

# Outer Billiards on Kites

by

Richard Evan Schwartz

# Preface

Outer billiards is a basic dynamical system defined relative to a convex shape in the plane. B.H. Neumann introduced outer billiards in the 1950s, and J. Moser popularized outer billiards in the 1970s as a toy model for celestial mechanics. Outer billiards is an appealing dynamical system because of its simplicity and also because of its connection to such topics as interval exchange maps, piecewise isometric actions, and area-preserving actions. There is a lot left to learn about these kinds of dynamical systems, and a good understanding of outer billiards might shed light on the more general situation.

The *Moser-Neumann question*, one of the central problems in this subject, asks *Does there exist an outer billiards system with an unbounded orbit?* Until recently, all the work on this subject has been devoted to proving that all the orbits are bounded for various classes of shapes. We will detail these results in the introduction.

Recently we answered the Moser-Neumann question in the affirmative by showing that outer billiards has an unbounded orbit when defined relative to the Penrose kite, the convex quadrilateral that arises in the famous Penrose tiling. Our proof involves special properties of the Penrose kite, and naturally raises questions about generalizations.

In this monograph we will give a more general and robust answer to the Moser-Neumann question. We will prove that outer billiards has unbounded orbits when defined relative to any irrational kite. A *kite* is probably best defined as a “kite-shaped” quadrilateral. (See the top of §1.2 for a non-circular definition.) The kite is irrational if it is not affinely equivalent to a quadrilateral with rational vertices. Our analysis uncovers some of the deep structure underlying outer billiards on kites, including connections to self-similar tilings, higher dimensional polytope exchange maps, Diophantine approximation, the modular group, and the universal odometer.

I discovered every result in this monograph by experimenting with my computer program, Billiard King, a Java-based graphical user interface. For the most part, the material here is logically independent from Billiard King, but I encourage the serious reader of this monograph to download Billiard King from my website <sup>1</sup> and play with it. My website also has an interactive guide to this monograph, in which many of the basic ideas and constructions are illustrated with interactive Java applets.

---

<sup>1</sup>[www.math.brown.edu/~res](http://www.math.brown.edu/~res)

There are a number of people I would like to thank. I especially thank Sergei Tabachnikov, whose great book *Geometry and Billiards* first taught me about outer billiards. Sergei has constantly encouraged me as I have investigated this topic, and he has provided much mathematical insight along the way.

I thank Yair Minsky for his work on the punctured-torus case of the Ending Lamination Conjecture. It might seem strange to relate outer billiards to punctured-torus bundles, but there seems to me to be a common theme. In both cases, one studies the limit of geometric objects indexed by rational numbers and controlled in some sense by the Farey triangulation.

I thank Eugene Gutkin for the explanations he has given me about his work on outer billiards. The work of Gutkin-Simanyi and others on the periodicity of the orbits for rational polygons provided the theoretical underpinnings for some of my initial computer investigations.

I thank Jeff Brock, Peter Doyle, Dmitry Dolgopyat, David Dumas, Giovanni Forni, Richard Kent, Howie Masur, Curt McMullen, John Smillie, and Ben Wieland, for various helpful conversations about this work.

I thank the National Science Foundation for their continued support, currently in the form of the grant DMS-0604426.

I thank my home institution, Brown University, for providing an excellent research environment during the genesis of most of this work. I also thank the Institut des Hautes Etudes Scientifiques for providing a similarly excellent research environment, during the summer of 2008.

I dedicate this monograph to my parents, Karen and Uri.

# Table of Contents

1. Introduction	6
<b>Part I</b>	22
2. The Arithmetic Graph	23
3. The Hexagrid Theorem	34
4. Period Copying	42
5. Proofs of the Basic Results	48
<b>Part II</b>	56
6. The Master Picture Theorem	57
7. The Pinwheel Lemma	66
8. The Torus Lemma	79
9. The Strip Functions	88
10. Proof of the Master Picture Theorem	95
11. Some Formulas	100
<b>Part III</b>	108
12. Proof of the Embedding Theorem	109
13. Extension and Symmetry	116
14. The Structure of the Doors	123
15. Proof of the Hexagrid Theorem I	128
16. Proof of the Hexagrid Theorem II	135
17. The Barrier Theorem	147
<b>Part IV</b>	156
18. Proof of the Superior Sequence Lemma	157
19. The Diophantine Lemma	164
20. Existence of Strong Sequences	174
21. Proof of the Decomposition Theorem	179

<b>Part V</b>	188
22. Odd Approximation Results	189
23. The Fundamental Orbit	194
24. Most of the Comet Theorem	208
25. Dynamical Consequences	220
26. Geometric Consequences	230
 <b>Part VI</b>	 238
27. Proof of the Copy Theorem	239
28. Pivot Arcs in the Even Case	247
29. Proof of the Pivot Theorem	260
30. Proof of the Period Theorem	273
31. The End of the Comet Theorem	280
 32. References	 295

# 1 Introduction

## 1.1 History of the Problem

B.H. Neumann [N] introduced *outer billiards* in the late 1950s. In the 1970s, J. Moser [M1] popularized outer billiards as a toy model for celestial mechanics. One appealing feature of polygonal outer billiards is that it gives rise to a piecewise isometric mapping of the plane. Such maps have close connections to interval exchange transformations and more generally to polygon exchange maps. See [T1] and [DT] for an exposition of outer billiards and many references.

To define an outer billiards system, one starts with a bounded convex set  $K \subset \mathbf{R}^2$  and considers a point  $x_0 \in \mathbf{R}^2 - K$ . One defines  $x_1$  to be the point such that the segment  $\overline{x_0x_1}$  is tangent to  $K$  at its midpoint and  $K$  lies to the right of the ray  $\overrightarrow{x_0x_1}$ . (See Figure 1.1 below.) The iteration  $x_0 \rightarrow x_1 \rightarrow x_2 \dots$  is called the *forwards outer billiards orbit* of  $x_0$ . It is defined for almost every point of  $\mathbf{R}^2 - K$ . The backwards orbit is defined similarly.

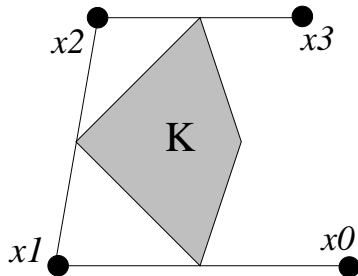


Figure 1.1: Outer Billiards

Moser [M2, p. 11] attributes the following question to Neumann *circa* 1960, though it is sometimes called *Moser's Question*.

**Question:** *Is there an outer billiards system with an unbounded orbit?*

This question is an idealized version of the question about the stability of the solar system. The Moser-Neumann question has been considered by various authors. Here is a list of the main results on the question.

- J. Moser [M] sketches a proof, inspired by K.A.M. theory, that outer billiards on  $K$  has all bounded orbits provided that  $\partial K$  is at least  $C^6$

smooth and positively curved. R. Douady gives a complete proof in his thesis, [D].

- P. Boyland [B] gives examples of  $C^1$  smooth convex domains for which an orbit can contain the domain boundary in its  $\omega$ -limit set.
- In [VS], [Ko], and (later, but with different methods) [GS], it is proved that outer billiards on a *quasirational polygon* has all orbits bounded. This class of polygons includes rational polygons and also regular polygons. In the rational case, all defined orbits are periodic.
- S. Tabachnikov analyzes the outer billiards system for the regular pentagon and shows that there are some non-periodic (but bounded) orbits. See [T1, p 158] and the references there.
- D. Genin [G] shows that all orbits are bounded for the outer billiards systems associated to trapezoids. He also makes a brief numerical study of a particular irrational kite based on the square root of 2, observes possibly unbounded orbits, and indeed conjectures that this is the case.
- Recently, in [S] we proved that outer billiards on the Penrose kite has unbounded orbits, thereby answering the Moser-Neumann question in the affirmative. The Penrose kite is the convex quadrilateral that arises in the Penrose tiling.
- Very recently, D. Dolgopyat and B. Fayad [DF] show that outer billiards around a semicircle has some unbounded orbits. Their proof also works for “circular caps” sufficiently close to the semicircle. This is a second affirmative answer to the Moser-Neumann question.

The result in [S] naturally raises questions about generalizations. The purpose of this monograph is to develop the theory of outer billiards on kites and show that the phenomenon of unbounded orbits for polygonal outer billiards is (at least for kites) quite robust. We think that the theory we develop here will work, to some extent, for polygonal outer billiards in general, though right now a general theory is beyond us.

We mention again that we discovered all the results in the monograph through computer experimentation. The interested reader can download my program, Billiard King, from my website <sup>2</sup>.

---

<sup>2</sup>[www.math.brown.edu/~res](http://www.math.brown.edu/~res)

## 1.2 The Basic Results

For us, a *kite* is a quadrilateral of the form  $K(A)$ , with vertices

$$(-1, 0); \quad (0, 1) \quad (0, -1) \quad (A, 0); \quad A \in (0, 1). \quad (1)$$

Figure 1.1 shows an example. We call  $K(A)$  *(ir)rational* iff  $A$  is (ir)rational. Outer billiards is an affinely invariant system, and any quadrilateral that is traditionally called a kite is affinely equivalent to some  $K(A)$ .

Let  $\mathbf{Z}_{\text{odd}}$  denote the set of odd integers. Reflection in each vertex of  $K(A)$  preserves  $\mathbf{R} \times \mathbf{Z}_{\text{odd}}$ . Hence, outer billiards on  $K(A)$  preserves  $\mathbf{R} \times \mathbf{Z}_{\text{odd}}$ . We say that a *special orbit* on  $K(A)$  is an orbit contained in  $\mathbf{R} \times \mathbf{Z}_{\text{odd}}$ . This monograph <sup>3</sup> only discusses special orbits.

We call an orbit *forwards erratic* if the forwards orbit is unbounded and also returns to every neighborhood of a kite vertex. We make the same definition for the backwards direction. We call an orbit *erratic* if it is both forwards and backwards erratic. Say that a *trimmed Cantor set* is a set of the form  $C - C'$ , where  $C$  is a Cantor set and  $C'$  is countable. Note that a trimmed Cantor set is an uncountable set. Here are our 3 basic results.

**Theorem 1.1 (Erratic Orbits)** *On any irrational kite, the union of special erratic orbits contains a trimmed Cantor set.*

**Theorem 1.2 (Dichotomy)** *On any irrational kite, every special orbit is either periodic or else unbounded in both directions.*

**Theorem 1.3 (Density)** *On any irrational kite, the union of periodic special orbits is open dense in  $\mathbf{R} \times \mathbf{Z}_{\text{odd}}$ .*

Thanks to the work mentioned above, we already know that all orbits are bounded on rational kites. The Erratic Orbits Theorem therefore has the following simple corollary.

**Corollary 1.4** *Outer billiards on a kite has an unbounded orbit if and only if the kite is irrational.*

Our monograph comes in 6 parts. Parts I-IV constitute a self-contained subset of the monograph designed to prove the results listed above. Parts V-VI go deeper into the subject, and establish the Comet Theorem, a fairly complete description of the set of unbounded special orbits.

---

<sup>3</sup>Some of our theory works for the general orbit, and there seems to be quite a lot to say, but we will not say it here. The special orbits are hard enough for us already.

### 1.3 The Comet Theorem

The Comet Theorem has a number of corollaries that are much easier to state than the result itself. We state some of these first. Let  $U_A$  denote the set of unbounded special orbits relative to an irrational  $A \in (0, 1)$ .

- $U_A$  is minimal: Every orbit in  $U_A$  is dense in  $U_A$ .
- $U_A$  is locally homogeneous: Every two points in  $U_A$  have arbitrarily small neighborhoods that are isometric to each other.
- $U_A$  has length 0. Hence, almost every point in  $\mathbf{R} \times \mathbf{Z}_{\text{odd}}$  is periodic.
- Let  $u(A)$  denote the Hausdorff dimension of  $U_A$ . The function  $u$  maps every open subset of  $[0, 1] - \mathbf{Q}$  onto  $[0, 1]$  and yet is almost everywhere constant. (We don't know "the constant".)
- Let  $\Gamma_2 \subset SL_2(\mathbf{Z})$  denote the subgroup consisting of matrices congruent to the identity mod 2. As usual,  $\Gamma_2$  acts on  $\mathbf{R} \cup \infty$  by linear fractional transformations. The function  $u$  is constant on  $\Gamma_2$ -orbits.

We will deduce these results, and many others, from the Comet Theorem in §25 and §26. We turn now to the statement of the Comet Theorem. Consider the regions

$$I = [0, 2] \times \{-1\}; \quad J = [-2, 2] \times \{-1, 1\} = \bigcup_{k=0}^3 (\psi')^k(I). \quad (2)$$

Here  $\psi'$  is the outer billiards map. The domains  $I$  and  $J$  turn out to be canonical domains for outer billiards on kites, as we have normalized them. The Comet Theorem provides a model for the way the unbounded orbits return to  $I$ .

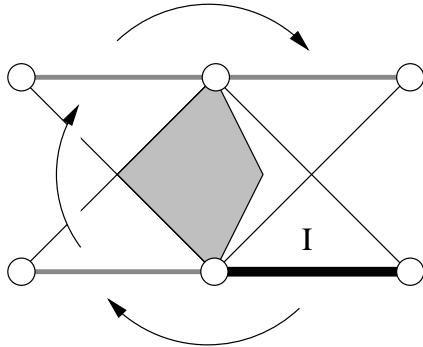


Figure 1.2:  $I$  is black and  $J$  is grey.

Say that  $p/q$  is *odd* or *even* according to whether  $pq$  is odd or even. There is a unique sequence  $\{p_n/q_n\}$  of distinct odd rationals, converging to  $A$ , such that  $p_0/q_0 = 1/1$  and  $|p_n q_{n+1} - q_n p_{n+1}| = 2$  for all  $n$ . We call this sequence the *inferior sequence*. See §4.2. This sequence is closely related to continued fractions.

We define

$$d_n = \text{floor}\left(\frac{q_{n+1}}{2q_n}\right); \quad n = 0, 1, 2, \dots \quad (3)$$

Say that a *superior term* is a term  $p_n/q_n$  such that  $d_n \geq 1$ . We will show that there are infinitely many superior terms. Say that the *superior sequence* is the subsequence of superior terms. Say that the *renormalization sequence* is the corresponding subsequence of  $\{d_n\}$ . We re-index so that the superior and renormalization sequences are indexed by  $0, 1, 2, \dots$ . The definitions that follow work entirely with the superior sequence.

We define  $\mathcal{Z}_A$  to be the inverse limit of the system

$$\dots \rightarrow \mathbf{Z}/D_3 \rightarrow \mathbf{Z}/D_2 \rightarrow \mathbf{Z}/D_1; \quad D_n = \prod_{i=0}^{n-1} (d_i + 1) \quad (4)$$

We equip  $\mathcal{Z}$  with a metric, defining  $d(x, y) = q_{n-1}^{-1}$ , where  $n$  is the smallest index such that  $[x]$  and  $[y]$  disagree in  $\mathbf{Z}/D_n$ . In case  $d_i + 1 = p$  for all  $i$ , the metric  $d$  is the  $p$ -adic metric. In general,  $\mathcal{Z}_A$  is a metric abelian group. The map  $x \rightarrow x + 1$  is a canonical self-homeomorphism called the *odometer map*.

We can identify the points of  $\mathcal{Z}_A$  with the sequence space

$$\Pi_A = \prod_{i=0}^{\infty} \{0, \dots, d_i\} \quad (5)$$

Our identification works like this

$$\phi_1 : \sum_{j=0}^{\infty} \tilde{k}_j D_j \in \mathcal{Z}_A \quad \longrightarrow \quad \{k_j\} \in \Pi_A. \quad (6)$$

The elements on the left hand side are formal series, and

$$\tilde{k}_j = \begin{cases} k_j & \text{if } p_j/q_j < A \\ d_j - k_j & \text{if } p_j/q_j > A \end{cases} \quad (7)$$

Our identification is a bit nonstandard, in that it uses  $\tilde{k}_j$  in place of the more obvious choice of  $k_j$ .

There is a map  $\phi_2 : \Pi_A \rightarrow \mathbf{R} \times \{-1\}$ , defined as follows.

$$\phi_2 : \{k_j\} \longrightarrow \left( \sum_{j=0}^{\infty} 2k_j \lambda_j, -1 \right); \quad \lambda_j = |Aq_j - p_j|. \quad (8)$$

We define  $C_A = \phi_2(\Pi_A)$ . Equivalently,

$$C_A = \phi(\mathcal{Z}_A); \quad \phi = \phi_2 \circ \phi_1. \quad (9)$$

It turns out that  $\phi : \mathcal{Z}_A \rightarrow C_A$  is a homeomorphism and  $C_A$  is a Cantor set whose convex hull is exactly  $I$ . Let  $C_A^\#$  denote the set obtained from  $C_A$  by deleting the endpoints of the complementary intervals in  $I - C_A$ .

The points  $\phi(-1), \phi(0) \in C_A$  are important points for us. It turns out that these points have well-defined orbits iff they lie in  $C_A^\#$ , which happens iff the superior sequence for  $A$  is not eventually monotone. Reflection in the midpoint of  $I$  preserves  $C_A$  and swaps  $\phi(-1)$  and  $\phi(0)$ .

Define

$$\mathbf{Z}[A] = \mathbf{Z} \oplus \mathbf{Z}A = \{mA + n \mid m, n \in \mathbf{Z}\}. \quad (10)$$

Say that the *excursion distance* of a portion of an outer billiards orbit is the maximum distance from a point on this orbit-portion to the origin.

**Theorem 1.5 (Comet)** *Let  $U_A$  denote the set of unbounded special orbits relative to an irrational  $A \in (0, 1)$ .*

1. *For any  $N$  there is an  $N'$  with the following property. If  $\zeta \in U_A$  satisfies  $\|\zeta\| < N$  then the  $k$ th outer billiards iterate of  $\zeta$  lies in  $I$  for some  $|k| < N'$ . Here  $N'$  only depends on  $N$  and  $A$ .*
2.  *$U_A \cap I = C_A^\#$ . The first return map  $\rho_A : C_A^\# \rightarrow C_A^\#$  is defined precisely on  $C_A^\# - \phi(-1)$ . The map  $\phi^{-1} \circ \rho_A \circ \phi$ , wherever defined on  $\mathcal{Z}_A$ , equals the odometer.*
3. *For any  $\zeta \in C_A^\# - \phi(-1)$ , the orbit-portion between  $\zeta$  and  $\rho_A(\zeta)$  has excursion distance in  $[c_1^{-1}d^{-1}, c_1d^{-1}]$  and length in  $[c_2^{-1}d^{-2}, c_2d^{-3}]$ . Here  $d = d(-1, \phi^{-1}(\zeta))$ , and  $c_1, c_2$  are universal positive constants.*
4.  *$C_A^\# = C_A - (2\mathbf{Z}[A] \times \{-1\})$ . Two points in  $U_A$  lie on the same orbit if and only if the difference of their first coordinates lies in  $2\mathbf{Z}[A]$ .*

**Remarks:**

(i) To use a celestial analogy, we think of  $I$  as the visible sky, and the special unbounded orbits as the comets. Item 1 says (in particular) that any comet visits  $I$ . Item 2 describes the exact locations and combinatorial structure of the visits. Item 3 gives a coarse model for the excursion distances and return times between visits. Item 4 gives an algebraic view. In short, the Comet Theorem tells us where and (approximately) when to point the telescope.

(ii) Item 1 of the Comet Theorem is somewhat loose, in that we don't know how  $N'$  depends on  $N$  and  $A$ . In principle, one could extract estimates from our proof, but we didn't try to do this.

(iii) Lemma 24.3 replaces our bounds in Item 3 with explicit estimates. The orders on all our bounds in Item 3 are sharp except perhaps for the length upper-bound. See the remarks following Lemma 24.3 for a discussion.

(iv) The Comet Theorem has an analogue for the backwards orbits. The statement is the same except that the point  $\phi(0)$  replaces the point  $\phi(-1)$  and the map  $x \rightarrow x - 1$  replaces the odometer.

(v) Our analysis will show that  $\phi(0)$  and  $\phi(-1)$  have well-defined orbits iff they lie in  $C_A^\#$ . Again, this happens iff the superior sequence for  $A$  is not eventually monotone. This happens for a full-measure set of parameters. Item 1 implies that the forwards orbit of  $\phi(-1)$ , when defined, only accumulates at  $\infty$ . The same goes for the backwards orbit of  $\phi(0)$ . We think of  $\phi(-1)$  as the “cosmic ejector”. When a comet comes close to this point, it gets ejected way out into space. Likewise, we think of  $\phi(0)$  as the “cosmic attractor”.

(vi) By symmetry  $U_A \cap J$  consists of 4 copies of  $C_A^\#$  arranged in a symmetric pattern about the two kite vertices  $(0, \pm 1)$ . Thus, the Comet Theorem completely controls how the unbounded special orbits return near the origin.

(vii) In §25.4 we will formalize the idea of constructing a model for the dynamics of the outer billiards map on  $U_A$ . The *solenoid*  $\mathcal{S}_A$  is the mapping cylinder for the odometer on  $\mathcal{Z}_A$ . We delete a point from  $\mathcal{S}_A$  and alter the metric so that this deleted point lies infinitely far away. That is, we create a cusp. There is a fairly canonical way to do this, and we call the result  $\mathcal{C}_A$  the

*cusped solenoid*. We will see that, in some sense the time-one map for the geodesic flow on  $\mathcal{C}_A$  serves as a good model for the dynamics on  $U_A$ . This result is really just a re-packaging of the Comet Theorem.

(viii) For almost all choices of  $A$ , the object  $\mathcal{Z}_A$  and its odometer coincide with the *universal odometer*. This is the profinite completion of  $\mathbf{Z}$  – i.e., the inverse limit over all finite cyclic groups. We call the corresponding object  $\mathcal{C}_A$  the *universal cusped solenoid*. As we formalize in §25.4 and §25.5, the time-one map of the geodesic flow on the universal cusped solenoid serves as a good model, in some sense, for the dynamics on  $U_A$  for almost all  $A$ . In particular, for almost all  $A$ , the return map to  $C_A^\#$  is conjugate (modulo a countable set) to the universal odometer.

(ix) By the Dichotomy Theorem, all well-defined orbits in  $I - C_A$  are periodic. Conjecture 25.3 describes the dynamics of these points. In brief, we can identify  $C_A$  with the ends of a certain directed tree. The first return map to  $C_A$  is induced by a certain automorphism of the directed tree. The complementary intervals in  $I - C_A$  are naturally in bijection with the forward cones of the directed tree. Conjecture 25.3 says that the first return map to  $I - C_A$  permutes these intervals just as the tree automorphism permutes the forward cones.

(x) The  $\Gamma_2$ -invariance of the dimension function  $\dim(U_A)$  is a small reflection of the beautiful structure of the sets  $C_A$ . This monograph only scratches the surface. Here is a structural result is outside the scope of the monograph. Letting  $C'_A$  denote the scaled-in-half version of  $C_A$  that lives in the unit interval, it seems that

$$C = \bigcup_{A \in [0,1]} (C'_A \times \{A\}) \subset [0, 1]^2 \subset \mathbf{RP}^2 \quad (11)$$

is the limit set of a semigroup  $S \subset SL_3(\mathbf{Z})$  that acts by projective transformations. ( $C_A$  can be defined even for rational  $A$ .) The group closure of  $S$  has finite index in a maximal cusp of  $SL_3(\mathbf{Z})$ . The projective geometry underlying the set  $C$  emerges almost immediately from a good plot. We might have included a plot here, but we don't know how to draw a good picture without producing a huge picture file. My website <sup>4</sup> has a picture of  $C$ . We produced this picture using the formula in Theorem 1.9 below.

---

<sup>4</sup>[www.math.brown.edu/~res/BilliardKing/Butterfly0](http://www.math.brown.edu/~res/BilliardKing/Butterfly0)

## 1.4 Rational Kites

We find it convenient to work with the square of the outer billiards map. Let  $O_2(x)$  denote the square outer billiards orbit of  $x$ . Let  $I$  be as above, and let

$$\Xi = \mathbf{R}_+ \times \{-1, 1\}. \quad (12)$$

When  $\epsilon \in (0, 2/q)$ , the orbit  $O_2(\epsilon, -1)$  has a combinatorial structure independent of  $\epsilon$ . See Lemma 2.2. Thus,  $O_2(1/q, -1)$  is a natural representative of this orbit. This orbit plays a crucial role in our proofs. Reflection The following result is our basic mechanism for producing unbounded orbits.

**Theorem 1.6** *Let  $p/q \in (0, 1)$  be any rational. Relative to  $A = p/q$  the following is true.*

- *If  $p/q$  is odd then  $O_2(1/q, -1)$  has diameter between  $(p+q)/2$  and  $p+q$ .*
- *If  $p/q$  is even then  $O_2(1/q, -1)$  has diameter between  $(p+q)$  and  $2(p+q)$ .*

Here is an amplification of the upper bound in Theorem 1.6.

**Theorem 1.7** *If  $p/q$  is odd let  $\lambda = 1$ . If  $p/q$  is even let  $\lambda = 2$ . Each special orbit intersects  $\Xi$  in exactly one set of the form  $I_k \times \{-1, 1\}$ , where*

$$I_k = (\lambda k(p+q), \lambda(k+1)(p+q)) \quad k = 0, 1, 2, 3\dots$$

*Hence, any special orbit intersects  $\Xi$  in a set of diameter at most  $\lambda \cdot (p+q)$ .*

Theorem 1.7 is similar in spirit to a result in [K]. See §3.4 for a discussion.

An outer billiards orbit on  $K(A)$  is called *stable* if there are nearby and combinatorially identical orbits on  $K(A')$  for all  $A'$  sufficiently close to  $A$ . Otherwise, the orbit is called *unstable*. In the odd case,  $O_2(1/q, \pm 1)$  is unstable. This fact is of crucial importance to all our proofs. Here is a classification of special orbits in terms of stability.

**Theorem 1.8** *In the even rational case, all special orbits are stable. In the odd case, the set  $I_k \times \{-1, 1\}$  contains exactly two unstable orbits,  $U_k^+$  and  $U_k^-$ , and these are conjugate by reflection in the  $x$ -axis. In particular, we have  $U_0^\pm = O_2(1/q, \pm 1)$ .*

The preceding results give effective but somewhat coarse global pictures of the special orbits. Here we describe a very precise picture of our fundamental orbit  $O_2(1/q, -1)$  near the origin. Any odd rational  $p/q$  appears as a term in a superior sequence, and the terms before  $p/q$  are uniquely determined by  $p/q$ . This is similar to what happens for continued fractions.

**Theorem 1.9** *Let  $\mu_i = |p_n q_i - q_n p_i|$ .*

$$O_2(1/q_n, -1) \cap I = \bigcup_{\kappa \in \Pi_n} (X_n(\kappa), -1); \quad X_n(\kappa) = \frac{1}{q_n} \left( 1 + \sum_{i=0}^{n-1} 2k_i \mu_i \right).$$

To prove the Comet Theorem, we will combine Theorem 1.6 and Theorem 1.9 and then take a geometric limit.

Here we show Theorem 1.9 in action. Relative to  $19/49$ , the intersection  $O_2(1/49) \cap \Xi$  has diameter between 34 and 68. The odd rational  $19/49$  determines the inferior sequence

$$\frac{p_0}{q_0} = \frac{1}{1}, \frac{1}{3}, \frac{5}{13}, \frac{19}{49} = \frac{p_3}{q_3}.$$

All terms are superior, so this is also the superior sequence.  $n = 3$  in our example, and the renormalization sequence is 1, 2, 1. The  $\mu$  sequence is 30, 8, 2. The first coordinates of the 12 points of  $O_2(1/49) \cap I$  are given by

$$\bigcup_{k_0=0}^1 \bigcup_{k_1=0}^2 \bigcup_{k_2=0}^1 \frac{2(30k_0 + 8k_1 + 2k_2) + 1}{49}.$$

Writing these numbers in a suggestive way, the union above works out to

$$\frac{1}{49} \times (1 \ 5 \quad 17 \ 21 \quad 33 \ 37 \quad \quad \quad 61 \ 65 \quad 77 \ 81 \quad 93 \ 97).$$

The reader can check this example, and many others, using Billiard King.

**Remarks:**

- (i) A version of Theorem 1.9 holds in the even case as well. We will discuss the even case of Theorem 1.9 in §23.7.
- (ii) Theorem 1.9 has a nice conjectural extension, which describes the entire return map to  $I$ . See §23.8.

## 1.5 The Arithmetic Graph

All our results about special orbits derive from our analysis of a fundamental object, which we call the *arithmetic graph*. One should think of the first return map to  $\Xi$ , for rational parameters, as an essentially combinatorial object. The idea behind the arithmetic graph is to give a 2 dimensional pictorial representation of this combinatorial object.

The principle guiding our construction is that sometimes it is better to understand the abelian group  $\mathbf{Z}[A] := \mathbf{Z} \oplus \mathbf{Z}A$  as a module over  $\mathbf{Z}$  rather than as a subset of  $\mathbf{R}$ . Our arithmetic graph is similar in spirit to the lattice vector fields studied by Vivaldi et. al. in connection with interval exchange transformations. See e.g. [VL]. In this section we will explain the idea behind the arithmetic graph. In §2.5 we will give a precise construction.

The arithmetic graph is most easily explained in the rational case. Let  $\psi$  be the square of the outer billiards map. Let  $\Xi = \mathbf{R}_+ \times \{-1, 1\}$  as above. It turns out that every orbit starting on  $\Xi$  eventually returns to  $\Xi$ . See Lemma 2.3. Thus we can define the return map

$$\Psi : \Xi \rightarrow \Xi. \quad (13)$$

We define the map  $T : \mathbf{Z}^2 \rightarrow 2\mathbf{Z}[A] \times \{-1, 1\}$  by the formula

$$T(m, n) = \left( 2Am + 2n + \frac{1}{q}, (-1)^{p+q+1} \right). \quad (14)$$

Here  $A = p/q$ .

Up to the reversal of the direction of the dynamics, every point of  $\Xi$  has the same orbit as a point of the form  $T(m, n)$ , where  $(m, n) \in \mathbf{Z}^2$ . For instance, the orbit of  $T(0, 0) = (1/q, -1)$  is the same as the orbit of our favorite point  $(1/q, -1)$  up to reversing the dynamics. The point here is that reflection in the  $x$ -axis conjugates the outer billiards map to its inverse.

We form the graph  $\widehat{\Gamma}(p/q)$  by joining the points  $(m_1, m_2)$  to  $(m_2, n_2)$  when these points are sufficiently close together and also  $T(m_1, n_1) = \Psi^{\pm 1}(m_2, n_2)$ . (The map  $T$  is not injective, so we have choices to make. That is the purpose of the *sufficiently close* condition.)

We let  $\Gamma(p/q)$  denote the component of  $\widehat{\Gamma}(p/q)$  that contains  $(0, 0)$ . This component tracks the orbit  $O_2(1/q, -1)$ , the main orbit of interest to us. When  $p/q$  is odd,  $\Gamma(p/q)$  is an infinite periodic polygonal arc, invariant under translation by the vector  $(q, -p)$ . Note that  $T(q, -p) = T(0, 0)$ . When  $p/q$

is even,  $\Gamma(p/q)$  is an embedded polygon. This difference causes us to prefer the odd case.

We prove many structural theorems about the arithmetic graph. Here we mention 3 central ones. We state these results vaguely here, and refer the reader to the chapters where the precise statements are given.

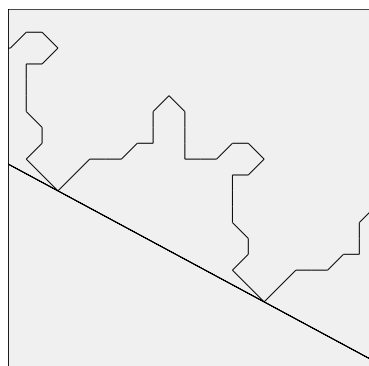
- **The Embedding Theorem** (§2):  $\widehat{\Gamma}(p/q)$  is a disjoint union of embedded polygons and infinite embedded polygonal arcs. Every edge of  $\widehat{\Gamma}(p/q)$  has length at most  $\sqrt{2}$ . The stable orbits correspond to closed polygons, and the unstable orbits correspond to infinite (but periodic) polygonal arcs.
- **The Hexagrid Theorem** (§3): The structure of  $\widehat{\Gamma}(p/q)$  is controlled by 6 infinite families of parallel lines. The *quasiperiodic* structure is similar to what one sees in DeBruijn’s famous pentagrid construction of the Penrose tilings. See [DeB].
- **The Copy Theorem:** (§19; also Lemmas 4.2 and Lemma 4.3.) If  $A_1$  and  $A_2$  are two rationals that are close in the sense of Diophantine approximation then the corresponding arithmetic graphs  $\Gamma_1$  and  $\Gamma_2$  have substantial agreement.

The Hexagrid Theorem causes  $\Gamma(p/q)$  to have an oscillation (relative to the line of slope  $-p/q$  through the origin) on the order of  $p + q$ . The Hexagrid Theorem is responsible for Theorems 1.6, 1.7, and 1.8. Referring to the superior sequence, the Copy Theorem guarantees that the structure the graph  $\Gamma(p_n/q_n)$  is copied by the graph  $\Gamma(p_{n+1}/q_{n+1})$ . The Copy Theorem is responsible for Theorem 1.9. Thus, the Hexagrid Theorem and the Copy Theorem serve as a kind of a team, with one result forcing large oscillations in certain orbits, and the other result guaranteeing that the oscillations are coherently organized in the family of arithmetic graphs corresponding to the superior sequence.

We illustrate these ideas with some pictures. Each picture shows  $\Gamma(p/q)$  in reference to the line of slope  $-p/q$  through the origin. The rationals

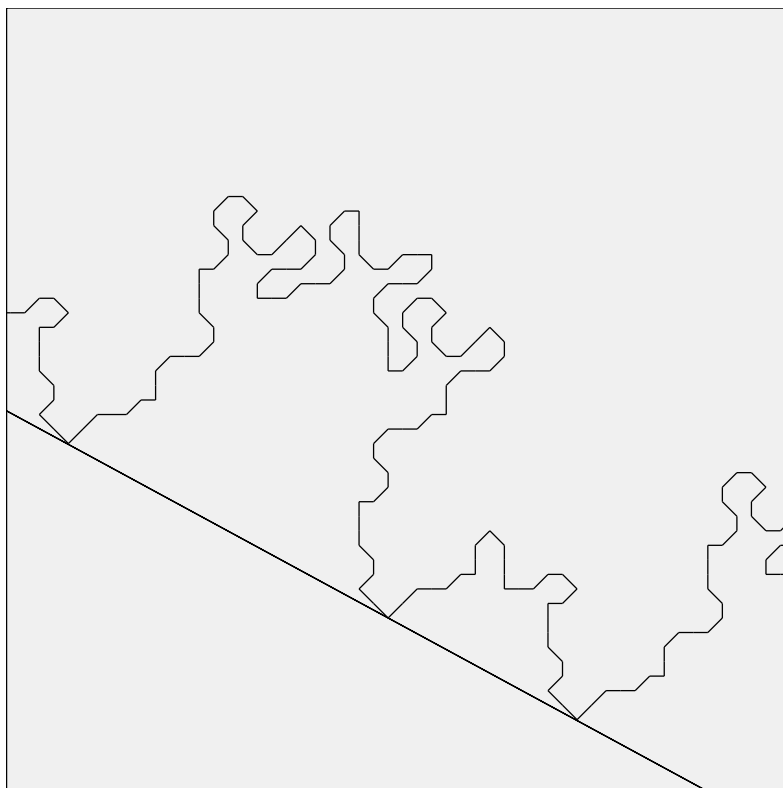
$$\frac{7}{13}, \frac{19}{35}, \frac{45}{83}$$

form 3 terms in a superior sequence. Figure 1.3 shows a bit more than one period of  $\Gamma(7/13)$ .



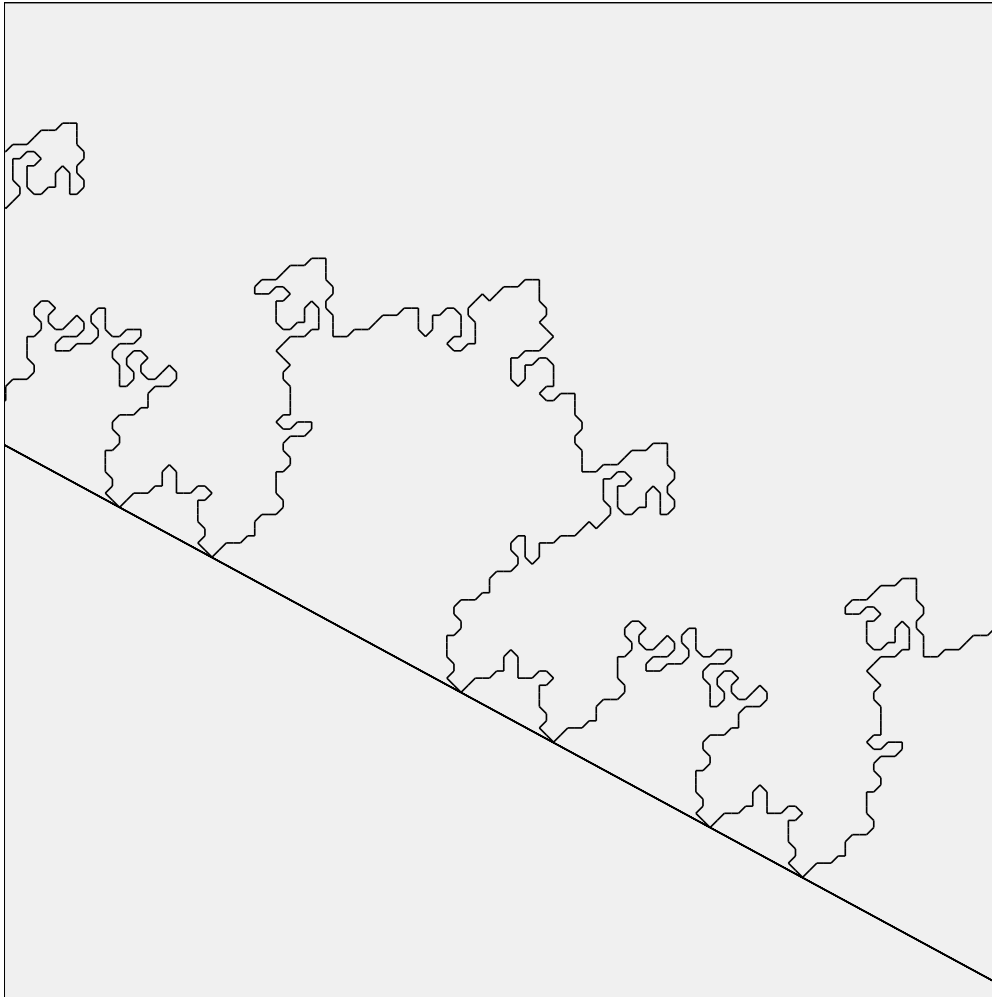
**Figure 1.3:** The graph  $\Gamma(7/13)$ .

Figure 1.4 shows a picture of  $\Gamma(19/35)$ . Notice that  $\Gamma(19/35)$  has a much wider oscillation, but also manages to copy a bit more than one period of  $\Gamma(7/13)$ . The reader can see many more pictures like this using either Billiard King or our interactive guide to the monograph



**Figure 1.4:** The graph  $\Gamma(19/35)$ .

Figure 1.5 shows the same phenomenon for  $\Gamma(45/83)$ . This graph oscillates on a large scale but still manages to copy a bit more than one period of  $\Gamma(19/35)$ . Hence  $\Gamma(45/83)$  copies a period of  $\Gamma(7/13)$  and a period of  $\Gamma(19/35)$ . That is,  $\Gamma(45/83)$  oscillates on 3 scales.



**Figure 1.5:** The graph  $\Gamma(45/83)$ .

What emerges in these pictures is both the wide excursions predicted by Theorem 1.6 and also the Cantor-like structure predicted by Theorem 1.9. Taking a limit of this process, we produce a graph that oscillates on all scales. This limiting graph tracks the sort of unbounded orbit discussed above.

## 1.6 The Master Picture Theorem

Essentially all of our results have a common source, the Master Picture Theorem. The Master Picture Theorem is, in some sense, a closed form expression for the arithmetic graph. We formulate and prove the Master Picture Theorem in Part II of the monograph. Here we will give the reader a feel for the result.

Recall that  $\Xi = \mathbf{R}_+ \times \{-1, 1\}$ . The arithmetic graph encodes the dynamics of the first return map  $\Psi : \Xi \rightarrow \Xi$ . It turns out that  $\Psi$  is an infinite interval exchange map. The Master Picture Theorem reveals the following structure.

1. There is a locally affine map  $\mu$  from  $\Xi$  into a union  $\widehat{\Xi}$  of two 3-dimensional tori.
2. There is a polyhedron exchange map  $\widehat{\Psi} : \widehat{\Xi} \rightarrow \widehat{\Xi}$ , defined relative to a partition of  $\widehat{\Xi}$  into 28 polyhedra.
3. The map  $\mu$  is a semi-conjugacy between  $\Psi$  and  $\widehat{\Psi}$ .

In other words, the return dynamics of  $\widehat{\Psi}$  has a kind of compactification into a 3 dimensional polyhedron exchange map. All the objects above depend on the parameter  $A$ , but we have suppressed them from our notation.

There is one master picture, a union of two 4-dimensional convex lattice polytopes partitioned into 28 smaller convex lattice polytopes, that controls everything. For each parameter, one obtains the 3-dimensional picture by taking a suitable slice.

The fact that nearby slices give almost the same picture is the source of our Copy Theorem. The interaction between the map  $\mu$  and the walls of our convex polytope partitions is the source of the Hexagrid Theorem. The Embedding Theorem follows from basic geometric properties of the polytope exchange map in an elementary way that is hard to summarize here.

My investigation of the Master Picture Theorem is really just starting, and this monograph only has the beginnings of a theory. First, I believe that a version of the Master Theorem should hold much more generally. (This is something that John Smillie and I hope to work out together.) Second, some recent experiments convince me that there is a renormalization theory for this object, grounded in real projective geometry. All of this is perhaps the subject of a future work.

## 1.7 Computational Issues

I discovered all the structure of outer billiards by experimenting with Billiard King. Ultimately, I am trying to verify the structure I noticed on the computer, and so one might expect there to be some computation in the proof. The proof here uses considerably less computation than the proof in [S], but I still use a computer-aided proof in several places. For example, I use the computer to check that various 4 dimensional convex integral polytopes have disjoint interiors.

To the reader who does not like computer-aided proofs (however mild) I would like to remark that the experimental method here has the advantage that I checked all the results with massive and visually-based computation. The reader can make the same checks, by downloading Billiard King or else playing with the interactive online guide to the monograph.

## 1.8 Organization of the Monograph

As we mentioned above, our monograph comes in 6 parts. Parts I-IV comprise the core of the monograph. In part I we define the arithmetic graph and state its basic properties, such as the Embedding Theorem and the Hexagrid Theorem. Modulo these structural results, Part I proves the results listed in §1.2, and all the results in §1.4 except Theorem 1.9.

Part II proves the Master Picture Theorem, our main structural result. Part III deduces the Embedding Theorem and the Hexagrid Theorem from the Master Picture Theorem. Part IV establishes various period copying results needed for the results in §1.2.

Parts V and VI describes the close connection between the arithmetic graph and the modular group. In Part V, we prove the Comet Theorem modulo technical details that we resolve in Part VI.

Before each part of the monograph, we include an overview of that part.

# Part I

Here is an overview of this part of the monograph.

- In §2 we establish some basic results that allow for the definition of the arithmetic graph. The arithmetic graph is our main object of study. We also state the Embedding Theorem, a basic structural result about the arithmetic graph that we prove in Part III of the monograph.
- In §3 we state our main structural result, the Hexagrid Theorem. We then deduce Theorems 1.6, 1.7, and 1.8 from the Hexagrid Theorem. We prove the Hexagrid Theorem in Part III of the monograph.
- In §4 we discuss the period copying results needed to prove the Erratic Orbits Theorem. Along the way, we introduce the inferior and superior sequences, two basic ingredients in our overall theory. To illustrate the connection between outer billiards and these sequences, we state the Decomposition Theorem, a basic structural result that helps with the period copying. We prove the period copying results and the Decomposition Theorem in Part IV.
- In §5 we assemble the ingredients from previous chapters and prove the Erratic Orbits Theorem. At the end of the chapter, we prove Theorems 1.2 and 1.3.

We mention several conventions that we use repeatedly throughout the monograph. Recall that  $p/q$  is an odd rational if  $pq$  is odd. When we say *odd rational* we mean that the odd rational lies in  $(0, 1)$ . On very rare occasions, we also consider the odd rational  $1/1$ . However, we never consider negative odd rationals, or odd rationals  $> 1$ . Also,  $A$  always stands for a kite parameter, and we write  $A = p/q$ . Similarly,  $A_n$  stands for  $p_n/q_n$ , and  $A_+$  stand for  $p_+/q_+$ , etc. Sometimes we will mention these conventions explicitly, and sometimes we will forget to mention them.

## 2 The Arithmetic Graph

### 2.1 Polygonal Outer Billiards

Let  $P$  be a polygon. We denote the outer billiards map by  $\psi'$ , and the square of the outer billiards map by  $\psi = (\psi')^2$ . Our convention is that a person walking from  $p$  to  $\psi'(p)$  sees the  $P$  on the right side. These maps are defined away from a countable set of line segments in  $\mathbf{R}^2 - P$ . This countable set of line segments is sometimes called the *limit set*.

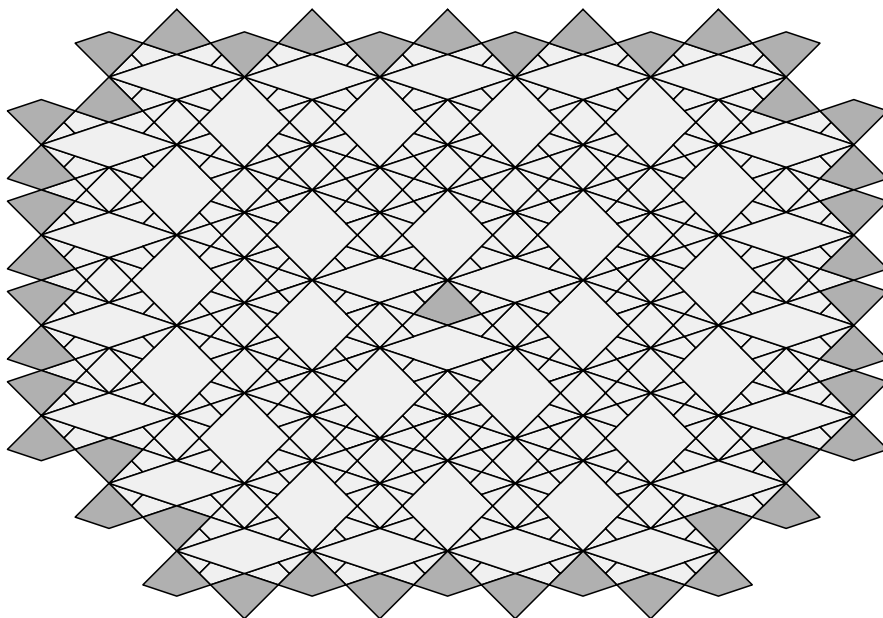


**Figure 2.1:** Part of the Tiling for  $K(1/3)$ .

The result in [VS], [K] and [GS] states, in particular, that the orbits for rational polygons are all periodic. In this case, the complement of the limit set is tiled by dynamically invariant convex polygons. Figure 2.1 shows the picture for the kite  $K(1/3)$ .

This is the simplest tiling <sup>5</sup> we see amongst all the kites. We have only drawn part of the tiling. The reader can draw more of these pictures, and in color, using Billiard King. The existence of these tilings was what motivated me to study outer billiards. I wanted to understand how the tiling changed with the rational parameter and saw that the kites gave rise to highly non-trivial pictures.

---

<sup>5</sup>Note that the picture is rotated by 90 degrees from our usual normalization.

## 2.2 Special Orbits

Until the last result in this section the parameter  $A = p/q$  is rational. Say that a *special interval* is an open horizontal interval of length  $2/q$  centered at a point of the form  $(a/q, b)$ , with  $a$  odd. Here  $a/q$  need not be in lowest terms.

**Lemma 2.1** *The outer billiards map is entirely defined on any special interval, and indeed permutes the special intervals.*

**Proof:** We note first that the order 2 rotations about the vertices of  $K(A)$  send the point  $(x, y)$  to the point:

$$(-2 - x, -y); \quad (-x, 2 - y); \quad (-x, -2 - y); \quad (2A - x, -y). \quad (15)$$

Let  $\psi'$  denote the outer billiards map on  $K(A)$ . The map  $\psi'$  is built out of the 4 transformations from Equation 15. The set  $\mathbf{R} \times \mathbf{Z}_{\text{odd}}$  is a countable collection of lines. Let  $\Lambda \subset \mathbf{R} \times \mathbf{Z}_{\text{odd}}$  denote the set of points of the form  $(2a+2bA, 2c+1)$ , with  $a, b, c \in \mathbf{Z}$ . The complementary set  $\Lambda^c = \mathbf{R} \times \mathbf{Z}_{\text{odd}} - \Lambda$  is the union of the special intervals.

Looking at Equation 15, we see that  $\psi'(x) \in \Lambda^c$  provided that  $x \in \Lambda^c$  and  $\psi'$  is defined on  $x$ . To prove this lemma, it suffices to show that  $\psi'$  is defined on any point of  $\Lambda^c$ .

To find the points of  $\mathbf{R} \times \mathbf{Z}_{\text{odd}}$  where  $\psi'$  is not defined, we extend the sides of  $K(A)$  and intersect them with  $\mathbf{R} \times \mathbf{Z}_{\text{odd}}$ . We get 4 families of points.

$$(2n, 2n + 1); \quad (2n, -2n - 1); \quad (2An, 2n - 1); \quad (2An, -2n + 1).$$

Here  $n \in \mathbf{Z}$ . Notice that all these points lie in  $\Lambda$ . ♠

Let  $\mathbf{Z}[A] = \mathbf{Z} \oplus \mathbf{Z}A$ . More generally, the same proof gives:

**Lemma 2.2** *Suppose that  $A \in (0, 1)$  is any number. Relative to  $K(A)$ , the entire outer billiards orbit of any point  $(\alpha, n)$  is defined provided that  $\alpha \notin 2\mathbf{Z}[A]$  and  $n \in \mathbf{Z}_{\text{odd}}$ .*

When  $A$  is irrational, the set  $2\mathbf{Z}[A]$  is dense in  $\mathbf{R}$ . However, it is always a countable set.

### 2.3 Structure of the Square Map

As we mentioned in §1.5, we have  $\psi(p) - p = V$ , where  $V$  is twice a vector that points from one vertex of  $K(A)$  to another. See Figure 1.2. There are 12 possibilities for  $V$ , namely

$$\pm(0, 4); \quad \pm(2, 2); \quad \pm(-2, 2); \quad \pm(2, 2A); \quad \pm(-2, 2A); \quad \pm(2+2A, 0). \quad (16)$$

These vectors are drawn, for the parameter  $A = 1/3$ , in Figure 2.2. The grey lines are present to guide the reader's eye.

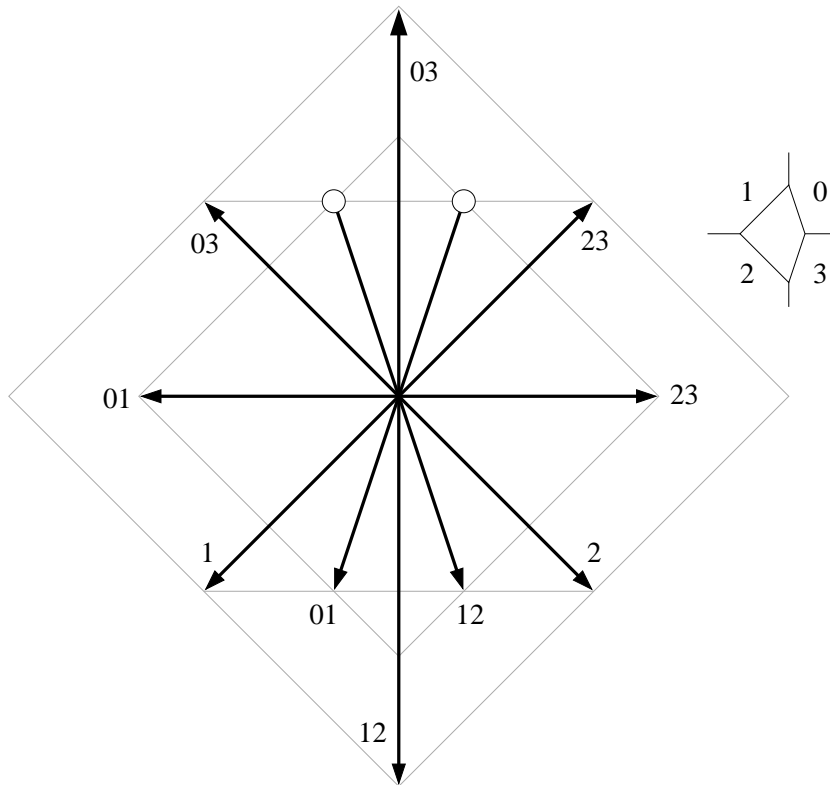


**Figure 2.2:** The 12 direction vectors

The labelling of the vectors works as follows. We divide the plane into its quadrants, according to the numbering scheme shown in Figure 2.2. A vector  $V$  gets the label  $k$  if there exists a parameter  $A$  and a point  $p \in Q_k$  such that  $\psi(v) - v = V$ . Here  $Q_k$  is the  $k$ th quadrant. For instance,  $(0, -4)$  gets the labels 1 and 2. The two vectors with dots never occur. In §7.5 we will give a much more precise version of Figure 2.2. For now, Figure 2.2 is sufficient for our purposes.

## 2.4 The Return Lemma

As in the introduction let  $\Xi = \mathbf{R}_+ \times \{-1, 1\}$ .

**Lemma 2.3 (Return)** *Let  $p \in \mathbf{R} \times \mathbf{Z}_{\text{odd}}$  be a point with a well-defined outer billiards orbit. Then there is some  $a > 0$  such that  $\psi^a(p) \in \Xi$ . Likewise, there is some  $b < 0$  such that  $\psi^b(p) \in \Xi$ .*

Consider the sequence  $\{\psi^k(p)\}$  for  $k = 1, 2, 3, \dots$ . We order the quadrants of  $\mathbf{R}^2 - \{0\}$  cyclically. Let  $Q_0$  be the  $(++)$  quadrant. We include the positive  $x$ -axis in  $Q$ . Let  $Q_{n+1}$  be the quadrant obtained by rotating  $Q_n$  clockwise by  $\pi/2$ . We take indices mod 4.

**Lemma 2.4** *The sequence  $\{\psi^k(p)\}$  cannot remain in a single quadrant.*

**Proof:** We prove this for  $Q_0$ . The other cases are similar. Let  $q = \psi^k(p)$  and  $r = \psi(q)$ . We write  $q = (q_1, q_2)$  and  $r = (r_1, r_2)$ . Looking at Figure 2.2, we see that either

1.  $r_2 \geq q_2 + 2$  and  $r_1 \leq q_1$ .
2.  $r_1 \leq q_1 - 2A$ .

Moreover, Option 1 cannot happen if the angle between  $\vec{0r}$  and the  $x$ -axis is sufficiently close to  $\pi/2$ . Hence, as we iterate, Option 2 occurs every so often until the first coordinate is negative and our sequence leaves  $Q_0$ . ♠

Call  $p \in \mathbf{R}^2 - K$  a *bad point* if  $p \in Q_k$  and  $\psi(p) \notin Q_k \cup Q_{k+1}$ .

**Lemma 2.5** *If  $q$  is bad, then either  $q$  or  $\psi(q)$  lies in  $\Xi$ .*

**Proof:** Let  $r = \psi(q)$ . If  $q$  is bad then  $q_2$  and  $r_2$  have opposite signs. If  $q_2 - r_2 = \pm 2$  then  $q_2 = \pm 1$  and  $r_2 = \pm 1$ . A short case-by-case analysis shows that this forces  $q_1$  and  $r_1$  to have opposite signs. The other possibility is that  $q_2 - r_2 = 4$ . But then  $r - q = \pm(0, 4)$ . A routine case-by-case analysis shows that  $r - q = (0, 4)$  only if  $q_1 > 0$  and  $r - q = (0, -4)$  only if  $q_1 < 0$ . But  $q$  is not bad in these cases. ♠

If the Return Lemma is false, then our sequence is entirely good. But then we must have some  $k$  such that  $\psi^k(p) \in Q_3$  and  $\psi^{k+1}(p) \in Q_0$ . Since the second coordinates differ by at most 4, we must have either  $\psi^k(p) \in \Xi$  or  $\psi^{k+1}(p) \in \Xi$ . This proves the first statement. The second statement follows from the first statement and symmetry.

## 2.5 The Return Map

The Return Lemma implies that the *first return map*  $\Psi : \Xi \rightarrow \Xi$  is well defined on any point with an outer billiards orbit. This includes the set

$$(\mathbf{R}_+ - 2\mathbf{Z}[A]) \times \{-1, 1\},$$

as we saw in Lemma 2.2.

Given the nature of the maps in Equation 15 comprising  $\psi$ , we see that

$$\Psi(p) - (p) \in 2\mathbf{Z}[A] \times \{-2, 0, 2\}.$$

In Part II, we will prove our main structural result about the first return map, namely the Master Picture Theorem. We will also prove the Pinwheel Lemma, in Part II. Combining these two results, we have a much stronger result about the nature of the first return map:

$$\Psi(p) - (p) = 2(A\epsilon_1 + \epsilon_2, \epsilon_3); \quad \epsilon_j \in \{-1, 0, 1\}; \quad \sum_{j=1}^3 \epsilon_j \equiv 0 \pmod{2}. \quad (17)$$

### Remarks:

(i) Some notion of the return map is also used in [K] and [GS]. This is quite a natural object to study.

(ii) We can at least roughly explain the first statement of Equation 17 in an elementary way. At least far from the origin, the square outer billiards orbit circulates around the kite in such a way as to nearly make an octagon with 4-fold symmetry. Compare Figure 11.3. The *return pair*  $(\epsilon_1(p), \epsilon_2(p))$  essentially measures the *approximation error* between the true orbit and the closed octagon.

(iii) On a nuts-and-bolts level, this monograph concerns how to determine  $(\epsilon_1(p), \epsilon_2(p))$  as a function of  $p \in \Xi$ . (The pair  $(\epsilon_1, \epsilon_2)$  and the parity condition determine  $\epsilon_3$ .) I like to tell people that this book is really about the infinite accumulation of small errors.

(iv) Reflection in the  $x$ -axis conjugates the map  $\psi$  to the map  $\psi^{-1}$ . Thus, once we understand the orbit of the point  $(x, 1)$  we automatically understand the orbit of the point  $(x, -1)$ . Put another way, the unordered pair of return points  $\{\Psi(p), \Psi^{-1}(p)\}$  for  $p = (x, \pm 1)$  only depends on  $x$ .

## 2.6 The Arithmetic Graph

Recall that  $\Xi = \mathbf{R}_+ \times \{-1, 1\}$ . Define  $M = M_{A,\alpha} : \mathbf{R} \times \{-1, 1\}$  by

$$M_{A,\alpha}(m, n) = (2Am + 2m + 2\alpha, (-1)^{m+n+1}) \quad (18)$$

The second coordinate of  $M$  is either 1 or  $-1$  depending on the parity of  $m+n$ . This definition is adapted to the parity condition in Equation 17. We call  $M$  a *fundamental map*. Each choice of  $\alpha$  gives a different map.

When  $A$  is irrational,  $M$  is injective. In the rational case,  $M$  is injective on any disk of radius  $q$ . Given  $p_1, p_2 \in \mathbf{Z}^2$ , we write  $p_1 \rightarrow p_2$  iff the following holds.

- $\zeta_j = M(p_j) \in \Xi$ .
- $\Psi(\zeta_1) = \zeta_2$ .
- $\|p_1 - p_2\| \leq \sqrt{2}$ .

The third condition is only relevant in the rational case. See Equation 17. Our construction gives a directed graph with vertices in  $\mathbf{Z}^2$ . We call this graph the *arithmetic graph* and denote it by  $\widehat{\Gamma}_\alpha(A)$ .

When  $A = p/q$ , any choice of  $\alpha \in (0, 2/q)$  gives the same result. This is a consequence of Lemma 2.1. To simplify our formulas, we choose  $\alpha = 0_+$ , where  $0_+$  is an infinitesimally small positive number. The reader who does not like infinitesimally small positive numbers can take

$$\alpha = \exp(-(\exp(q))).$$

When we write our formulas, we usually take  $\alpha = 0$ , but we always use the convention that the lattice point  $(m, n)$  tracks the orbits just to the right of the points  $(2Am + 2n, \pm 1)$ . With this convention, we have

$$\widehat{\Gamma}(p/q) = \widehat{\Gamma}_{0_+}(p/q); \quad M(m, n) = (2(p/q)m + 2n, (-1)^{m+n+1}) \quad (19)$$

We say that the *baseline* of  $\widehat{\Gamma}(A)$  is the line  $M^{-1}(0)$ . We think of the baseline essentially as the line  $L$  of slope  $-A$  through the origin. However, we really want to think of the baseline as lying infinitesimally beneath  $L$ , so that the entire arithmetic graph lies above the baseline.

we will prove the following result.

**Theorem 2.6 (Embedding)** *Any well-defined arithmetic graph is the disjoint union of embedded polygons and bi-infinite embedded polygonal curves.*

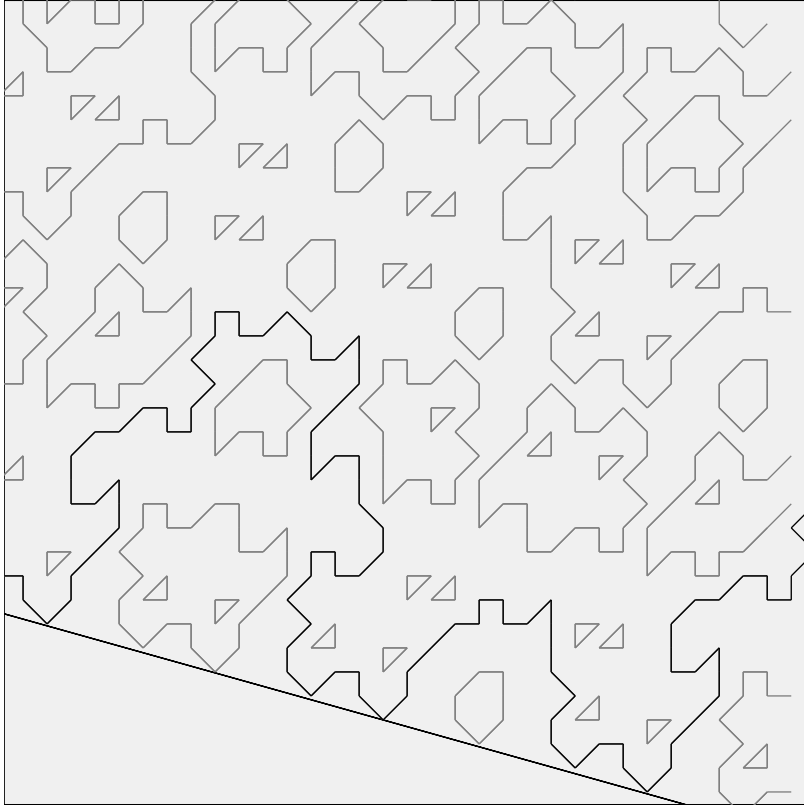


**Figure 2.3:** Some of  $\widehat{\Gamma}(7/25)$ , with  $\Gamma(7/25)$  in black

**Remark:** In the arithmetic graph, there are some lattice points having no edges emanating from them. These isolated points correspond to points where the return map is the identity and hence the orbit is periodic in the simplest possible way. We usually ignore these trivial components.

We are mainly interested in the component of  $\widehat{\Gamma}$  that contains  $(0, 0)$ . We denote this component by  $\Gamma$ . In the rational case,  $\Gamma(p/q)$  encodes the structure of the orbit  $O_2(1/q, -1)$ . The orbit  $O_2(1/q, 1)$ , the subject of Theorems 1.6 and 1.9, is conjugate to  $O_2(1/q, -1)$  *via* reflection in the  $x$ -axis. As we have said several times above,  $\Gamma(p/q)$  really tracks the orbit of the special interval bounded by  $(0, -1)$  and  $(2/q, -1)$ .

## 2.7 The Continuity Principle

Given two compact subsets  $K_1, K_2 \subset \mathbf{R}^2$ , we define  $d(K_1, K_2)$  to be the infimal  $\epsilon > 0$  such that  $K_1$  is contained in the  $\epsilon$ -tubular neighborhood of  $K_2$ , and *vice versa*. The function  $d(K_1, K_2)$  is known as the *Hausdorff metric*. A sequence  $\{C_n\}$  of closed subsets of  $\mathbf{R}^2$  is said to *Hausdorff converge* to  $C \subset \mathbf{R}^2$  if  $d(C_n \cap K, C \cap K) \rightarrow 0$  for every compact subset  $K \subset \mathbf{R}^2$ .

In the cases of interest to us,  $C_n$  will always be an arc of an arithmetic graph that contains  $(0, 0)$ . In this case, the Hausdorff convergence has a simple meaning.  $\{C_n\}$  converges to  $C$  if and only if the following property holds true. For any  $N$  there some  $N'$  such that  $n > N'$  implies that the first  $N$  steps of  $C_n$  away from  $(0, 0)$  in either direction agree with the corresponding steps of  $C$ .

Given a parameter  $A \in (0, 1)$  and a point  $\zeta \in \Xi$ , we say that a pair  $(A, \zeta)$  is *N-defined* if the first  $N$  iterates of the outer billiards map of  $\zeta$  are defined relative to  $A$ , in both directions. We let  $\Gamma(A, \zeta)$  be as much of the arithmetic graph as is defined. We call  $\Gamma(A, \zeta)$  a *partial arithmetic graph*.

**Lemma 2.7 (Continuity Principle)** *Let  $\{\zeta_n\} \in \Xi$  converge to  $\zeta \in \Xi$ . Let  $\{A_n\}$  converge to  $A$ . Suppose the orbit of  $\zeta$  is defined relative to  $A$ . Then for any  $N$  there is some  $N'$  such that  $n > N'$  implies that  $(\zeta_n, A_n)$  is  $N$ -defined. The corresponding sequence  $\{\Gamma(A_n, \zeta_n)\}$  of partially defined arithmetic graphs Hausdorff converges to  $\Gamma(A, \zeta)$ .*

**Proof:** Let  $\psi'_n$  be the outer billiards map relative to  $A_n$ . Let  $\psi'$  be the outer billiards map defined relative to  $A$ . If  $p_n \rightarrow p$  and  $\psi'$  is defined at  $p$  then  $\psi'_n$  is defined at  $p_n$  for  $n$  sufficiently large and  $\psi'_n(p_n) \rightarrow \psi(p)$ . This follows from the fact that  $K(A_n) \rightarrow K(A)$  and from the fact that a piecewise isometric map is defined and continuous in open sets. Our continuity principle now follows from induction. ♠

In case the orbit of  $\zeta_n$  relative to  $A_n$  is already well defined, the partial arithmetic graph is the same as one component of the ordinary arithmetic graph. In this case, we can state the Continuity Principle more simply.

**Corollary 2.8** *Let  $\{\zeta_n\} \in \Xi$  converge to  $\zeta \in \Xi$ . Let  $\{A_n\}$  converge to  $A$ . Suppose the orbit of  $\zeta$  is defined relative to  $A$  and the orbit of  $\zeta_n$  is defined relative to  $A_n$  for all  $n$ . Then  $\{\Gamma(A_n, \zeta_n)\}$  Hausdorff converges to  $\Gamma(A, \zeta)$ .*

We will have occasion to use both versions in our arguments.

## 2.8 Low Vertices and Parity

Let  $A$  be any kite parameter. We define the *parity* of a low vertex  $(m, n)$  to be the parity of  $m + n$ . Here we explain the structure of the arithmetic graph at low vertices. Our answer will be given in terms of a kind of phase portrait. Given a point  $(x, A) \in (0, 2) \times (0, 1)$ , we have

$$\Psi^{\pm 1}(x, -1) = (x, -1) + 2(\epsilon_1^{\pm} A + \epsilon_2^{\pm}, \epsilon_3^{\pm}). \quad (20)$$

For the point  $(x, t)$  we associate the directed graph

$$(\epsilon_1^-, \epsilon_2^-) \rightarrow (0, 0) \rightarrow (\epsilon_1^+, \epsilon_2^+).$$

This gives a local picture of the arithmetic at the low vertex  $(m, n)$  such that  $M_A(m, n) = (x, -1)$ . If  $M_A(m, n) = (x, 1)$  then we get the local picture by reversing the edges. Figure 2.2 shows the final result. The grey edges in the picture, present for reference, connect  $(0, 0)$  to  $(0, -1)$ . The grey triangle represents the places where the return map is the identity.

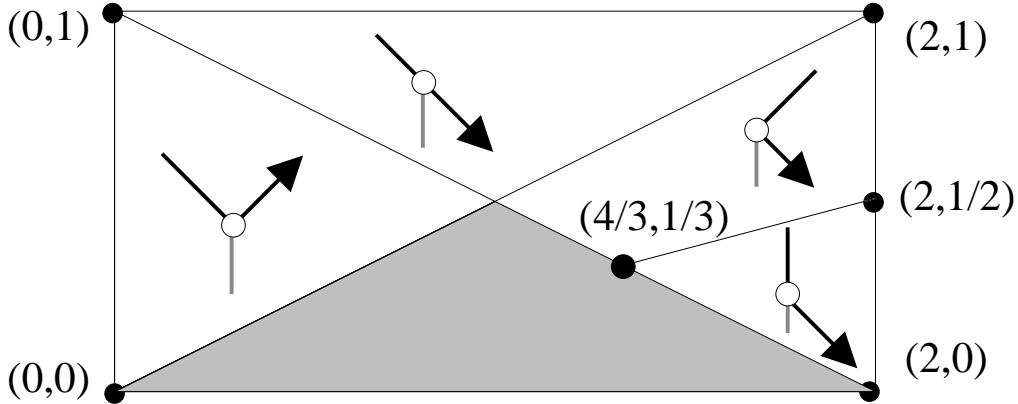


**Figure 2.4:** Low vertex phase portrait

**Example:** Relative to  $A = 1/3$ , the vertex  $-7, 3$  is a low vertex. We compute that

$$M_{1/3}(A) = (4/3 + \alpha, -1).$$

Here  $\alpha$  is an infinitesimally small positive number. To see the local picture of the arithmetic graph  $\Gamma(1/3)$  at  $(-7, 3)$  we observe that the point  $p = (4/3 + \alpha, 1/3)$  lies infinitesimally to the right of the point  $(4/3, 1/3)$ . Hence  $(\epsilon_1^-, \epsilon_2^-) = (0, 1)$  and  $(\epsilon_1^+, \epsilon_2^+) = (1, -1)$ .



To finish our proof, we just have to show that a component of  $\widehat{\Gamma}$  right-travels at a low vertex  $v$  if and only if  $v$  has even parity. We will show that a component of  $\widehat{\Gamma}$  always right-travels at low vertices of even parity. Let us explain why this suffices. Recall that the fundamental map  $M$  maps vertices of even parity to  $\mathbf{R}_+ \times \{-1\}$  and vertices of odd parity to  $\mathbf{R} \times \{1\}$ . Also, recall that reflection in the  $x$ -axis conjugates the return map  $\Psi$  to  $\Psi^{-1}$ . It follows from this symmetry that  $\widehat{\Gamma}$  left-travels at all low vertices of odd parity if and only if  $\widehat{\Gamma}$  right-travels at all vertices of even parity. But a glance at Figure 2.4 shows that  $\widehat{\Gamma}$  right travels at all vertices of even parity. The grey line segment always lies on the right. ♠

**Corollary 2.10** *Let  $A$  be any rational parameter. Let  $\xi_{\pm}$  be any point in  $(0, 2) \times \{\pm 1\}$  with a well defined orbit relative to  $A$ . Then the two orbits  $O_2(\xi_+)$  and  $O_2(\xi_-)$  are disjoint.*

**Proof:** Our orbits are either disjoint or identical. By perturbing  $\xi_{\pm}$  slightly we arrange that  $\xi_{\pm} = M(m_{\pm}, n_{\pm})$ . Here  $(m_+, n_+)$  has odd parity and  $(m_-, n_-)$  has even parity. If we have  $O_2(\xi_+) = O_2(\xi_-)$  then one and the same component of  $\widehat{\Gamma}(A)$  contains both  $(m_+, n_+)$  and  $(m_-, n_-)$ . But this contradicts our previous result. ♠

### 3 The Hexagrid Theorem

#### 3.1 The Arithmetic Kite

In this section we describe a certain quadrilateral, which we call the *arithmetic kite*. This object is meant to “live” in the same plane as the arithmetic graph. The diagonals and sides of this quadrilateral define 6 special directions. In the next section we describe a grid made from 6 infinite families of parallel lines, based on these 6 directions.

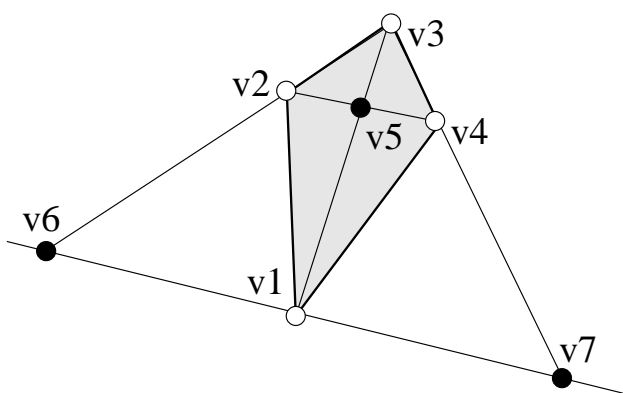


**Figure 3.1:** The arithmetic kite

Let  $A = p/q$ . Figure 3.1 shows a schematic picture of  $\mathcal{K}(A)$ . The vertices are given by the equations.

1.  $v_1 = (0, 0)$ .
2.  $v_2 = \frac{1}{2}(0, p + q)$ .
3.  $v_3 = \frac{1}{2q}(2pq, (p + q)^2 - 2p^2)$ .
4.  $v_4 = \frac{1}{2(p+q)}(4pq, (p + q)^2 - 4p^2)$ .
5.  $v_5 = \frac{1}{2(p+q)}(2pq, (p + q)^2 - 2p^2)$ .
6.  $-v_6 = v_7 = (q, -p)$ .

A short calculation, which we omit, shows that  $K(A)$  and  $\mathcal{K}(A)$  are actually affinely equivalent.  $\mathcal{K}(A)$  does not have Euclidean bilateral symmetry,

but it does have affine bilateral symmetry. We especially single out the vectors  $V = v_7$  and  $W = v_5$ . That is,

$$V = (q, -p); \quad W = \left( \frac{pq}{p+q}, \frac{pq}{p+q} + \frac{q-p}{2} \right). \quad (21)$$

The *hexagrid*  $G(A)$  consists of two interacting grids, which we call the *room grid*  $RG(A)$  and the *door grid*  $DG(A)$ .

**Room Grid:** When  $A$  is an odd rational,  $RG(A)$  consists of the lines obtained by extending the diagonals of  $\mathcal{K}(A)$  and then taking the orbit under the lattice  $\mathbf{Z}[V/2, W]$ . These are the black lines in Figure 3.2. In case  $A$  is an even rational, we would make the same definition, but use the lattice  $\mathbf{Z}[V, 2W]$  instead.

**Door Grid:** The *door grid*  $DG(A)$  is the same for both even and odd rationals. It is obtained by extending the sides of  $\mathcal{K}(A)$  and then taking their orbit under the one dimensional lattice  $\mathbf{Z}[V]$ . These are the grey lines in Figure 3.2.

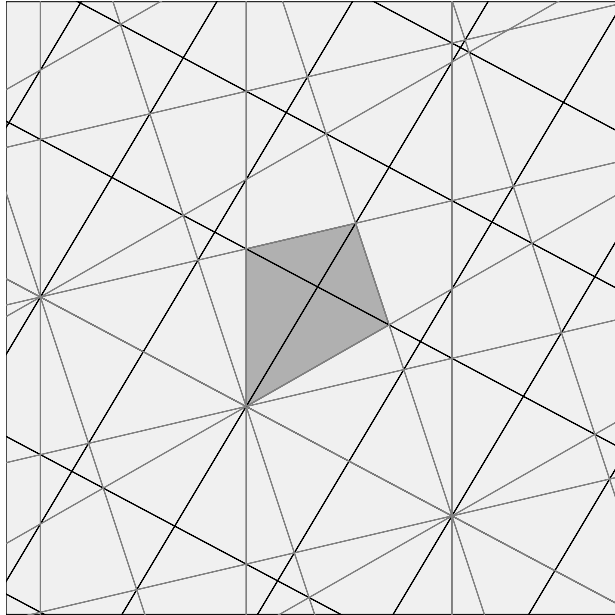


**Figure 3.2:**  $G(25/47)$ . and  $\mathcal{K}(25/47)$ .

## 3.2 The Hexagrid Theorem

The Hexagrid Theorem relates two kinds of objects, *wall crossings* and *doors*. Informally, the Hexagrid Theorem says that the arithmetic graph only crosses a wall at a door. Here are formal definitions.

**Rooms and Walls:**  $RG(A)$  divides  $\mathbf{R}^2$  into different connected components which we call *rooms*. Say that a *wall* is the line segment of positive slope that divides two adjacent rooms.

**Doors:** When  $p/q$  is odd, we say that a *door* is a point of intersection between a wall of  $RG(A)$  and a line of  $DG(A)$ . When  $p/q$  is even, we make the same definition, except that we exclude crossing points of the form  $(x, y)$ , where  $y$  is a half-integer. Every door is a triple point, and every wall has one door. The first coordinate of a door is always an integer. (See Lemma 14.2.) In exceptional cases – when the second coordinate is also an integer – the door lies in the corner of the room. In this case, we associate the door to both walls containing it. The door  $(0, 0)$  has this property.

**Crossing Cells:** Say that an edge  $e$  of  $\hat{\Gamma}$  *crosses a wall* if  $e$  intersects a wall at an interior point. Say that a union of two incident edges of  $\Gamma$  *crosses a wall* if the common vertex lies on a wall, and the two edges point to opposite sides of the wall. The point  $(0, 0)$  has this property. We say that a *crossing cell* is either an edge or a union of two edges that crosses a wall in the manner just described. For instance  $(-1, 1) \rightarrow (0, 0) \rightarrow (1, 1)$  is a crossing cell for any  $A \in (0, 1)$ .

In Part III of the monograph we will prove the following result. Let  $\underline{y}$  denote the greatest integer less than  $y$ .

**Theorem 3.1 (Hexagrid)** *Let  $A \in (0, 1)$  be rational.*

1.  $\hat{\Gamma}(A)$  never crosses a floor of  $RG(A)$ . Any edges of  $\hat{\Gamma}(A)$  incident to a vertex contained on a floor rise above that floor (rather than below it.)
2. There is a bijection between the set of doors and the set of crossing cells. If  $y$  is not an integer, then the crossing cell corresponding to the door  $(m, y)$  contains  $(m, \underline{y}) \in \mathbf{Z}^2$ . If  $y$  is an integer, then  $(x, y)$  corresponds to 2 doors. One of the corresponding crossing cells contains  $(x, y)$  and the other one contains  $(x, y - 1)$ .

**Remark:** We really only care about the odd case of the hexagrid theorem. We include the even case for the sake of completeness.

Figure 3.3 illustrates the Hexagrid Theorem for  $p/q = 25/47$ . We will explain the shaded parallelogram  $R(25/47)$  in the next section. We have only drawn the unstable components in Figure 3.3. The reader can see much better pictures of the Hexagrid Theorem using either Billiard King or our interactive guide to the monograph. (The interactive guide only shows the odd case, but Billiard King also shows the even case.)

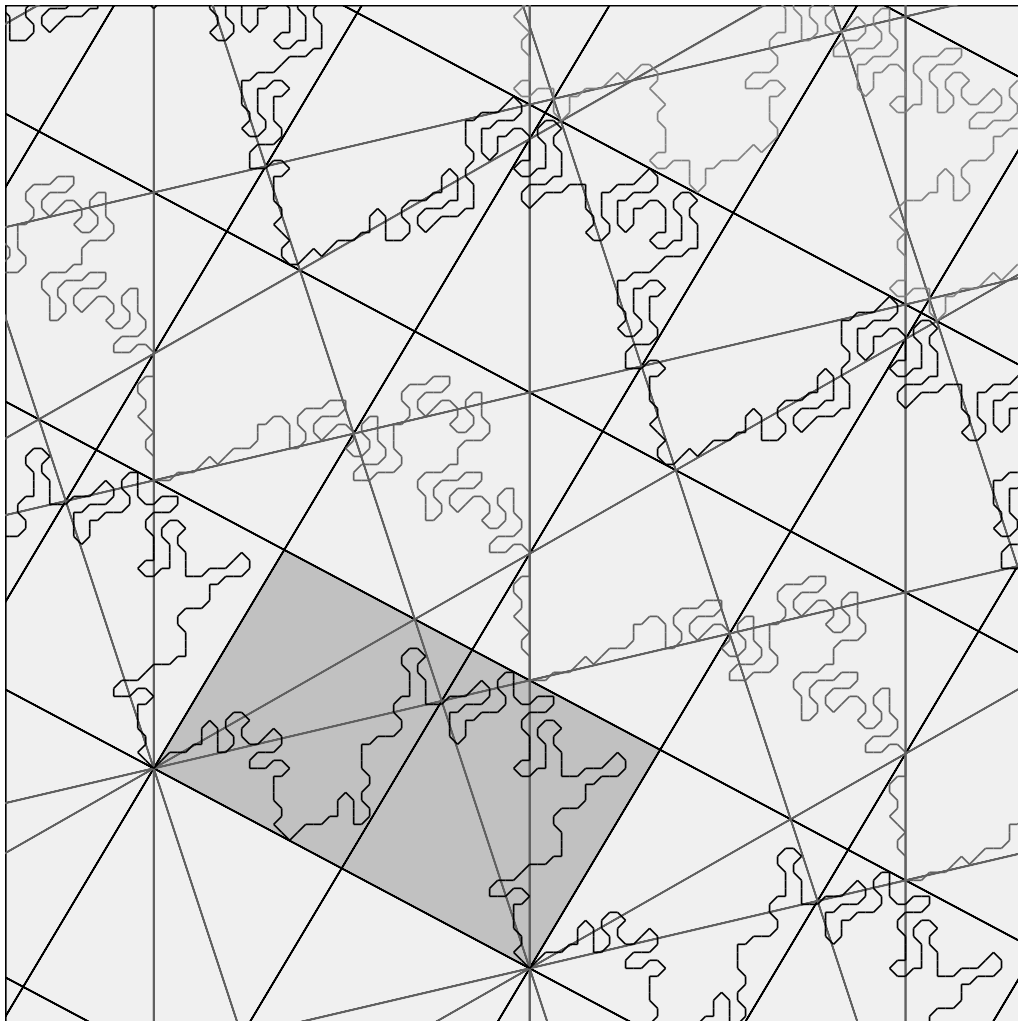


**Figure 3.3:**  $G(25/47)$ ,  $R(25/47)$ , and some of  $\hat{\Gamma}(25/47)$ .

### 3.3 The Room Lemma

Let  $R(p/q)$  denote the parallelogram whose vertices are

$$(0, 0); \quad V; \quad W; \quad V + W. \quad (22)$$

Here  $V$  and  $W$  are as in Equation 21. See Figure 3.3. We also define

$$d_0 = (x, \underline{y}); \quad x = \frac{p+q}{2}; \quad y = \frac{q^2 - p^2}{4q} \quad (23)$$

$d_0$  lies within 1 vertical unit of the centerline of  $R(p/q)$ , above the center.  $d_0$  is just below the door contained inside the shaded parallelogram in Figure 3.3. Figure 3.1 is an enlargement of this parallelogram.

**Lemma 3.2 (Room)**  $\Gamma(p/q)$  is an open polygonal curve. One period of  $\Gamma(p/q)$  connects  $(0, 0)$  to  $d_0$  to  $(q, -p)$ . This period is contained in  $R(p/q)$ .

**Proof:** First of all, for any value of  $A$ , it is easy to check that  $\Gamma(A)$  contains the arc  $(-1, 1) \rightarrow (0, 0) \rightarrow (1, 1)$ . This is to say that  $\Gamma(p/q)$  enters  $R(p/q)$  from the left at  $(0, 0)$ . Now,  $R(p/q)$  is the union of two adjacent rooms,  $R_1$  and  $R_2$ . Note that  $(0, 0)$  is the only door on the left wall of  $R_1$  and  $(x, y)$  is the only door on the wall separating  $R_1$  and  $R_2$ , and  $(q, -p)$  is the only door on the right wall of  $R_2$ . Here  $(x, y)$  is as in Equation 23. From the Hexagrid Theorem and the Embedding Theorem,  $\Gamma(p/q)$  must connect  $(0, 0)$  to  $d_0$  to  $(q, -p)$ . The arithmetic graph  $\widehat{\Gamma}(p/q)$  is invariant under translation by  $(q, -p)$ , and so the whole picture repeats endlessly to the left and the right of  $R(p/q)$ . Hence  $\Gamma(p/q)$  is an open polygonal curve. ♠

We remark that we did not really need the Embedding Theorem in our proof above. All we require is that  $\Gamma(p/q)$  cannot backtrack as we travel from one corner of  $R(p/q)$  to the other. Lemma 3.3 below gives a self-contained proof of what we need.

**Lemma 3.3**  $\Gamma(p/q)$  has valence 2 at every vertex.

**Proof:** As in our proof of the Room Lemma,  $\Gamma(p/q)$  has valence 2 at  $(0, 0)$ . But  $\Gamma(p/q)$  describes the forward orbit of  $p = (1/q, 1)$  under  $\Psi$ . If some vertex of  $\Gamma(p/q)$  has valence 1 then  $\Psi$  has order 2 when evaluated at the corresponding point. But then  $\Psi$  has order 2 when evaluated at  $v$ . But then  $\Gamma(p/q)$  has valence 1 at  $(0, 0)$ . This is a contradiction. ♠

### 3.4 Proof of Theorems 1.6 and 1.7

The bounds in Theorem 1.7 imply the upper bound in Theorem 1.6. First we establish the lower bound in Theorem 1.6. Suppose that  $p/q$  is an odd rational. Let  $M_1$  be the first coordinate for the fundamental map associated to  $p/q$ . We compute that  $M_1(d_0) > (p+q)/2$ , at least when  $p > 1$ . Technically,  $\Gamma(p/q)$  describes  $O_2(1/q, -1)$ , but the two orbits  $O_2(1/q, 1)$  and  $O_2(1/q, -1)$  are conjugate by reflection in the  $x$ -axis.

Now suppose that  $p/q$  is even. Referring to the plane containing the arithmetic graph, let  $S_0$  be the line segment connecting the origin to  $v_3$ , the very tip of the arithmetic kite. Then  $S_0$  is bounded by two consecutive doors on  $L_0$ . The bottom endpoint of  $S_0$  is  $(0, 0)$ , one of the vertices of  $\Gamma(0, 0)$ . We know already that  $\Gamma(p/q)$  is a closed polygon. By the hexagrid Theorem,  $\Gamma(p/q)$ , cannot cross  $S_0$  except within 1 unit of the door  $v_3$ . Hence,  $\Gamma(p/q)$  must engulf all but the top 1 unit of  $S_0$ .

Essentially the same calculation as in the odd case now shows that  $\Gamma(p/q)$  rises up at least  $(p+q)$  units from the baseline when  $p > 1$ . When  $p = 1$  the same result holds, but the calculation is a bit harder. The reason why we get an extra factor of 2 in the even case is that  $v_3$  is twice as far from the baseline as is the door near  $d_0$ . See Equation 23.

First suppose that  $p/q$  is odd. Let  $M_1$  be the first coordinate of the fundamental map associated to  $p/q$ . Since  $p$  and  $q$  are relatively prime, we can realize any integer as an integer combination of  $p$  and  $q$ . From this we see that every point of the form  $s/q$ , with  $s$  odd, lies in the image of  $M_1$ . Hence, some point of  $\mathbf{Z}^2$ , above the baseline of  $\hat{\Gamma}(p/q)$ , corresponds to the orbit of either  $(s/q, 1)$  or  $(s/q, -1)$ .

Let the *floor grid* denote the lines of negative slope in the room grid. These lines all have slope  $-p/q$ . The  $k$ th line  $L_k$  of the floor grid contains the point

$$\zeta_k = \left(0, \frac{k(p+q)}{2}\right).$$

Modulo translation by  $V$ , the point  $\zeta_k$  is the only lattice point on  $L_k$ . Statement 1 of the Hexagrid Theorem contains that statement that the edges of  $\Gamma$  incident to  $\zeta_k$  lie between  $L_k$  and  $L_{k+1}$  (rather than between  $L_{k-1}$  and  $L_k$ ).

We compute that

$$M_1(\zeta_k) = k(p+q) + \frac{1}{q}.$$

For all lattice points  $(m, n)$  between  $L_k$  and  $L_{k+1}$  we therefore have

$$M_1(m, n) \in I_k, \quad (24)$$

the interval from Theorem 1.7. Theorem 1.7 now follows from Equation 24, Statement 1 of the Hexagrid Theorem, and our remarks about  $\zeta_k$ .

The proof of Theorem 1.7 in the even case is exactly the same, except that we get a factor of 2 due to the different definition of the room grid.

**Remark:** We compare Theorem 1.7 to a result in [K]. The result in [K] is quite general, and so we will specialize it to kites. In this case, a kite is quasi-rational iff it is rational. The (special case of the) result in [K], interpreted in our language, says that every special orbit is contained in one of the intervals  $J_0, J_1, J_2, \dots$ , where

$$J_a = \bigcup_{i=0}^{p+q-1} I_{ak+i}.$$

The endpoints of the  $J$  intervals correspond to *necklace orbits*. A necklace orbit (in our case) is an outer billiards orbit consisting of copies of the kite, touching vertex to vertex. Compare Figure 2.1.

### 3.5 Proof of Theorem 1.8

Let  $p/q$  be some rational and let  $\hat{\Gamma}$  be the corresponding arithmetic graph. Let  $O_2(m, n)$  denote the orbit corresponding to the component  $\hat{\Gamma}(m, n)$ .

**Lemma 3.4** *A periodic orbit  $O_2(m, n)$  is stable iff  $\hat{\Gamma}(m, n)$  is a polygon.*

**Proof:** Let  $K$  be the period of  $\Psi$  on  $p_0$ . Tracing out  $\hat{\Gamma}(m, n)$ , we get integers  $(m_k, n_k)$  such that

$$\Psi^k(p_0) - p_0 = (2m_k A + 2n_k, 2\epsilon_k); \quad k = 1, \dots, K. \quad (25)$$

Here  $\epsilon_k \in \{0, 1\}$ , and  $\epsilon_k = 0$  iff  $m_k + n_k$  is even. The integers  $(m_k, n_k)$  are determined by the combinatorics of a finite portion of the orbit. Hence, Equation 25 holds true for all nearby parameters  $A$ .

If  $\hat{\Gamma}(m, n)$  is a closed polygon, then  $(m_K, n_K) = 0$ . But then  $\Psi^k(p_0) = p_0$  for all parameters near  $A$ . If  $O_2(m, n)$  is stable then  $(m_K, n_K) = (0, 0)$ . Otherwise, the equation  $m_K A + n_K = 0$  would force  $A = -n_K/m_K$ . ♠

**Odd Case:** Assume that  $A = p/q$  is an odd rational. Say that a *suite* is the region between two floors of the room grid. Each suite is partitioned into rooms. Each room has two walls, and each wall has a door in it. From the Hexagrid Theorem, we see that there is an infinite polygonal arc of  $\widehat{\Gamma}(p/q)$  that lives in each suite. Let  $\Gamma_k(p/q)$  denote the infinite polygonal arc that lies in the  $k$ th suite. Here  $\Gamma_0(p/q) = \Gamma(p/q)$ .

We have just described the infinite family of unstable components listed in Theorem 1.8. All the other components of  $\widehat{\Gamma}(p/q)$  are closed polygons and must be confined to single rooms. The corresponding orbits are stable, by Lemma 3.4. The already-described polygonal arcs use up all the doors.

Each vertex  $(m, n)$  in the arithmetic graph corresponds to the two points  $(M_1(m, n), \pm 1)$ . Thus, each component of  $\widehat{\Gamma}$  tracks either 1 or 2 orbits. By the parity result in Equation 17, these two points lie on different  $\psi$ -orbits. Therefore, each component of  $\widehat{\Gamma}$  tracks two special orbits. In particular, there are exactly two unstable orbits  $U_k^+$  and  $U_k^-$  contained in the interval  $I_k$ , and these correspond to  $\Gamma_k(p/q)$ . This completes the proof in the odd case.

**Even Case:** Now let  $p/q$  be even. By Lemma 3.4, it suffices to show that all nontrivial components of  $\widehat{\Gamma}$  are polygons. Suppose  $\widehat{\Gamma}(m, n)$  is not a polygon. Let  $R$  denote reflection in the  $x$ -axis. We have

$$R\Psi R^{-1} = \Psi^{-1}; \quad R(M(m, n)) = M(m + q, n - p). \quad (26)$$

From this equation we see that translation by  $(q, -p)$  preserves  $\widehat{\Gamma}$  but reverses the orientation of all components. But then  $(m, n) + (q, -p) \notin \widehat{\Gamma}(m, n)$ .

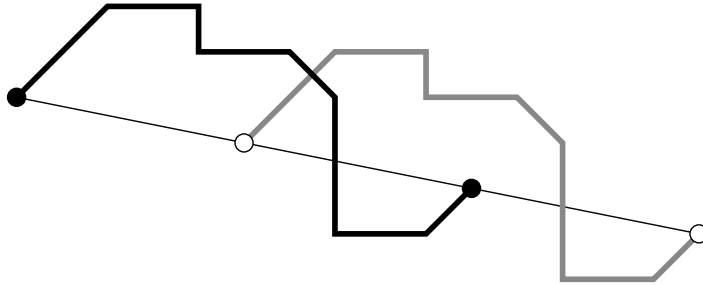


**Figure 3.4:**  $\gamma$  and  $\gamma + (q, -p)$ .

Since all orbits are periodic,  $(m, n) + k(p, -q) \in \widehat{\Gamma}(m, n)$  for some integer  $k \geq 2$ . Let  $\gamma$  be the arc of  $\widehat{\Gamma}(m, n)$  connecting  $(m, n)$  to  $(m, n) + k(q, -p)$ . By the Embedding Theorem,  $\gamma$  and  $\gamma' = \gamma + (q, -p)$  are disjoint. But this situation violates the Jordan Curve Theorem. See Figure 3.4.

## 4 Period Copying

### 4.1 Inferior and Superior Predecessors

Let  $p/q \in (0, 1)$  be any odd rational. There are unique rationals  $p_-/q_-$  and  $p_+/q_+$  such that

$$\frac{p_-}{q_-} < \frac{p}{q} < \frac{p_+}{q_+}; \quad \max(q_-, q_+) < q; \quad qp_{\pm} - pq_{\pm} = \pm 1. \quad (27)$$

See §18 for more details.

We define the odd rational

$$\frac{p'}{q'} = \frac{|p_+ - p_-|}{|q_+ - q_-|}, \quad (28)$$

$p'/q'$  is the unique odd rational satisfying the equation

$$q' < q; \quad |pq' - qp'| = 2. \quad (29)$$

We call  $p'/q'$  the *inferior predecessor* of  $p/q$ , and we write  $p'/q' \leftarrow p/q$  or  $p/q \rightarrow p'/q'$ . We can iterate this procedure. Any  $p/q$  belongs to a finite chain

$$\frac{1}{1} \leftarrow \frac{p_1}{q_1} \leftarrow \dots \leftarrow \frac{p_n}{q_n} = \frac{p}{q}. \quad (30)$$

Corresponding to this sequence we define

$$d_k = \text{floor}\left(\frac{q_{k+1}}{2q_k}\right). \quad (31)$$

We define the *superior predecessor* of  $p/q$  to be  $p_k/q_k$ , where  $k$  is the largest index such that  $d_k \geq 1$ . It might happen that the inferior and superior predecessors coincide, and it might not.

Here is an example, where the terms are highlighted in a suggestive way.

$$\frac{\mathbf{1}}{\mathbf{1}} \leftarrow \frac{1}{3} \leftarrow \frac{\mathbf{1}}{\mathbf{5}} \leftarrow \frac{3}{13} \leftarrow \frac{\mathbf{5}}{\mathbf{21}} \leftarrow \frac{13}{55} \leftarrow \frac{\mathbf{21}}{\mathbf{89}} \leftarrow \frac{55}{233} \leftarrow \frac{\mathbf{89}}{\mathbf{377}} \dots$$

$3/13$  has  $1/5$  both a superior and an inferior predecessor.  $5/21$  has  $3/13$  as an inferior predecessor and  $1/5$  as a superior predecessor. The implied limit of this sequence is  $\sqrt{5} - 2$ , the Penrose kite parameter.

## 4.2 Inferior and Superior Sequences

The inferior predecessor construction organizes all the odd rationals into a directed tree of infinite valence. The rational  $1/1$  is the terminal node of this tree. The nodes incident to  $1/1$  are  $1/3$ ,  $3/5$ ,  $5/7$ , etc. Figure 4.1 shows part of this tree. The edges are labelled with the  $d$  values from Equation 31.

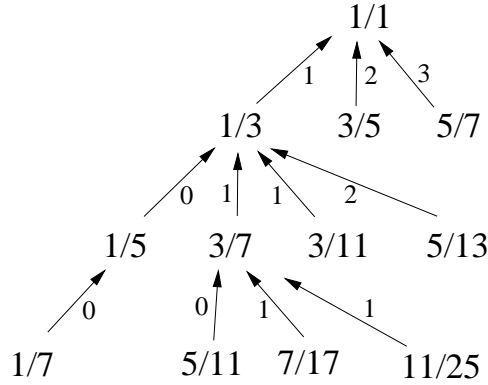


**Figure 4.1:** The odd tree.

The next result identifies certain of the ends of this tree with the irrationals in  $(0, 1)$ . In Part IV, we prove the following result.

**Lemma 4.1 (Superior Sequence)** *Let  $A \in (0, 1)$  be irrational. There is a unique sequence  $\{p_n/q_n\}$  of odd rationals such that*

$$\frac{p_0}{q_0} = \frac{1}{1}; \quad \frac{p_{n+1}}{q_{n+1}} \rightarrow \frac{p_n}{q_n} \quad \forall n; \quad A = \lim_{n \rightarrow \infty} \frac{p_n}{q_n}. \quad (32)$$

*There are infinitely many indices  $n$  such that  $2q_n < q_{n+1}$ .*

We call the sequence  $\{p_n/q_n\}$  the *inferior sequence*. We call  $n$  a *superior index* if  $2q_n < q_{n+1}$ . In terms of Equation 31, the index  $n$  is superior if and only if  $d_n \geq 1$ . We define the *superior sequence* to be the subsequence that is indexed by the superior indices. Though there are many inferior and superior sequences containing  $p_n/q_n$ , the initial parts of these sequences are determined by  $p_n/q_n$ . This comes from the directed tree structure we have already mentioned.

**Remark:** The converse result is also true. Any inferior sequence with infinitely many superior terms as an irrational limit. This is a consequence of Lemma 18.4.

### 4.3 Strong Sequences

Let  $A_1$  and  $A_2$  be two odd rationals. Let  $\Gamma_1$  and  $\Gamma_2$  be the corresponding arithmetic graphs. We fix

$$\epsilon = \frac{1}{8}. \quad (33)$$

This is an arbitrary but convenient choice.

Let  $V_1 = (q_1, -p_1)$ . Let  $\Gamma_1^1$  denote the period of  $\Gamma_1$  connecting  $(0, 0)$  to  $V_1$ . Let  $\Gamma_1^{-1}$  denote the period of  $\Gamma_1$  connecting  $(0, 0)$  to  $-V_1$ . We define

$$\Gamma_1^{1+\epsilon} = \Gamma_1^1 \cup \left( \Gamma_1 \cap B_{\epsilon q_1}(V_1) \right); \quad \Gamma_1^{-1-\epsilon} = \Gamma_1^{-1} \cup \left( \Gamma_1 \cap B_{\epsilon q_1}(-V_1) \right). \quad (34)$$

We are extending one period of  $\Gamma_1$  slightly beyond one of its endpoints. Call a monotone convergent sequence of odd rationals  $\{p_n/q_n\}$  *strong* if it has the following properties.

1.  $|A - A_n| < Cq_n^{-2}$  for some universal constant  $C$ .
2. If  $A_n < A_{n+1}$  then  $\Gamma_n^{1+\epsilon} \subset \Gamma_{n+1}^1$ .
3. If  $A_n > A_{n+1}$  then  $\Gamma_n^{-1-\epsilon} \subset \Gamma_{n+1}^{-1}$ .

In other words,  $\Gamma_{n+1}$  copies about  $1 + \epsilon$  periods of  $\Gamma_n$  for every  $n$ . As usual, we have set  $A_n = p_n/q_n$ .

In Part IV we will prove the following result.

**Lemma 4.2** *Any superior sequence has a strong subsequence. In particular, any irrational in  $(0, 1)$  is the limit of a strong subsequence.*

In the next chapter we will prove that any limit of a strong sequence satisfies the conclusions of the Erratic Orbits Theorem. Thus, Lemma 4.2 is one of the key ingredients in the proof of the Erratic Orbits Theorem. The proof of Lemma 4.2, however, is rather involved. We can prove a result nearly as strong as the Erratic Orbits Theorem based on a slightly weaker result that is much easier to prove. We now describe this alternate result.

Let  $\Delta_k \subset (0, 1)$  denote the set of irrationals  $A$  such that the equation

$$0 < \left| A - \frac{p}{q} \right| < \frac{1}{kq^2}; \quad p, q \in \mathbf{Z}_{\text{odd}} \quad (35)$$

holds infinitely often.

In Part IV we prove the following result.

**Lemma 4.3** *Let  $A_j = p_j/q_j$  be odd rationals such that  $|A_1 - A_2| < 1/(2q_1^2)$ .*

- *If  $A_1 < A_2$  then  $\Gamma_1^{1+\epsilon} \subset \Gamma_2^1$ .*
- *If  $A_1 > A_2$  then  $\Gamma_1^{-1-\epsilon} \subset \Gamma_2^{-1}$ .*

**Corollary 4.4** *Every  $A \in \Delta_2$  is the limit of a strong sequence.*

**Proof:** If  $A \in \Delta_2$ , then there exists a monotone sequence of solutions to Equation 35 for  $k = 2$ . This sequence is strong, by Lemma 4.3. ♠

Combining the last corollary with our work in the next chapter, we obtain the proof of the Erratic Orbits Theorem for all  $A \in \Delta_2$ . The reader who is satisfied with this result can skip most of Part IV. The proof of Lemma 4.3 is really much easier than the proof of Lemma 4.2. We close this discussion with some observations on the size of the sets  $\Delta_k$ .

**Lemma 4.5**  *$\Delta_k$  has full measure in  $(0, 1)$  for any  $k$ .*

**Proof:** Any block of 3 consecutive odd terms  $\geq k$  in the continued fraction expansion of  $A$  guarantees a solution to Equation 35. It follows from the ergodicity of the Gauss map (or the ergodicity of the geodesic flow on the modular surface) that almost every  $A$  has infinitely many such blocks. Hence  $\Delta_k$  has full measure in  $(0, 1)$ . ♠

As Curt McMullen pointed out to me, every irrational in  $(0, 1)$  belongs to  $\Delta_1$ . This result is similar in spirit to Lagrange's famous theorem that every irrational  $A$  satisfies

$$\left| A - \frac{p}{q} \right| < \frac{1}{\sqrt{5}q^2}$$

infinitely often. Lagrange's theorem doesn't imply that every irrational lies in  $\Delta_2$  because the conditions on  $\Delta_2$  involve a parity restriction.

For the interested reader, we sketch here McMullen's argument that  $\Delta_1 = (0, 1) - \mathcal{Q}$ . Consider the usual horodisk packing associated to the modular group. Remove all horodisks except those based at odd rationals. Dilate each disk (in the Euclidean sense) by a factor of 2 about its basepoint. Observe that the complement of these inflated disks, in the hyperbolic plane has infinitely many components. Interpret this result in terms of  $\Delta_1$ , using the usual connection between the modular horodisk packing and rational approximation.

## 4.4 The Decomposition Theorem

Given an odd rational  $A = p/q$ , we construct the even rationals  $A_{\pm} = p_{\pm}/q_{\pm}$ . We let  $A'$  be the inferior predecessor of  $A$  and we let  $A^*$  be the superior predecessor. For each rational, we use Equation 21 to construct the corresponding  $V$  and  $W$  vectors. For instance,  $V_+ = (q_+, -p_-)$  and  $V_* = (q_*, -p_*)$ . Now we define the following lines.

- $L_0^-$  is the line parallel to  $V$  and containing  $W$ .
- $L_1^-$  is the line parallel to  $V$  and containing  $W^*$ .
- $L$  is the line parallel to  $V$  through the  $(0, 0)$ .
- $L_0^+$  is the line parallel to  $W$  through  $(0, 0)$ .
- If  $q_+ > q_-$  then  $L_1^+$  is the line parallel to  $W$  through  $-V_-$ .
- If  $q_+ < q_-$  then  $L_1^+$  is the line parallel to  $W$  through  $+V_+$ .
- If  $q_+ > q_-$  then  $L_2^+$  is the line parallel to  $W$  through  $+V_+$ .
- If  $q_+ < q_-$  then  $L_2^+$  is the line parallel to  $W$  through  $-V_-$ .

Now we define the following parallelograms:

- $R_1$  is the parallelogram bounded by  $L$  and  $L_1^-$  and  $L_0^+$  and  $L_1^+$ .
- $R_2$  is the parallelogram bounded by  $L$  and  $L_0^-$  and  $L_0^+$  and  $L_2^+$ .

The parallelogram  $R_2$  is the bigger of the two parallelograms. It is both wider and taller. Note that translation by  $V$  carries the leftmost edge of  $R_1 \cup R_2$  to the rightmost edge.

These might look like complicated definitions, but they are exactly adapted to the structure of the arithmetic graph. In Part IV we establish the following result.

**Theorem 4.6 (Decomposition)**  $R_1 \cup R_2$  contains a period of  $\Gamma$ .

The Decomposition Theorem is an improvement on the containment result in the Room Lemma. It is our main tool for Lemma 4.2 and many of the results we prove in Part VI.



**Figure 4.2:**  $\Gamma(29/69)$  and  $R_1(29/69)$  and  $R_2(29/69)$ .

Figure 4.2 shows the example  $A = 29/69$ . In this case,

$$A_- = 21/50; \quad A_+ = 8/19; \quad A' = A^* = 13/31.$$

Since  $q_+ < q_-$ , the smaller  $R_1$  lies to the right of the origin. The ratio of heights of the two parallelograms is  $q^*/q = 31/69$ . The ratio of widths is  $q_+/q_- = 19/50$ .

Notice that the containment is extremely efficient. Notice also that each piece  $\Gamma \cap R_1$  and  $\Gamma \cap R_2$  has approximate bilateral symmetry. This situation always happens. We will explain this symmetry in §13.

## 5 Proofs of the Main Results

### 5.1 Proof of the Erratic Orbits Theorem

the Erratic Orbits Theorem follows from Lemma 4.2, Lemma 5.5 and Lemma 5.1 (stated below). For the reader who wants to take a shortcut, we remark again that we prove the Erratic Orbits Theorem for all  $A \in \Delta_2$ , when we use the much easier Lemma 4.3 in place of Lemma 4.2.

**Lemma 5.1** *Suppose that  $A$  is the limit of a strong sequence  $\{p_n/q_n\}$ . Then the Erratic Orbits Theorem holds for  $A$ .*

In our proof, we will consider the monotone increasing case. The other case is essentially the same. Note that our sequence remains strong if we pass to a subsequence. Passing to a subsequence, we arrange that

$$\epsilon q_{n+1} > 10q_n \quad (36)$$

Let  $V_n = (q_n, -p_n)$ . Define

$$\Gamma_n^2 = \Gamma_n^1 + V_{n+1}, \quad (37)$$

**Lemma 5.2**

$$\Gamma_n^1 \subset \Gamma_{n+1}^1; \quad \Gamma_n^2 \subset \Gamma_m^1 \quad \forall m \geq n+2. \quad (38)$$

**Proof:** We have

$$\Gamma_n^{1+\epsilon} \subset \Gamma_{n+1}^1$$

by definition, and

$$\Gamma_n^1 + V_{n+1} \subset \Gamma_{n+1}^1$$

because  $\Gamma_{n+1}^1$  is invariant under translation by  $V_{n+1}$ . Our choice of subsequence gives

$$\Gamma_n^{1+\epsilon} \subset B_{10q_n}(0,0) \subset B_{\epsilon q_{n+1}}(0,0) \cap \Gamma_{n+1}^1. \quad (39)$$

The first containment comes from the Room Lemma. Translating by  $V_{n+1}$ , we have

$$\Gamma_n^1 + V_{n+1} \subset B_{\epsilon q_{n+1}}(V_{n+1}) \cap \Gamma_{n+1}^1 \subset \Gamma_{n+1}^{1+\epsilon} \subset \Gamma_{n+2}^1. \quad (40)$$

Equation 38 follows immediately. ♠

It follows from Equation 38 and induction that

$$\omega_n = \omega(\sigma) := \sum_{k=1}^{n-1} \epsilon_k V_{2k+1} \quad (41)$$

is a vertex of  $\Gamma_{2n}^1$  for any binary sequence  $\epsilon_1, \dots, \epsilon_{n-1}$ . Let  $\Pi$  denote the set of not-eventually-constant sequences. Given any  $\sigma \in \Pi$ , we form the sequence of translated graphs

$$\Gamma'_n = \Gamma_{2n}^1 - \omega_n. \quad (42)$$

Here  $\omega_n$  is based on the first  $n - 1$  terms of  $\sigma$ , as in Equation 41.

**Lemma 5.3**  $\{\Gamma'_n\}$  Hausdorff converges to  $\Gamma$ , an open polygonal arc that rises unboundedly far, in both directions from the line  $L$  of slope  $(-A)$  through the origin.

**Proof:** Figure 5.1 shows the sort of binary structure that we have established. In this figure, the notation  $ij$  stands for  $\Gamma_i^j$ .

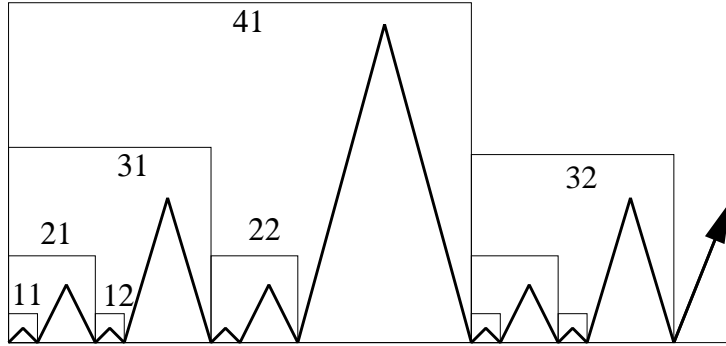


**Figure 5.1:** large scale Cantor set structure

Figure 5.2 shows a simpler picture that retains the structure of interest to us.

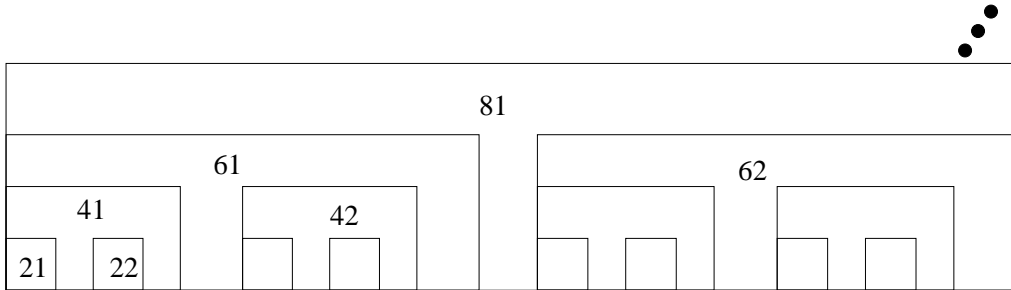


**Figure 5.2:** large scale Cantor set structure

To make sense of Figures 5.1 and 5.2, we say that the *box* containing  $\Gamma_n^1$  is  $R_n = R(A_n)$ , the box from the Room Lemma. For instance, the 8 smallest boxes in Figure 5.2 are

$$R_2 + \epsilon_1 V_3 + \epsilon_2 V_5 + \epsilon_3 V_7; \quad \epsilon_j \in \{0, 1\}. \quad (43)$$

The larger boxes have a similar description. The boxes are not quite nested, on account of the tiny mismatches between the slopes of their boundaries, but they are very nearly nested. See Property 4 below. We rank each box according to the label of its leftmost translate. The smallest boxes have rank 2. The next-smallest have rank 4. And so on. The following structure emerges.

1. If two boxes have the same rank, then the corresponding arcs are translates of each other.
2. The boxes of rank  $n$  have diameter  $O(q_n)$ .
3. The arc inside a box of rank  $n$ , a translate of  $\Gamma_{2n}^1$ , contains the bottom corners of the box containing it and rises up  $O(q_n)$  units towards the top of this box. This is a consequence of the Room Lemma.
4. The bottom edge of a box of rank  $n$  lies within  $O(1/q_n)$  of the bottom edge of the box of rank  $n + 1$  that nearly contains it. First we prove this for  $R_n$  and  $R_{n+1}$ . The bottoms of these boxes meet at the origin. The difference in slopes of  $O(1/q_n^2)$ . The length of the bottom edge of  $R(A_n)$  is  $O(q_n)$ . The estimate follows immediately. Once we note that  $V_{n+1}$  is  $O(1/q_{n+1})$  units away from the bottom of  $R_{n+1}$ , we get the same result for  $R_n + V_{n+1}$  and  $R_{n+1}$ . The general case now follows from translation.

By construction, the pattern of boxes surrounding  $\omega_n$  stabilizes when we view any fixed-radius neighborhood of  $\omega_n$ . More formally, for any  $R$ , there is some  $N$  such that  $m, n > N$  implies that  $\Gamma_{2m}^1 \cap B_R(\omega_m)$  is a translate of  $\Gamma_{2n}^1 \cap B_R(\omega_n)$ . Here we are crucially using the fact that  $\sigma \in \Pi$ , so that our common pattern of boxes grows both to the left and to the right of the points of interest. Hence, the sequence  $\{\Gamma'_n\}$  Hausdorff converges to a limit  $\Gamma$ .

From the 4 properties listed above,  $\Gamma$  is an infinite open polygonal arc that rises unboundedly far, in both directions, from  $L$ . ♠

It remains to recognize  $\Gamma$ . Let  $M$  be the map from Equation 19, relative to the limit parameter  $A$ . Given  $\sigma = \{\epsilon_k\} \in \Pi$ , the point

$$\alpha(\sigma) = \left( \sum_{k=1}^{\infty} 2\epsilon_k (Aq_{2k+1} - p_{2k+1}), -1 \right) \quad (44)$$

is well defined because the  $k$ th term in the series has size  $O(1/q_{2k+1})$ , and the sequence  $\{q_{2k+1}\}$  grows exponentially. The union of such limits, taken over all of  $\Pi$ , contains a pruned Cantor set. Throwing out a countable subset of  $\Pi$ , we can arrange that our pruned Cantor set is disjoint from  $2\mathbf{Z}[A]$ . But then, and  $\alpha = \alpha(\sigma)$  we consider has a well-defined orbit, by Lemma 2.2.

**Lemma 5.4**  $\Gamma$  is the arithmetic graph of  $\alpha$ .

**Proof:** Define

$$\alpha_n = M_{2n}(\sigma_n) = \left( \sum_{k=1}^{n-1} 2\epsilon_k (A_{2n}q_{2k+1} - p_{2k+1}), -1 \right) \quad (45)$$

An easy argument shows that  $\alpha_n \rightarrow \alpha$ . By construction,  $\Gamma'_n$  is one period of the arithmetic graph of  $\alpha_n$  relative to  $A_{2n}$ . The distance that  $\Gamma'_n$  extends from the origin, in either direction, tends to  $\infty$  with  $n$ . By the Continuity Principle,  $\{\Gamma'_n\}$  converges to the arithmetic graph of  $\alpha$ . ♠

Given the structure of  $\Gamma$ , we know that  $\alpha$  has an unbounded orbit. To finish our proof of Lemma 5.1, we just need to show that  $\alpha$  has an erratic orbit. Call an arc of  $\Gamma'_n$  *stable* if this same arc also belongs to  $\Gamma'_m$  for  $m > n$ . By construction, we get the following result. For any  $k$ , there is some  $n$  such that  $\Gamma'_n$  contains a stable arc of the form  $\beta - \omega_n$ . Here  $\beta$  is a full period of  $\Gamma_k$ , but contained in  $\Gamma_{2n}^1$ . Some vertex  $v$  of  $\beta$  has the form

$$\sum_{j=k}^{n-1} \epsilon_j V_{2j+1} \quad (46)$$

The distance from  $v$  to the baseline of  $\Gamma_{2n}$  is  $O(1/q_{2k+1})$ . But then, the distance from  $v - \omega_n$  to the baseline of  $\Gamma'_n$  is  $O(1/q_{2k+1})$ . But  $v - \omega_n$  is also a vertex of  $\Gamma$  (by stability) and its distance to the baseline of  $\Gamma$  is also  $O(1/q_{2k+1})$ . We can choose our arc  $\beta - \omega_n$  either to the left or to the right of the origin. Hence, both sides of the limit  $\Gamma$  come arbitrarily close to the baseline of  $\Gamma$ .

## 5.2 Proof of Theorem 1.2

The following result combines with the Erratic Orbits Theorem to prove Theorem 1.2: Every special orbit is either periodic or else unbounded in both directions. Note that the result does not quite require the existence of erratic orbits, but only the existence of orbits that come fairly close to the kite vertex.

**Lemma 5.5** *Suppose that  $A$  is a parameter, and  $p \in (0, 2) \times \{1\}$  has an orbit that is unbounded in both directions. Then all special orbits relative to  $A$  are either periodic or else unbounded in both directions.*

**Proof:** We write  $p = (2\zeta, 1)$ . By hypothesis,  $\zeta \in (0, 1)$ . Suppose that  $\beta$  has an aperiodic orbit that is forwards bounded. (The backwards case is similar.) For ease of exposition, we suppose that  $\beta \notin 2\mathbf{Z}[A]$ , so that all components of the arithmetic graph  $\widehat{\Gamma}$  associated to  $\beta$  are well defined. In case  $\beta \in 2\mathbf{Z}[A]$ , we simply apply our argument to a sequence  $\{\beta_n\}$  converging to  $\beta$  and invoke the Continuity Principle. Our robust geometric limit argument works the same way with only notational complications.

Let  $\Gamma$  be the component of  $\widehat{\Gamma}$  that tracks  $\beta$ . The forwards direction  $\Gamma_+$  remains within a bounded distance of the baseline  $L$  of  $\widehat{\Gamma}$  and yet is not periodic. Hence,  $\Gamma_+$  travels infinitely far either to the left or to the right. Since  $L$  has irrational slope, we can find a sequence of vertices  $\{v_n\}$  of  $\Gamma_+$  such that the vertical distance from  $v_n$  to  $L$  converges to  $\zeta + N$  for some integer  $N$ . Let  $w_n = v_n - (0, N)$ . Let  $\gamma_n$  be the component of  $\widehat{\Gamma}_n$  containing  $w_n$ . Note that  $M(w_n) \rightarrow p$ . Here  $M$  is as in Equation 19.

Let  $T_n$  be a translation so that  $T_n(w_n) = (0, 0)$ . By compactness, we can choose our sequence so that  $\{T_n(\Gamma_+)\}$  converges to an infinite polygonal arc  $X$  that remains within a bounded distance of any line parallel to  $L$ . By construction  $X$  travels infinitely far both to the left and to the right. At the same time,  $\{T_n(\gamma_n)\}$  converges to the arithmetic graph  $Y$  of  $\zeta$ . Here  $Y$  starts at  $(0, 0)$ , a point within 1 unit of the baseline  $L_\infty = \lim T_n(L)$  and rises unboundedly far from  $L_\infty$ . Hence  $Y$  starts out below  $X$  and rises above  $X$ , contradicting the Embedding Theorem. ♠

### 5.3 The Rigidity Lemma

Here we prove a technical convergence result that helps in the proofs of both Theorem 1.3 and Theorem 1.5.

**Lemma 5.6 (Rigidity)** *Let  $A_n$  be any sequence of parameters converging to the irrational parameter  $A$ . Let  $\zeta_n \in [0, 2] \times \{1\}$  be a sequence of points converging to  $(0, 1)$ . Let  $\Gamma(\zeta_n, A)$  be the arithmetic graph of  $\zeta_n$  relative to  $A$ . Then the sequence  $\{\Gamma(\zeta_n, A)\}$  Hausdorff converges.*

We think of our result as a rigidity result because it implies that all possible limits we can take in the above manner are the same.

Given  $\epsilon > 0$ , let  $\Sigma_\epsilon(A) \subset (0, 1)^2$  denote those pairs  $(s, A')$  where  $s \in (0, \epsilon)$  and  $|A' - A| < \epsilon$ . Let  $O(s; A')$  denote the outer billiards orbit of  $(s, 1)$  relative to  $K(A')$ .

**Lemma 5.7** *For any  $N$  there is some  $\epsilon > 0$  with the following property. The first  $N$  iterates of  $O(s; A')$ , forwards and backwards, are well defined provided that  $(s, A') \in \Sigma_\epsilon(A)$ .*

**Proof:** Inspecting the proof of Lemma 2.1, we draw the following conclusion. If  $O(s; A')$  is not defined after  $N$  iterates, then  $s = 2A'm + 2n$  for integers  $m, n \in (-N', N')$ . Here  $N'$  depends only on  $N$ . Rearranging this equation, we get

$$|A' - \frac{m}{n}| < \frac{s}{2m}.$$

For  $s$  sufficiently small and  $A'$  sufficiently close to  $A$ , this is impossible. ♠

**Corollary 5.8** *For any  $N$  there is some  $\epsilon > 0$  with the following property. The combinatorics of the first  $N$  forward iterates of  $O(s; A')$  is independent of the choice of point  $(s, A') \in \Sigma_\epsilon(A)$ . The same goes for the first  $N$  backwards iterates.*

**Proof:** If all orbits in some interval are defined, then all orbits in that interval have the same combinatorial structure. ♠

The Rigidity Lemma is now a consequence of Corollary 5.8 and the Return Lemma. The Return Lemma guarantees that as  $N \rightarrow \infty$ , the number of returns to  $\Xi$  tends to  $\infty$  as well.

## 5.4 Proof of Theorem 1.3

First of all, since outer billiards is a piecewise isometry, the set of periodic orbits is open in  $\mathbf{R} \times \mathbf{Z}_{\text{odd}}$ . We just need to prove density.

Let  $A$  be an irrational parameter. Let  $\widehat{\Gamma}$  be an arithmetic graph associated to  $A$ , such that  $\Gamma$  tracks an erratic orbit. Since  $A$  is irrational, we can find a sequence of vertices  $\{(m_k, n_k)\}$  of odd parity that converges to the baseline of  $A$ . Let  $\gamma_k$  be the component of  $\widehat{\Gamma}$  that contains  $(m_k, n_k)$ . Note that  $\gamma_k \neq \Gamma$  because  $\Gamma$  only contains vertices of even parity. By the Embedding Theorem,  $\gamma_k$  is trapped underneath  $\Gamma$ . Hence  $\gamma_k$  is a polygon. Let  $|\gamma_k|$  denote the maximal distance between a pair of low vertices on  $\gamma_k$ .

**Lemma 5.9**  $|\gamma_k| \rightarrow \infty$  as  $k \rightarrow \infty$ .

**Proof:** By the Rigidity Lemma, a very long arc of  $\gamma_k$ , with one endpoint  $(m_k, n_k)$ , agrees with the Hausdorff limit  $\lim_{n \rightarrow \infty} \Gamma(p_n/q_n)$ . Here  $\{p_n/q_n\}$  is an approximating strong sequence. But this limit has vertices within  $\epsilon$  of the baseline and at least  $1/\epsilon$  apart for any  $\epsilon > 0$ . Our result now follows from Hausdorff continuity. ♠

Let  $S_k$  denote the set of components  $\gamma'$  of  $\widehat{\Gamma}$  such that  $\gamma'$  is translation equivalent to  $\gamma_k$  and the corresponding vertices are low. The vertex  $(m, n)$  is low if the baseline of  $\widehat{\Gamma}$  separates  $(m, n)$  and  $(m, n - 1)$ .

**Lemma 5.10** *There is some constant  $N_k$  so that every point of  $L$  is within  $N_k$  units of a member of  $S_k$ .*

**Proof:** Say that a lattice point  $(m, n)$  is *very low* if it has depth less than  $1/100$  (but still positive.) The polygon  $\gamma_k$  corresponds to a periodic orbit  $\xi_k$ . Since  $\xi_k$  is periodic, there is an open neighborhood  $U_k$  of  $\xi_k$  such that all orbits in  $U_k$  are combinatorially identical to  $\xi_k$ . Let  $M$  be fundamental map associated to  $\widehat{\Gamma}$ . Then  $M^{-1}(U_k)$  is an open strip, parallel to  $L$ . Since  $L$  has irrational slope, there is some constant  $N_k$  so that every point of  $L$  is within  $N_k$  of some point of  $M^{-1}(U_k) \cap \mathbf{Z}^2$ . But the components of  $\widehat{\Gamma}$  containing these points are translation equivalent to  $\gamma_k$ . Choosing  $U_k$  small enough, we can guarantee that the translations taking  $\gamma_k$  to the other components carry the very low vertices of  $\gamma_k$  to low vertices. ♠

Given two polygonal components  $X$  and  $Y$  of  $\widehat{\Gamma}$ , we write  $X \bowtie Y$  if one low vertex of  $Y$  lies to the left of  $X$  and one low vertex of  $Y$  lies to the right of  $X$ . See Figure 5.3. In this case,  $X$  is trapped underneath  $Y$ , by the Embedding Theorem.

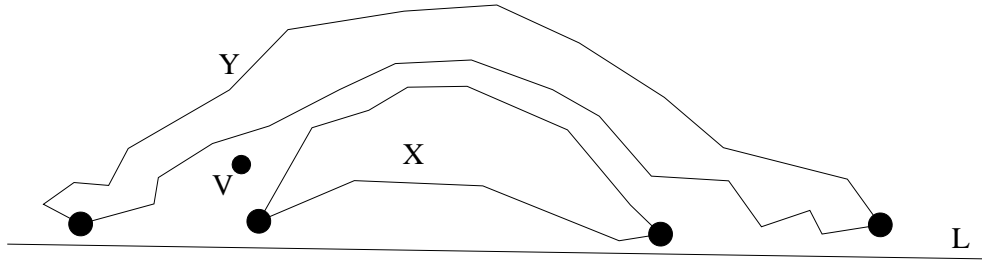


**Figure 5.3:** One polygon overlaying another.

Now we pass to a subsequence so that

$$|\gamma_{k+1}| > 10(N_k + |\gamma_k|). \quad (47)$$

Equation 47 has the following consequence. For any integer  $N$ , we can find components  $\gamma_j$  of  $S_j$ , for  $j = N, \dots, 2N$  such  $\gamma_N \bowtie \dots \bowtie \gamma_{2N}$ . Let  $L_N$  denote the portion of  $L$  between the two distinguished low points of  $\gamma_N$ . Let  $\Lambda_N$  denote the set of lattice points within  $N$  units of  $L_N$ . The set  $\Lambda_N$  is a parallelogram whose base is  $L_N$ , a segment whose length tends to  $\infty$  with  $N$ . The height of  $\Lambda_N$  tends to  $\infty$  as well.

**Lemma 5.11** *The set  $M(\mathbf{Z}^2 \cap \Lambda_N)$  consists entirely of periodic orbits.*

**Proof:** Let  $V$  be a vertical ray whose  $x$ -coordinate is an integer. If  $V$  starts out on  $L_n$  then  $V$  must travel upwards at least  $N$  units before escaping from underneath  $\gamma_{2N}$ . This is an application of the pidgeonhole principle. The point is that  $V$  must intersect each  $\gamma_j$  for  $j = N, \dots, 2N$ , in a different lattice point. Hence, any point of  $\Lambda_N$  is trapped beneath  $\gamma_{2N}$ . ♠

Given the fact that both base and height of  $\Lambda_N$  are growing unboundedly, and the fact that  $A$  is an irrational parameter, the union  $\bigcup_{N=1}^{\infty} M(\Lambda_N \cap \mathbf{Z}^2)$  is dense in  $\mathbf{R}_+$ . Hence, the set of periodic orbits starting in  $\mathbf{R}_+ \times \{-1, 1\}$  is dense in the set of all special orbits. Our proof of the Pinwheel Lemma in Part II shows that every special orbit eventually lands in  $\mathbf{R}_+ \times \{-1, 1\}$ . Hence, the set of periodic special orbits is dense in  $\mathbf{R} \times \mathbf{Z}_{\text{odd}}$ .

# Part II

In this part of the monograph we will state and prove the Master Picture Theorem. All the auxiliary theorems left over from Part I rely on this central result. Here is an overview of the material.

- In §6 we will state the Master Picture Theorem. Roughly, the Master Picture Theorem says that the structure of the return map  $\Psi$  is determined by a pair of maps into a flat 3-torus,  $\mathbf{R}^3/\Lambda$ , together with a partition of  $\mathbf{R}^3/\Lambda$  into polyhedra. Here  $\Lambda$  is a certain 3-dimensional lattice that depends on the parameter.
- In §7, we will prove the Pinwheel Lemma, a key technical step along the way to our proof of the Master Picture Theorem. The Pinwheel Lemma states that we can factor the return map  $\Psi$  into a composition of 8 simpler maps, which we call *strip maps*. A strip map is a very simple map from the plane into an infinite strip.
- In §8 we prove the Torus Lemma, another key result. The Torus Lemma implies that there exists some partition of our torus into open regions, such that the regions determine the structure of the arithmetic graph. The Torus Lemma reduces the Master Picture Theorem to a rough determination of the singular set. The singular set is the (closure of the) set of points in the torus corresponding to points where the return map is not defined.
- In §9 we verify, with the aid of symbolic manipulation, certain functional identities that arise in connection with the Torus Lemma. These function identities are the basis for our analysis of the singular set.
- In §10 we combine the Torus Lemma with the functional identities to prove the Master Picture Theorem.
- in §11 we will explain how one actually makes computations with the Master Picture Theorem. §11.2 will be very important for Part IV of the monograph.

## 6 The Master Picture Theorem

### 6.1 Coarse Formulation

Recall that  $\Xi = \mathbf{R}_+ \times \{-1, 1\}$ . We distinguish two special subsets of  $\Xi$ .

$$\Xi_+ = \bigcup_{k=0}^{\infty} (2k, 2k+2) \times \{(-1)^k\}; \quad \Xi_- = \bigcup_{k=1}^{\infty} (2k, 2k+2) \times \{(-1)^{k-1}\}. \quad (48)$$

Each set is an infinite disconnected union of open intervals of length 2. Reflection in the  $x$ -axis interchanges  $\Xi_+$  and  $\Xi_-$ . The union  $\Xi_+ \cup \Xi_-$  partitions  $(\mathbf{R}_+ - 2\mathbf{Z}) \times \{\pm 1\}$ .

Define

$$R_A = [0, 1 + A] \times [0, 1 + A] \times [0, 1] \quad (49)$$

$R_A$  is a fundamental domain for the action of a certain lattice  $\Lambda_A$ . We have

$$\Lambda_A = \begin{bmatrix} 1 + A & 1 - A & -1 \\ 0 & 1 + A & -1 \\ 0 & 0 & 1 \end{bmatrix} \mathbf{Z}^3 \quad (50)$$

We mean to say that  $\Lambda_A$  is the  $\mathbf{Z}$ -span of the column vectors of the above matrix.

We define  $\mu_+ : \Xi_+ \rightarrow R_A$  and  $\mu_- : \Xi_- \rightarrow R_A$  by the equations

$$\mu_{\pm}(t, *) = \left( \frac{t-1}{2}, \frac{t+1}{2}, \frac{t}{2} \right) \pm \left( \frac{1}{2}, \frac{1}{2}, 0 \right) \pmod{\Lambda}. \quad (51)$$

The maps only depend on the first coordinate. In each case, we mean to map  $t$  into  $\mathbf{R}^3$  and then use the action of  $\Lambda_A$  to move the image into  $R_A$ . It might happen that there is not a unique representative in  $R_A$ . (There is the problem with boundary points, as usual with fundamental domains.) However, if  $t \notin 2\mathbf{Z}[A]$ , this situation does not happen. The maps  $\mu_+$  and  $\mu_-$  are locally affine.

Here is a coarse formulation of the Master Picture Theorem. We will state the entire result in terms of  $(+)$ , with the understanding that the same statement holds with  $(-)$  replacing  $(+)$  everywhere. Let  $\Psi$  be the first return map.

**Theorem 6.1** *For each parameter  $A$  there is a partition  $(\mathcal{P}_A)_+$  of  $R_A$  into finitely many convex polyhedra. If  $\Psi$  is defined on  $\xi_1, \xi_2 \in \Xi_+$  and  $\mu_+(\xi_1)$  and  $\mu_+(\xi_2)$  lie in the same open polyhedron of  $(\mathcal{P}_A)_+$ , then  $\Psi(\xi_1) - \xi_1 = \Psi(\xi_2) - \xi_2$ .*

## 6.2 The Walls of the Partitions

In order to make Theorem 6.1 precise, we need to describe the nature of the partitions  $(\mathcal{P}_A)_\pm$ , and also the rule by which the polygon in the partition determines  $\Psi(\xi) - \xi$ . We will make several passes through the description, adding a bit more detail each time.

The polyhedra of  $(\mathcal{P}_A)_\pm$  are cut out by the following 4 families of planes.

- $\{x = t\}$  for  $t = 0, A, 1, 1 + A$ .
- $\{y = t\}$  for  $t = 0, A, 1, 1 + A$ .
- $\{z = t\}$  for  $t = 0, A, 1 - A, 1$ .
- $\{x + y - z = t\}$  for  $t = -1 + A, A, 1 + A, 2 + A$ .

The complements of the union of these planes are the open polyhedra in the partitions.

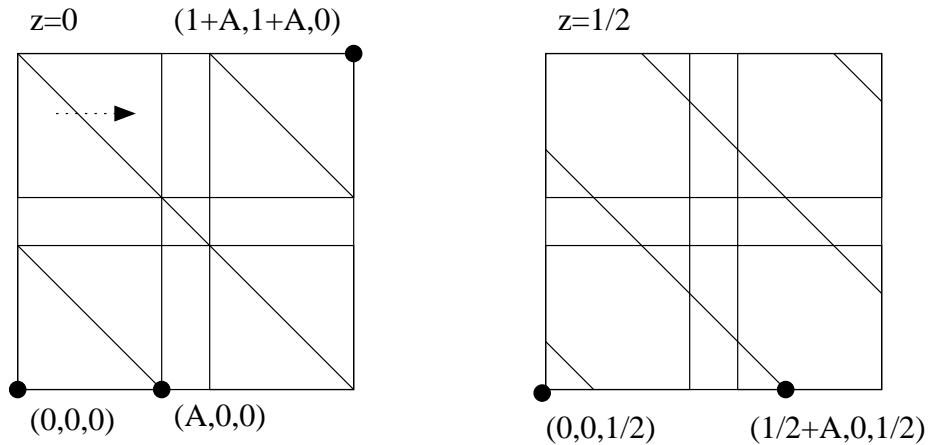


**Figure 6.1:** Two slices of the partition for  $A = 2/3$ .

Figure 6.1 shows a picture of two slices of the partition for the parameter  $A = 2/3$ . We have sliced the picture at  $z = 0$  and  $z = 1/2$ . We have labelled several points just to make the coordinate system more clear. The little arrow in the picture indicate the “motion” the diagonal lines would make were we to increase the  $z$ -coordinate and show a kind of movie of the partition. The reader can see this partition for any parameter and slice using Billiard King.

### 6.3 The Partitions

For each parameter  $A$  we get a solid body  $R_A$  partitioned into polyhedra. We can put all these pieces together into a single master picture. We define

$$R = \bigcup_{A \in (0,1)} R_A \times \{A\} \subset \mathbf{R}^4. \quad (52)$$

Each 2-plane family discussed above gives rise to a hyperplane family in  $\mathbf{R}^4$ . These hyperplane families are now all defined over  $\mathbf{Z}$ , because the variable  $A$  is just the 4th coordinate of  $\mathbf{R}^4$  in our current scheme. Given that we have two maps  $\mu_+$  and  $\mu_-$ , it is useful for us to consider two identical copies  $R_+$  and  $R_-$  of  $R$ .

We have a fibration  $f : \mathbf{R}^4 \rightarrow \mathbf{R}^2$  given by  $f(x, y, z, A) = (z, A)$ . This fibration in turn gives a fibration of  $R$  over the unit square  $B = (0, 1)^2$ . Figure 6.1 draws the fiber  $f^{-1}(3/2, 1/2)$ . The base space  $B$  has a partition into 4 regions, as shown in Figure 6.2.

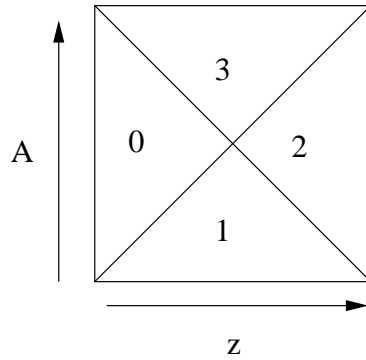


**Figure 6.2:** The Partition of the Base Space

All the fibers above the same open region in the base space have the same combinatorial structure. Figure 6.3 explains precisely how the partition assigns the value of the return map. Given a point  $\xi \in \Xi_+$ , we have a pair of integers  $(\epsilon_1^+(\xi), \epsilon_2^+(\xi))$  such that

$$\Psi(\xi) - \xi = 2(\epsilon_1^+, \epsilon_2^+, *). \quad (53)$$

The second coordinate,  $\pm 2$ , is determined by the parity relation in Equation 17. Similarly, we have  $(\epsilon_1^-, \epsilon_2^-)$  for  $\xi \in \Xi_-$ .

Figure 6.3 shows a schematic picture of  $R$ . For each of the 4 open triangles in the base, we have drawn a cluster of 4 copies of a representative fiber over

that triangle. The  $j$ th column of each cluster determines the value of  $\epsilon_j^\pm$ . The first row of each cluster determines  $\epsilon_j^+$  and the second row determines  $\epsilon_j^-$ . A light shading indicates a value of  $+1$ . A dark shading indicates a value of  $-1$ . No shading indicates a value of  $0$ .

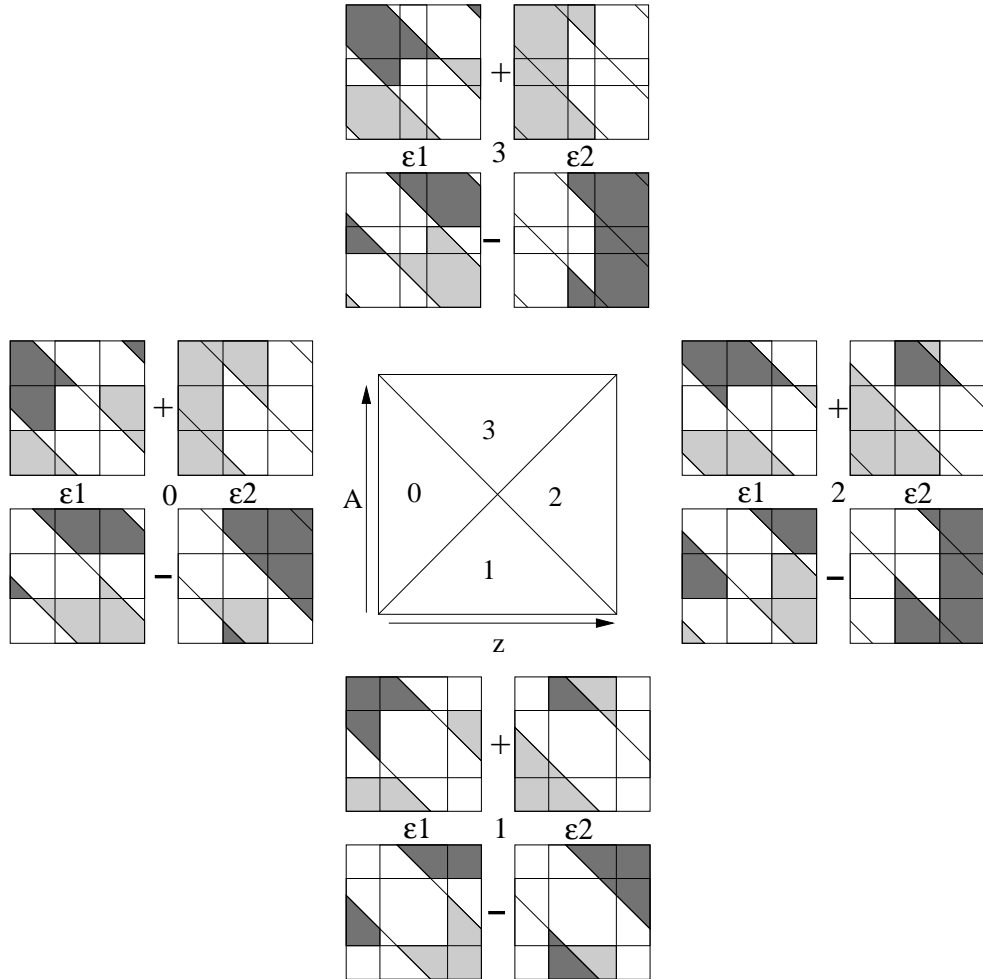


**Figure 6.3:** The decorated fibers

Given a generic point  $\xi \in \Xi_\pm$ , the image  $\mu_\pm(\xi)$  lies in some fiber. We then use the coloring scheme to determine  $\epsilon_j^\pm(\xi)$  for  $j = 1, 2$ . (See below for examples.) Theorem 6.1, together with the description in this section, constitutes the Master Picture Theorem. In §11 we explain with more traditional formulas how to compute these values. The reader can get a vastly superior understanding of the partition using Billiard King.

## 6.4 A Typical Example

Here we will explain how the Master Picture Theorem determines the local structure of the arithmetic graph  $\Gamma(3/5)$  at the point  $(4, 2)$ . Letting  $M$  be the fundamental map associated to  $A = 3/5$  (and  $\alpha = 1/(2q) = 1/10$ ).

$$M(4, 2) = \left( (8)(3/5) + (4) + (1/5), (-1)^{4+2+1} \right) = (9, -1) \in \Xi_-.$$

So,  $\mu_-(9, -1)$  determines the forwards direction and  $\mu_+(9, 1)$  determines the backwards direction. (Reflection in the  $x$ -axis conjugates  $\Psi$  to its inverse.)

We compute

$$\mu_+(9, 1) = \left( \frac{9}{2}, \frac{11}{2}, \frac{9}{2} \right) \equiv \left( \frac{1}{10}, \frac{3}{2}, \frac{1}{2} \right) \pmod{\Lambda};$$

$$\mu_-(9, -1) = \left( \frac{7}{2}, \frac{9}{2}, \frac{9}{2} \right) \equiv \left( \frac{7}{10}, \frac{1}{2}, \frac{1}{2} \right) \pmod{\Lambda}.$$

(In §11 we will explain algorithmically how to make these computations.) We have  $(z, A) = (1/2, 3/5)$ . There we need to look at Cluster 3, the cluster of fibers above region 3 in the base. Here is the plot of the two points in the relevant fiber. When we look up the regions in Figure 6.3, we find that  $(\epsilon_1^+, \epsilon_2^+) = (-1, 1)$  and  $(\epsilon_1^-, \epsilon_2^-) = (1, 0)$ . The bottom right of Figure 6 shows the corresponding local picture for the arithmetic graph.

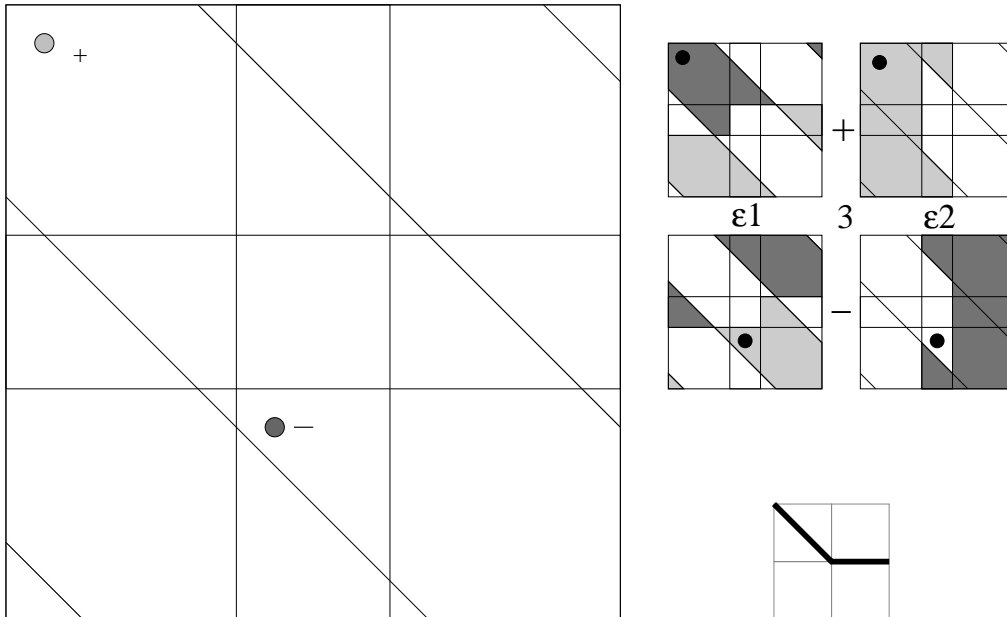


**Figure 6.4:** Points in the fiber.

## 6.5 A Singular Example

Sometimes it is an annoyance to deal with the tiny positive constant  $\alpha$  that arises in the definition of the fundamental map. In this section we will explain an alternate method for applying the Master Picture Theorem. One situation where this alternate approach proves useful is when we need to deal with the fibers at  $z = \alpha$ . We much prefer to draw the fibers at  $z = 0$ , because these do not contain any tiny polygonal regions. All the pieces of the partition can be drawn cleanly. However, in order to make sense of the Master Picture Theorem, we need to slightly redefine how the partition defines the return map.

Our method is to redefine our polygonal regions to include their *lower* edges. A lower edge is an edge first encountered by a line of slope 1. Figure 6.5 shows what we have in mind.

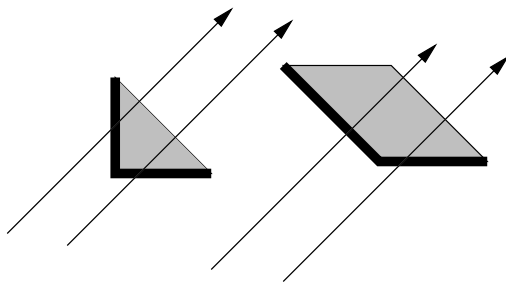


**Figure 6.5:** Polygons with their lower boundaries included.

We then set  $\alpha = 0$  and determine the relevant edges of the arithmetic graph by which *lower bordered* polygon contains our points. if it happens that  $z \in \{0, A, 1 - A\}$ , Then we think of the fiber at  $z$  as being the geometric limit of the fibers at  $z + \epsilon$  for  $\epsilon > 0$ . That is, we take a right-sided limit of the pictures. When  $z$  is not one of these special values, there is no need to do this, for the fiber is completely defined already.

We illustrate our approach with the example  $A = 3/5$  and  $(m, n) = (0, 8)$ . We compute that  $t = 8 + \alpha$  in this case. The relevant slices are the ones we get by setting  $z = \alpha$ . We deal with this by setting  $\alpha = 0$  and computing

$$\mu_+(16, 1) = (8, 9, 8) \equiv \left(\frac{4}{5}, 1, 0\right) \pmod{\Lambda}$$

$$\mu_-(16, -1) = (7, 8, 8) \equiv \left(0, \frac{7}{5}, 0\right) \pmod{\Lambda}.$$

Figure 6.6 draws the relevant fibers. The bottom right of Figure 6.6 shows the local structure of the arithmetic graph. For instance,  $(\epsilon_1^+, \epsilon_2^+) = (0, 1)$ .

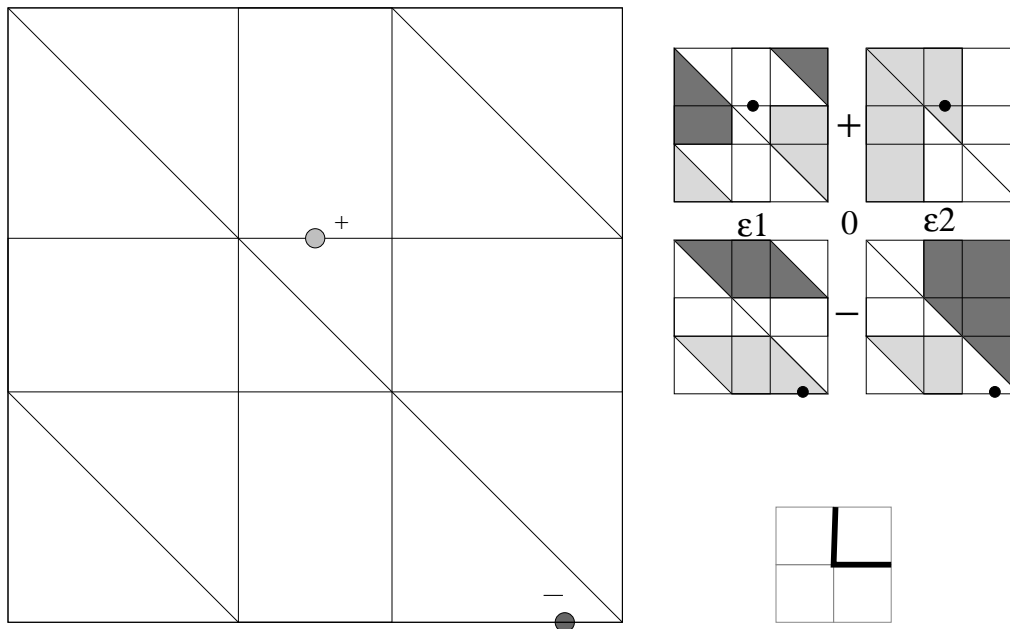


**Figure 6.6:** Points in the fiber.

The only place where we need to use our special definition of a lower bordered polygon is for the point in the lower left fiber. This fiber determines the  $x$  coordinate of the edge corresponding to  $\mu_-$ . In this case, we include our point in the lightly shaded parallelogram, because our point lies in the lower border of this parallelogram.

There is one exception to our construction that requires an explanation. Referring to the lower right fiber, suppose that the bottom point actually was the bottom right vertex, as shown in Figure 6.7. In this case, the point is simultaneously the bottom left vertex, and we make the definition using the bottom left vertex. The underlying reason is that a tiny push along the line of slope 1 moves the point into the region on the left.

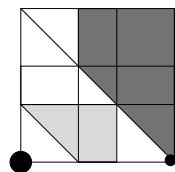


**Figure 6.7:** An exceptional case.

## 6.6 The Integral Structure

### 6.6.1 An Affine Action

We can describe Figure 6.3, and hence the Master Picture Theorem, in a different way. Let  $\mathbf{Aff}$  denote the 4 dimensional affine group. We define a discrete affine group action  $\Lambda \subset \mathbf{Aff}$  on the infinite slab  $\tilde{R} = \mathbf{R}^3 \times (0, 1)$ . The group  $\Lambda$  is generated by the 3 maps  $\gamma_1, \gamma_2, \gamma_3$ . Here  $\gamma_j$  acts on the first 3 coordinates as translation by the  $j$ th column of the matrix  $\Lambda_A$ , and on the 4th coordinate as the identity. We think of the  $A$ -variable as the 4th coordinate. Explicitly, we have

$$\begin{aligned} \gamma_1 \begin{bmatrix} x \\ y \\ z \\ A \end{bmatrix} &= \begin{bmatrix} x + 1 + A \\ y \\ z \\ A \end{bmatrix} \\ \gamma_2 \begin{bmatrix} x \\ y \\ z \\ A \end{bmatrix} &= \begin{bmatrix} x + 1 - A \\ y + 1 + A \\ z \\ A \end{bmatrix}; \\ \gamma_3 \begin{bmatrix} x \\ y \\ z \\ A \end{bmatrix} &= \begin{bmatrix} x - 1 \\ y - 1 \\ z + 1 \\ A \end{bmatrix}. \end{aligned} \tag{54}$$

These are all affine maps of  $\mathbf{R}^4$ . The quotient  $\tilde{R}/\Lambda$  is naturally a fiber bundle over  $(0, 1)$ . Each fiber  $(\mathbf{R}^3 \times \{A\})/\Lambda$  is isomorphic to  $\mathbf{R}^3/\Lambda_A$ .

The region  $R$ , from Equation 52, is a fundamental domain for the action of  $\Lambda$ . Note that  $R$  is naturally an *integral polytope*. That is, all the vertices of  $R$  have integer coordinates.  $R$  has 16 vertices, and they are as follows.

$$(\epsilon_1, \epsilon_2, \epsilon_3, 0); \quad (2\epsilon_1, 2\epsilon_2, \epsilon_3, 1); \quad \epsilon_1, \epsilon_2, \epsilon_3 \in \{0, 1\}. \tag{55}$$

### 6.6.2 Integral Polytope Partitions

Implicit in Figure 10.3 is the statement that the regions  $R_+$  and  $R_-$  are partitioned into smaller convex polytopes. The partition is defined by the 4 families of hyperplanes discussed above. An alternate point of view leads to a simpler partition.

For each pair  $(\epsilon_1, \epsilon_2) \in \{-1, 0, 1\}$ , we let  $R_+(\epsilon_1, \epsilon_2)$  denote the closure of the union of regions that assign  $(\epsilon_1, \epsilon_2)$ . It turns out that  $R(\epsilon_1, \epsilon_2)$  is a finite union of convex integral polytopes. There are 14 such polytopes, and they give an integral partition of  $R_+$ . We list these polytopes in §11.4.

Let  $\iota : R_+ \rightarrow R_-$  be given by the map

$$\iota(x, y, z, A) = (1 + A - x, 1 + A - y, 1 - z, A). \quad (56)$$

Geometrically,  $\iota$  is a reflection in the 1-dimensional line. We have the general equation

$$R_-(-\epsilon_1, -\epsilon_2) = \iota(R_+(\epsilon_1, \epsilon_2)). \quad (57)$$

Thus, the partition of  $R_-$  is a mirror image of the partition of  $R_+$ . (See Example 11.5 for an example calculation.)

We use the action of  $\Lambda$  to extend the partitions of  $R_+$  and  $R_-$  to two integral polytope tilings of  $\tilde{R}$ . (Again, see §11.5 for an example calculation.) These 4 dimensional tilings determine the structure of the special orbits.

### 6.6.3 Notation

Suppose that  $\hat{\Gamma}$  is an arithmetic graph. Let  $M$  be the fundamental map associated to  $\hat{\Gamma}$ . We define

$$M_+ = \mu_+ \circ M; \quad M_- = \mu_- \circ \rho \circ M. \quad (58)$$

Here  $\rho$  is reflection in the  $x$ -axis. Given a point  $p \in \mathbf{Z}^2$ , the polytope of  $R_+$  containing  $M_+(p)$  determines the forward edge of  $\hat{\Gamma}$  incident to  $p$ , and the polytope of  $R_-$  containing  $M_-(p)$  determines the backward edge of  $\hat{\Gamma}$  incident to  $p$ . Concretely, we have

$$\begin{aligned} M_+(m, n) &= (s, s + 1, s) \pmod{\Lambda}; \\ M_-(m, n) &= (s - 1, s, s) \pmod{\Lambda}; \\ s &= Am + n + \alpha. \end{aligned} \quad (59)$$

As usual,  $\alpha$  is the offset value. Note that  $\mu_+$  and  $\mu_-$  only depend on the first coordinate, and this first coordinate is not changed by  $\rho$ . The map  $\rho$  is present mainly for bookkeeping purposes, because  $\rho(\Xi_+) = \Xi_-$ , and the domain of  $\mu_{\pm}$  is  $\Xi_{\pm}$ .

## 7 The Pinwheel Lemma

### 7.1 The Main Result

The Pinwheel Lemma gives a formula for the return map  $\Psi : \Xi \rightarrow \Xi$  in terms of maps we call *strip maps*. Similar objects are considered in [GS] and [S].

Consider a pair  $(\Sigma, L)$ , where  $\Sigma$  is an infinite planar strip and  $L$  is a line transverse to  $\Sigma$ . The pair  $(L, \Sigma)$  determines two vectors,  $V_+$  and  $V_-$ , each of which points from one boundary component of  $\Sigma$  to the other and is parallel to  $L$ . Clearly  $V_- = -V_+$ .

For almost every point  $p \in \mathbf{R}^2$ , there is a unique integer  $n$  such that

$$E(p) := p + nV_+ \in \Sigma. \quad (60)$$

We call  $E$  the *strip map* defined relative to  $(\Sigma, L)$ . The map  $E$  is well-defined except on a countable collection of parallel and evenly spaced lines.

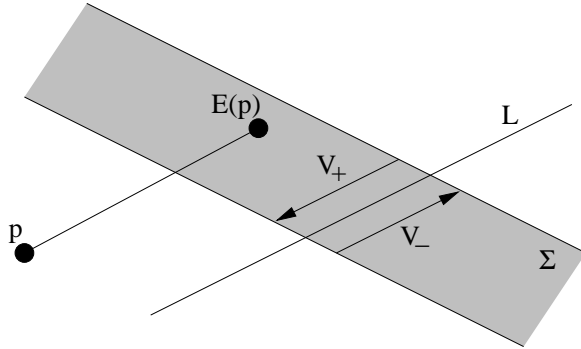


**Figure 7.1:** A strip map

Figure 7.2 shows 4 strips we associate to our kite. To describe the strips in Figure 7.2 write  $(v_1, v_2, v_3)^t$  (a column vector) to signify that  $L = \overline{v_2 v_3}$  and  $\partial\Sigma = \overline{v_1 v_2} \cup I(\overline{v_1 v_2})$ , where  $I$  is the order 2 rotation fixing  $v_3$ . Here is the data for the strip maps  $E_1, E_2, E_3, E_4$ .

$$\begin{bmatrix} (-1, 0) \\ (0, 1) \\ (0, -1) \end{bmatrix}; \quad \begin{bmatrix} (A, 0) \\ (0, -1) \\ (-1, 0) \end{bmatrix}; \quad \begin{bmatrix} (0, 1) \\ (A, 0) \\ (-1, 0) \end{bmatrix}; \quad \begin{bmatrix} (-1, 0) \\ (0, -1) \\ (0, 1) \end{bmatrix}. \quad (61)$$

We set  $\Sigma_{j+4} = \Sigma_j$  and  $V_{j+4} = -V_j$ . Then  $\Sigma_{j+4} = \Sigma_j$ . The reader can also reconstruct the strips from the information given in Figure 7.2. Figure 7.2 shows the parameter  $A = 1/3$ , but the formulas in the picture are listed for

general  $A$ . In particular, the point  $(3, 0)$  is independent of  $A$ . Here is an explicit formula for the vectors involved.

$$V_1 = (0, 4); \quad V_2 = (-2, 2); \quad V_3 = (-2 - 2A, 0); \quad V_4 = (-2, -2) \quad (62)$$

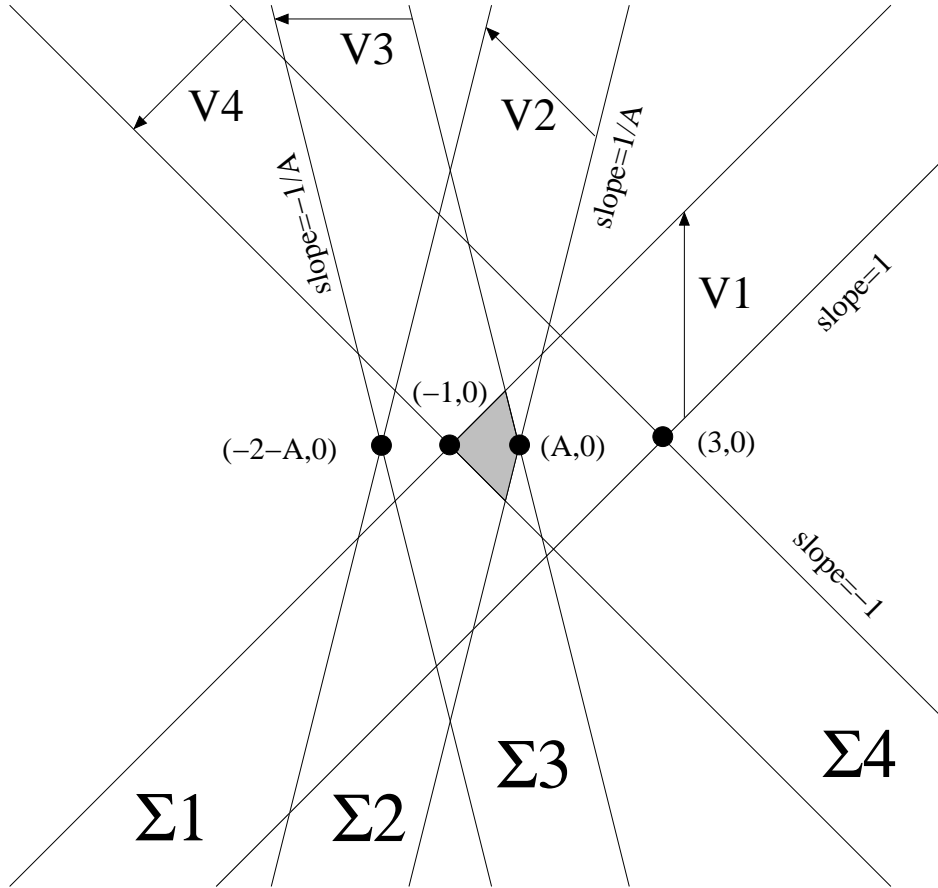


**Figure 7.2:** The 4 strips for the parameter  $A = 1/3$ .

We also define a map  $\chi : \mathbf{R}_+ \times \mathbf{Z}_{\text{odd}} \rightarrow \Xi$  by the formula

$$\chi(x, 4n \pm 1) = (x, \pm 1) \quad (63)$$

**Lemma 7.1 (Pinwheel)**  $\Psi$  exists for any point of  $\Xi$  having a well-defined outer billiards orbit. In all cases,  $\Psi = \chi \circ (E_8 \dots E_1)$ .

We call the map in the Pinwheel Lemma the *pinwheel map*. In §11.1 we give concrete formulas for this map.

## 7.2 Some Corollaries

Before we prove the Pinwheel Lemma, we list two corollaries.

**Corollary 7.2** *The parity equation in Equation 17 is true.*

**Proof:** The Pinwheel Lemma tells us that

$$\Psi(x, 1) - (x, 1) = 2(\epsilon_1 A + \epsilon_2, \epsilon_3); \quad (\epsilon_1, \epsilon_2, \epsilon_3) \in \mathbf{Z}^2 \times \{-1, 0, 1\}. \quad (64)$$

Given Equation 62, we see that the sum of the integer coefficients in each vector  $V_j$  is divisible by 4. (For instance,  $-2 - 2A$  yields  $-2 - 2 = -4$ .) Hence  $\epsilon_1 + \epsilon_2 + \epsilon_3$  is even. ♠

The Pinwheel Lemma gives a formula for the quantities in Equation 17.

For  $j = 0, \dots, 7$  we define points  $p_{j+1}$  and integers  $n_j$  by the following equations.

$$p_{j+1} = E_{j+1}(p_j) = p_j + n_j V_{j+1}. \quad (65)$$

Given the equations

$$V_1 = (0, 4); \quad V_2 = (-2, 2); \quad V_3 = (-2 - 2A, 0); \quad V_4 = (-2, -2) \quad (66)$$

we find that

$$\epsilon_1 = n_2 - n_6; \quad \epsilon_2 = n_1 + n_2 + n_3 - n_5 - n_6 - n_7; \quad (67)$$

We call  $(n_1, \dots, n_7)$  the *length spectrum* of  $p_0$ .

The precise bound in Equation 17 follows from the Master Picture Theorem, but here we give a heuristic explanation. If we define

$$m_1 = n_7; \quad m_2 = n_6; \quad m_3 = n_5; \quad (68)$$

then we have

$$\epsilon_1(p) = n_2 - m_2; \quad \epsilon_2(p) = (n_1 - m_1) + (n_2 - m_2) + (n_3 - m_3). \quad (69)$$

The path with vertices  $p_0, p_1, \dots, p_7, p_8, \chi(p_8)$  uniformly close to an octagon with dihedral symmetry. See Figure 7.3 below. For this reason, there is a universal bound to  $|n_i - m_i|$ . This is a heuristic explanation of the bound in Equation 17.

### 7.3 The Simplest Case

Here we prove the Pinwheel for points of  $\Xi$  far from  $K$ . Figure 7.3 shows a decomposition of  $\mathbf{R}^2 - K'$  into 8 regions,  $S_0, \dots, S_7$ . Here  $K'$  is a suitably large compact set. Let  $V_1, \dots, V_4$  be the vectors associated to our special strip maps. We set  $V_{4+j} = -V_j$ . A calculation shows that

$$x \in S_j; \quad \implies \quad \psi(x) - x = V_j. \quad (70)$$

One can easily see this using Billiard King or else our interactive guide to the monograph.

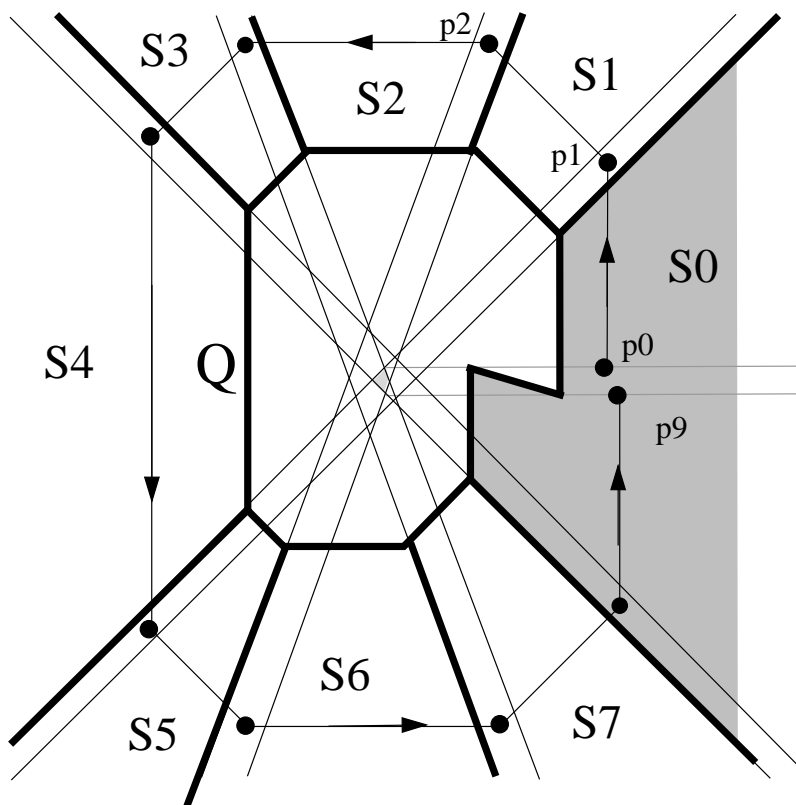


**Figure 7.3:** The Simplest Sequence of Regions

Equation 70 tells the whole story for points of  $\Xi$  far away from  $K$ . As above, let  $p_{j+1} = E_{j+1}(p_j)$  for  $j = 0, \dots, 7$ . let  $p_9 = \chi(p_8)$ . Here we have set  $E_{j+4} = E_j$ . By induction and Equation 70,  $p_{j+1}$  lies in the forward orbit of  $p_j$  for each  $j = 0, \dots, 8$ . But then  $p_9 = \Psi(p_1) = \chi \circ E_8 \dots E_1(p_0)$ .

## 7.4 Discussion of the General Case

As we have just seen, the Pinwheel Lemma is a fairly trivial result for points that are far from the origin. For points near the origin, the Pinwheel Lemma is a surprising and nontrivial result. In fact, it only seems to work because of a lucky accident. The fact that we consider the Pinwheel Lemma to be an accident probably means that we don't yet have a good understanding of what is going on.

Verifying the Pinwheel Lemma for any given parameter  $A$  is a finite calculation. We just have to check, on a fine enough mesh of points extending out sufficiently far away from  $K(A)$ , that the equation in the Pinwheel Lemma holds. The point is that all the maps involved are piecewise isometries for each parameter. We took this approach in [S] when we proved the Pinwheel Lemma for  $A = \phi^{-3}$ .

Using Billiard King, we computed that the Pinwheel Lemma holds true at the points  $(x, \pm 1)$  relative to the parameter  $A$  for all

$$A = \frac{1}{256}, \dots, \frac{255}{256}; \quad x = \epsilon + \frac{1}{1024}, \dots, \epsilon + \frac{16384}{1024}; \quad \epsilon = 10^{-6}.$$

The tiny number  $\epsilon$  is included to make sure that the outer billiards orbit is actually defined for all the points we sample. This calculation does not constitute a proof of anything. However, we think that it serves as a powerful sanity check that the Pinwheel Lemma is correct. We have fairly well carpeted the region of doubt about the Pinwheel Lemma with instances of its truth.

Our proof of the Pinwheel Lemma essentially boils down to finding the replacement equation for Equation 70. We will do this in the section. As the reader will see, the situation in general is much more complicated. There is a lot of information packed into the next section, but all this information is easily seen visually on Billiard King. We have programmed Billiard King so that the reader can see pictures of all the regions involved, as well as their interactions, for essentially any desired parameter.

We think of the material in the next section as something like a written description of a photograph. The written word is probably not the right medium for the proof of the Pinwheel Lemma. To put this in a different way, Billiard King relates to the proof given here much in the same way that an ordinary research paper would relate to one that was written in crayon.

## 7.5 A Partition of the Plane

Let  $\psi = \psi_A$  be the square of the outer billiards map relative to  $K(A)$ . For each  $x \in \mathbf{R}^2 - K$  on which  $\psi$  is defined, there is a vector  $v_x$  such that

$$\psi(x) - x = v_x.$$

This vector is twice the difference between 2 vertices of  $K$ , and therefore can take on 12 possible values. It turns out that 10 of these values occur. We call these vectors  $V_j$ , with  $j = 1, 2, 3, 4, 4^\sharp, 5, 6^\flat, 6, 7, 8$ . With this ordering, the argument of  $V_j$  increases monotonically with  $j$ . Compare Figure 7.4. For each of our vectors  $V$ , there is an open region  $R \subset \mathbf{R}^2 - K$  such that  $x \in R$  if and only if  $\psi(x) - x = V$ . The regions  $R_1, \dots, R_8$  are unbounded. The two regions  $R_4^\sharp$  and  $R_6^\flat$  are bounded.

One can find the entire partition by extending the sides of  $K$  in one direction, in a pinwheel fashion, and then pulling back these rays by the outer billiards map. To describe the regions, we use the notation  $\vec{q}_1, p_1, \dots, p_k, \vec{q}_2$  to indicate that

- The two unbounded edges are  $\{p_1 + tq_1 \mid t \geq 0\}$  and  $\{p_k + tq_2 \mid t \geq 0\}$ .
- $p_2, \dots, p_{k-1}$  are any additional intermediate vertices.

To improve the typesetting on our list, we set  $\lambda = (A - 1)^{-1}$ . Figure 6.3 shows the picture for  $A = 1/3$ . The reader can see any parameter using Billiard King.

$$\begin{array}{ll}
 V_1 = (0, 4) & R_1 : \overrightarrow{(1, -1)}, (1, -2), \overrightarrow{(1, 1)}. \\
 V_2 = (-2, 2) & R_2 : \overrightarrow{(1, 1)}, (1, -2), (0, -1), \overrightarrow{(A, 1)}. \\
 V_3 = (-2 - 2A, 0) & R_3 : \overrightarrow{(A, 1)}, (2A, 1), \lambda(2A^2, -1 - A), \overrightarrow{(-A, 1)}. \\
 V_4 = (-2, -2) & R_4 : \overrightarrow{(-A, 1)}, \lambda(2A, A - 3), \overrightarrow{(-1, 1)}. \\
 V_{4^\sharp} = (-2A, -2) & R_{4^\sharp} : (A, 0), (2A, 1), \lambda(2A^2, -1 - A) \\
 V_5 = (0, -4) & R_5 : \overrightarrow{(-1, 1)}, \lambda(2A, A - 3), (-A, 2), \lambda(2A, 3A - 1), \overrightarrow{(-1, -1)} \\
 V_{6^\flat} = (2A, -2) & R_{6^\flat} : (0, 1), (-A, 2), \lambda(2A, 3A - 1) \\
 V_6 = (2, -2) & R_6 : \overrightarrow{(-1, -1)}, \lambda(2, A + 1), \overrightarrow{(-A, -1)} \\
 V_7 = (2 + 2A, 0) & R_7 : \overrightarrow{(-A, -1)}, \lambda(2, A + 1), (-2, -1), \overrightarrow{(A, -1)} \\
 V_8 = (2, 2) & R_8 : \overrightarrow{(A, -1)}, (-2, -1), (-1, 0), \overrightarrow{(1, -1)}.
 \end{array}$$

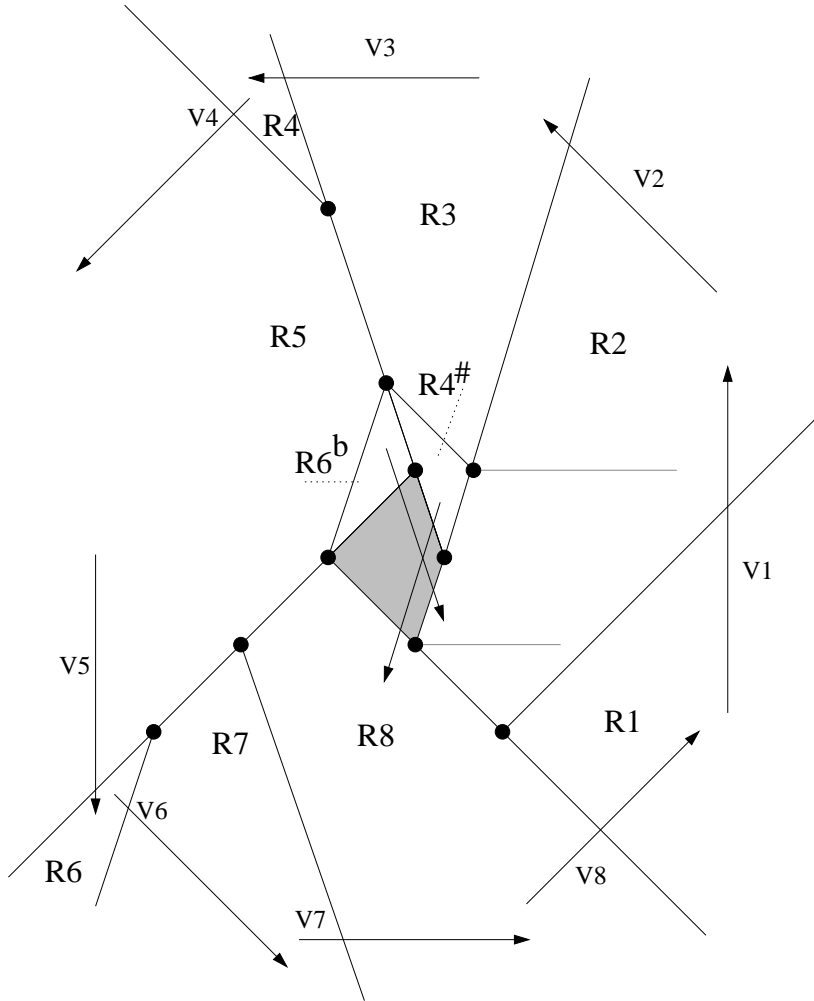


**Figure 7.4:** The Partition for  $A = 1/3$ .

It is convenient to set

$$\widehat{R}_a = R_a + V_a = \{p + V_a \mid p \in R_a\}. \quad (71)$$

One symmetry of the partition is that reflection in the  $x$ -axis interchanges  $\widehat{R}_a$  with  $R_{10-a}$ , for all values of  $a$ . (To make this work, we set  $R_9 = R_1$ , and use the convention  $4^\# + 6^\flat = 10$ .)

We are interested in *transitions* between one region  $R_a$ , and another region  $R_b$ . If  $\widehat{R}_a \cap R_b \neq \emptyset$  for some parameter  $A$  it means that there is some  $p \in R_a$  such that  $\psi_A(p) \in R_b$ . (We think of our regions as being open.) We create a *transition matrix* using the following rules.

- A 0 in the  $(ab)$ th spot indicates that  $\widehat{R}_a \cap R_b = \emptyset$  for all  $A \in (0, 1)$ .
- A 1 in the  $(ab)$ th spot indicates that  $\widehat{R}_a \cap R_b \neq \emptyset$  for all  $A \in (0, 1)$ .
- A  $t^+$  in the  $(ab)$ th spot indicates that  $R_a \cap R_b \neq \emptyset$  iff  $A \in (t, 1)$ .
- A  $t^-$  in the  $(ab)$ th spot indicates that  $R_a \cap R_b \neq \emptyset$  iff  $A \in (0, t)$ .

	$R_1$	$R_2$	$R_3$	$R_4$	$R_{4^\sharp}$	$R_5$	$R_{6^\flat}$	$R_6$	$R_7$	$R_8$	
$\widehat{R}_1$	1	1	$(\frac{1}{3})^+$	0	0	0	0	0	0	0	
$\widehat{R}_2$	0	1	1	$(\frac{1}{3})^-$	1	1	1	0	0	0	
$\widehat{R}_3$	0	0	1	1	$(\frac{1}{2})^+$	1	0	0	0	0	
$\widehat{R}_4$	0	0	0	1	0	1	0	0	0	0	
$\widehat{R}_{4^\sharp}$	0	0	0	0	0	$(\frac{1}{3})^+$	$(\frac{1}{3})^+$	0	0	1	(72)
$\widehat{R}_5$	0	0	0	0	0	1	$(\frac{1}{3})^+$	1	1	1	
$\widehat{R}_{6^\flat}$	0	1	0	0	0	0	0	0	$(\frac{1}{2})^+$	1	
$\widehat{R}_6$	0	0	0	0	0	0	0	0	1	$(\frac{1}{3})^-$	
$\widehat{R}_7$	$(\frac{1}{3})^+$	1	0	0	0	0	0	0	0	1	
$\widehat{R}_8$	1	1	1	0	1	0	0	0	0	0	

We have programmed Billiard King so that the interested reader can see each of these relations at a single glance. Alternatively, they can easily be established using routine linear algebra. For example, interpreting  $\widehat{R}_3$  and  $R_2$  as projectivizations of open convex cones  $\widehat{C}_3$  and  $C_2$  in  $\mathbf{R}^3$ , we easily verifies that the vector  $(-1, A, -2 - A)$  has positive dot product with all vectors in  $\widehat{C}_3$  and negative dot product with all vectors in  $C_2$ . Hence  $R_2 \cap \widehat{R}_3 = \emptyset$ .

We can relate all the nonempty intersections to our strips. As with the list of intersections, everything can be seen at a glance using Billiard King, or else proved using elementary linear algebra. First we list the intersections that comprise the complements of the strips.

- $\widehat{R}_2 \cap R_2$  and  $\widehat{R}_6 \cap R_6$  are the components of  $\mathbf{R}^2 - (\Sigma_1 \cup \Sigma_2)$ .
- $\widehat{R}_4 \cap R_4$  and  $\widehat{R}_8 \cap R_8$  are the components of  $\mathbf{R}^2 - (\Sigma_3 \cup \Sigma_4)$ .
- $\widehat{R}_3 \cap (R_3 \cup R_{4^\sharp})$  and  $(\widehat{R}_{6^\flat} \cup \widehat{R}_7) \cap R_7$  are the components of  $\mathbf{R}^2 - (\Sigma_2 \cup \Sigma_3)$ .
- $\widehat{R}_1 \cap R_1$  and  $(\widehat{R}_{4^\sharp} \cup \widehat{R}_5) \cap (R_5 \cup R_{6^\flat})$  are the components of  $\mathbf{R}^2 - (\Sigma_1 \cup \Sigma_4)$ .

Now we list the intersections that are contained in single strips. To make our typesetting nicer, we use the term *u-component* to denote an unbounded connected component. We use the term *b-component* to denote a bounded connected component.

- $\widehat{R}_1 \cap R_2$  and  $\widehat{R}_5 \cap R_6$  are the two *u*-components of  $\Sigma_1 - (\Sigma_2 \cup \Sigma_4)$ .
- $\widehat{R}_8 \cap R_1$  and  $\widehat{R}_4 \cap R_5$  are the two *u*-components of  $\Sigma_4 - (\Sigma_1 \cup \Sigma_3)$ .
- $\widehat{R}_3 \cap R_4$  and  $(\widehat{R}_{6^b} \cup \widehat{R}_7) \cap R_8$  are the two *u*-components of  $\Sigma_3 - (\Sigma_2 \cup \Sigma_4)$ .
- $\widehat{R}_6 \cap R_7$  and  $\widehat{R}_2 \cap (R_3 \cup R_{4^\sharp})$  are the two *u*-components of  $\Sigma_2 - (\Sigma_1 \cup \Sigma_3)$ .
- $\widehat{R}_{6^b} \cap R_7$  is contained in the *b*-component of  $\Sigma_1 - (\Sigma_2 \cup \Sigma_3)$ .
- $\widehat{R}_3 \cap R_{4^\sharp}$  is contained in the *b*-component of  $\Sigma_4 - (\Sigma_2 \cup \Sigma_3)$ .
- $\widehat{R}_{4^\sharp} \cap (R_5 \cup R_{6^b})$  is contained in the *b*-component of  $\Sigma_3 - (\Sigma_1 \cup \Sigma_4)$ .
- $(\widehat{R}_{4^\sharp} \cup \widehat{R}_5) \cap R_{6^b}$  is contained in the *b*-component of  $\Sigma_2 - (\Sigma_1 \cup \Sigma_4)$ .

Now we list the intersections of regions that are contained in double intersections of strips. In this case, all the components are bounded: Any two strips intersect in a bounded region of the plane.

- $\widehat{R}_1 \cap R_3$  and  $\widehat{R}_5 \cap R_7$  are the components of  $(\Sigma_1 \cap \Sigma_2) - (\Sigma_3 \cup \Sigma_4)$ .
- $\widehat{R}_7 \cap R_1$  and  $\widehat{R}_3 \cap R_5$  are the components of  $(\Sigma_3 \cap \Sigma_4) - (\Sigma_1 \cup \Sigma_2)$ .
- $\widehat{R}_2 \cap R_4$  and  $\widehat{R}_6 \cap R_8$  are bounded components of  $(\Sigma_2 \cap \Sigma_3) - (\Sigma_1 \cup \Sigma_4)$ .
- $\widehat{R}_8 \cap R_2 = (\Sigma_1 \cap \Sigma_4) - (\Sigma_2 \cup \Sigma_3)$ .

Now we list all the intersections of regions that are contained in triple intersections of strips.

- $\widehat{R}_2 \cap (R_5 \cup R_{6^b}) = \Sigma_2 \cap \Sigma_3 \cap \Sigma_4 - \Sigma_1$ .
- $\widehat{R}_8 \cap (R_3 \cup R_{4^\sharp}) = \Sigma_1 \cap \Sigma_2 \cap \Sigma_4 - \Sigma_3$ .
- $(\widehat{R}_{4^\sharp} \cup \widehat{R}_5) \cap R_8 = \Sigma_1 \cap \Sigma_2 \cap \Sigma_3 - \Sigma_4$ .
- $(\widehat{R}_{6^b} \cup \widehat{R}_7) \cap R_2 = \Sigma_1 \cap \Sigma_3 \cap \Sigma_4 - \Sigma_2$ .

Here we list a bit more information about the two regions  $R_{4^\sharp}$  and  $R_{6^\flat}$  some of the information is redundant, but it is useful to have it all in one place.

- $R_{4^\sharp} \subset \Sigma_4 - \Sigma_3$ .
- $R_{4^\sharp} + V_3 = \Sigma_3 - (\Sigma_2 \cup \Sigma_4)$ .
- $R_{6^\flat} \subset \Sigma_2 - \Sigma_1$ .
- $R_{6^\flat} + V_5 \subset \Sigma_1 - \Sigma_2$ .
- $R_{6^\flat} + V_5 - V_6 = \Sigma_2 - (\Sigma_1 \cup \Sigma_3)$ .

Finally, we mention two crucial relations between our various vectors:

- $V_3 - V_4 + V_5 = V_{4^\sharp}$ .
- $V_5 - V_6 + V_7 = V_{6^\flat}$ .

These two relations are responsible for the lucky cancellation that makes the Pinwheel Lemma hold near the kite.

We will change our notation slightly from the simplest case considered above. Given any point  $z_1 \in \Xi$ , we can associate the *sequence of regions*

$$R_{a_1} \rightarrow \dots \rightarrow R_{a_k} \tag{73}$$

through which the forwards orbit of  $z_1$  transitions until it returns as  $\Psi(z_1)$ . The simplest possible sequence is the one where  $a_j = j$  for  $j = 1, \dots, 9$ . See Figure 7.2. We already analyzed this case above. We let  $z_j$  denote the first point in the forward orbit of  $z_1$  that lies in  $R_{a_j}$ .

To prove the Pinwheel Lemma in general, we need to analyze all allowable sequences and see that the equation in the Pinwheel Lemma always holds. We will break the set of all sequences into three types, and then analyze the types one at a time. Here are the types.

1. Sequences that do not involve the indices  $4^\sharp$  or  $6^\flat$ .
2. Sequences that involve  $4^\sharp$  but not  $6^\flat$ .
3. Sequences that involve  $6^\flat$ .

## 7.6 No Sharps or Flats

**Lemma 7.3** *If  $j < k$  then  $\widehat{R}_j \cap R_k \subset \Sigma_j \cap \dots \cap \Sigma_{k-1}$ .*

**Proof:** This is a corollary of the the intersections listed above. ♠

Suppose by induction we have shown that

$$z_j = E_{a_j-1} E_{a_j-2} \dots E_1(z_1). \quad (74)$$

By construction and Lemma 7.3,

$$z_{j+1} = E_{a_j}(z_j) \in \widehat{R}_{a_j} \cap R_{a_{j+1}} \subset \Sigma_{a_j} \cap \dots \cap \Sigma_{a_{j+1}-1}.$$

Therefore,  $E_{a_j}, \dots, E_{a_{j+1}-1}$  all act trivially on  $z_{j+1}$ , forcing

$$z_{j+1} = E_{a_{j+1}-1} E_{a_{j+1}-2} \dots E_1(z_1).$$

Hence, Equation 74 holds true for all indices  $j$ .

By the Intersection Lemma, we eventually reach either a point  $z_9$  or  $z_{10}$ . (That is, we wrap all the way around and return either to  $R_9 = R_1$  or else to  $R_{10} = R_2$ .) We will consider these two cases one at a time.

**Case 1:** If we reach  $z_9 = (x_9, y_9) \in R_9$  then we have

$$z_9 = E_8 \dots E_1(z_1); \quad x_9 > 0; \quad y_9 \leq 1. \quad (75)$$

From this we get that  $\Psi(z_1) = \chi \circ (E_4 \dots E_1)^2(z_1)$ , as desired. The last inequality in Equation 75 requires explanation. By the Intersection Lemma, the point preceding  $z_9$  on our list must lie in  $R_a$  for some  $a \in \{6^b, 6, 7, 8\}$ . However, the distance between any point on  $\mathbf{R}_+ \times \{3, 5, 7, \dots\}$  to any point in  $R_a$  exceeds the length of vector  $V_a$ .

**Case 2:** If we arrive at  $z_{10} = (x_{10}, y_{10})$ , then the Intersection Lemma tells us that the point preceding  $z_{10}$  lies in  $V_a$  for  $a = \{6^b, 6, 7, 8\}$  and  $z_{10} \in \Sigma_9$ . Hence  $E_9(z_{10}) = z_{10}$ . That is

$$z_{10} = E_8 \dots E_1(z_1); \quad x_{10} > 0; \quad y_{10} < 3.$$

The last inequality works just as in Case 1. All points in  $R_{10}$  have  $y$ -coordinate at least  $-2$ . Hence  $y_{10} = \pm 1$ . Hence  $\chi(z_{10}) = z_{10}$ . Putting everything together gives the same result as Case 1.

## 7.7 Dealing with Four Sharp

In this section we will deal with orbits whose associated sequence has a  $4^\sharp$  in it, but not a  $6^\flat$ . The following result is an immediate consequence the intersections discussed above.

**Lemma 7.4** *The following holds for all parameters.*

$$\widehat{R}_{4^\sharp} \cap R_{4^\sharp} = \emptyset; \quad R_{4^\sharp} \subset \Sigma_4 - \Sigma_3; \quad R_{4^\sharp} + V_3 \in \Sigma_3 - \Sigma_4; \quad \widehat{R}_{4^\sharp} \cap R_8 \subset \Sigma_1 \cap \Sigma_2 \cap \Sigma_3$$

Let  $z$  be the first point in the forward orbit of  $z_1$  such that  $z \in R_{4^\sharp}$ . Using Lemma 7.3 and the same analysis as in the previous section, we get

$$\exists n \in \mathbf{N} \cup \{0\} \quad z = E_2 E_1(z_1) + nV_3, \quad (76)$$

From Lemma 7.3 and Item 1 of Lemma 7.4, the next point in the orbit is

$$w = z + V_{4^\sharp} \in R_5 \cup R_8. \quad (77)$$

Items 2 and 3 of Lemma 7.4 give

$$E_3 E_2 E_1(z_1) = E_3(z) = z + V_3; \quad E_4 E_3(z) = z + V_3 - V_4.$$

Figure 7.5 shows what is going on. Since  $V_3 - V_4 + V_5 = V_{4^\sharp}$ ,

$$w = z + V_{4^\sharp} = z + V_3 - V_4 + V_5 = E_4 E_3(z) + V_5 = E_4 E_3 E_2 E_1(z_1) + V_5. \quad (78)$$

The rest of the analysis is as in the previous section. We use Item 4 of Lemma 7.4 as an *addendum* to Lemma 7.3 in case  $w \in R_8$ .

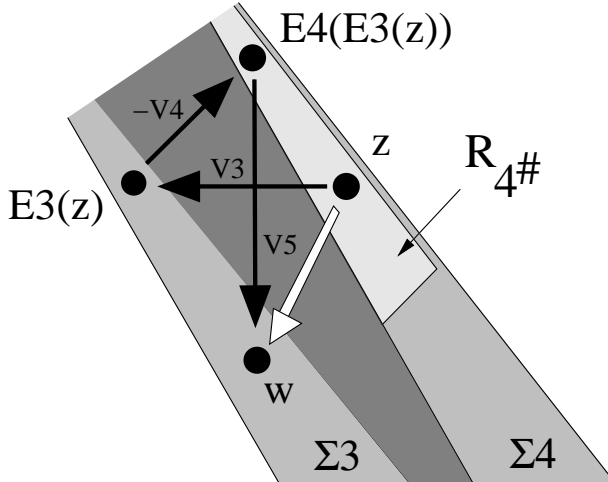


**Figure 7.5:** The orbit near  $R_{4^\sharp}$ .

## 7.8 Dealing with Six Flat

Here is another immediate consequence of the intersections listed above.

**Lemma 7.5** *The following is true for all parameters.*

$$\begin{aligned} V_{6^b} &\subset \Sigma_2 - \Sigma_1; & V_{6^b} + R_5 &\subset \Sigma_1 - \Sigma_2; \\ \widehat{R}_{6^b} \cap R_2 &\subset \Sigma_3 \cap \Sigma_4 \cap \Sigma_1; & \widehat{R}_2 \cap R_{6^b} &\subset \Sigma_2 \cap \Sigma_3 \cap \Sigma_4; \end{aligned}$$

Let  $z$  be the first point in the forwards orbit of  $z_1$  such that  $z \in R_{6^b}$  and let  $w = \psi(z)$ . The same arguments as in the previous section give

$$z = E_4 E_3 E_2 E_1(z_1) + nV_5; \quad w = z + V_{6^b} \in R_7 \cup R_2. \quad (79)$$

Here  $n \in \mathbf{N} \cup \{0\}$ . (The possibility of  $w \in R_{6^b}$  is ruled out by Item 1 of Lemma 7.4 and the reflection symmetry.) Items 2 and 3 of Lemma 7.5 give

$$E_5 E_4 E_3 E_2 E_1(z_1) = E_5(z) = z + V_5; \quad E_6 E_5 E_4 E_3 E_2 E_1(z) = z + V_5 - V_6$$

Figure 7.6 shows what is going on. Since  $V_5 - V_6 + V_7 = V_{6^b}$ ,

$$w = E_6 E_5 E_4 E_3 E_2 E_1(z) + V_7. \quad (80)$$

The rest of the analysis is as in the previous cases. We use Item 3 of Lemma 7.5 as an *addendum* to Lemma 7.3 in case  $w \in R_2$ .

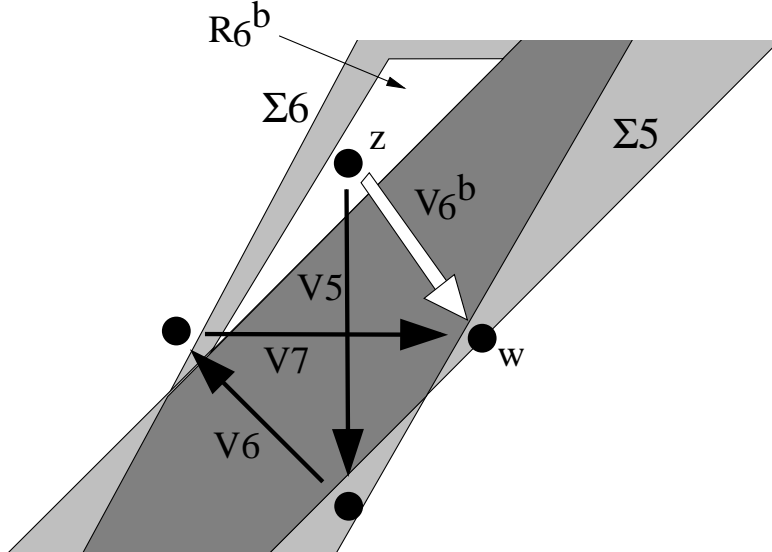


**Figure 7.6:** The orbit near  $R_{6^b}$ .

## 8 The Torus Lemma

### 8.1 The Main Result

For ease of exposition, we state and prove the (+) halves of our results. The (−) halves have the same formulation and proof.

Let  $T^4 = \tilde{R}/\Lambda$ , the 4 dimensional quotient discussed in §6.6. Topologically,  $T^4$  is the product of a 3-torus with  $(0, 1)$ . Let  $(\mu_+)_A$  denote the map  $\mu_+$  as defined for the parameter  $A$ . We now define  $\mu_+ : \Xi_+ \times (0, 1) \rightarrow T^4$  by the obvious formula  $\mu_+(p, A) = ((\mu_+)_A(p), A)$ . We are just stacking all these maps together.

The Pinwheel Lemma tells us that  $\Psi(p) = \chi \circ E_8 \dots E_1(p)$  whenever both maps are defined. This map involves the sequence  $\Sigma_1, \dots, \Sigma_8$  of strips. We are taking indices mod 4 so that  $\Sigma_{j+4} = \Sigma_j$  and  $E_{4+j} = E_j$ . Let  $p \in \Xi_+$ . We set  $p_0 = p$  and inductively define

$$p_j = E_j(p_{j-1}) \in \Sigma_j. \quad (81)$$

We also define

$$\theta(p) = \min \theta_j(p); \quad \theta_j(p) = \text{distance}(p_j, \partial \Sigma_j). \quad (82)$$

The quantity  $\theta(p)$  depends on the parameter  $A$ , so we will write  $\theta(p, A)$  when we want to be clear about this.

**Lemma 8.1 (Torus)** *Let  $(p, A), (q^*, A^*) \in \Xi_+ \times (0, 1)$ . There is some  $\eta > 0$ , depending only on  $\theta(p, A)$  and  $\min(A, 1 - A)$ , with the following property. Suppose that the pinwheel map is defined at  $(p, A)$ . Suppose also that  $\mu_+(p, A)$  and  $\mu_+(q^*, A^*)$  are within  $\eta$  of each other. Then the pinwheel map is defined at  $(q^*, A^*)$  and  $(\epsilon_1(q^*), \epsilon_2(q^*)) = (\epsilon_1(p), \epsilon_2(p))$ .*

**Remark:** My proof of the Torus Lemma owes a big intellectual debt to many sources. I discovered the Torus Lemma experimentally, but I got some inspiration for its proof by reading [T2], an account of unpublished work by Chris Culter about the existence of periodic orbits for polygonal outer billiards. Culter’s proof is closely related to ideas in [K]. The paper [GS] implicitly has some of these same ideas, though they are treated from a different point of view. If all these written sources aren’t enough, I was also influenced by some conversations with John Smillie.

## 8.2 Input from the Torus Map

We first prove the Torus Lemma under the assumption that  $A = A^*$ . We set  $q = q^*$ . In this section, we explain the significance of the map  $\mu_+$ . We introduce the quantities

$$\widehat{\lambda}_j = \lambda_0 \times \dots \times \lambda_j; \quad \lambda_j = \frac{\text{Area}(\Sigma_{j-1} \cap \Sigma_j)}{\text{Area}(\Sigma_j \cap \Sigma_{j+1})}; \quad j = 1, \dots, 7. \quad (83)$$

Let  $p = (x, \pm 1)$  and  $q = (y, \pm 1)$ . We have

$$\mu_+(q) - \mu_+(p) = (t, t, t) \bmod \Lambda; \quad t = \frac{y - x}{2}. \quad (84)$$

**Lemma 8.2** *If  $\text{dist}(\mu_+(x), \mu_+(y)) < \delta$  in  $T^3$ , then there is an integer  $I_k$  such that  $t\widehat{\lambda}_k$  is within  $\epsilon$  of  $I_k$  for all  $k$ ,*

**Proof:** We compute

$$\begin{aligned} \text{Area}(\Sigma_0 \cap \Sigma_1) &= 8; & \text{Area}(\Sigma_1 \cap \Sigma_2) &= \frac{8 + 8A}{1 - A}; \\ \text{Area}(\Sigma_2 \cap \Sigma_3) &= \frac{2(1 + A)^2}{A}; & \text{Area}(\Sigma_3 \cap \Sigma_4) &= \frac{8 + 8A}{1 - A}. \end{aligned} \quad (85)$$

This leads to

$$\widehat{\lambda}_0 = \widehat{\lambda}_4 = 1; \quad \widehat{\lambda}_1 = \widehat{\lambda}_3 = \widehat{\lambda}_5 = \widehat{\lambda}_7 = \frac{1 - A}{1 + A}; \quad \widehat{\lambda}_2 = \widehat{\lambda}_6 = \frac{4A}{(1 + A)^2}. \quad (86)$$

The matrix

$$H = \begin{bmatrix} \frac{1}{1+A} & \frac{A-1}{(1+A)^2} & \frac{2A}{(1+A)^2} \\ 0 & \frac{1}{1+A} & \frac{1}{1+A} \\ 0 & 0 & 1 \end{bmatrix} \quad (87)$$

conjugates the columns of the matrix defining  $\Lambda$  to the standard basis. Therefore, if  $\mu_+(x)$  and  $\mu_+(y)$  are close in  $T^3$  then  $H(t, t, t)$  is close to a point of  $\mathbf{Z}^3$ . We compute

$$H(t, t, t) = \left( \frac{4A}{(1 + A)^2}, \frac{2}{1 + A}, 1 \right) t = (\widehat{\lambda}_2, \widehat{\lambda}_1 - 1, 1)t. \quad (88)$$

Equations 86 and 88 now finish the proof. ♠

### 8.3 Pairs of Strips

Suppose  $(S_1, S_2, V_2)$  is triple, where  $V_2$  is a vector pointing from one corner of  $S_1 \cap S_2$  to an opposite corner. Let  $p_1 \in S_1$  and  $p_2 = E_2(p_1) \in S_2$ . Here  $E_2$  is the strip map associated to  $(S_2, V_2)$ . We define  $n$  and  $\alpha$  by the equations

$$p_2 - p_1 = nV_2; \quad \alpha = \frac{\text{area}(B)}{\text{area}(S_1 \cap S_2)}; \quad \sigma_j = \frac{\|p_j - p'_j\|}{\|V_2\|} \quad (89)$$

All quantities are affine invariant functions of the quintuple  $(S_1, S_2, V_2, p_1, p_2)$ .

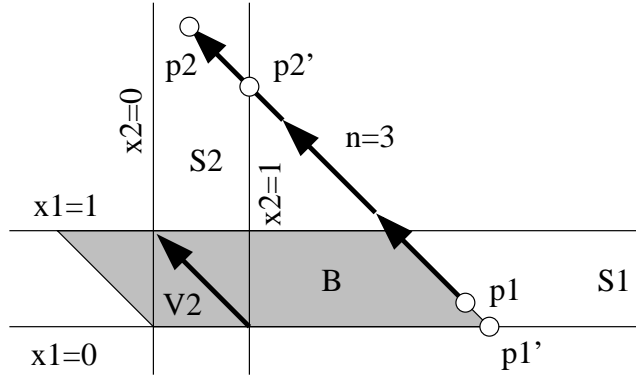


**Figure 8.1:** Strips and associated objects

Figure 8.1 shows what we call the *standard pair* of strips, where  $\Sigma_j$  is the strip bounded by the lines  $x_j = 0$  and  $x_j = 1$ . To get a better picture of the quantities we have defined, we consider them on the standard pair. We have a

$$\alpha = p_{11} + p_{12} = p_{21} + p_{22}; \quad \sigma_1 = p_{12}; \quad \sigma_2 = 1 - p_{22}; \quad n = \text{floor}(p_{11}). \quad (90)$$

Here  $p_{ij}$  is the  $j$ th coordinate of  $p_i$ . These equations lead to the following affine invariant relations.

$$n = \text{floor}(\alpha - \sigma_1); \quad \sigma_2 = 1 - [\alpha_1 - \sigma_1] \quad (91)$$

Here  $[x]$  denotes the fractional part of  $x$ . Again, the relations in Equation 91 hold for any pair of strips.

In our next result, we hold  $(S_1, S_2, V_2)$  fixed but compare all the quantities for  $(p_1, p_2)$  and another pair  $(q_1, q_2)$ . Let  $n(p) = n(S_1, S_2, V_2, p_1, p_2)$ , etc. Also,  $N$  stands for an integer.

**Lemma 8.3** *Let  $\epsilon > 0$ . There is some  $\delta > 0$  with the following property. If  $|\sigma(p_1) - \sigma(q_1)| < \delta$  and  $|\alpha(q) - \alpha(p) - N| < \delta$  then  $|\sigma(p_2) - \sigma(q_2)| < \epsilon$  and  $N = n(q) - n(p)$ . The number  $\delta$  only depends on  $\epsilon$  and the distance from  $\sigma(p_1)$  and  $\sigma(p_2)$  to  $\{0, 1\}$ .*

**Proof:** If  $\delta$  is small enough then  $[\alpha(p) - \sigma(p_1)]$  and  $[\alpha(q) - \sigma(q_1)]$  are very close, and relatively far from 0 or 1. Equation 91 now says that  $\sigma(p_2)$  and  $\sigma(q_2)$  are close. Also, the following two quantities are both near  $N$  while the individual summands are all relatively far from integers.

$$\alpha(q) - \alpha(p); \quad (\alpha(q) - \sigma(q_1)) - (\alpha(p) - \sigma(p_1))$$

But the second quantity is near the integer  $n(q) - n(p)$ , by Equation 91. ♠

Suppose now that  $S_1, S_2, S_3$  is a triple of strips, and  $V_2, V_3$  is a pair of vectors, such that  $(S_1, S_2, V_2)$  and  $(S_2, S_3, V_3)$  are as above. Let  $p_j \in S_j$  for  $j = 1, 2, 3$  be such that  $p_2 = E_2(p_1)$  and  $p_3 = E_3(p_2)$ . Define,

$$\alpha_j = \alpha(S_j, S_{j+1}, V_{j+1}, p_j, p_{j+1}); \quad j = 1, 2; \quad \lambda = \frac{\text{Area}(S_1 \cap S_2)}{\text{Area}(S_2 \cap S_3)}. \quad (92)$$

It is convenient to set  $\sigma_2 = \sigma(p_2)$ .

**Lemma 8.4** *There are constants  $C$  and  $D$  such that  $\alpha_2 = \lambda\alpha_1 + C\sigma_2 + D$ . The constants  $C$  and  $D$  depend on the strips.*

**Proof:** We normalize, as above, so that Equation 90 holds. Then

$$p_2 = (1 - \sigma_2, \alpha_1 + \sigma_2 - 1). \quad (93)$$

There is a unique orientation preserving affine transformation  $T$  such that  $T(S_{j+1}) = S_j$  for  $j = 1, 2$ , and  $T$  the line  $y = 1$  to the line  $x = 0$ . Given that  $S_1 \cap S_2$  has unit area, we have  $\det(T) = \lambda$ . Given the description of  $T$ , we have

$$T(x, y) = \begin{pmatrix} a & \lambda \\ -1 & 0 \end{pmatrix} (x, y) + (b, 1) = (ax + b + \lambda y, 1 - x). \quad (94)$$

Here  $a$  and  $b$  are constants depending on  $S_2 \cap S_3$ . Setting  $q = T(p_2)$ , Equation 90 gives  $\alpha = q_1 + q_2$ . Hence

$$\alpha_2 = a(1 - \sigma_2) + b + \lambda(\alpha_1 + \sigma_2 - 1) + \sigma_2 = \lambda\alpha_1 + C\sigma_2 + D. \quad (95)$$

This completes the proof. ♠

## 8.4 Single Parameter Proof

We are still working under the assumption, in the Torus Lemma, that  $A = A^*$ . Our main argument relies on the Equation 67, which gives a formula for the return pairs in terms of the strip maps. We define the point  $q_j$  relative to  $q$  just as we defined  $p_j$  relative to  $p$ .

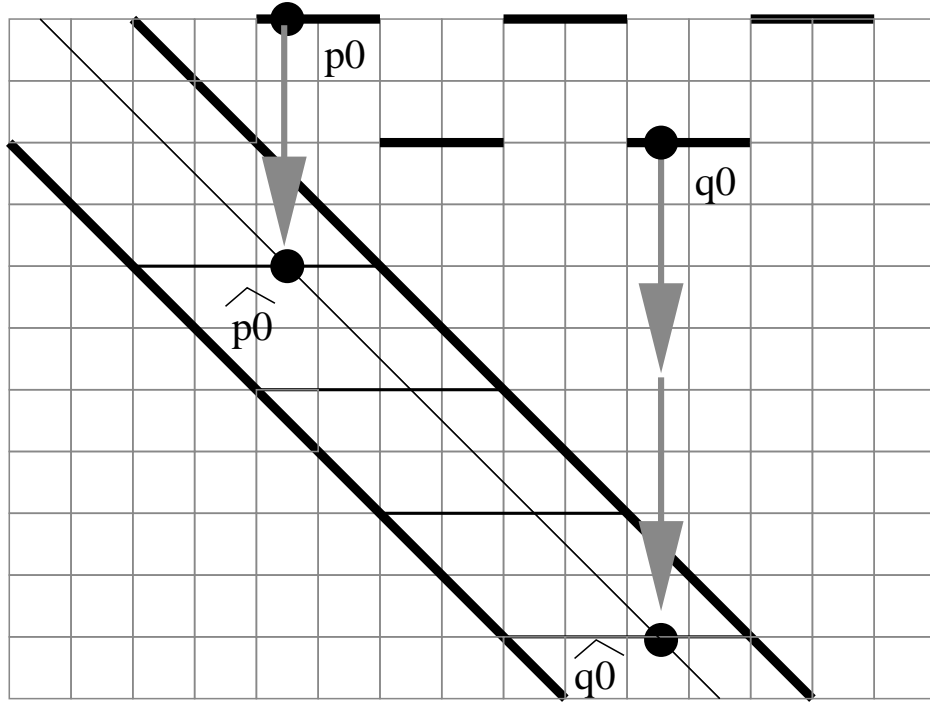


**Figure 8.2:** The points  $\hat{p}_0$  and  $\hat{q}_0$ .

We would like to apply Lemmas 8.2, 8.3, and 8.4 inductively. One inconvenience is that  $p_0$  and  $q_0$  do not lie in any of our strips. To remedy this situation we start with the two points

$$\hat{p}_0 = E_0(p_0); \quad \hat{q}_0 = E_0(q_0). \quad (96)$$

We have  $\hat{p}_0, \hat{q}_0 \in \Sigma_0$ . Let  $t$  be the near-integer from Lemma 8.2. Looking at Figure 8.4, we see that  $|\sigma(\hat{q}_0) - \sigma(\hat{p}_0)|$  tends to 0 as  $\eta$  tends to 0.

We define

$$\alpha_k(p) = \alpha(\Sigma_k, \Sigma_{k+1}, V_{k+1}, p_k, p_{k+1}) \quad (97)$$

It is also convenient to write

$$\sigma_k(p) = \sigma(p_k); \quad \Delta\sigma_k = \sigma_k(q) - \sigma_k(p). \quad (98)$$

For  $k = 0$ , we use  $\widehat{p}_0$  in place of  $p_0$  and  $\widehat{q}_0$  in place of  $q_0$  for these formulas.

**Lemma 8.5** *As  $\eta \rightarrow 0$ , the pairwise differences between the 3 quantities*

$$\alpha_k(q) - \alpha_k(p); \quad n_k(q) - n_k(p); \quad t\widehat{\lambda}_k$$

*converge to 0 for all  $k$ .*

**Proof:** Referring to Figure 8.2, we have

$$\text{Area}(\Sigma_0 \cap \Sigma_1) = 8; \quad \text{Area}(B(\widehat{p}_0)) - \text{Area}(B(\widehat{q}_0)) = 4y - 4x.$$

This gives us  $\alpha_0(q) - \alpha_0(p) = t$ . Applying Lemma 8.4 inductively, we find that

$$\alpha_k = \alpha_0\widehat{\lambda}_k + \sum_{i=1}^k \xi_i\sigma_i + C_k. \quad (99)$$

for constants  $\xi_1, \dots, \xi_k$  and  $C_k$  that depend analytically on  $A$ . Therefore

$$\alpha_k(q) - \alpha_k(p) = t\widehat{\lambda}_k + \sum_{i=1}^k \xi_i\Delta\sigma_i; \quad k = 1, \dots, 7 \quad (100)$$

By Lemma 8.2, the term  $t\lambda_k$  is near an integer for all  $k$ . By Lemma 8.3 and induction, the remaining terms on the right hand side are near 0. This lemma now follows from Lemma 8.3. ♠

Combining our last result with Equation 86, we see that

$$\begin{aligned} n_1(q) - n_1(p) &= n_3(q) - n_3(p) = n_5(q) - n_5(p) = n_7(q) - n_7(p); \\ n_2(q) - n_2(p) &= n_6(q) - n_6(p). \end{aligned} \quad (101)$$

once  $\eta$  is small enough. Given the dependence of constants in Lemma 8.3, the necessary bound on  $\eta$  only depends on  $\min(A, 1 - A)$  and  $\theta(p)$ . Equation 67 now tells us that  $\epsilon_j(p) = \epsilon_j(q)$  for  $j = 1, 2$  once  $\eta$  is small enough.

## 8.5 A Generalization of Lemma 8.3

Now we turn to the proof of the Torus Lemma in the general case. Our first result is the key step that allows us to handle pairs of distinct parameters. Once we set up the notation, the proof is almost trivial. Our second result is a variant that will be useful in the next chapter.

Suppose that  $(S_1, S_2, V_2, p_1, p_2)$  and  $(S_1^*, S_2^*, V_2^*, q_1^*, q_2^*)$  are two quintuples. To fix the picture in our minds we imagine that  $(S_1, S_2, V_2)$  is near  $(S_1^*, S_2^*, V_2^*)$ , though this is not necessary for the proof of the result to follow. We can define the quantities  $\alpha, \rho_j, n$  for each of these quintuples. We put a  $(*)$  by each quantity associated to the second triple.

**Lemma 8.6** *Let  $\epsilon > 0$ . There is some  $\delta > 0$  with the following property. If  $|\sigma(p_1) - \sigma(q_1^*)| < \delta$  and  $|\alpha(q^*) - \alpha(p) - N| < \delta$  then  $|\sigma(p_2) - \sigma(q_2^*)| < \epsilon$  and  $N = n(q^*) - n(p)$ . The number  $\delta$  only depends on  $\epsilon$  and the distance from  $\sigma(p_1)$  and  $\sigma(p_2)$  to  $\{0, 1\}$ .*

**Proof:** There is an affine transformation such that  $T(X^*) = X$  for each object  $X = S_1, S_2, V_2$ . We set  $q_j = T(q_j^*)$ . Then  $\alpha(q_1^*) = \alpha(q_1)$ , by affine invariance. Likewise for the other quantities. Now we apply Lemma 8.3 to the triple  $(S_1, S_2, V_2)$  and the pairs  $(p_1, p_2)$  and  $(q_1, q_2)$ . The conclusion involves quantities with no  $(*)$ , but returning the  $(*)$  does not change any of the quantities. ♠

For use in the next chapter, we state a variant of Lemma 8.6. Let  $[x]$  denote the image of  $x \in \mathbf{R}/\mathbf{Z}$ .

**Lemma 8.7** *Let  $\epsilon > 0$ . There is some  $\delta > 0$  with the following property. If  $|\sigma(p_1) - \sigma(q_1^*)| < \delta$  and  $|\alpha(q^*) - \alpha(p) - N| < \delta$  then the distance from  $[\sigma(p_2)]$  and  $[\sigma(q_2)^*]$  in  $\mathbf{R}/\mathbf{Z}$  is less than  $\epsilon$ .  $|\sigma(p_2) - \sigma(q_2^*)| < \epsilon$  and  $N = n(q^*) - n(p)$ . The number  $\delta$  only depends on  $\epsilon$  and the distance from  $\sigma(p_1)$  to  $\{0, 1\}$ .*

**Proof:** Using the same trick as in Lemma 8.3, we reduce to the single variable case. In this case, we mainly repeat the proof of Lemma 8.3. If  $\delta$  is small enough then  $[\alpha(p) - \sigma(p_1)]$  and  $[\alpha(q) - \sigma(q_1)]$  are very close, and relatively far from 0 or 1. Equation 91 now says that  $[\sigma(p_2)]$  and  $[\sigma(q_2)]$  are close in  $\mathbf{R}/\mathbf{Z}$ . ♠

## 8.6 Proof in the General Case

We no longer suppose that  $A = A^*$ , and we return to the original notation  $(q^*, A^*)$  for the second point. In our proof of this result, we attach a  $(*)$  to any quantity that depends on  $(q^*, A^*)$ . We first need to repeat the analysis from §8.2, this time keeping track of the parameter. Let  $\eta$  be as in the Torus Lemma. We use the big  $O$  notation.

**Lemma 8.8** *There is an integer  $I_k$  such that  $|\alpha_0^* \widehat{\lambda}_k^* - \alpha_0 \lambda_k - I_k| < O(\eta)$ .*

**Proof:** Let  $[V]$  denote the distance from  $V \in \mathbf{R}^3$  to the nearest point in  $\mathbf{Z}^3$ . Let  $p = (x, \pm 1)$  and  $q^* = (x^*, \pm 1)$ . Recalling the definition of  $\mu_+$ , the hypotheses in the Torus Lemma imply that

$$\left[ H^* \left( \frac{x^*}{2}, \frac{x^*}{2} + 1, \frac{x^*}{2} \right) - H \left( \frac{x}{2}, \frac{x}{2} + 1, \frac{x}{2} \right) \right] < O(\eta) \quad (102)$$

We compute that  $\alpha_0 = x/2 + 1/2$ , independent of parameter. Therefore

$$H \left( \frac{x}{2}, \frac{x}{2} + 1, \frac{x}{2} \right) = H(\alpha_0, \alpha_0, \alpha_0) + \frac{1}{2} H(-1, 1, -1).$$

The same goes with the starred quantities. Therefore,

$$[(\widehat{\lambda}_2^*, \widehat{\lambda}_1^* - 1, 1)\alpha_0^* - (\widehat{\lambda}_2, \widehat{\lambda}_1 - 1, 1)\alpha_0] =$$

$$[H^*(\alpha_0^*, \alpha_0^*, \alpha_0^*) - H(\alpha_0, \alpha_0, \alpha_0)] < O(\eta) + \|(H^* - H)(-1, 1, -1)\| < O(\eta).$$

Our lemma now follows immediately from Equation 86. ♠

The integer  $I_k$  of course depends on  $(p, A)$  and  $(q^*, A^*)$ , but in all cases Equation 86 gives us

$$I_0 = I_4; \quad I_1 = I_3 = I_5 = I_7; \quad I_2 = I_6, \quad (103)$$

**Lemma 8.9** *As  $\eta \rightarrow 0$ , the pairwise differences between the 3 quantities  $\alpha_k^* - \alpha_k$  and  $n_k^* - n_k$  and  $I_k$  tends to 0 for all  $k$ .*

**Proof:** Here  $\alpha_k^*$  stands for  $\alpha_k(q^*)$ , etc. Equation 99 works separately for each parameter. The replacement for Equation 100 is

$$\alpha_k^* - \alpha_k = W + X + Y; \quad W = \alpha_0^* \widehat{\lambda}_k^* - \alpha_0 \widehat{\lambda}_k \quad (104)$$

$$X = \sum_{i=1}^k \xi_i^* \sigma_i^*(q^*) - \sum_{i=1}^k \xi_i \sigma_i(p) = \sum_{i=1}^k \xi_i (\sigma_i^* - \sigma_i) + O(|A - A^*|); \quad (105)$$

$$Y = \sum_{i=1}^k C_i^* - \sum_{i=1}^k C_i = O(|A - A^*|). \quad (106)$$

The estimates on  $X$  and  $Y$  comes from the fact  $\xi_i$  and  $C_i$  vary smoothly with  $A$ . Putting everything together, we get the following.

$$\alpha_k^* - \alpha_k = \left( \alpha_0^* \widehat{\lambda}_k^* - \alpha_0 \lambda_k \right) + \sum_{i=1}^k \xi_i (\sigma_i^* - \sigma_i) + O(|A - A^*|). \quad (107)$$

In light of Lemma 8.8, it suffices to show that  $\sigma_i^* - \sigma_i$  tends to 0 as  $\eta$  tends to 0. The same argument as in the single parameter case works here, with Lemma 8.6 used in place of Lemma 8.3. ♠

Similar to the single parameter case, Equations 67 and 103 now finish the proof.

## 9 The Strip Functions

### 9.1 The Main Result

The purpose of this chapter is to understand the functions  $\sigma_j$  that arose in the proof of the Master Picture Theorem. We call these functions the *strip functions*.

Let  $W_k \subset \Xi_+ \times (0, 1)$  denote the set of points where  $E_k \dots E_1$  is defined but  $E_{k+1} E_k \dots E_1$  is not defined. Let  $S_k$  denote the closure of  $\mu_+(W_k)$  in  $R$ . Finally, let

$$W'_k = \bigcup_{j=0}^{k-1} W_j; \quad S'_k = \bigcup_{j=0}^{k-1} S_j; \quad k = 1, \dots, 7. \quad (108)$$

The Torus Lemma applies to any point that does not lie in the *singular set*

$$S = S_0 \cup \dots \cup S_7. \quad (109)$$

If  $p \in \Xi_+ - W'_k$  then the points  $p = p_0, \dots, p_k$  are defined. Here, as in the previous chapter,  $p_j = E_j(p_{j-1})$ . The functions  $\sigma_1, \dots, \sigma_k$  and  $\alpha_1, \dots, \alpha_k$  are defined for such a choice of  $p$ . Again,  $\sigma_j$  measures the position of  $p_j$  in  $\Sigma_j$ , relative to  $\partial\Sigma_j$ . Even if  $E_{k+1}$  is not defined on  $p_k$ , the equivalence class  $[p_{k+1}]$  is well defined in the cylinder  $\mathbf{R}^2 / \langle V_{k+1} \rangle$ . The corresponding function  $\sigma_{k+1}(q) = \sigma(q_{k+1})$  is well defined as an element of  $\mathbf{R}/\mathbf{Z}$ .

Let  $\pi_j : \mathbf{R}^4 \rightarrow \mathbf{R}$  be the  $j$ th coordinate projection. Let  $[x]$  denote the image of  $x$  in  $\mathbf{R}/\mathbf{Z}$ . The following identities refer to the (+) case. We discuss the (-) case at the end of the chapter.

$$\sigma_1 = \left[ \frac{2 - \pi_3}{2} \right] \circ \mu_+ \quad \text{on } \Xi_+ \quad (110)$$

$$\sigma_2 = \left[ \frac{1 + A - \pi_2}{1 + A} \right] \circ \mu_+ \quad \text{on } \Xi_+ - W'_1 \quad (111)$$

$$\sigma_3 = \left[ \frac{1 + A - \pi_1}{1 + A} \right] \circ \mu_+ \quad \text{on } \Xi_+ - W'_2 \quad (112)$$

$$\sigma_4 = \left[ \frac{1 + A - \pi_1 - \pi_2 + \pi_3}{2} \right] \circ \mu_+ \quad \text{on } \Xi_+ - W'_3 \quad (113)$$

In the next chapter we deduce the Master Picture Theorem from these identities and the Torus Lemma. In this chapter, we prove the identities.

## 9.2 Continuous Extension

Let  $g = \sigma_j$  for  $j = 0, \dots, k + 1$ . since the image  $\mu_+(\Xi \times (0, 1))$  is dense in  $R - S'_k$ , we define

$$\tilde{g}(\tau) := \lim_{n \rightarrow \infty} g(p_n, A_n); \quad \tau \in R - S'_k. \quad (114)$$

Here  $(p_n, A_n)$  is chosen so that all functions are defined and  $\mu_+(p_n, A_n) \rightarrow \tau$ . Note that the sequence  $\{p_n\}$  need not converge.

**Lemma 9.1** *The functions  $\tilde{\sigma}_1, \dots, \tilde{\sigma}_{k+1}$ , considered as  $\mathbf{R}/\mathbf{Z}$ -valued functions, are well defined and continuous on  $R - S'_k$ .*

**Proof:** For the sake of concreteness, we will give the proof in the case  $k = 2$ . This representative case explains the idea. First of all, the continuity follows from the well-definedness. We just have to show that the limit above is always well defined.  $\tilde{\sigma}_1$  is well defined and continuous on all of  $R$ , by Equation 110.

Since  $S'_1 \subset S'_2$ , we see that  $\tau \in R - S'_1$ . Hence  $\tau$  does not lie in the closure of  $\mu_+(W_0)$ . Hence, there is some  $\theta_1 > 0$  such that  $\theta_1(p_n, A_n) > \theta_1$  for all sufficiently large  $n$ . Note also that there is a positive and uniform lower bound to  $\min(A_n, 1 - A_n)$ . Note that  $[\alpha_1(p_n, A_n)] = [\pi_3(\mu_+(p_n, A_n))]$ . Hence  $\{[\alpha_1(p_n, A_n)]\}$  is a Cauchy sequence in  $\mathbf{R}/\mathbf{Z}$ .

Lemma 8.7 now applies uniformly to

$$(p, A) = (p_m, A_m); \quad (q^*, A^*) = (p_n, A_n)$$

for all sufficiently large pairs  $(m, n)$ . Since  $\{\mu_+(p_n, A_n)\}$  forms a Cauchy sequence in  $R$ , Lemma 8.7 implies that  $\{\sigma_2(\tau_m, A_m)\}$  forms a Cauchy sequence in  $\mathbf{R}/\mathbf{Z}$ . Hence,  $\tilde{\sigma}_2$  is well defined on  $R - S'_1$ , and continuous.

Since  $\tau \in R - S'_2$ , we see that  $\tau$  does not lie in the closure of  $\mu_+(W_1)$ . Hence, there is some  $\theta_2 > 0$  such that  $\theta_j(p_n, A_n) > \theta_j$  for  $j = 1, 2$  and all sufficiently large  $n$ . As in our proof of the General Torus Lemma, Equation 107 now says that shows that  $\{\alpha_2(p_n, A_n)\}$  forms a Cauchy sequence in  $\mathbf{R}/\mathbf{Z}$ . We now repeat the previous argument to see that  $\{\sigma_3(\tau_m, A_m)\}$  forms a Cauchy sequence in  $\mathbf{R}/\mathbf{Z}$ . Hence,  $\tilde{\sigma}_3$  is well defined on  $R - S'_2$ , and continuous. ♠

Implicit in our proof above is the function

$$\beta_k = [\alpha_k] \in \mathbf{R}/\mathbf{Z}. \quad (115)$$

This function will come in handy in our next result.

### 9.3 Quality of the Extension

Let  $X = R - \partial R \subset \mathbf{R}^4$ . Note that  $X$  is open and convex

**Lemma 9.2** *Suppose  $X \subset R - S'_k$ . Then  $\tilde{\sigma}_{k+1}$  is locally affine on  $X_A$ .*

**Proof:** Since  $\tilde{\sigma}_{k+1}$  is continuous on  $X$ , it suffices to prove this lemma for a dense set of  $A$ . We can choose  $A$  so that  $\mu_+(\Xi_+)$  is dense in  $X_A$ .

We already know that  $\tilde{\sigma}_1, \dots, \tilde{\sigma}_{k+1}$  are all defined and continuous on  $X$ . We already remarked that Equation 110 is true by direct inspection. As we already remarked in the previous proof,  $\beta_0 = \pi_3 \circ \mu_+$ . Thus, we define  $\tilde{\beta}_0 = [\pi_3]$ . Let  $\tilde{\beta}_0 = [\pi_3]$ . Both  $\tilde{\sigma}_0$  and  $\tilde{\beta}_0$  are locally affine on  $X_A$ .

Let  $m \leq k$ . The second half of Equation 91 tells us that  $\tilde{\sigma}_m$  is a locally affine function of  $\tilde{\sigma}_{m-1}$  and  $\tilde{\beta}_{m-1}$ . Below we will prove that  $\tilde{\beta}_m$  is defined on  $X_A$ , and locally affine, provided that  $\tilde{\sigma}_1, \dots, \tilde{\sigma}_m$  are locally affine. Our lemma follows from this claim and induction.

Now we prove the claim. All the addition below is done in  $\mathbf{R}/\mathbf{Z}$ . Since  $\mu_+(\Xi_+)$  is dense in  $X_A$ , we can at least define  $\tilde{\beta}_m$  on a dense subset of  $X_A$ . Define

$$p = (x, \pm 1); \quad p' = (x', \pm 1); \quad \tau = \mu_+(p); \quad \tau' = \mu_+(p'); \quad t = \frac{x' - x}{2}. \quad (116)$$

We choose  $p$  and  $p'$  so that the pinwheel map is entirely defined.

From Equation 100, we have

$$\tilde{\beta}_m(\tau') - \tilde{\beta}_m(\tau) = [t\hat{\lambda}_k] + \sum_{j=1}^m [\xi_j \times (\tilde{\sigma}_j(\tau') - \tilde{\sigma}_j(\tau))]. \quad (117)$$

Here  $\xi_1, \dots, \xi_m$  are constants that depend on  $A$ . Let  $H$  be the matrix in Equation 87. We have  $H(t, t, t) \equiv H(\tau' - \tau) \pmod{\mathbf{Z}^3}$  because  $(t, t, t) \equiv \tau' - \tau \pmod{\Lambda}$ . Our analysis in §8.2 shows that

$$[t\hat{\lambda}_k] = [\pi \circ H(t, t, t) - \epsilon t] = [(\pi - \epsilon\pi_3) \circ H(\tau' - \tau)]. \quad (118)$$

Here  $\epsilon \in \{0, 1\}$  and  $\pi$  is some coordinate projection. The choice of  $\epsilon$  and  $\pi$  depends on  $k$ . We now see that

$$\tilde{\beta}_m(\tau') = \tilde{\beta}_m(\tau) + (\pi + \epsilon_3\pi) \circ H(\tau' - \tau) + \sum_{j=1}^m [\xi_j \times (\tilde{\sigma}_j(\tau') - \tilde{\sigma}_j(\tau))]. \quad (119)$$

The right hand side is everywhere defined and locally affine. Hence, we define  $\tilde{\beta}_m$  on all of  $X_A$  using the right hand side of the last equation. ♠

**Lemma 9.3** *Suppose  $X \subset R - S'_k$ . Then  $\sigma_{k+1}$  is analytic on  $X$ .*

**Proof:** The constants  $\xi_j$  in Equation 117 vary analytically with  $A$ . Our argument in Lemma 9.2 therefore shows that the linear part of  $\sigma_{k+1}$  varies analytically with  $A$ . We just have to check the linear term. Since  $X_A$  is connected we can compute the linear term of  $\sigma_{k+1}$  at  $A$  from a single point. We choose  $p = (\epsilon, 1)$  where  $\epsilon$  is very close to 0. The fact that  $A \rightarrow \sigma_k(p, A)$  varies analytically follows from the fact that our strips vary analytically. ♠

**Remark:** We have  $S_k \subset \tilde{\sigma}_{k+1}^{-1}([0])$ . Given Equation 110, we see that  $X \subset R - S'_1$ . Hence  $\sigma_2$  is defined on  $X$ . Hence  $\sigma_2$  is analytic on  $X$  and locally affine on each  $X_A$ . We use these two properties to show that Equation 111 is true. But then  $X \subset R - S'_2$ . etc. So, we will know at each stage of our verification that Lemmas 9.2 and 9.3 apply to the function of interest.

Equations 111, 112, and 113 are formulas for  $\tilde{\sigma}_2$ ,  $\tilde{\sigma}_3$ , and  $\tilde{\sigma}_4$  respectively. Let  $f_{k+1} = \tilde{\sigma}_{k+1} - \sigma'_{k+1}$ , where  $k = 2, 3, 4$ . Here  $\sigma'_{k+1}$  is the right hand side of the identity for  $\tilde{\sigma}_{k+1}$ . Our goal is to show that  $f_{k+1} \equiv [0]$  for  $k = 1, 2, 3$ . Call a parameter  $A$  *good* if  $f_{k+1} \equiv [0]$  on  $X_A$ . Call a subset  $S \subset (0, 1)$  *substantial* if  $S$  is dense in some open interval of  $(0, 1)$ . By analyticity,  $f_{k+1} \equiv [0]$  provided that a substantial set of parameters is good.

In the next section we explain how to verify that a parameter is good. If  $f_{k+1}$  was a locally affine map from  $X_A$  into  $\mathbf{R}$ , we would just need to check that  $f_{k+1} = 0$  on some tetrahedron on  $X_A$  to verify that  $A$  is a good parameter. Since the range of  $f_{k+1}$  is  $\mathbf{R}/\mathbf{Z}$ , we have to work a bit harder.

## 9.4 Irrational Quintuples

We will give a construction in  $\mathbf{R}^3$ . When the time comes to use the construction, we will identify  $X_A$  as an open subset of a copy of  $\mathbf{R}^3$ .

Let  $\zeta_1, \dots, \zeta_5 \in \mathbf{R}^3$  be 5 points. By taking these points 4 at a time, we can compute 5 volumes,  $v_1, \dots, v_5$ . Here  $v_j$  is the volume of the tetrahedron obtained by omitting the  $j$ th point. We say that  $(\zeta_1, \dots, \zeta_5)$  is an *irrational quintuple* if there is no rational relation

$$\sum_{i=1}^5 c_i \zeta_i = 0; \quad c_j \in \mathbf{Q}; \quad c_1 c_2 c_3 c_4 c_5 = 0. \quad (120)$$

If we allow all the constants to be nonzero, then there is always a relation.

**Lemma 9.4** *Let  $C$  be an open convex subset of  $\mathbf{R}^3$ . Let  $f : C \rightarrow \mathbf{R}/\mathbf{Z}$  be a locally affine function. Suppose that there is an irrational  $(\zeta_1, \dots, \zeta_5)$  such that  $\zeta_j \in C$  and  $f(\zeta_j)$  is the same for all  $j$ . Then  $f$  is constant on  $C$ .*

**Proof:** Since  $C$  is simply connected, we can lift  $f$  to a locally affine function  $F : C \rightarrow \mathbf{R}$ . But then  $F$  is affine on  $C$ , and we can extend  $F$  to be an affine map from  $\mathbf{R}^3$  to  $\mathbf{R}$ . By construction  $F(\zeta_i) - F(\zeta_j) \in \mathbf{Z}$  for all  $i, j$ . Adding a constant to  $F$ , we can assume that  $F$  is linear. There are several cases.

**Case 1:** Suppose that  $F(\zeta_j)$  is independent of  $j$ . In this case, all the points lie in the same plane, and all volumes are zero. This violates the irrationality condition.

**Case 2:** Suppose we are not in Case 1, and the following is true. For every index  $j$  there is a second index  $k$  such that  $F(\zeta_k) = F(\zeta_j)$ . Since there are 5 points total, this means that the set  $\{F(\zeta_j)\}$  only has a total of 2 values. But this means that our 5 points lie in a pair of parallel planes,  $\Pi_1 \cup \Pi_2$ , with 2 points in  $\Pi_1$  and 3 points in  $\Pi_2$ . Let's say that that  $\zeta_1, \zeta_2, \zeta_3 \in \Pi_1$  and  $\zeta_4, \zeta_5 \in \Pi_2$ . But then  $v_4 = v_5$ , and we violate the irrationality condition.

**Case 3:** If we are not in the above two cases, then we can relabel so that  $F(\zeta_1) \neq F(\zeta_j)$  for  $j = 2, 3, 4, 5$ . Let

$$\zeta'_j = \zeta_j - \zeta_1.$$

Then  $\zeta'_1 = (0, 0, 0)$  and  $F(\zeta'_1) = 0$ . But then  $F(\zeta'_j) \in \mathbf{Z} - \{0\}$  for  $j = 2, 3, 4, 5$ . Note that  $v'_j = v_j$  for all  $j$ . For  $j = 2, 3, 4, 5$ , let

$$\zeta''_j = \frac{\zeta'_j}{F(\zeta'_j)}.$$

Then  $v''_j/v'_j \in \mathbf{Q}$  for  $j = 2, 3, 4, 5$ . Note that  $F(\zeta''_j) = 1$  for  $j = 2, 3, 4, 5$ . Hence there is a plane  $\Pi$  such that  $\zeta''_j \in \Pi$  for  $j = 2, 3, 4, 5$ .

There is always a rational relation between the areas of the 4 triangles defined by 4 points in the plane. Hence, there is a rational relation between  $v''_2, v''_3, v''_4, v''_5$ . But then there is a rational relation between  $v_2, v_3, v_4, v_5$ . This contradicts the irrationality condition. ♠

## 9.5 Verification in the Plus Case

Proceeding somewhat at random, we define

$$\phi_j = \left(8jA + \frac{1}{2j}, 1\right); \quad j = 1, 2, 3, 4, 5. \quad (121)$$

We check that  $\phi_j \in \Xi_+$  for  $A$  near  $1/2$ . Letting  $\zeta_j = \mu_+(\phi_j)$ , we check that  $f_{k+1}(\zeta_j) = [0]$  for  $j = 1, 2, 3, 4, 5$ .

**Example Calculation:** Here is an example of what we do automatically in Mathematica. Consider the case  $k = 1$  and  $j = 1$ . When  $A = 1/2$ , the length spectrum for  $\phi_1$  starts out  $(1, 1, 2, 1)$ . Hence, this remains true for nearby  $A$ . Knowing the length spectrum allows us to compute, for instance, that

$$E_2E_1(\phi_1) = \phi_1 + V_1 + V_2 = \left(\frac{-3}{2} + 8A, 7\right) \in \Sigma_2$$

for  $A$  near  $1/2$ . The affine functional

$$(x, y) \rightarrow (x, y, 1) \cdot \frac{(-1, A, A)}{2 + 2A} \quad (122)$$

takes on the value 0 on the line  $x = Ay + A$  and 1 on the line  $x = Ay - 2 - A$ . These are the two edges of  $\Sigma_2$ . (See §11.1.) Therefore,

$$\sigma_2(\phi_1) = \left(\frac{-3}{2} + 8A, 7, 1\right) \cdot \frac{(-1, A, A)}{2 + 2A} = \frac{3}{4 + 4A}.$$

At the same time, we compute that

$$\mu_+(\phi_1) = \frac{1}{4}(-7 + 24A, 1 + 4A, -7 + 16A),$$

at least for  $A$  near  $1/2$ . When  $A$  is far from  $1/2$  this point will not lie in  $R_A$ . We then compute

$$\frac{1 + A - \pi_2(\mu_+(\phi_1))}{1 + A} = \frac{3}{4 + 4A}.$$

This shows that  $f_2(\zeta_2) = [0]$  for all  $A$  near  $1/2$ . The verifications for the other pairs  $(k, j)$  are similar.

**Checking Irrationality:** It only remains to check that the points  $(\zeta_1, \dots, \zeta_5)$  form an irrational quintuple for a dense set of parameters  $A$ . In fact this will true in the complement of a countable set of parameters.

The 5 volumes associated to our quintuple are as follows.

- $v_5 = 5/24 - 5A/12 + 5A^2/24.$
- $v_4 = 71/40 + 19A/20 - 787A^2/120 - 4A^3.$
- $v_3 = 119/60 + 7A/60 - 89A^2/15 - 4A^3$
- $v_2 = -451/240 - 13A/40 + 1349A^2/240 + 4A^3$
- $v_1 = -167/80 - 13A/40 + 533A^2/80 + 4A^3.$

If there is an open set of parameters for which the first 4 of these volumes has a rational relation, then there is an infinite set on which the same rational relation holds. Since every formula in sight is algebraic, this means that there must be a single rational relation that holds for all parameters. But then the curve  $A \rightarrow (v_5, v_4, v_3, v_2)$  lies in a proper linear subspace of  $\mathbf{R}^4$ .

We evaluate this curve at  $A = 1, 2, 3, 4$  and see that the resulting points are linearly independent in  $\mathbf{R}^4$ . Hence, there is no global rational relation. Hence, on a dense set of parameters, there is no rational relation between the first 4 volumes listed. A similar argument rules out rational relations amongst any other 4-tuple of these volumes.

## 9.6 The Minus Case

In the  $(-)$  case, Equations 111 and 112 do not change, except that  $\mu_-$  replaces  $\mu_+$  and all the sets are defined relative to  $\Xi_-$  and  $\mu_-$ . Equations 110 and 113 become

$$\sigma_1 = \left[ \frac{1 - \pi_3}{2} \right] \circ \mu_- \quad \text{on } \Xi_-. \quad (123)$$

$$\sigma_4 = \left[ \frac{A - \pi_1 - \pi_2 + \pi_3}{2} \right] \circ \mu_- \quad \text{on } \Xi_- - S'_3. \quad (124)$$

Lemma 9.2 and Lemma 9.3 have the same proof in the  $(-)$  case. We use the same method as above, except that we use the points

$$\phi_j + (2, 0); \quad j = 1, 2, 3, 4, 5. \quad (125)$$

These points all lie in  $\Xi_-$  for  $A$  near  $1/2$ . The rest of the verification is essentially the same as in the  $(+)$  case.

## 10 Proof of the Master Picture Theorem

### 10.1 The Main Argument

Let  $S$  be the singular set defined in Equation 109. Let  $\tilde{S}$  denote the union of hyperplanes listed in §6.2. let  $d$  denote distance on the polytope  $R$ . In this chapter we will prove

**Lemma 10.1 (Hyperplane)**  $S \subset \tilde{S}$  and  $\theta(p, A) \geq d(\mu_+(p, A), \tilde{S})$ .

We finish the proof of the Master Picture Theorem assuming the Hyperplane Lemma.

Say that a *ball of constancy* in  $R - \tilde{S}$  is an open ball  $B$  with the following property. If  $(p_0, A_0)$  and  $(p_1, A_1)$  are two pairs and  $\mu_+(p_j, A_k) \in B$  for  $j = 0, 1$ , then  $(p_0, A_0)$  and  $(p_1, A_1)$  have the same return pair. Here is a consequence of the Torus Lemma.

**Corollary 10.2** *Any point  $\tau$  of  $R - \tilde{S}$  is contained in a ball of constancy.*

**Proof:** If  $\tau$  is in the image of  $\mu_+$ , this result is an immediate consequence of the Torus Lemma. In general, the image  $\mu_+(\Xi_+ \times (0, 1))$  is dense in  $R$ . Hence, we can find a sequence  $\{\tau_n\}$  such that  $\tau_n \rightarrow \tau$  and  $\tau_n = \mu_+(p_n, A_n)$ . Let  $2\theta_0 > 0$  be the distance from  $\tau$  to  $S$ . From the triangle inequality and the second statement of the Hyperplane Lemma,  $\theta(p_n, A_n) \geq \theta_0 = \theta_1 > 0$  for large  $n$ . By the Torus Lemma,  $\tau_n$  is the center of a ball  $B_n$  of constancy whose radius depends only on  $\theta_0$ . In particular – and this is really all that matters in our proof – the radius of  $B_n$  does not tend to 0. Hence, for  $n$  large enough,  $\tau$  itself is contained in  $B_n$ . ♠

**Lemma 10.3** *Let  $(p_0, A_0)$  and  $(p_1, A_1)$  be two points of  $\Xi_+ \times (0, 1)$  such that  $\mu_+(p_0, A_0)$  and  $\mu_+(p_1, A_1)$  lie in the same path connected component of  $R - \tilde{S}$ . Then the return pair for  $(p_0, A_0)$  equals the return pair for  $(p_1, A_1)$ .*

**Proof:** Let  $L \subset R - \tilde{S}$  be a path joining points  $\tau_0 = \mu_+(p_0, A_0)$  and  $\tau_1 = \mu_+(p_1, A_1)$ . By compactness, we can cover  $L$  by finitely many overlapping balls of constancy. ♠

Now we just need to see that the Master Picture Theorem holds for one component of the partition of  $R - \tilde{S}$ . Here is an example calculation that does the job. For each  $\alpha = j/16$  for  $j = 1, \dots, 15$ , we plot the image

$$\mu_A(2\alpha + 2n); \quad n = 1, \dots, 2^{15}; \quad (126)$$

The image is contained in the slice  $z = \alpha$ . We see that the Master Picture Theorem holds for all these points. The reader can use Billiard King to plot and inspect millions of points for any desired parameter.

We have really only proved the half of the Master Picture Theorem that deals with  $\Xi_+$  and  $\mu_+$ . The half that deals with  $\Xi_-$  and  $\mu_-$  is exactly the same. In particular, both the Torus Lemma and the Hyperplane Lemma hold *verbatim* in the  $(-)$  case. The proof of the Hyperplane Lemma in the  $(-)$  case differs only in that the two identities in Equation 123 replace Equations 110 and 113. We omit the details in the  $(-)$  case.

## 10.2 The First Four Singular Sets

Our strip function identities make short work of the first four pieces of the singular set.

- Given Equation 110,

$$S_0 \subset \{z = 0\} \cup \{z = 1\}. \quad (127)$$

- Given Equation 111,

$$S_1 \subset \{y = 0\} \cup \{y = 1 + A\}. \quad (128)$$

- Given Equation 112,

$$S_2 \subset \{x = 0\} \cup \{x = 1 + A\}. \quad (129)$$

- Give Equation 113,

$$S_3 \subset \{x + y - z = 1 + A\} \cup \{x + y - z = -1 + A\}. \quad (130)$$

### 10.3 Symmetry

We use symmetry to deal with the remaining pieces. Suppose we start with a point  $p \in \Xi_+$ . We define  $p_0 = p$  and  $p_j = E_j(p)$ . As we go along in our analysis, these points will be defined for increasingly large values of  $j$ . However, for the purposes of illustration, we assume that all points are defined.

Let  $\rho$  denote reflection in the  $x$ -axis. Then

$$\rho(\Sigma_9 - j) = \Sigma_j; \quad q_j = \rho(p_{9-j}); \quad j = 1, 2, 3, 4. \quad (131)$$

Figure 10.1 shows a picture. The disk in the center is included for artistic purposes, to cover up some messy intersections. In the picture, we have included the coordinates for the vectors  $-V_1$  and  $-V_2$  and  $-V_2$  to remind the reader of their values. It is convenient to write  $-V_k$  rather than  $V_k$  because there are far fewer minus signs involved.

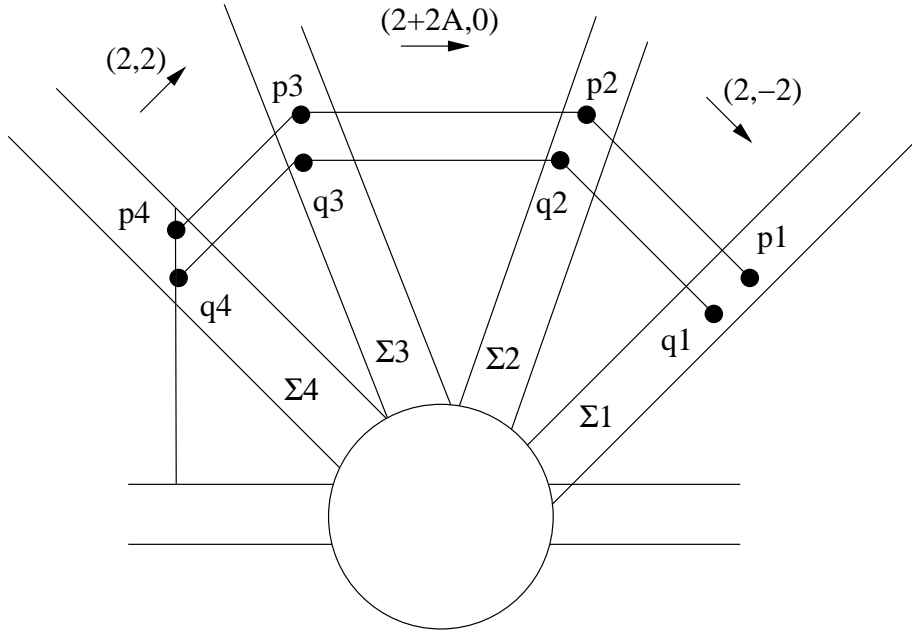


**Figure 10.1:** Reflected points

Here is a notion we will use in our estimates. Say that a strip  $\Sigma$  *dominates* a vector  $V$  if we can translate  $V$  so that it is contained in the interior of the strip. This is equivalent to the condition that we can translate  $V$  so that one endpoint of  $V$  lies on  $\partial\Sigma$  and the other one lies in the interior.

## 10.4 The Remaining Pieces

### 10.4.1 The set $S_4$

Suppose  $p \in W_4$ . Then  $p_5$  and  $q_4$  are defined and  $q_4 \in \partial\Sigma_4$ . Given that  $V_5 = (0, -4)$  and the  $y$ -coordinates of all our points are odd integers, we have  $p_4 - q_4 = (0, 2) + k(0, 4)$  for some  $k \in \mathbf{Z}$ . Given that  $\Sigma_4$  dominates  $p_4 - q_4$  we have  $k \in \{-1, 0\}$ . Hence  $p_4 = q_4 \pm (0, 2)$ . If  $p_5 \in \partial\Sigma_5$  then  $q_4 \in \partial\Sigma_4$ . Any vertical line intersects  $\Sigma_4$  in a segment of length 4. From this we see that  $p_4$  lies on the centerline of  $\Sigma_4$ . That is,  $\sigma_4(p) = 1/2$ . Given Equation 113, we get

$$S_4 \subset \{x + y - z = A\} \cup \{x + y - z = 2 + A\}.$$

### 10.4.2 The Set $S_5$

Suppose that  $p \in W_5$ . Then  $p_6$  and  $q_3$  are defined, and  $q_3 \in \partial\Sigma_3$ . Given that  $V_6 = -V_4 = (-2, 2)$ , we see that

$$p_3 - q_3 = \epsilon(0, 2) + k(2, 2); \quad \epsilon \in \{-1, 1\}; \quad k \in \mathbf{Z}.$$

The criterion that  $\Sigma_3$  dominates a vector  $(x, y)$  is that  $|x + Ay| < 2 + 2A$ .

$\Sigma_3$  dominates the vector  $q_3 - p_3$ . If  $\epsilon = 1$  then  $|2k + 2 + 2Ak| < 2 + 2A$ , forces  $k \in \{-1, 0\}$ . If  $\epsilon = -1$ , then the condition  $|2k - 2 + 2Ak| < 2 + 2A$  forces  $k \in \{0, 1\}$ . Hence  $p_3 - q_3$  is one of the vectors  $(\pm 2, 0)$  or  $(0, \pm 2)$ . Now we have a case-by-case analysis.

Suppose that  $q_3$  lies in the right boundary of  $\Sigma_3$ . Then we have either  $p_3 = q_3 - (2, 0)$  or  $p_3 = q_3 + (0, 2)$ . Any horizontal line intersects  $\Sigma_3$  in a strip of width  $2 + 2A$ . So,  $\sigma_3(p)$  equals either  $1/(1 + A)$  or  $A/(1 + A)$  depending on whether or not  $p_3 = q_3 - (2, 0)$  or  $p_3 = q_3 + (0, 2)$ . A similar analysis reveals the same two values when  $q_3$  lies on the left boundary of  $\Sigma_3$ . Given Equation 112 we get

$$S_5 \subset \{x = A\} \cup \{x = 1\}.$$

### 10.4.3 The Set $S_6$

Suppose that  $p \in W_6$ . Then  $p_7$  and  $q_2$  are defined, and  $q_2 \in \partial\Sigma_2$ . We have

$$p_2 - q_2 = (p_3 - q_3) + k(2 + 2A, 0). \quad (132)$$

The criterion that  $\Sigma_3$  dominates a vector  $(x, y)$  is that  $|x - Ay| < 2 + 2A$ .

Let  $X_1, \dots, X_4$  be the possible values for  $p_3 - q_3$ , as determined in the previous section. Using the values of the vectors  $X_j$ , and the fact that  $\Sigma_2$  dominates  $p_2 - q_2$ , we see that

$$p_2 - q_2 = X_j + \epsilon(2A, 2); \quad \epsilon \in \{-1, 0, 1\}; \quad j \in \{1, 2, 3, 4\}. \quad (133)$$

Note that the vector  $(2A, 2)$  is parallel to the boundary of  $\Sigma_2$ . Hence, for the purposes of computing  $\sigma_2(p)$ , this vector plays no role. Essentially the same calculation as in the previous section now gives us the same choices for  $\sigma_2(p)$  as we got for  $\sigma_3(p)$  in the previous section. Given Equation 111 we get

$$S_6 \subset \{y = A\} \cup \{y = 1\}.$$

#### 10.4.4 The Set $S_7$

Suppose that  $p \in W_7$ . Then  $p_8$  and  $q_1$  are defined, and  $q_1 \in \partial\Sigma_1$ . We have

$$p_1 - q_1 = (p_2 - q_2) + k(-2, 2). \quad (134)$$

Note that the vector  $(2, 2)$  is parallel to  $\Sigma_1$ . For the purposes of finding  $\sigma_1(p)$ , we can do our computation modulo  $(2, 2)$ . For instance,  $(2, -2) \equiv (0, 4) \pmod{(2, 2)}$ . Given Equation 133, we have

$$p_1 - q_1 = \epsilon_1(0, 2) + \epsilon_2(2A, 2) + k(0, 4) \pmod{(2, 2)}. \quad (135)$$

Here  $\epsilon_1, \epsilon_2 \in \{-1, 0, 1\}$ . Given that any vertical line intersects  $\Sigma_1$  in a segment of length 4, we see that the only choices for  $\sigma_1(p)$  are

$$\left[ \frac{k}{2} + 2\epsilon A \right]; \quad \epsilon \in \{-1, 0, 1\}; \quad k \in \mathbf{Z}.$$

Given Equation 110 we see that  $S_7 \subset \{z = A\} \cup \{z = 1 - A\}$ .

## 10.5 Proof of The Second Statement

Our analysis above establishes the first statement of the Hyperplane Lemma. For the second statement, suppose that  $d(\mu_+(p, A), \tilde{S}) = \epsilon$ . Given Equations 110, 111, 112, and 113, we have

$$\theta_j(p) \geq \epsilon; \quad j = 1, 2, 3, 4.$$

Given our analysis of the remaining points using symmetry, the same bound holds for  $j = 5, 6, 7, 8$ . In these cases,  $\theta_j(p, A)$  is a linear function of the distance from  $\mu_+(p, A)$  to  $S_{j-1}$ , and the constant of proportionality is the same as it is for the index  $9 - j$ .

## 11 Some Formulas

### 11.1 Formulas for the Pinwheel Map

In this section we explain how to implement the pinwheel map. We define

$$\begin{aligned} V_1 &= (0, 4); & V_2 &= (-2, 2); \\ V_3 &= (-2 - 2A, 0); & V_4 &= (-2, -2). \end{aligned} \tag{136}$$

Next, we define vectors

$$\begin{aligned} W_1 &= \frac{1}{4}(-1, 1, 3); & W_2 &= \frac{1}{2 + 2A}(-1, A, A); \\ W_3 &= \frac{1}{2 + 2A}(-1, -A, A); & W_4 &= \frac{1}{4}(-1, -1, 3); \end{aligned} \tag{137}$$

For a point  $p \in \mathbf{R}^2$ , we define

$$F_j(p) = W_j \cdot (p_1, p_2, 1). \tag{138}$$

$F(j, p)$  measures the position of  $p$  relative to the strip  $\Sigma_j$ . This quantity lies in  $(0, 1)$  iff  $p$  lies in the interior of  $\Sigma_j$ .

**Example:** Let  $p = (2A, 1)$  and  $q = (-2, 1)$ , we compute that

$$F_2(p) = \frac{1}{2 + 2A}(-1, A, A) \cdot (2A, 1, 1) = 0.$$

$$F_2(q) = \frac{1}{2 + 2A}(-1, A, A) \cdot (-2, 1, 1) = 1.$$

This checks out, because  $p$  lies in one component of  $\partial\Sigma_2$  and  $q$  lies in the other component of  $\partial\Sigma_2$ .

Here is a formula for our strip maps.

$$E_j(p) = p - \text{floor}(F_j(p))V_j. \tag{139}$$

If we set  $V_{4+j} = -V_j$  and  $F_{j+4} = -F_j$  then we get the nice formulas

$$dF_j(V_j) = dF_j(V_{j+1}) = 1. \tag{140}$$

with indices taken mod 8.

## 11.2 The Reduction Algorithm

Let  $A \in (0, 1)$  and  $\alpha \in \mathbf{R}_+$  and  $(m, n) \in \mathbf{Z}^2$  be a point above the baseline of  $\Gamma_\alpha(A)$ . In this section we describe how we compute the points

$$\mu_\pm(M_\alpha(m, n)).$$

This algorithm will be important when we prove the Copy Theorems in Part IV of the monograph.

1. Let  $z = Am + n + \alpha$ .
2. Let  $Z = \text{floor}(z)$ .
3. Let  $y = z + Z$ .
4. Let  $Y = \text{floor}(y/(1 + A))$ .
5. Let  $x = y - Y(1 - A) - 1$ .
6. Let  $X = \text{floor}(x/(1 + A))$ .

We then have

$$\mu_-(M_\alpha(m, n)) = \begin{pmatrix} x - (1 + A)X \\ y - (1 + A)Y \\ z - Z \end{pmatrix} \quad (141)$$

The description of  $\mu_+$  is identical, except that the third step above is replaced by

$$y = z + Z + 1. \quad (142)$$

**Example:** Referring to §6.4, consider the case when  $A = 3/5$  and  $\alpha = 1/10$  and  $(m, n) = (4, 2)$ . We get

$$z = \frac{9}{2}; \quad Z = 4; \quad y = \frac{17}{2}; \quad Y = \text{floor}\left(\frac{17/2}{8/5}\right) = 5.$$

$$x = \frac{17}{2} - 5\left(\frac{2}{5}\right) - 1 = \frac{11}{2}; \quad X = \text{floor}\left(\frac{11/2}{8/5}\right) = 3.$$

$$\mu_-(M(4, 2)) = \left(\frac{11}{2} - 3\left(\frac{8}{5}\right), \frac{17}{2} - 5\left(\frac{8}{5}\right), \frac{9}{2} - 4\right) = \left(\frac{7}{10}, \frac{1}{2}, \frac{1}{2}\right).$$

## 11.3 Computing the Partition

Here we describe how Billiard King applies the Master Picture Theorem.

### 11.3.1 Step 1

Suppose  $(a, b, c) \in R_A$  lies in the range of  $\mu_+$  or  $\mu_-$ . Now we describe how to attach a 5-tuple  $(n_0, \dots, n_4)$  to  $(a, b, c)$ .

- Determining  $n_0$ :
  - If we are interested in  $\mu_+$ , then  $n_0 = 0$ .
  - If we are interested in  $\mu_-$ , then  $n_0 = 1$ .
- Determining  $n_1$ :
  - If  $c < A$  and  $c < 1 - A$  then  $n_1 = 0$ .
  - If  $c > A$  and  $c < 1 - A$  then  $n_1 = 1$ .
  - If  $c > A$  and  $c > 1 - A$  then  $n_1 = 2$ .
  - If  $c < A$  and  $c > 1 - A$  then  $n_1 = 3$ .
- Determining  $n_2$ :
  - If  $a \in (0, A)$  then  $n_2 = 0$ .
  - If  $a \in (A, 1)$  then  $n_2 = 1$ .
  - If  $a \in (1, 1 + A)$  then  $n_2 = 2$ .
- Determining  $n_3$ :
  - If  $b \in (0, A)$  then  $n_3 = 0$ .
  - If  $b \in (A, 1)$  then  $n_3 = 1$ .
  - If  $b \in (1, 1 + A)$  then  $n_3 = 2$ .
- Determining  $n_4$ :
  - Let  $t = a + b - c$ .
  - Let  $n_4 = \text{floor}(t - A)$ .

Notice that each 5-tuple  $(n_0, \dots, n_4)$  corresponds to a (possibly empty) convex polyhedron in  $R_A$ . The polyhedron doesn't depend on  $n_0$ . It turns out that this polyhedron is empty unless  $n_4 \in \{-2, -1, 0, 1, 2\}$ .

### 11.3.2 Step 2

Let  $n = (n_0, \dots, n_4)$ . We now describe two functions  $\epsilon_1(n) \in \{-1, 0, 1\}$  and  $\epsilon_2(n) \in \{-1, 0, 1\}$ .

Here is the definition of  $\epsilon_1(n)$ .

- If  $n_0 + n_4$  is even then:
  - If  $n_2 + n_3 = 4$  or  $x_2 < x_3$  set  $\epsilon_1(n) = -1$ .
- If  $n_0 + n_4$  is odd then:
  - If  $n_2 + n_3 = 0$  or  $x_2 > x_3$  set  $\epsilon_1(n) = +1$ .
- Otherwise set  $\epsilon_1(n) = 0$ .

Here is the definition of  $\epsilon_2(n)$ .

- If  $n_0 = 0$  and  $n_1 \in \{3, 0\}$ .
  - If  $n_2 = 0$  let  $\epsilon_2(n) = 1$ .
  - If  $n_2 = 1$  and  $n_4 \neq 0$  let  $\epsilon_2(n) = 1$ .
- If  $n_0 = 1$  and  $n_1 \in \{0, 1\}$ .
  - if  $n_2 > 0$  and  $n_4 \neq 0$  let  $\epsilon_2(n) = -1$ .
  - If  $n_2 < 2$  and  $n_3 = 0$  and  $n_4 = 0$  let  $\epsilon_2(n) = 1$ .
- If  $n_0 = 0$  and  $n_1 \in \{1, 2\}$ .
  - If  $n_2 < 2$  and  $n_4 \neq 0$  let  $\epsilon_2(n) = 1$ .
  - If  $n_2 > 0$  and  $n_3 = 2$  and  $n_4 = 0$  let  $\epsilon_2(n) = -1$ .
- If  $n_0 = 1$  and  $n_1 \in \{2, 3\}$ .
  - If  $n_2 = 2$  let  $\epsilon_2(n) = -1$ .
  - If  $n_2 = 1$  and  $n_4 \neq 0$  let  $\epsilon_2(n) = -1$ .
- Otherwise let  $\epsilon_2(n) = 0$ .

### 11.3.3 Step 3

Let  $A \in (0, 1)$  be any parameter and let  $\alpha > 0$  be some parameter such that  $\alpha \notin 2\mathbf{Z}[A]$ . Given any lattice point  $(m, n)$  we perform the following construction.

- Let  $(a_{\pm}, b_{\pm}, c_{\pm}) = \mu_{\pm}(A, m, n)$ . See §11.2.
- Let  $n_{\pm}$  be the 5-tuple associated to  $(a_{\pm}, b_{\pm}, c_{\pm})$ .
- Let  $\epsilon_1^{\pm} = \epsilon_1(n_{\pm})$  and  $\epsilon_2^{\pm} = \epsilon_2(n_{\pm})$ .

The Master Picture Theorem says that the two edges of  $\Gamma_{\alpha}(m, n)$  incident to  $(m, n)$  are  $(m, n) + (\epsilon_1^{\pm}, \epsilon_2^{\pm})$ .

## 11.4 The List of Polytopes

Referring to the simpler partition from §6.6, we list the 14 polytopes that partition  $R_+$ . In each case, we list some vectors, followed by the pair  $(\epsilon_1, \epsilon_2)$  that the polytope determines.

$$\begin{array}{cccccccc}
 \begin{bmatrix} 0 \\ 0 \\ 0 \\ 0 \end{bmatrix} & \begin{bmatrix} 0 \\ 0 \\ 0 \\ 1 \end{bmatrix} & \begin{bmatrix} 0 \\ 0 \\ 1 \\ 0 \end{bmatrix} & \begin{bmatrix} 0 \\ 1 \\ 0 \\ 1 \end{bmatrix} & \begin{bmatrix} 0 \\ 1 \\ 1 \\ 1 \end{bmatrix} & \begin{bmatrix} 1 \\ 0 \\ 0 \\ 1 \end{bmatrix} & \begin{bmatrix} 1 \\ 0 \\ 1 \\ 0 \end{bmatrix} & \begin{bmatrix} 1 \\ 0 \\ 1 \\ 1 \end{bmatrix} & \begin{bmatrix} 1 \\ 1 \\ 1 \\ 1 \end{bmatrix} & (1, 1) \\
 \begin{bmatrix} 0 \\ 0 \\ 0 \\ 0 \end{bmatrix} & \begin{bmatrix} 0 \\ 1 \\ 0 \\ 0 \end{bmatrix} & \begin{bmatrix} 0 \\ 1 \\ 0 \\ 1 \end{bmatrix} & \begin{bmatrix} 0 \\ 2 \\ 0 \\ 1 \end{bmatrix} & \begin{bmatrix} 0 \\ 2 \\ 1 \\ 1 \end{bmatrix} & \begin{bmatrix} 1 \\ 1 \\ 0 \\ 1 \end{bmatrix} & \begin{bmatrix} 1 \\ 1 \\ 1 \\ 1 \end{bmatrix} & \begin{bmatrix} 1 \\ 1 \\ 1 \\ 1 \end{bmatrix} & \begin{bmatrix} 1 \\ 2 \\ 1 \\ 1 \end{bmatrix} & (-1, 1) \\
 \begin{bmatrix} 0 \\ 1 \\ 0 \\ 0 \end{bmatrix} & \begin{bmatrix} 0 \\ 1 \\ 0 \\ 0 \end{bmatrix} & \begin{bmatrix} 1 \\ 1 \\ 0 \\ 0 \end{bmatrix} & \begin{bmatrix} 1 \\ 1 \\ 1 \\ 1 \end{bmatrix} & \begin{bmatrix} 1 \\ 2 \\ 1 \\ 1 \end{bmatrix} & \begin{bmatrix} 2 \\ 1 \\ 1 \\ 1 \end{bmatrix} & & & & (-1, -1) \\
 \begin{bmatrix} 0 \\ 1 \\ 0 \\ 0 \end{bmatrix} & \begin{bmatrix} 0 \\ 2 \\ 0 \\ 1 \end{bmatrix} & \begin{bmatrix} 1 \\ 0 \\ 0 \\ 0 \end{bmatrix} & \begin{bmatrix} 1 \\ 1 \\ 0 \\ 0 \end{bmatrix} & \begin{bmatrix} 1 \\ 1 \\ 0 \\ 1 \end{bmatrix} & \begin{bmatrix} 1 \\ 1 \\ 1 \\ 0 \end{bmatrix} & \begin{bmatrix} 1 \\ 2 \\ 0 \\ 1 \end{bmatrix} & \begin{bmatrix} 1 \\ 2 \\ 1 \\ 1 \end{bmatrix} & & (0, 1) \\
 \begin{bmatrix} 0 \\ 0 \\ 0 \\ 0 \end{bmatrix} & \begin{bmatrix} 0 \\ 0 \\ 1 \\ 0 \end{bmatrix} & \begin{bmatrix} 0 \\ 1 \\ 0 \\ 1 \end{bmatrix} & \begin{bmatrix} 0 \\ 1 \\ 1 \\ 0 \end{bmatrix} & \begin{bmatrix} 0 \\ 1 \\ 1 \\ 1 \end{bmatrix} & \begin{bmatrix} 0 \\ 2 \\ 1 \\ 1 \end{bmatrix} & \begin{bmatrix} 0 \\ 1 \\ 1 \\ 0 \end{bmatrix} & \begin{bmatrix} 1 \\ 0 \\ 1 \\ 1 \end{bmatrix} & \begin{bmatrix} 1 \\ 1 \\ 1 \\ 1 \end{bmatrix} & (0, 1)
 \end{array}$$



## 11.5 Calculating with the Polytopes

We will illustrate a calculation with the polytopes we have listed. Let  $\iota$  and  $\gamma_2$  be the maps from Equation 6.6.  $R_+(0, 0)$  consists of two polygons,  $P_1$  and  $P_2$ . These are the last two listed above. We will show that

$$\iota(P_2) + (1, 1, 0, 0) = \gamma_2(P_2).$$

As above, the coordinates for  $P_2$  are

$$\begin{bmatrix} 0 \\ 0 \\ 0 \\ 0 \end{bmatrix} \begin{bmatrix} 0 \\ 1 \\ 0 \\ 0 \end{bmatrix} \begin{bmatrix} 0 \\ 1 \\ 1 \\ 0 \end{bmatrix} \begin{bmatrix} 1 \\ 0 \\ 0 \\ 0 \end{bmatrix} \begin{bmatrix} 1 \\ 0 \\ 0 \\ 1 \end{bmatrix} \begin{bmatrix} 1 \\ 0 \\ 1 \\ 0 \end{bmatrix} \begin{bmatrix} 1 \\ 1 \\ 0 \\ 1 \end{bmatrix} \begin{bmatrix} 1 \\ 1 \\ 1 \\ 0 \end{bmatrix} \begin{bmatrix} 1 \\ 1 \\ 1 \\ 1 \end{bmatrix} \begin{bmatrix} 2 \\ 0 \\ 0 \\ 1 \end{bmatrix} \begin{bmatrix} 2 \\ 0 \\ 1 \\ 1 \end{bmatrix} \begin{bmatrix} 2 \\ 1 \\ 1 \\ 1 \end{bmatrix}$$

Recall that  $\iota(x, y, z, A) = (1 + A - x, 1 + A - y, 1 - z, A)$ . For example,  $\iota(0, 0, 0, 0) = (1, 1, 1, 0)$ . The coordinates for  $\iota(P_2)$  are

$$\begin{bmatrix} 1 \\ 1 \\ 1 \\ 0 \end{bmatrix} \begin{bmatrix} 1 \\ 0 \\ 1 \\ 0 \end{bmatrix} \begin{bmatrix} 1 \\ 0 \\ 0 \\ 0 \end{bmatrix} \begin{bmatrix} 0 \\ 1 \\ 1 \\ 0 \end{bmatrix} \begin{bmatrix} 1 \\ 2 \\ 1 \\ 1 \end{bmatrix} \begin{bmatrix} 0 \\ 1 \\ 0 \\ 0 \end{bmatrix} \begin{bmatrix} 1 \\ 1 \\ 1 \\ 1 \end{bmatrix} \begin{bmatrix} 0 \\ 0 \\ 0 \\ 0 \end{bmatrix} \begin{bmatrix} 1 \\ 1 \\ 0 \\ 1 \end{bmatrix} \begin{bmatrix} 0 \\ 2 \\ 1 \\ 1 \end{bmatrix} \begin{bmatrix} 0 \\ 2 \\ 0 \\ 1 \end{bmatrix} \begin{bmatrix} 0 \\ 1 \\ 1 \\ 1 \end{bmatrix}$$

The coordinates for  $\iota(P_2) + (1, 1, 0, 0)$  are

$$\begin{bmatrix} 2 \\ 2 \\ 1 \\ 0 \end{bmatrix} \begin{bmatrix} 2 \\ 1 \\ 1 \\ 0 \end{bmatrix} \begin{bmatrix} 2 \\ 1 \\ 0 \\ 0 \end{bmatrix} \begin{bmatrix} 1 \\ 2 \\ 1 \\ 0 \end{bmatrix} \begin{bmatrix} 2 \\ 3 \\ 1 \\ 1 \end{bmatrix} \begin{bmatrix} 1 \\ 2 \\ 0 \\ 0 \end{bmatrix} \begin{bmatrix} 2 \\ 2 \\ 1 \\ 1 \end{bmatrix} \begin{bmatrix} 1 \\ 1 \\ 0 \\ 0 \end{bmatrix} \begin{bmatrix} 2 \\ 2 \\ 0 \\ 1 \end{bmatrix} \begin{bmatrix} 1 \\ 2 \\ 0 \\ 1 \end{bmatrix} \begin{bmatrix} 1 \\ 3 \\ 1 \\ 1 \end{bmatrix} \begin{bmatrix} 1 \\ 3 \\ 0 \\ 1 \end{bmatrix}$$

We have  $\gamma_2(x, y, z, A) = (x + 1 - A, y + 1 + A, z, A)$ . For instance, we compute that  $\gamma_2(0, 0, 0, 0) = (1, 1, 0, 0)$ . The coordinates for  $\gamma(P_2)$  are

$$\begin{bmatrix} 1 \\ 1 \\ 0 \\ 0 \end{bmatrix} \begin{bmatrix} 1 \\ 2 \\ 0 \\ 0 \end{bmatrix} \begin{bmatrix} 1 \\ 2 \\ 1 \\ 0 \end{bmatrix} \begin{bmatrix} 2 \\ 1 \\ 0 \\ 0 \end{bmatrix} \begin{bmatrix} 1 \\ 2 \\ 0 \\ 1 \end{bmatrix} \begin{bmatrix} 2 \\ 1 \\ 1 \\ 0 \end{bmatrix} \begin{bmatrix} 1 \\ 3 \\ 0 \\ 1 \end{bmatrix} \begin{bmatrix} 2 \\ 2 \\ 1 \\ 0 \end{bmatrix} \begin{bmatrix} 1 \\ 3 \\ 1 \\ 1 \end{bmatrix} \begin{bmatrix} 2 \\ 2 \\ 0 \\ 1 \end{bmatrix} \begin{bmatrix} 2 \\ 2 \\ 1 \\ 1 \end{bmatrix} \begin{bmatrix} 2 \\ 3 \\ 1 \\ 1 \end{bmatrix}$$

These are the same vectors as listed for  $\iota(P_2) + (1, 1, 0, 0)$  but in a different order.

## 11.6 The Phase Portrait

Here we explain how to derive the phase portrait described in Figure 2.4. Our discussion refers to §11. Consider the two rectangles

$$Q_+ = \{(t, t+1, t) \mid t \in (0, 1)\} \times [0, 1];$$

$$Q_- = \{(t-1, t, t) \mid t \in (0, 1)\} \times [0, 1].$$

Intersect  $Q_{\pm}$  with the polytope  $R_{\pm}$ . These intersections partition  $Q_+$  and  $Q_-$  into a small finite number of polygons. The partition of  $Q_{\pm}$  tells the behavior of  $\Psi^{\pm}$  on points of  $(0, 2) \times \{1\}$ . By symmetry, the partition of  $Q_{\mp}$  tells the behavior of  $\Psi^{\pm}$  on  $(0, 2) \times \{-1\}$ . The partition of  $Q_{\pm}$  gives us the information needed to build Figure 2.4. Given the simplicity of the partitions involved, we can determine the picture just by plotting (say) 10000 fairly dense points in our rectangles. This is what we do.

# Part III

In this part of the monograph we use the Master Picture Theorem to prove all the results quoted in Part I of the monograph.

- In §12 we prove the Embedding Theorem.
- In §13 we prove some results about the symmetries of the arithmetic graph and the hexagrid.
- In §14 we establish some information about the doors. These special points were defined in connection with the Hexagrid Theorem.
- In §15 we prove Statement 1 of the Hexagrid theorem, namely that the arithmetic graph does not cross any floor lines.
- In §16 we prove Statement 2 of the Hexagrid theorem, namely that the arithmetic graph only crosses the walls near the doors. The two statements of the Hexagrid Theorem have similar proofs, though Statement 2 has a more elaborate proof.
- In §17 we prove a variant of Statement 1 of the Hexagrid Theorem. We call the result that Barrier Theorem. Though we don't need this result until Part VI, the proof fits best right after the proof of the Hexagrid Theorem.

Many of the proofs in this part of the monograph require us to prove various disjointness results about some 4 dimensional polytopes. We will give short computer-aided proofs of these disjointness results. The proofs only involve a small amount of integer arithmetic. An energetic mathematician could do them all by hand in an afternoon. To help make the proofs surveyable, we will include extensive computer pictures of 2 dimensional slices of our polytopes. These pictures, all reproducible on Billiard King, serve as sanity checks for the computer calculations.

## 12 Proof of the Embedding Theorem

Let  $\widehat{\Gamma} = \widehat{\Gamma}_\alpha(A)$  be the arithmetic graph for a parameter  $A$  and some number  $\alpha \notin 2\mathbf{Z}[A]$ . In this chapter we prove that  $\widehat{\Gamma}$  is a disjoint union of embedded polygons and infinite polygonal arcs. This is the Embedding Theorem.

### 12.1 Step 1

We will first prove that every nontrivial vertex of  $\widehat{\Gamma}$  has valence 2. Each point  $p \in \widehat{\Gamma}$  is connected to two points  $q_+$  and  $q_-$ . Hence, each non-trivial vertex has valence either 1 or 2. The following two cases are the only cases that lead to valence 1 vertices:

- $p = q_+$  and  $q_+ \neq q_-$ .
- $q_+ = q_-$  and  $q_\pm \neq p$ .

The following lemma rules out the first of these cases.

**Lemma 12.1** *If  $p = q_+$  or  $p = q_-$  then  $p = q_+ = q_-$ .*

**Proof:** Our proof refers to §6.6. Recall that  $R_+(0, 0)$  consists of 2 convex integer polytopes. Likewise  $R_-(0, 0)$  consists of 2 convex integer polytopes. It suffices to show that

$$(t, t + 1, t) \in R_+(0, 0) \iff (t - 1, t, t) \in R_-(0, 0). \quad (143)$$

This is equivalent to the statement that

$$R_-(0, 0) + (1, 1, 0, 0) \subset \Lambda R_+(0, 0)$$

Here  $\Lambda R_+(0, 0)$  is the orbit of  $R_+(0, 0)$  under the action of  $\Lambda$ . Let  $\iota$  be the involution from Equation 56. Recall that  $R_-(0, 0) = \iota(R_+(0, 0))$ . Hence, Equation 143 equivalent to the statement that

$$\iota(R_+(0, 0)) + (1, 1, 0, 0) \subset \Lambda R_+(0, 0). \quad (144)$$

Let  $P_1$  and  $P_2$  denote the two polytopes comprising  $R_+(0, 0)$ , as listed at the end of §6. Let  $\gamma_2$  be the element of  $\Lambda$  described in §6.6. We compute that

$$\iota(P_1) + (1, 1, 0, 0) = P_1; \quad \iota(P_2) + (1, 1, 0, 0) = \gamma_2(P_2). \quad (145)$$

We did the second calculation in §11.5, and the first computation is similar. This does it for us. ♠

## 12.2 Step 2

Our next goal is to rule out the possibility that  $p \neq q_{\pm}$ , but  $q_+ = q_-$ . This situation happens iff there is some  $(\epsilon_1, \epsilon_2) \in \{-1, 0, 1\}$  such that

$$\Lambda R_+(\epsilon_1, \epsilon_2) \cap (R_-(\epsilon_1, \epsilon_2) + (1, 1, 0, 0)) \neq \emptyset. \quad (146)$$

A visual inspection and/or a compute computer search – we did both – reveals that at least one of the two sets above is empty unless  $(\epsilon_1, \epsilon_2)$  is one of

$$(1, 1); \quad (-1, -1); \quad (1, 0); \quad (-1, 0). \quad (147)$$

To rule out Equation 146 for each of these pairs, we need to consider all possible pairs  $(P_1, P_2)$  of integral convex polytopes such that

$$P_1 \subset \Lambda R_+(\epsilon_1, \epsilon_2); \quad P_2 \subset (R_-(\epsilon_1, \epsilon_2) + (1, 1)) \quad (148)$$

Recall that  $\Lambda$  is generated by the three elements  $\gamma_1, \gamma_2, \gamma_3$ . Let  $\Lambda' \subset \Lambda$  denote the subgroup generated by  $\gamma_1$  and  $\gamma_2$ . We also define  $\Lambda'_{10} \subset \Lambda'$  by the equation

$$\Lambda'_{10} = \{a_1\gamma_1 + a_2\gamma_2 \mid |a_1|, |a_2| \leq 10\}. \quad (149)$$

**Lemma 12.2** *Let  $\gamma \in \Lambda - \Lambda'$ . Suppose that*

$$P_1 = \gamma(Q_1); \quad Q_1 \subset R_+(\epsilon_1, \epsilon_2); \quad P_2 \subset R_-(\epsilon_1, \epsilon_2) + (1, 1, 0, 0).$$

*Then  $P_1$  and  $P_2$  have disjoint interiors.*

**Proof:** The third coordinates of points in  $P_1$  lies between  $n$  and  $n + 1$  for some  $n \neq 0$  whereas the third coordinates of points in  $P_2$  lie in  $[0, 1]$ . ♠

**Lemma 12.3** *Let  $\gamma \in \Lambda' - \Lambda'_{10}$ .*

$$P_1 = \gamma(Q_1); \quad Q_1 \subset R_+(\epsilon_1, \epsilon_2); \quad P_2 \subset R_-(\epsilon_1, \epsilon_2) + (1, 1, 0, 0).$$

*Then  $P_1$  and  $P_2$  have disjoint interiors.*

**Proof:**  $Q_1$  is contained in the ball of radius 4 about  $P_2$ , but  $\gamma$  moves this ball entirely off itself. ♠

The last two results leave us with a finite problem. Given a pair  $(\epsilon_1, \epsilon_2)$  from our list above, and

$$\gamma \in \Lambda'_{10}; \quad P_1 = \gamma(Q_1); \quad Q_1 \subset R_+(\epsilon_1, \epsilon_2); \quad P_2 \subset R_-(\epsilon_1, \epsilon_2) + (1, 1, 0, 0),$$

we produce a vector

$$w = w(P_1, P_2) \in \{-1, 0, 1\}^4 \tag{150}$$

such that

$$\max_{v \in \text{vtx}(P_1)} v \cdot w \leq \min_{v \in \text{vtx}(P_2)} v \cdot w. \tag{151}$$

This means that a hyperplane separates the interior of  $P_1$  from  $P_2$ . In each case we find  $v(P_1, P_2)$  by a short computer search, and perform the verification using integer arithmetic. It is a bit surprising to us that such a simple vector works in all cases, but that is how it works out.

Using Billiard King, the interested reader can draw arbitrary  $(z, A)$  slices of the sets  $\Lambda R_+(\epsilon_1, \epsilon_2)$  and  $\Lambda R_-(\epsilon_1, \epsilon_2) + (1, 1, 0, 0)$ , and see that the interiors of the polygons from the first set are disjoint from the interiors of the polygons from the second set. We will illustrate this with pictures in §12.4.

### 12.3 Step 3

Given that every nontrivial vertex of  $\widehat{\Gamma}$  has valence 2, and also that the edges of  $\widehat{\Gamma}$  have length at most  $\sqrt{2}$ , the only way that  $\widehat{\Gamma}$  can fail to be embedded is if there is situation like the one shown in Figure 12.1.

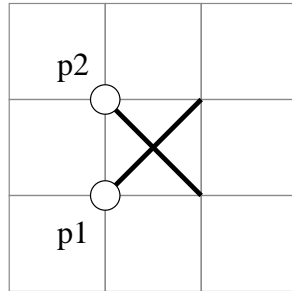


**Figure 12.1:** Embedding Failure

Let  $M_+$  and  $M_-$  be the maps from §6.6.3. Given the Master Picture Theorem, this situation arises only in the following 4 cases:

- $M_+(p_1) \in \Lambda R_+(1, 1)$  and  $M_+(p_2) \in \Lambda R_+(1, -1)$ .
- $M_-(p_1) \in \Lambda R_-(1, 1)$  and  $M_-(p_2) \in \Lambda R_-(1, -1)$ .
- $M_-(p_1) \in \Lambda R_-(1, 1)$  and  $M_+(p_2) \in \Lambda R_+(1, -1)$ .
- $M_+(p_1) \in \Lambda R_+(1, 1)$  and  $M_-(p_2) \in \Lambda R_-(1, -1)$ .

Note that  $p_2 = p_1 + (0, 1)$  and hence

$$M_{\pm}(p_2) = M_{\pm}(p_1) + (1, 1, 1, 0) \bmod \Lambda. \quad (152)$$

In particular, the two points  $M(p_1)$  and  $M(p_2)$  lie in the same fiber of  $R$  over the  $(z, A)$  square. We inspect the picture and see that this situation never occurs for the types  $(1, 1)$  and  $(1, -1)$ . Hence, Cases 1 and 2 do not occur. More inspection shows that there are  $R_+(1, -1) = \emptyset$ . Hence, Case 3 does not occur. This leaves Case 4, the only nontrivial case.

Case 4 leads to the statement that

$$(t, t, t, A) + (0, 1, 0, 0) \in \Lambda R_+(1, 1);$$

$$(t, t, t, A) - (1, 0, 0, 0) + (1, 1, 1, 0) = (t, t, t, A) + (0, 1, 1, 0) \in \Lambda R_-(1, -1). \quad (153)$$

Setting  $p$  equal to the first of the two points above, we get

$$p \in \Lambda R_+(1, 1); \quad p + (0, 0, 1, 0) \in \Lambda R_-(1, -1). \quad (154)$$

Letting  $\gamma_3 \in \Lambda$  be as in Equation 54, we have

$$p + (1, 1, 0, 0) = \gamma_3^{-1}(p + (0, 0, 1, 0)) \in \Lambda R_-(1, -1). \quad (155)$$

For any subset  $S \subset \tilde{R}$ , we have

$$(\Lambda S) + (a, b, c, 0) = \Lambda(S + (a, b, c, 0)). \quad (156)$$

The point here is that  $\Lambda$  acts as a group of translations on each set of the form  $R^3 \times \{A\}$ , and addition by  $(x, y, z, 0)$  commutes with this action on every such set. Equations 155 and 156 combine to give

$$p \in \Lambda(R_-(1, -1) - (1, 1, 0, 0)) \quad (157)$$

Now we see that

$$\Lambda R_+(1, 1) \cap \Lambda(R_-(1, -1) - (1, 1, 0, 0)) \neq \emptyset.$$

Since the whole picture is  $\Lambda$ -equivariant, we have

$$\Lambda R_+(1, 1) \cap (R_-(1, -1) - (1, 1, 0, 0)) \neq \emptyset. \quad (158)$$

We mean that there is a pair  $(P_1, P_2)$  of polytopes, with  $P_1$  in the first set and  $P_2$  in the second set, such that  $P_1$  and  $P_2$  do not have disjoint interiors.

We rule out this intersection using exactly the same method as in Step 2. In §12.4 we illustrate this with a convincing picture.

## 12.4 A Visual Tour

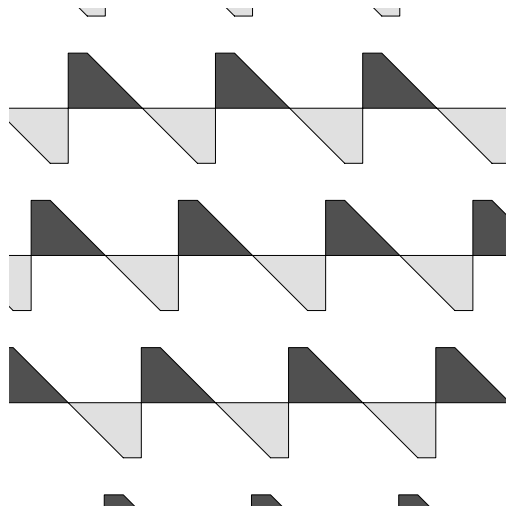
The theoretical part of our proof amounts to reducing the Embedding Theorem to the statement that finitely many pairs of polytopes have disjoint interiors. The computer-aided part of the proof amounts to verifying the disjointness finitely many times. Our verification used a very fragile disjointness test. We got a lucky, because many of our polytope pairs share a 2-dimensional face. Thus, a separating hyperplane has to be chosen very carefully. Needless to say, if our simple-minded approach did not work, we would have used a more robust disjointness test.

If we could write this monograph on 4-dimensional paper, we could simply replace the computer-aided part of the proof with a direct appeal to the visual sense. Since we don't have 4-dimensional paper, we need to rely on the computer to "see" for us. In this case, "seeing" amounts to finding a hyperplane that separates the interiors of the two polytopes. In other words, we are getting the computer to "look" at the pair of polytopes in such a way that one polytope appears on one side and the other polytope appears on the other side.

We do not have 4 dimensional paper, but we can draw slices of all the sets we discussed above. The interested user of Billiard King can see any desired slice. We will just draw typical slices. In our pictures below, we will draw the slices of  $R_+$  with dark shading and the slices of  $R_-$  with light shading. In our discussion, the *base space*  $B$  refers to the  $(z, A)$  square over which our picture fibers. Let  $B_j$  denote the  $j$ th component of  $B$ , as determined by the characteristic  $n_1$  discussed in §11.3.

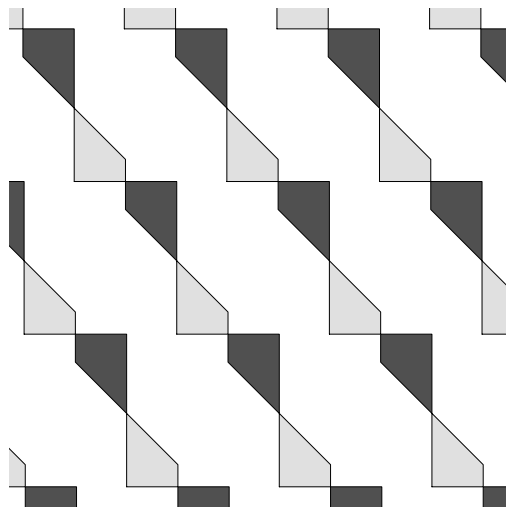
In reference to Step 2, our pictures for the pair  $(-\epsilon_1, -\epsilon_2)$  look like rotated versions of the pictures for the pair  $(\epsilon_1, \epsilon_2)$ . Accordingly, we will just draw pictures for  $(1, 1)$  and  $(1, 0)$ .

Figure 12.2 shows a slice of  $\Lambda R_+(1, 1)$  and  $\Lambda(R_-(1, 1) + (1, 1, 0, 0))$  over  $B_0$ . Both slices are nonempty over  $B_1$  as well, and the picture is similar.



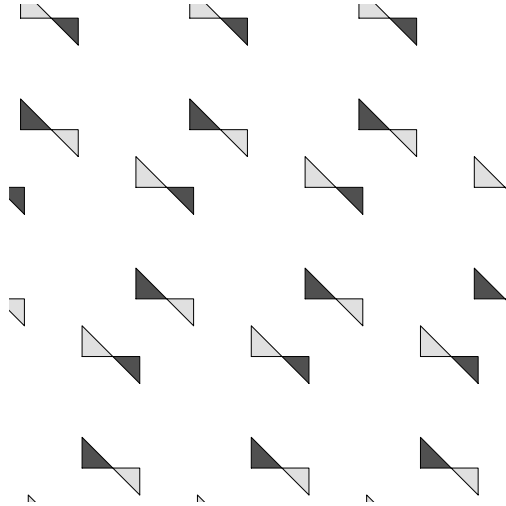
**Figure 12.2:** A slice of  $\Lambda R_+(1, 1)$  and  $\Lambda(R_-(1, 1) + (1, 1, 0, 0))$

Figure 12.3 shows a slice of  $\Lambda R_+(1, 0)$  and  $\Lambda(R_-(1, 0) + (1, 1, 0, 0))$  over  $B_0$ . The picture over  $B_1$  is similar. Figure 12.4 shows a slice of  $\Lambda R_+(1, 0)$  and  $\Lambda(R_-(1, 0) + (1, 1, 0, 0))$  over  $B_2$ . The picture over  $B_3$  is similar.



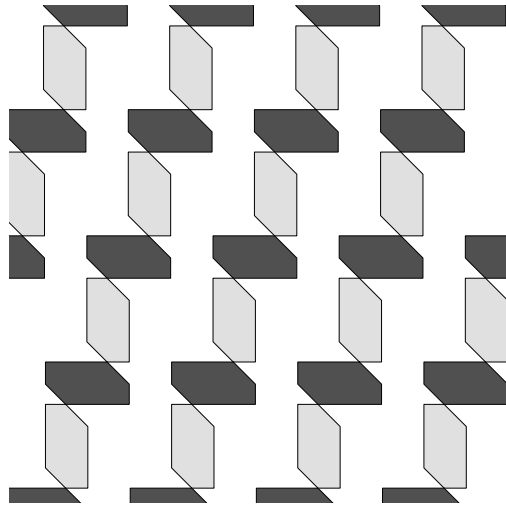
**Figure 12.3:** A slice of  $\Lambda R_+(1, 1)$  and  $\Lambda(R_-(1, -1) - (1, 1, 0, 0))$ .

Figure 12.4 shows a slice of  $\Lambda R_+(1, 0)$  and  $\Lambda(R_-(1, 0) + (1, 1, 0, 0))$  over  $B_2$ . The picture over  $B_3$  is similar.



**Figure 12.4:** A slice of  $\Lambda R_+(1, 1)$  and  $\Lambda(R_-(1, -1) - (1, 1, 0, 0))$ .

Figure 12.5 shows a slice of  $\Lambda R_+(1, 1)$  and  $\Lambda(R_-(1, -1) - (1, 1, 0, 0))$  over  $B_2$ . The picture looks similar over  $B_3$  and otherwise at least one of the slices is empty.



**Figure 12.5:** A slice of  $\Lambda R_+(1, 1)$  and  $\Lambda(R_-(1, -1) - (1, 1, 0, 0))$ .

## 13 Extension and Symmetry

### 13.1 Translational Symmetry

Referring to §6.6.3, the maps  $M_+$  and  $M_-$  are defined on all of  $\mathbf{Z}^2$ . This gives the extension of the arithmetic graph to all of  $\mathbf{Z}^2$ .

**Lemma 13.1** *The extended arithmetic graph does not cross the baseline.*

**Proof:** By the Pinwheel Lemma, the arithmetic graph describes the dynamics of the pinwheel map,  $\Phi$ . Note that  $\Phi$  is generically defined and invertible on  $\mathbf{R}_+ \times \{-1, 1\}$ . Reflection in the  $x$ -axis conjugates  $\Phi$  to  $\Phi^{-1}$ . By the Pinwheel Lemma,  $\Phi$  maps  $\mathbf{R}_+ \times \{-1, 1\}$  into itself. By symmetry the same goes for  $\Phi^{-1}$ . Hence  $\Phi$  and  $\Phi^{-1}$  also map  $\mathbf{R}_- \times \{-1, 1\}$  into itself. If some edge of  $\hat{\Gamma}$  crosses the baseline, then one of  $\Phi$  or  $\Phi^{-1}$  would map a point of  $\mathbf{R}^+ \times \{-1, 1\}$  into  $\mathbf{R}_- \times \{-1, 1\}$ . This is a contradiction. ♠

Let  $\lambda(p/q) = 1$  if  $p/q$  is odd, and  $\lambda(p/q) = 2$  if  $p/q$  is even. Define

$$\Theta = \mathbf{Z}V + \mathbf{Z}V'; \quad V' = \lambda^2 \left( 0, \frac{(p+q)^2}{4} \right); \quad \lambda = \lambda(p/q). \quad (159)$$

**Lemma 13.2** *The arithmetic graph  $\hat{\Gamma}(p/q)$  is invariant under  $\Theta$ .*

**Proof:** We will give the proof in the case when  $p/q$  is odd. The even case is similar. We have already seen that  $\hat{\Gamma}$  is invariant under  $V$ . We just have to show invariance for  $V'$ . By the Master Picture Theorem, it suffices to prove that  $(t, t, t) \in \Lambda$  when  $t$  is the second coordinate of  $V'$ . Here  $\Lambda$  is as in Equation 50.

We have  $(t, t, t) \equiv (2t, 2t, 0) \pmod{\Lambda}$  because  $t$  is an integer. Setting

$$a = pq; \quad b = \frac{pq + q^2}{2}, \quad (160)$$

We compute that

$$a \begin{bmatrix} 1 + A \\ 0 \\ 0 \end{bmatrix} + b \begin{bmatrix} 1 - A \\ 1 + A \\ 0 \end{bmatrix} = \begin{bmatrix} 2t \\ 2t \\ 0 \end{bmatrix}. \quad (161)$$

This completes the proof. ♠

**Lemma 13.3** *the hexagrid is invariant under the action of  $\Theta$ .*

**Proof:** Again, we treat the odd case only. Let  $G = G(p/q)$  denote the hexagrid. As in the previous result, we just have to show that  $G$  is invariant under  $V'$ . Let

$$W = \left( \frac{pq}{p+q}, \frac{pq}{p+q} + \frac{q-p}{2} \right)$$

be the vector from the definition of the hexagrid  $G$ . It suffices to prove that 6 lines of  $G$  contain  $V'$ . We compute that

$$V' = -\frac{p}{2}V + \frac{p+q}{2}W. \tag{162}$$

The second coefficient is an integer. Given that the room grid  $RG$  is invariant under the lattice  $\mathbf{Z}[V/2, W]$ , we see that  $RG$  is also invariant under translation by  $V'$ . This gives 2 lines,  $L_1$  and  $L_2$ , one from each family of  $RG$ .

Note that  $DG$  is only invariant under  $\mathbf{Z}[V]$ , so we have to work harder. We need to produce 4 lines of  $DG$  that contain  $V'$ . Here they are.

- The vertical line  $L_3$  through the origin certainly contains  $V'$ . This line extends the bottom left edge of  $Q$  and hence belongs to  $DG$ .
- Let  $L_4$  be the line containing  $V'$  and point  $-(p+q)V/2 \in \mathbf{Z}[V]$ . We compute that the slope of  $L_4$  coincides with the slope of the top left edge of  $Q$ . The origin contains a line of  $DG$  parallel to the top left edge of  $Q$ , and hence every point in  $\mathbf{Z}[V]$  contains such a line. Hence  $L_4$  belongs to  $DG$ . To avoid a repetition of words below, we call our argument here the *translation principle*.
- Let  $L_5$  be the line containing  $V'$  and point  $-pV \in \mathbf{Z}[V]$ . We compute that the slope of  $L_5$  coincides with the slope of the bottom right edge of  $Q$ . The translation principle shows that  $L_5$  belongs to  $DG$ .
- Let  $L_6$  be the line containing  $V'$  and point  $(q-p)V/2 \in \mathbf{Z}[V]$ . We compute that the slope of  $L_6$  coincides with the slope of the top right edge of  $Q$ . The translation principle shows that  $L_6$  belongs to  $DG$ .

The reader can see these lines, for any desired parameter, using Billiard King.



## 13.2 Rotational Symmetry

Let  $p/q$  be an odd rational. Let  $p_+/q_+$  be as in Equation 27. Let  $\iota$  be the rotation

$$\iota(m, n) = V_+ - (m, n). \quad (163)$$

Here  $V_+ = (q_+, -p_+)$ . The fixed point of  $\iota$  is  $(1/2)V_+$ . This point lies very close to the baseline of  $\hat{\Gamma}(p/q)$ . Figure 13.1 shows  $\Gamma(7/17)$  centered on this fixed point.

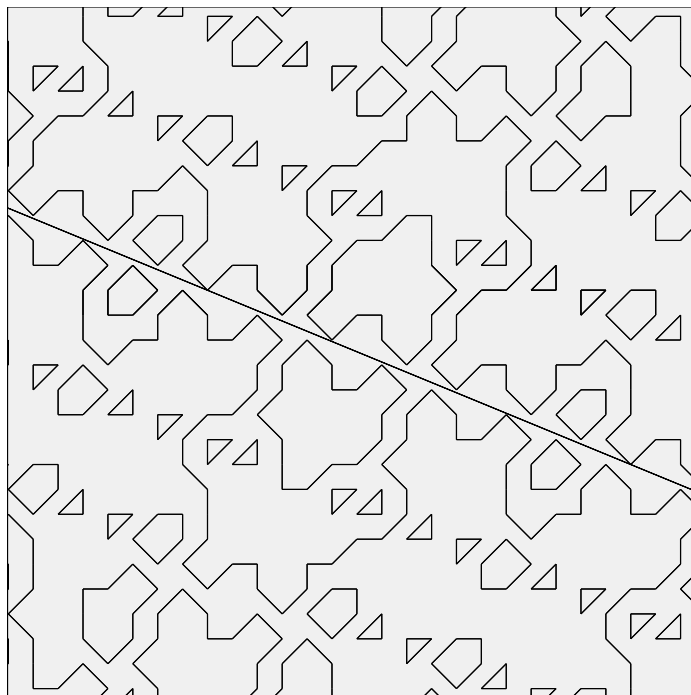


**Figure 13.1:**  $\hat{\Gamma}(7/17)$  centered on the point  $(12, -5)/2$ . point of symmetry.

Below we prove that  $\iota(\tilde{\Gamma}) = \hat{\Gamma}$ , as suggested by Figure 13.1. Combining this result with the translation symmetry above, we see that rotation by  $\pi$  about any of the points

$$\beta + \theta; \quad \beta = (1/2)V_+; \quad \theta \in \Theta \quad (164)$$

is a symmetry of  $\hat{\Gamma}$ .

**Remark:** In particular, there is an involution swapping  $(0, 0)$  and  $V_+ + dV$  for any  $d \in \mathbf{Z}$ .

**Lemma 13.4**  $\iota(\tilde{\Gamma}) = \tilde{\Gamma}$ .

**Proof:** Let  $M_+$  and  $M_-$  be as in §6.6.3. As usual, we take  $\alpha = 1/(2q)$ . We will first compare  $M_+(m, n)$  with  $M_-(\iota(m, n))$ . We have

$$M_+(m, n) = (t, t+1, t) \bmod \Lambda; \quad \frac{pm}{q} + n + \frac{1}{2q} \quad (165)$$

Next, using the fact that  $q_+p - p_+q = -1$ , we have

$$\begin{aligned} M_-(\iota(m, n)) &= (t' - 1, t', t') \bmod \Lambda; \\ t' &= \left( \frac{q_+p}{q} - p_+ \right) - \left( \frac{pm}{q} + n \right) + \frac{1}{2q} = - \left( \frac{pm}{q} + n \right) - \frac{1}{2q} = -t. \end{aligned}$$

In short

$$M_-(\iota(m, n)) = (-t - 1, -t, -t) \bmod \Lambda. \quad (166)$$

Recall that  $R_A$  is the fundamental domain for the action of  $\Lambda = \Lambda_A$ . We mean to equate  $\Lambda$  with the  $\mathbf{Z}$  span of its columns. There is some  $v \in \Lambda$  such that

$$(s_1, s_2, s_3) = (t, t+1, t) + (v_1, v_2, v_3) \in R_A \quad (167)$$

Given Equation 50, we have  $(2 + A, A, 1) \in \Lambda$ . Hence

$$w = (-v_1 + 2 + A, -v_2 + A, -v_3 + 1) \in \Lambda. \quad (168)$$

We compute that

$$(-t - 1, -t, -t) + w = (1 + A, 1 + A, 1) - (s_1, s_2, s_3). \quad (169)$$

So, we have

$$M_+(m, n) = \rho \circ M_-(\iota(m, n)), \quad (170)$$

where  $\rho$  is reflection through the midpoint of the space  $R_A$ . Similarly,

$$M_-(m, n) = \rho \circ M_+(\iota(m, n)), \quad (171)$$

But now we just verify by inspection that our partition of  $R_A$  is symmetric under  $\rho$ , and has the labels appropriate to force the type determined by

$$\rho \circ M_+(m, n), \quad \rho \circ M_-(m, n)$$

to be the 180 degree rotation of the type forced by

$$M_-(m, n), \quad M_+(m, n)$$

Indeed, we can determine this with an experiment performed on any rational large enough such that all regions are sampled. ♠

### 13.3 Near Bilateral Symmetry

Our pictures of arithmetic graphs show that they have an approximate bilateral symmetry. For example, in Figure 4.2 the two arcs  $\Gamma \cap R_1$  and  $\Gamma \cap R_2$  both have near bilateral symmetry. In Figure 13.1 we see a similar phenomenon. Here we will explain this near-symmetry.

We say that a map  $\mathbf{J}$  from  $\widehat{\Gamma}$  to  $\widehat{\Gamma}$  is a *combinatorial isomorphism* if  $\mathbf{J}$  maps vertices to vertices and edges to edges. We say that  $\mathbf{J}$  is *pseudo-linear* if there is a linear isomorphism  $J : \mathbf{R}^2 \rightarrow \mathbf{R}^2$  such that  $J$  is a bounded distance from  $\mathbf{J}$  (in the sup norm.) In this case, we call  $J$  the *model* for  $\mathbf{J}$ . Here is our main result.

**Lemma 13.5** *For any irrational  $A$ , there exists an involution  $\mathbf{J} : \widehat{\Gamma} \rightarrow \widehat{\Gamma}$  with the following properties.*

1.  $\mathbf{J}$  is a combinatorial isomorphism that swaps the components of  $\widehat{\Gamma}$  above the baseline with the ones below.
2.  $\mathbf{J}$  is a translation when restricted to low vertices. More precisely, if  $v$  is a low vertex then  $\mathbf{J}(v) = v - (0, 1)$ .
3.  $\mathbf{J}$  is pseudo-linear, modelled on the affine map  $J$  such that  $J(V) = V$  and  $J(W) = -W$ . Here  $V$  and  $W$  are as in Equation 21.

**Remarks:**

(i) We think that  $\mathbf{J}$  is within 2 units of  $J$ . Probably an analysis similar to what we did for the Pinwheel Lemma would prove this.

(ii) Let  $\iota$  be the symmetry discussed in the previous section. Then  $\iota \circ \mathbf{J}$  permutes the components of  $\widehat{\Gamma}$  above the baseline. In particular,  $\iota \circ \mathbf{J}$  preserves  $\Gamma$  but reverses its direction. This is the near-bilateral symmetry that we see in the pictures.

(iii) One can probably see the action of  $\mathbf{J}$  by looking at Figure 13.1 again. Notice the symmetry between components above the baseline and components below it.

The construction of  $\mathbf{J}$  is almost completely soft. It only uses the easy case of the Pinwheel Lemma, and basic symmetries of the outer billiards map. Our construction uses the following definition. Say that a *low component* is a component of  $\widehat{\Gamma}$  above the baseline that contains a low vertex.

**Constructing the Involution:** We turn now to the construction of  $\mathbf{J}$ . Recall that  $\Xi = \mathbf{R}_+ \times \{-1, 1\}$ . Let  $\Xi_{\pm} = \mathbf{R}_{\pm} \times \{-1, 1\}$ . Then  $\Xi = \Xi_+$ . Recall that  $\Psi : \Xi_+ \rightarrow \Xi_+$  is the first return map. We can extend  $\Psi$  to that it is also the return map from  $\Xi_-$  to  $\Xi_-$ . The points of the arithmetic graph below the baseline correspond to this extended notion of  $\Psi$ .

Let  $\Psi^{1/2}$  denote the first return map to  $\mathbf{R} \times \{-1, 1\}$ . Then  $\Psi$  is the square of  $\Psi^{1/2}$ . In terms of the Pinwheel Lemma, we start with (say) a point in  $\Xi_+$  and then watch it wind halfway around the kite until it lands in  $\Xi_-$ . This is the point  $\Psi^{1/2}(\xi)$ . The correspondence  $\xi \rightarrow \Psi^{1/2}(\xi)$  gives a bijection between  $\Psi$ -orbits in  $\Xi_+$  and  $\Psi$ -orbits in  $\Xi_-$ .

In terms of the arithmetic graph, there is a combinatorial isomorphism  $\mathbf{J}_+$  of  $\widehat{\Gamma}$  that swaps the components above the baseline with the ones below it. Here  $\mathbf{J}_+(m, n) = (m', n')$ , where  $(m, n)$  corresponds to  $\xi$  and  $(m', n')$  corresponds to  $\Psi^{1/2}(\xi)$ . There is a second involution that is equally good. We used the forwards direction of  $\Psi$  to define  $\mathbf{J}_+$ , but we could have used the backwards direction. That is, we would match  $\xi \in \Xi_+$  to the point  $\Psi^{-1/2}(\xi) \in \Xi_-$ . Call this map  $\mathbf{J}_-$ .

Our map  $\mathbf{J}$  is made from  $\mathbf{J}_+$  and  $\mathbf{J}_-$  in a not-completely-canonical way. We will define  $\mathbf{J}$  on components above the baseline. We then define  $\mathbf{J}$  for components below the baseline so as to make  $\mathbf{J}$  an involution.

Recall that the *parity* of a low vertex  $(m, n)$  to be the parity of  $m + n$ . By Lemma 2.9, a low component only has vertices of one kind of parity. We call the low component *even* or *odd* depending on the parity of its low vertices. If  $\gamma$  is a component of  $\widehat{\Gamma}$  above the baseline that is not low, we use (say)  $\mathbf{J} = \mathbf{J}_+$ . (We don't care about these components.) For even low components we use  $\mathbf{J} = \mathbf{J}_+$ . For odd low components, we use  $\mathbf{J} = \mathbf{J}_-$ . From the discussion above, we see that  $\mathbf{J}$  is a graph isomorphism of  $\widehat{\Gamma}$ .

**Remark:** There might be a canonical choice of  $\mathbf{J}_-$  or  $\mathbf{J}_+$  for components that are not low, but we don't know this.

**Action on Low Vertices:** Let's see what happens to low vertices. Let  $(m, n)$  be an even low vertex and let  $(x, -1) = M(m, n)$ . We compute easily that

$$\Psi^{1/2}(x, -1) = \psi^2(x, -1) = (x - 2, 1) = M(m, n - 1). \quad (172)$$

Hence,  $\mathbf{J}(m, n) = (m, n - 1)$ . Similarly, if  $(m, n)$  has odd parity, then

$$\Psi^{-1/2}(x, 1) = \psi^{-2}(x, 1) = (x - 2, -1) = M(m, n - 1). \quad (173)$$

Hence  $\mathbf{J}(v) = v - (0, 1)$  when  $v$  is a low vertex.

**Pseudo-Linearity:** It remains to show that  $\mathbf{J}$  is pseudo-linear, modelled on  $J$ . Since we don't need this final result for any purpose, we will only sketch the argument. Let  $(x, 1)$  be a point on  $\Xi_+$  about  $N$  units from the origin, we roughly trace out the Pinwheel map. First we some integer multiple of the vector  $(0, 4)$ , then we add some integer multiple of the vector  $(-2, 2)$ , etc. When we reach  $\Xi_-$  we have a vector of the form

$$(x + 2Am_1 + 2n_1, \pm 1),$$

where the pair  $(n_1, m_1)$  depends linearly on  $N$ , up to a uniformly bounded error. But, for the corresponding point  $v \in \widehat{\Gamma}$ , we have  $\mathbf{J}(v) = v + (m_1, n_1)$ . This shows that  $\mathbf{J}$  is pseudo-linear, and a simple calculation shows that  $\mathbf{J}$  is modelled on  $J$ .

## 14 The Structure of the Doors

### 14.1 The Odd Case

We suppose that  $p/q$  is an odd rational. Say that a *wall line* is a line of positive slope in the room grid. The doors are the intersection points of lines in the door grid with the wall lines. Let  $L_0$  be the wall line through  $(0, 0)$ . Let  $L_1$  be the wall line through  $V/2$ .

**Lemma 14.1** *Any two wall lines are equivalent mod  $\Theta$ .*

**Proof:** We check explicitly that the vector

$$V' + \frac{p+1}{2}V \in \Theta \cap L_1$$

Hence  $L_0$  and  $L_1$  are equivalent mod  $\Theta$ . But any other wall line is obtained from one of  $L_0$  or  $L_1$  by adding a suitable integer multiple of  $V$ . ♠

**Lemma 14.2** *The first coordinate of any door is an integer.*

**Proof:** Any wall line is equivalent mod  $\Theta$  to  $L_0$ . Since  $\Theta$  acts by integer translations, it suffices to door lies on  $L_0$ . Such a door is an integer multiple of the point  $v_3$  in Figure 3.1. That is, our door has coordinates

$$\frac{k}{2q}(2pq, (p+q)^2 - 2p^2). \tag{174}$$

The first coordinate here is certainly an integer. ♠

It could happen that the second coordinate of a door is an integer. Call such a door exceptional.

**Lemma 14.3** *Modulo the action of  $\Theta$ , there are only two exceptional doors.*

**Proof:** The point  $(0, 0)$  gives rise to two exceptional doors with (the same) integer coordinates. One of these doors is associated to the wall above  $(0, 0)$ , and one of these doors is associated to the door below. Hence, it suffices to show that any door with integer coordinates lies in  $\Theta$ .

As in the preceding result, it suffices to consider doors on  $L_0$ . Given Equation 174, we see that

$$k \frac{(p+q)^2 - 2p^2}{2q} \in \mathbf{Z}$$

for an exceptional door. Expanding this out, and observing that  $q$  divides both  $q^2$  and  $pq$ , we get that

$$k \frac{q^2 - p^2}{2q} \in \mathbf{Z}.$$

But  $q$  and  $q^2 - p^2$  are relatively prime. Hence  $k = jq$  for some  $j \in \mathbf{Z}$ . But

$$qv_3 = 2V' + V \in \Theta.$$

Hence  $jqv_3 = kv_3 \in \Theta$  as well. ♠

Here is a related result.

**Lemma 14.4** *Any lattice point on a wall line is equivalent to  $(0, 0) \bmod \Theta$ .*

**Proof:** By symmetry, it suffices to consider the cases when  $(m, n) \in L_0$ .

Looking at Figure 3.1, we see that any point on  $L_0$  has the form

$$sv_5 = \frac{s}{2(p+q)}(2pq, (p+q)^2 - 2p^2). \quad (175)$$

In order for this point to lie in  $\mathbf{Z}^2$ , the first coordinate must be an integer. Since  $p$  and  $q$  are relatively prime,  $pq$  and  $p+q$  are relatively prime. Hence, the first coordinate is an integer only if  $s = k(p+q)$  for some  $k \in \mathbf{Z}$ . Hence  $(m, n)$  is an integer multiple of the point

$$(p+q)v_5 = \left( pq, \frac{(p+q)^2}{2} - p^2 \right) = 2V' + pV \in \Theta.$$

Here  $V$  and  $V'$  are the vectors generating  $\Theta$ , as in Equation 159. ♠

The vertical lines in the door grid have the form  $x = kq$  for  $k \in \mathbf{Z}$ . Say that a *Type 1 door* is the intersection of such a line with a wall line.

**Lemma 14.5** *Let  $(kq, y)$  be a Type 1 door. Then  $py \in \mathbf{Z}$ .*

**Proof:** The group  $\Theta$  acts transitively, by integer translations, on the vertical lines of the door grid. Hence, it suffices to prove this lemma for the case  $k = 0$ . In other words, we need to show that  $py \in \mathbf{Z}$  if  $(0, y)$  lies on a wall line.

We order the wall lines according to the order in which they intersect the line of slope  $-A = -p/q$  through the origin. Let  $y_n$  be such that  $(0, y_n)$  lies on the  $k$ th wall line. The sequence  $\{y_n\}$  is an arithmetic progression. Hence, it suffices to prove our result for two consecutive values of  $n$ . Note that  $(0, 0)$  is a type A door. We might as well normalize so that  $y_0 = 0$ . Then  $(0, y_1)$  lies on the wall line  $L_1$  through  $(-q, p)$ . Referring to Equation 21, two points on  $L_1$  are  $-V$  and  $-V + W$ . These points are given by

$$-V = (-q, p); \quad -VW = (-q, p) + \left( \frac{pq}{p+q}, \frac{pq}{p+q} + \frac{q-p}{2} \right).$$

From this information, we compute that  $y_1 = (p+q)^2/2p$ . Since  $p+q$  is even,  $py_1 = (p+q)^2/2 \in \mathbf{Z}$ . ♠

Recall that  $\underline{y}$  is the greatest integer less than  $y$ .

**Corollary 14.6** *Suppose that  $(x, y)$  is a door of type 1, then  $y - \underline{y} \neq 1/2$ .*

**Proof:**  $p(y - \underline{y}) = p/2$  is an integer, by the previous result. But  $p/2$  is not an integer. This is a contradiction. ♠

Say that a *Type 2* door is a door on  $L_0$  that is not of Type 1. One obtains a Type 2 door by intersecting  $L_0$  with a line of the door grid that is parallel to the top left (or right) edge of the arithmetic kite.

**Lemma 14.7** *The Type 2 doors are precisely the points on  $L_0$  of the form  $(kp, y_k)$ , where  $k \in \mathbf{Z}$  and  $y_k$  is a number that depends on  $k$ .*

**Proof:** Referring to Figure 3.1, two consecutive doors on  $L_0$  are  $(0, 0)$  and  $v_3 = (p, y_1)$ . Our lemma now follows from the fact that the sequence of doors on  $L_0$  forms an arithmetic progression. ♠

## 14.2 The Even Case

Now we revisit all the results above in case  $p/q$  is even.

**Lemma 14.8** *Any two wall lines are equivalent mod  $\Theta$ .*

**Proof:** This is easy in the even case. Translation by  $V$  maps each wall line to the adjacent one. ♠

**Lemma 14.9** *The first coordinate of any door is an integer.*

**Proof:** The first door on  $L_0$  is the same in the even case as in the odd case. The rest of the proof is the same as in the odd case. ♠

**Lemma 14.10** *Modulo the action of  $\Theta$ , there are only two exceptional doors.*

**Proof:** As in the odd case, we just have to show that any door with integer coordinates is equivalent to  $(0, 0) \bmod \Theta$ . As in the odd case, the doors on  $L_0$  have the form  $kv_3$ . As in the odd case, this leads to the statement that

$$k \frac{q^2 - p^2}{2q} \in \mathbf{Z}.$$

Now the proof is a bit different. Here  $2q$  and  $q^2 - p^2$  are relatively prime. Hence  $k = 2jq$  for some  $j \in \mathbf{Z}$ . But

$$2qv_3 = V' + 2V \in \Theta.$$

Hence  $2jqv_3 = kv_3 \in \Theta$  as well. ♠

**Lemma 14.11** *Any lattice point on a wall line is equivalent to  $(0, 0) \bmod \Theta$ .*

**Proof:** As in the proof of Lemma 14.4, we see that

$$sv_5 = \frac{s}{2(p+q)}(2pq, (p+q)^2 - 2p^2) \in \mathbf{Z}. \quad (176)$$

As in the odd case, we look at the first coordinate and deduce the fact that  $s = k(p+q)$  for some  $k \in \mathbf{Z}$ . This is not enough for us in the even case. Looking now at the second coordinate, we see that

$$\frac{k(p+q)}{2} - kp^2 \in \mathbf{Z}.$$

Hence  $k$  is even. Hence  $(m, n)$  is an integer multiple of the point

$$2(p+q)v_5 = (2pq, (p+q)^2 - 2p^2) = V' + 2pV \in \Theta.$$

♠

We don't repeat the proof of Lemma 14.5 because we don't need it. We only need the even version of Corollary 14.6. In the even case, we have simply forced Corollary 14.6 to be true by eliminating the crossings for which it fails.

We say that a *Type 2* door is a door on  $L_0$  that is not of Type 1, and also is not one of the crossings we have eliminated. Once we make this redefinition, we have the following result

**Lemma 14.12** *The Type 2 doors are precisely the points on  $L_0$  of the form  $(kp, y_k)$ , where  $k \in \mathbf{Z}$  is not an odd multiple of  $q$ , and  $y_k$  is a number that depends on  $k$ .*

**Proof:** The Type two doors are as in the odd case, except that we eliminate the points  $(kp, y_k)$  where  $k$  is an odd multiple of  $q$ . ♠

## 15 Proof of the Hexagrid Theorem I

### 15.1 The Key Result

We will assume that  $p/q$  is an odd rational until the end of the chapter.

Say that a *floor line* is a negatively sloped line of the floor grid. Say that a *floor point* is a point on a floor line. Such a point need not have integer coordinates. Let  $M_+$  and  $M_-$  denote the maps from Equation 6.6.3.

**Lemma 15.1** *If  $(m, n)$  is a floor point, then  $M_-(m, n)$  is equivalent mod  $\Lambda$  to a point of the form  $(\beta, 0, 0)$ .*

**Proof:** The map  $M_-$  is constant when restricted to each floor line, because these lines have slope  $-A$ . Hence, it suffices to prove this result for one point on each floor line. The points

$$(0, t); \quad t = \frac{k(p+q)}{2}; \quad k \in \mathbf{Z}. \quad (177)$$

form a sequence of floor points, one per floor line. Note that  $t$  is an integer, because  $p+q$  is even.

To compute the image of the point  $(0, t)$ , we just have to subject the point  $t$  to our reduction algorithm from §11.2. The first 4 steps of the algorithm lead to the following result.

1.  $z = t$ .
2.  $Z = \text{floor}(t) = t$ , because  $t$  is an integer.
3.  $y = 2t = k(p+q) = kq(1+A)$ .
4.  $Y = \text{floor}(y/(1+A)) = kq$ .

Hence  $z = Z$  and  $y = (1+A)Y$ . Hence

$$M_-(0, t) = (x - (1+A)X, y - (1+A)Y, z - Z) = (\beta, 0, 0), \quad (178)$$

for some number  $\beta \in \mathbf{R}$  that depends on  $A$  and  $k$ . ♠

## 15.2 Two Special Planes

Let  $\Pi_- \subset \mathbf{R}^3$  denote the plane given by  $y = z$ . We can think of  $\Pi_-$  as the plane through the origin generated by the vectors  $(1, 0, 0)$  and  $(1, 1, 1)$ . In particular, the vector  $(1, 1, 1)$  is contained in  $\Pi_-$ . Let  $\Pi_-(0)$  denote the line through the origin parallel to  $(1, 0, 0)$ . Then  $\Pi_-(0)$  is a line in  $\Pi_-$ . Define

$$\Pi_+ = \Pi_- + (1, 1, 0); \quad \Pi_+(0) = \Pi_-(0) + (1, 1, 0). \quad (179)$$

**Lemma 15.2** *If  $(m, n)$  is a floor point, then  $M_{\pm}(m, n)$  is equivalent mod  $\Lambda$  to a point in  $\Pi_{\pm}(0)$ .*

**Proof:** The  $(-)$  case of this result is just a restatement of Lemma 15.1. The  $(+)$  case follows from the  $(-)$  case and symmetry. That is, we just translate the  $(-)$  case by the vector  $(1, 1, 0)$  to get the  $(+)$  case. ♠

Define

$$\Pi_{\pm}(r) = \Pi_{\pm}(0) + (r, r, r). \quad (180)$$

Let  $\Pi_{\pm}(r, s)$  denote the open infinite strip that is bounded by  $\Pi_{\pm}(r)$  and  $\Pi_{\pm}(s)$ . In the case of interest to us, we will have  $r = 0$  and  $s = \lambda > 0$ .

For each pair  $(\epsilon_1, \epsilon_2) \in \{-1, 0, 1\}^2$ , let  $\Sigma(\epsilon_1, \epsilon_2)$  denote the set of lattice points  $(m, n)$  such that  $(m, n)$  and  $(m, n) + (\epsilon_1, \epsilon_2)$  are separated by some floor line. The set  $\Sigma(\epsilon_1, \epsilon_2)$  is obtained by intersecting  $\mathbf{Z}^2$  with an infinite union of evenly spaced infinite strips, each of which has a floor line as one boundary component. For our purposes, it suffices to consider the pairs

$$(-1, 0); \quad (-1, -1); \quad (0, -1); \quad (1, -1). \quad (181)$$

For these pairs, the floor lines are the lower boundaries of the strips. We define

$$\lambda(\epsilon_1, \epsilon_2) = -(A\epsilon_1 + \epsilon_2). \quad (182)$$

**Lemma 15.3** *Let  $\lambda = \lambda(\epsilon_1, \epsilon_2)$ . Suppose that  $(m, n) \in \Sigma(\epsilon_1, \epsilon_2)$ . Then  $M_{\pm}(m, n) \in \Pi_{\pm}(0, \lambda)$ .*

**Proof:** We consider the case of  $M_-$  and the pair  $(-1, 0)$ . The other cases have essentially the same proof. If  $(m, n) \in \Sigma(-1, 0)$ , Then there is some  $x \in (m - 1, m)$  such that  $(x, n)$  is a floor point. Then  $M_+(x, n)$  is  $\Lambda$ -equivalent to a point  $p$  in  $\Pi(0)$ . But then  $M_+(m, n)$  is  $\Lambda$ -equivalent to  $p + (m - x)(A, A, A) \in \Pi(0, A) = \Pi(0, \lambda(-1, 0))$ . ♠

### 15.3 Critical Points

Say that a point  $v \in \Sigma(\epsilon_1, \epsilon_2)$  is *critical for*  $(\epsilon_1, \epsilon_2)$  if the arithmetic graph contains the edge joining  $(m, n)$  to  $(m + \epsilon_1, n + \epsilon_2)$ . Statement 1 of the Hexagrid Theorem says, in particular, that there are no such points like this.

**Lemma 15.4** *There are no critical points.*

**Proof:** Let  $\mathcal{R}_+$  denote the tiling of  $\mathbf{R}^3$  by polyhedra, according to the Master Picture Theorem. Let  $\mathcal{P}_+$  denote the intersection of  $\mathcal{R}_+$  with the plane  $\Pi$ . We make the same definitions in the  $(-)$  case. If  $(m, n)$  is critical for  $(\epsilon_1, \epsilon_2)$ , then one of two things is true.

1.  $\Pi_+(0, \lambda)$  nontrivially intersects a polygon of  $\mathcal{P}_+$  labelled by  $(\epsilon_1, \epsilon_2)$ .
2.  $\Pi_-(0, \lambda)$  nontrivially intersects a polygon of  $\mathcal{P}_-$  labelled by  $(\epsilon_1, \epsilon_2)$ .

Here we have set  $\lambda = \lambda(\epsilon_1, \epsilon_2)$ . Considering the 4 pairs of interest to us, and the 2 possible signs, we have 8 conditions to rule out. We check, in all cases, that the relevant strip is disjoint from the relevant polygons.

We can check the disjointness for all parameters at once. The union

$$S_{\pm}(\epsilon_1, \epsilon_2) := \bigcup_{A \in (0,1)} \left( \Pi_{\pm}(\epsilon_1, \epsilon_2; A) \times \{A\} \right)$$

is a polyhedral subset of  $\mathbf{R}^4$ . To get an honest polyhedron, we observe that  $S$  is invariant the action of the lattice element  $\gamma_1$  from Equation 54, and we take a polyhedron whose union under translates by  $\gamma_3$  tiles  $S$ . In practice, we simply restrict the  $x$ -coordinate to lie in  $[0, 2]$ .

We check that  $S_{\pm}(\epsilon_1, \epsilon_2)$ , or rather the compact polyhedron replacing it, is disjoint from all  $\Lambda$ -translates of the polytope  $P_{\pm}(\epsilon_1, \epsilon_2)$ , the polytope listed in §11.3. In practice, most translates are very far away, and we only need to check a small finite list. This is a purely algebraic calculation. ♠

Rather than dwell on the disjointness calculation, which gives no insight into what is going on, we will draw pictures for the parameter  $A = 1/3$ . The combinatorial type changes with the parameter, but not the basic features of interest to us. The interested reader can see the pictures for any parameter using Billiard King.

To draw pictures, we identify the planes  $\Pi_{\pm}$  with  $\mathbf{R}^2$  using the projection  $(x, y, z) \rightarrow (x, (y + z)/2)$ . Under this identification, all the polygons in question are rectangles! The coordinates of the rectangle vertices are small rational combinations of 1 and  $A$ , and can easily be determined by inspection. The whole picture is invariant under translation by  $(1 + A, 0)$ . The thick line in the first picture corresponds to  $\Pi_-(0)$ . In terms of  $\mathbf{R}^2$  coordinate, this is the  $x$ -axis. The black dot is  $(0, 0)$ . dot is  $(4/3, 0) = (1 + A, 0)$ .

We explain by example the notation on the right hand side of the figure. The label  $\lambda(-1, -1)$  denotes the line  $\Pi(\lambda)$ , where  $\lambda = \lambda(-1, -1)$ . In each case, the relevant strip lies below the relevant shaded piece. While the combinatorics of the picture changes as the parameter changes, the basic disjointness stays the same.

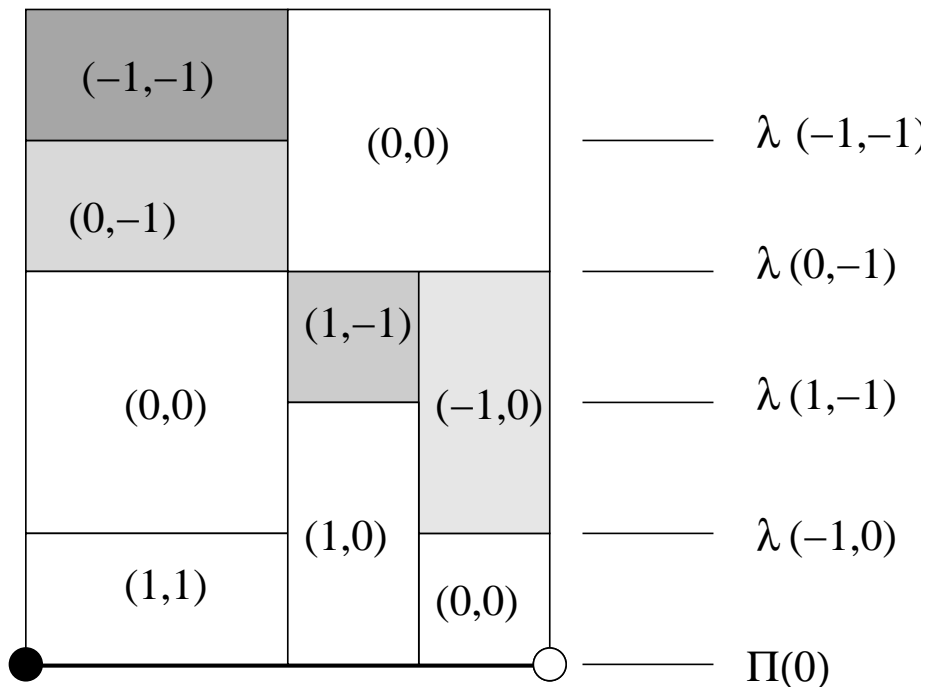


**Figure 15.1:** The  $(-)$  picture for  $A = 1/3$ .

Figure 15.2 shows the same thing for the  $(+)$  case. This time the black dot is  $(1/2, 1/2)$  and the white dot is  $(1/2, 1/2) + (1 + A, 0)$ . The thick line represents  $\Pi_+(0)$ . In  $\mathbf{R}^2$  coordinates, this is the line  $y = 1/2$ . In the  $(+)$  case is isn't even a close call.

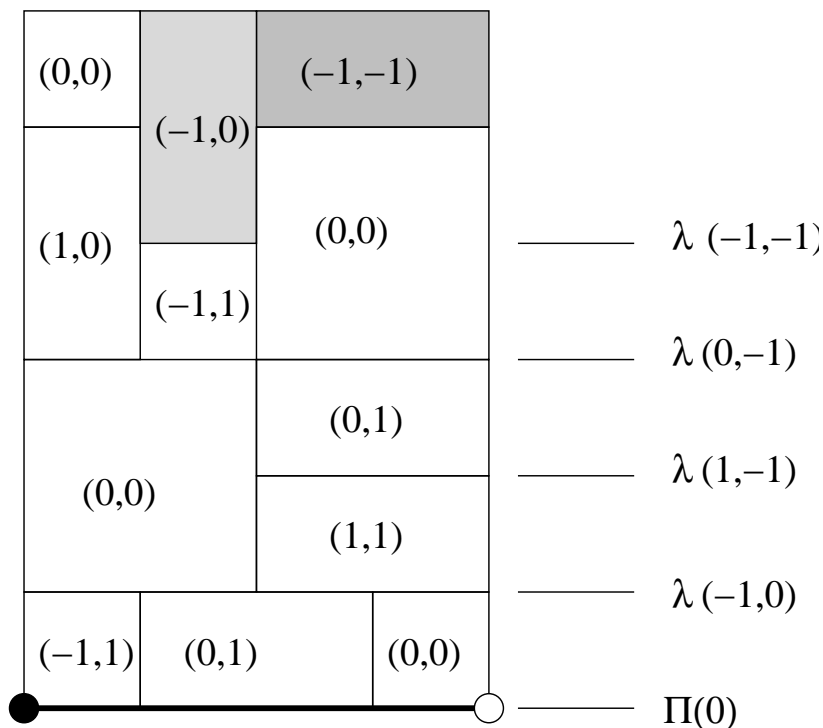


Figure 15.2: The (+) picture for  $A = 1/3$ .

## 15.4 The End of the Proof

Now we know that there are no critical points. The only other way that the arithmetic graph could cross a floor line would be at a floor point that was also a lattice point. It might happen that one edge emanating from such a floor point lies above the floor line, and the other lies below.

Define

$$\zeta_k = \left(0, \frac{k(p+q)}{2}\right); \quad k \in \mathbf{Z}. \quad (183)$$

**Lemma 15.5** *Modulo the symmetry group  $\Theta$ , the only lattice floor points are the ones listed in Equation 183.*

**Proof:** If  $(m, n)$  is a lattice floor point, then  $2Am + 2n \in \mathbf{Z}$ . But this means that  $q$  divides  $m$ . Subtracting off a suitable multiple of  $V = (q, -p) \in \Theta$ , we can arrange that the first coordinate of our lattice floor point is 0. But, now we must have one of the points in Equation 183. ♠

The slices as shown in Figure 6.3 determine the nature of the edges of the arithmetic graph, although the slices currently of interest to us are not shown there. We are interested in following the method discussed in §6.5, where we set  $\alpha = 0$  and consider the singular situation. The points  $M_-(\zeta_k)$  and  $M_+(\zeta_k)$  both lie in the  $(0, A)$  slices of our partitions. Figure 15.1 does for these slices what Figure 6.3 does for the generic slice. The point  $M_-(\zeta_k)$  always lies along the bottom edge of the fiber, and the point  $M_+(\zeta_k)$  just above the edge contained in the line  $y = 1$ . The relevant edges are highlighted.

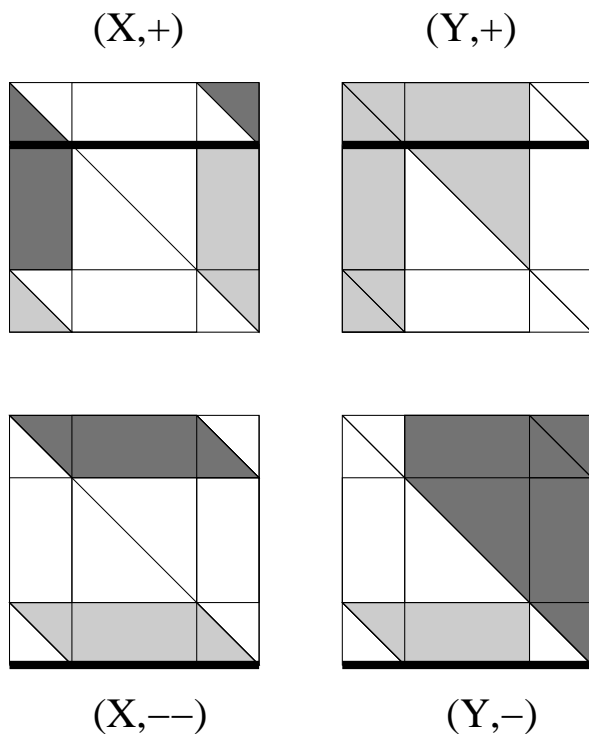


**Figure 15.1:** The  $(0, A)$  slices.

From this picture we can see that the only edges emanating from  $\zeta_k$  are those corresponding to the pairs

$$(0, 1); \quad (1, 0); \quad (1, 1); \quad (-1, 1).$$

All of these edges point into the halfplane above the relevant floor line. This what we wanted to establish.

## 15.5 The Even Case

The only place where we used the fact that  $p/q$  is odd was in Lemma 15.1. We needed to know that the number  $t$  in Equation 15.1 was odd. This no longer works when  $p + q$  is odd. However, when  $p/q$  is even, the floor grid has a different definition: Only the even floor lines are present in the grid. That is, the number  $k$  in Equation 15.1 is an even integer. Hence, for the floor lines in the even case, the number  $t$  is an integer. The rest of the proof of Lemma 15.1 works word for word. The rest of the proof of Statement 1 goes through word for word.

## 16 Proof of the Hexagrid Theorem II

### 16.1 The Basic Definitions

As in the previous chapter, we will take  $p/q$  odd until the very end. It turns out that the secret to proving Statement 2 of the Hexagrid Theorem is to use variants of the maps  $M_+$  and  $M_-$  from Equation 6.6.3. Let  $A \in (0, 1)$  be any parameter. Let  $\Lambda$  the lattice from the Master Picture Theorem. Let  $\Pi \subset \mathbf{R}^3$  be the plane defined by the relation  $x + y = A$ .

For  $(m, n) \in \mathbf{R}^2$  we define  $\Delta_+(m, n) = (x, y, z)$ , where

$$x = 2A(1 - m + n) - m; \quad y = A - x; \quad z = Am. \quad (184)$$

We also define

$$\Delta_-(m, n) = \Delta_+(m, n) + (-A, A, 0). \quad (185)$$

Note that  $\Delta_{\pm}(m, n) \in \Pi$ . Indeed,  $\Delta$  is an affine isomorphism from  $\mathbf{R}^2$  onto  $\Pi$ .

**Lemma 16.1** *Suppose that  $(m, n) \in \mathbf{Z}^2$ . Then  $\Delta_{\pm}(m, n)$  and  $M_{\pm}(m, n)$  are equivalent mod  $\Lambda$ .*

**Proof:** Let  $v_1, v_2, v_3$  be the three columns of the matrix defining  $\Lambda$ . So,  $v_1 = (1 + A, 0, 0)$  and  $v_2 = (1 - A, 1 + A, 0)$  and  $v_3 = (-1, -1, 1)$ . Let

$$c_1 = -1 + 2m; \quad c_2 = 1 - m + 2n; \quad c_3 = n.$$

We compute directly that

$$M_+(m, n) - \Delta_+(m, n) = c_1v_1 + c_2v_2 + c_3v_3.$$

$$M_-(m, n) - \Delta_-(m, n) = c_1v_1 + (c_2 - 1)v_2 + c_3v_3.$$

This completes the proof. ♠

We introduce the vector

$$\zeta = (-A, A, 1) \in \Lambda. \quad (186)$$

Referring to the proof of our last result, we have  $\zeta = v_2 + v_3$ . This explains why  $\zeta \in \Lambda$ . Note that  $\Pi$  is invariant under translation by  $\zeta$ .

## 16.2 Interaction with the Hexagrid

Now we will specialize to the case when  $A = p/q$  is an odd rational. The results above hold, and we can also define the hexagrid. We will see how the maps  $\Delta_+$  and  $\Delta_-$  interact with the Hexagrid. Let  $L_0$  denote the wall line through the origin.

**Lemma 16.2**  $\Delta_{\pm}(L_0)$  is parallel to  $\zeta$  and contains  $(-2A, A, 0)$ .

**Proof:** We refer to the points in Figure 3.1. The points  $v_5$  and  $v_1$  both lie on  $L_0$ . We compute

$$\Delta_+(v_5) - \Delta_+(v_1) = \frac{p^2}{p+q}\zeta.$$

Hence  $\Delta_+(L_0)$  is parallel to  $\zeta$ . We compute that  $\Delta_+(0, 0) = (2A, -A, 0)$ . ♠

We introduce the notation  $\Pi(x)$  to denote the line in  $\Pi$  that is parallel to  $\zeta$  and contains the point  $(x, A - x, 0)$ . For instance,

$$\Delta_+(0, 0) \subset \Pi(2A); \quad \Delta_-(0, 0) \subset \Pi(A). \quad (187)$$

Let  $\Pi(r, s)$  denote the infinite strip bounded by the lines  $\Pi(r)$  and  $\Pi(s)$ .

For each pair of indices  $(\epsilon_1, \epsilon_2) \in \{-1, 0, 1\}^2$ , we let  $\Sigma(\epsilon_1, \epsilon_2)$  denote the set of lattice points  $(m, n)$  such that  $L_0$  separates  $(m, n)$  from  $(m + \epsilon_1, n + \epsilon_2)$ . Now we define constants

$$\begin{aligned} \lambda(0, 1) &= 2A & \lambda(-1, -1) &= 1 - A^2; \\ \lambda(-1, 0) &= 1 + 2A - A^2 & \lambda(-1, 1) &= 1 + 4A - A^2 \end{aligned} \quad (188)$$

**Lemma 16.3** *Let  $(\epsilon_1, \epsilon_2)$  be any of the 4 pairs listed above. Let  $\lambda = \lambda(\epsilon_1, \epsilon_2)$ . The following 3 statements are equivalent.*

1.  $(m, n) \in \Sigma(\epsilon_1, \epsilon_2)$ .
2.  $\Delta_+(m, n)$  is congruent mod  $\Lambda$  to a point in the interior of  $\Pi(2A - \lambda, 2A)$ .
3.  $\Delta_-(m, n)$  is congruent mod  $\Lambda$  to a point in the interior of  $\Pi(A - \lambda, A)$ .

**Proof:** The formula  $\Delta_- = \Delta_+ + (-A, A, 0)$  immediately implies the equivalence of the second and third statements. So, it suffices to prove the equivalence of the first two statements. We will consider the pair  $(-1, 0)$ . The other cases have the same treatment. The set  $\Sigma(-1, 0)$  is the intersection of  $\mathbf{Z}^2$  with the interior of some infinite strip, one of whose boundaries is  $L_0$ . To find the image of this strip under  $\Delta_+$ , we just have to see what  $\Delta_+$  does to two points, one per boundary component of the strip. We choose the points  $(0, 0)$  and  $(1, 0)$ . We already know that  $\Delta_+(0, 0) \subset \Pi(2A)$ . We just have to compute  $\Delta_+(1, 0)$ . We compute

$$\Delta(1, 0) = (1, A - 1, A) \subset \Pi(1 - A^2).$$

This gives us  $\lambda(-1, 0) = 1 + 2A - A^2$ . Our lemma follows from this fact, and from the fact that  $\Delta_+$  is an affine isomorphism from  $\mathbf{R}^2$  to  $\Pi$ . ♠

### 16.3 Determining the Local Picture

A crossing cell can consist of either 1 edge or 2, depending on whether or not a vertex of the cell lies on a wall line. According to Lemma 14.4, the only crossing cells with one edge are equivalent mod  $\Theta$  to the one whose center vertex is  $(0, 0)$ . For these *special* crossing cells, Statement 2 of the Hexagrid Theorem is obvious. The door is just the central vertex.

The remaining crossing cells are what we call *generic*. Each generic crossing cell has one vertex in one of our sets  $\Sigma(\epsilon_1, \epsilon_2)$ , for one of the 4 pairs considered above. We call  $v \in \Sigma(\epsilon_1, \epsilon_2)$  a *critical* for  $(\epsilon_1, \epsilon_2)$ .  $v$  and  $v + (\epsilon_1, \epsilon_2)$  are the two vertices of a crossing cell. To prove Statement 2 of the Hexagrid Theorem, we need to understand the critical vertices. This means that we need to understand the local picture of the arithmetic graph in terms of the maps  $\Delta_+$  and  $\Delta_-$ .

We want to draw pictures as in the previous chapter, but here we need to be more careful. In the previous chapter, our plane  $\Pi$  contained the vector  $(1, 1, 1)$ . Thus, we could determine the structure of the arithmetic graph just by looking at the intersection  $\Pi \cap \mathcal{R}$ . Here  $\mathcal{R}$  is the polyhedron partition for the given parameter. The situation here is different. The vector  $(1, 1, 1)$  is transverse to the plane  $\Pi$ . What we really need to do is to understand the way that the plane  $\Pi_\alpha$  intersects the our partition. Here  $\Pi_\alpha$  is the plane satisfying the equation  $x + y = A + 2\alpha$ . We think of  $\alpha$  an infinitesimally

small but positive number. More formally, we take the geometric limit of the set  $\Pi_\alpha \cap \mathcal{R}$  as  $\alpha \searrow 0$ .

We say that a subset  $S \subset \Pi$  is *painted*  $(\epsilon_1, \epsilon_2, +)$  if  $\Delta_+(m, n) \in S$  implies that  $\Delta_+(m, n)$  determines the pair  $(\epsilon_1, \epsilon_2)$ . This is to say that  $S$  is contained in the Hausdorff limit of  $\Pi_\alpha \cap \mathcal{R}_+(\epsilon_1, \epsilon_2)$  as  $\alpha \rightarrow 0$ . We make the same definition with  $(+)$  in place of  $(-)$ . We think of  $(\epsilon_1, \epsilon_2, \pm)$  as a kind of color, because these regions are assigned various colors in Billiard King. For instance  $(0, 1, \pm)$  is green. There is essentially one *painting* of  $\Pi$  for  $(+)$  and one for  $(-)$ .

To visualize the painting, we identify  $\Pi$  with  $\mathbf{R}^2$  using the map  $(x, y, z) \rightarrow (x, z)$ . We just drop the second coordinate. The vector  $\zeta$  maps to the  $(-A, 1)$ . Thus, our whole painting is invariant under translation by this vector. Each wall of  $\mathcal{R}$  intersects  $\Pi$  in a line segment whose image in  $\mathbf{R}^2$  is either horizontal or vertical. The endpoints of each such segment have coordinates that are simple rational combinations of 1 and  $A$ . For this reason, we can determine the intersection we seek just by inspecting the output from Billiard King. In practice, we take  $\alpha = 10^{-5}$ , examine the resulting picture, and then adjust the various vertices slightly so that their coordinates are small rational combinations of 1 and  $A$ .

## 16.4 An Extended Example

We consider the pair  $(0, 1)$  in detail. We will draw pictures for the parameter  $A = 1/3$ , though the same argument works for any parameter. There is no polyhedron  $\mathcal{R}_-(0, 1)$ , so no points are painted  $(0, 1, -)$ . The interesting case is  $(0, 1, +)$ . First of all, we only care about points in our strip  $\Sigma(0, 1)$ . So, we only need to understand the portion of our painting that lies in our strip  $\Pi(0, 2A)$ . In  $\mathbf{R}^2$  (considered as the  $xz$  plane), our strip is bounded by the lines  $x = -zA$  and  $x = -zA + 2A$ .

We will first study the picture when  $z = 0$ . Referring to Figure 16.1, the shaded triangles correspond to  $\mathcal{R}(0, 1)$ . The thick line corresponds to the intersection of  $\Pi$  with our fiber. The black dot is the point  $(A, 0, 0, A)$ . Moving away from the black dot, the white dots are

$$(0, A, 0, A); \quad (-A, 2A, 0, A); \quad (-1, 1 + A, 0, A).$$

It we move the thick line an infinitesimal amount in the direction of  $(1, 1)$ , we see that it crosses through a shaded region whose diagonal edge is bounded

by the points  $(0, A)$  and  $(A, 0)$ . The only tricky part of the analysis is that the point  $(A, 0)$  determines the pair  $(0, 0)$  and the point  $(0, A)$  determines the pair  $(-1, 1)$ .

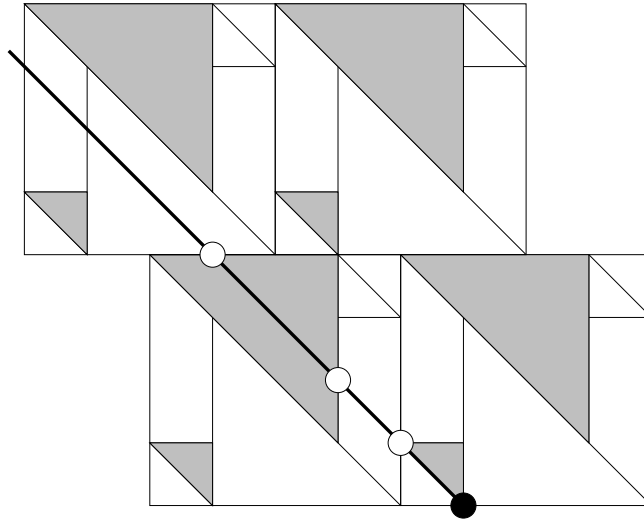


**Figure 16.1:** Slicing the 0 fiber.

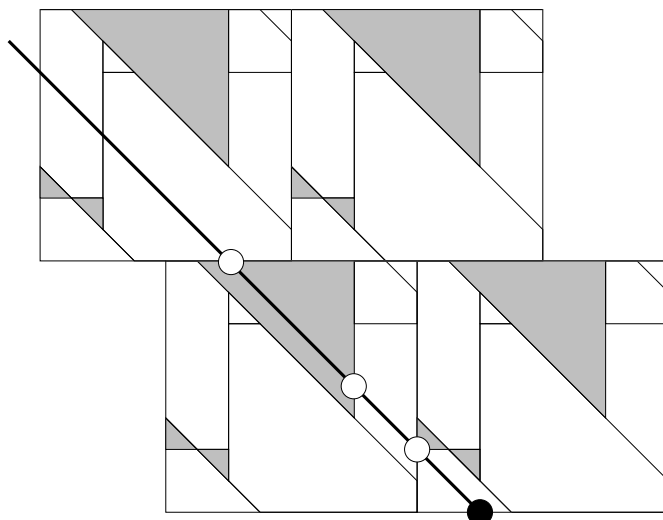
From this discussion, we conclude that  $(0, A) \times \{0\}$  is painted  $(0, 1, +)$ . For later use, we remark that  $(0, 0)$  is painted  $(-1, 1, +)$  and  $(A, 0)$  is painted  $(0, 0, +)$ . Looking at the picture, we also see that  $(-1, -A) \times \{0\}$  is painted  $(0, 1, +)$ . Notice, however, that this set lies outside our strip. It is irrelevant.

Figure 16.2 shows the picture for a typical parameter  $z \in (0, 1)$ . We choose  $z = 1/6$ , though the features of interest are the same for any choice of  $z$ . The interested reader can see essentially any slice (and in color) using Billiard King.

The black dot and the white dots have the same coordinates as in Figure 16.1. Notice that the point  $(0, A, z, A)$  lies at the bottom corner of a shaded region. This remains true for all  $z$ . We conclude that the open line segment  $\{0\} \times (0, 1)$  is painted  $(0, 1, +)$ . Similarly, the rectangle  $(-1, -A) \times [0, 1]$  is painted  $(0, 1, +)$ . However, this rectangle is disjoint from the interior of our strip. Again, it is irrelevant.

Recalling that our painting is invariant under translation by  $(0, 1, +)$ , we can now draw the portion of plane painted  $(0, 1, +)$  that is relevant to our analysis. To give the reader a sense of the geometry, we also draw one copy of the irrelevant rectangle. Again, we draw the picture for the parameter

$A = 1/3$ . The interested reader can see the picture for any parameter using Billiard King.



**Figure 16.2:** Slicing a typical fiber.

In Figure 16.3, the arrow represents the vector  $(-A, 1)$ . The black dot is  $(0, 0)$  and the white dot is  $(A, 0)$ . The thick zig-zag, which is meant to go on forever in both directions, is the relevant part of the painting. The lightly shaded region is the strip of interest to us.

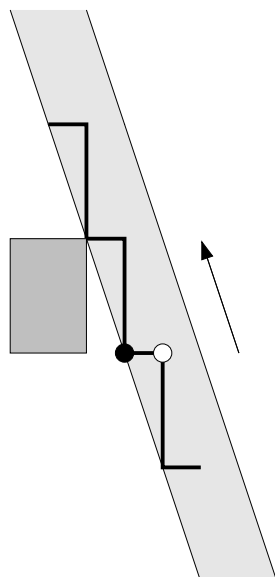


**Figure 16.3:** The relevant part of the  $(0, 1, +)$  painting.

## 16.5 The Rest of the Painting

We determine the rest of the painting using the same techniques. The interested reader can see everything plotted on Billiard King. The left side of figure 19.4 shows the relevant part of the (+) painting. The right side shows the relevant part of the (-) painting. The dots are exceptional points in the painting. The two grey dots at the endpoints correspond to the right endpoints of the special crossing cells. We have shown a “fundamental domain” for the paintings. The whole painting is obtained taking the orbit under the group  $\langle \zeta \rangle$ . In our picture,  $\zeta$  acts as translation by the vector  $(-A, 1)$ , because we are leaving off the  $y$  coordinate. In particular, the two endpoints of the  $L$  are identified when we translate by this group.

The small double-braced labels, such as  $((0, 1))$ , indicate the paint colors. The large labels, such as  $(0, 0)$ , indicate the coordinates in the plane. Note that the point  $(x, z)$  in the plane actually corresponds to  $(x, A - z, y)$  in  $\Pi$ . The grey vertices on the left corresponds to  $\Delta_+(0, 0)$ . The grey vertices correspond to the various images of points on the special crossing cell. These vertices are not relevant to our analysis of the points that are critical relative to our 4 pairs.

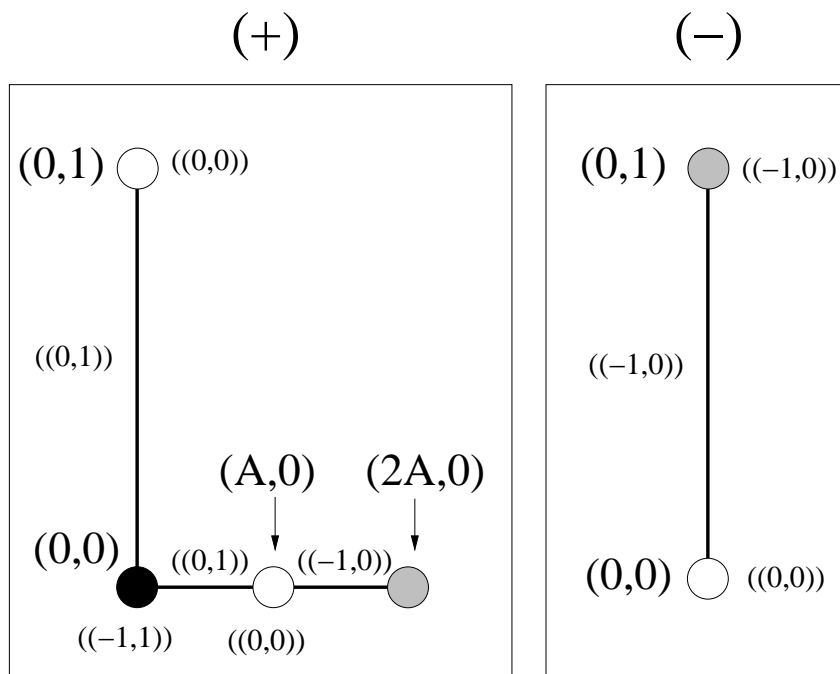
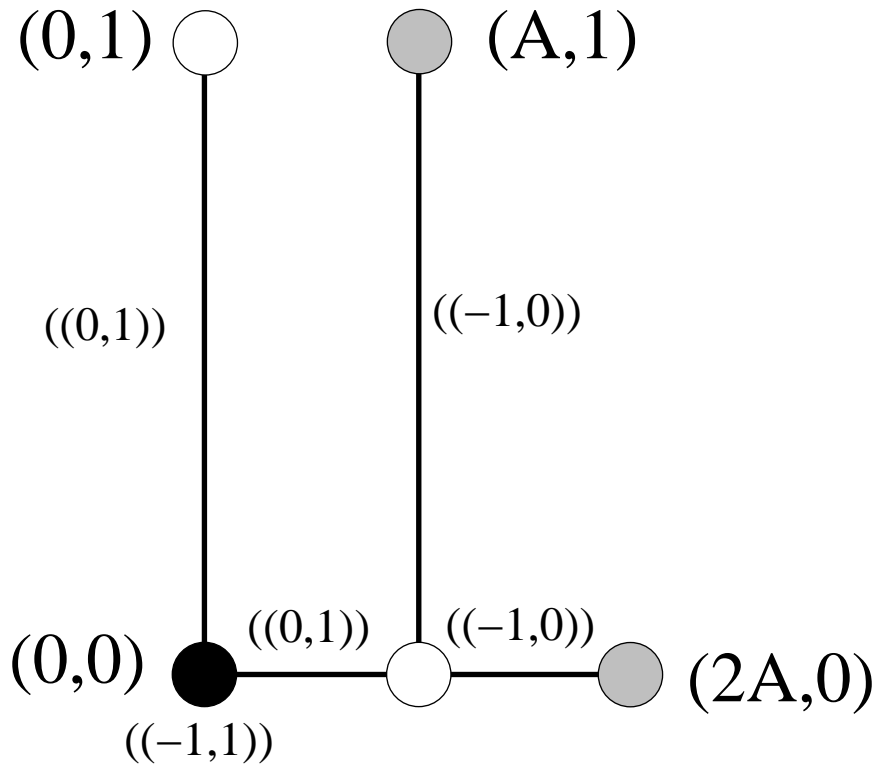


Figure 16.4: The relevant part of the (+) painting

Say that a vertex  $v = (m, n)$  is *critical* if it either lies in  $\Theta$  or else is critical for one of our strips. The point  $(0, 0)$  is the center vertex of a special crossing cell. Hence, By Lemma 14.4, the critical vertices are in bijection with the crossing cells. Given our analysis above, we see that  $v \in \mathbf{Z}^2$  is *critical* if and only if it satisfies the following criterion. *Modulo the action of  $\Lambda$ , the point  $\Delta_+(v)$  (respectively the point  $\Delta_-(v)$ ) lies in one of the colored parts of the painting on the left (respectively right) in Figure 16.4.*

Recalling that  $\Delta_+ = \Delta_- + (A, -A, 0)$ , we can eliminate  $\Delta_-$  from our discussion. We translate the right hand side of Figure 16.4 by  $(A, 0)$  and then superimpose it over the left hand side. (This translation does not reflect the way the two halves of Figure 16.4 are related to each other on the page.) See Figure 16.5. The result above has the following reformulation.

**Lemma 16.4 (Critical)** *A vertex  $v$  is critical if and only if  $\Delta_+(v)$  is equivalent mod  $\Lambda$  to a point colored portion of Figure 16.5.*



**Figure 16.5:** Superimposed paintings

Our drawing of Figure 16.5 somewhat hides the symmetry of our picture. In Figure 16.6, we show several translates of this fundamental domain at the same time, without the labels. We also show the strip  $\Pi(0, 2A)$ . The pattern is meant to repeat endlessly in both directions. The line on the left is  $\Pi(0)$  and the line on the right is  $\Pi(2A)$ . Again, we are drawing the picture for the parameter  $A = 1/3$ . The combinatorial pattern is the same for any  $A$ .

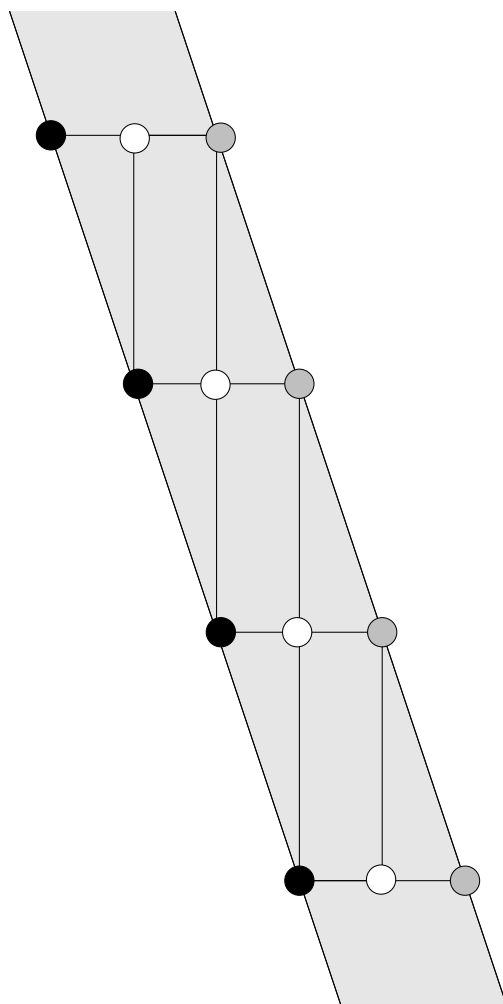


**Figure 16.6:** Superimposed paintings

To prove the hexagrid theorem, it only remains to identify the lattice points in the Critical Lemma with the doors from the Hexagrid Theorem.

## 16.6 The End of the Proof

Now we interpret the Critical Lemma algebraically. A vertex  $v \in \mathbf{Z}^2$  is *critical* if and only if  $\Delta_+(v)$  is equivalent mod  $\Lambda$  to one of the following kinds of points.

1.  $(2A, -A, 0)$ .
2.  $(0, A, 0)$ .
3.  $(x, A - x, 0)$ , where  $x \in (0, 2A) - \{A\}$ .
4.  $(0, A, z)$ , where  $z \in (0, 1)$ .

As we point out in our subsection headings, each case corresponds to a different feature of our painting in Figures 16.5 and 16.6

### 16.6.1 Case 1: The Grey Dots

Note that  $\Delta_+(0, 0) = (2A, -A, 0)$ . Moreover,  $\Delta_+(v) \equiv \Delta_+(v') \pmod{\Lambda}$  iff  $M_+(v) \equiv M_-(v) \pmod{\Lambda}$  iff  $v \equiv v' \pmod{\Theta}$ . Hence, Case 1 above corresponds precisely to the special crossing cells. The door associated to  $v$  is precisely  $v$ . In this case, the door is associated to the wall above it.

### 16.6.2 Case 2: The Black Dots

Note that  $\Delta_+(0, -1) = (0, A, 0)$ . Hence the second case occurs iff  $v$  is equivalent mod  $\Theta$  to  $(0, -1)$ . But  $(0, -1)$  is the vertex of a crossing cell whose other vertex is  $(-1, 0)$ . The door associated to  $(0, -1)$  is  $(0, 0)$ . In this case, the door is associated to the wall below it.

### 16.6.3 Case 3: Horizontal Segments

We are going to demonstrate the bijection between the Type 1 doors not covered in Cases 1 and 2 and the critical points that arise from Case 3 above.

Let  $v$  be a critical point. Using the symmetry of  $\Theta$ , we can arrange that our point  $v$  is closer to  $L_0$  than to any other wall line. In this case,  $\Delta_+(v)$  lies in the strip  $\Pi(0, 2A)$ . Hence  $v \in \Sigma(0, 1)$ . Hence  $L_0$  separates  $v$  from  $v + (0, 1)$ . Let  $y \in (n, n + 1)$  be such that  $(m, y) \in L_0$ .

The third coordinate of  $\Delta_+(v)$  is an integer. Setting  $v = (m, n)$ , we see that  $Am \in \mathbf{Z}$ . Hence  $q$  divides  $m$ . Hence  $v = (kq, n)$  for some  $k \in \mathbf{Z}$ . Hence  $(kq, y)$  is a Type 1 door.

For the converse, suppose that the point  $(kq, y)$  is a Type 1 door and that  $n = \underline{y}$ . Let  $v = (kq, n)$ . We want to show that  $v$  is critical. By construction  $(kq, \underline{n}) \in \Sigma(0, 1)$ . Hence  $\Delta_+(kq, n) \in \Pi(0, 2A)$ . But the third coordinate of  $\Delta_+(kq, n)$  is an integer. Hence  $\Delta_+(kq, n)$  is equivalent mod  $\Lambda$  to a point of the form  $(x, A - x, 0)$ . Here  $x \in (0, 2A)$ .

If  $x = A$  then  $v$  lies on the centerline of the strip  $\Sigma(0, 1)$ . But then  $y - \underline{y} = 1/2$ . This contradicts Lemma 14.6. Hence  $A \neq x$ .

Now we know that  $\Delta_+(kq, n)$  satisfies Case 3 above. Hence  $(kq, n)$  is critical, either for  $(0, 1)$  or for  $(-1, 0)$ . These are the relevant labellings in Figure 16.5. Note that  $L_0$  has positive slope greater than 1. Hence

$$(kq, n) \in \Sigma_+(0, 1) \cap \Sigma_+(-1, 0).$$

If  $\Delta'_+(v)$  is colored  $(0, 1)$ , then  $v$  is critical for  $(0, 1)$ . If  $\Delta'_+(v)$  is colored  $(-1, 0)$ , then  $v$  is critical for  $(-1, 0)$ . So,  $v$  is always vertex of a crossing cell.

#### 16.6.4 Case 4: Vertical Segments

We are going to demonstrate the bijection between Type 2 doors and the critical points that arise from Case 4 above.

We use the symmetry of  $\Theta$  to guarantee that our critical point is closer to  $L_0$  than to any other wall line. As in Case 3, the point  $\Delta_+(v) \in \Pi(0, A)$ . Hence  $v \in \Sigma(0, 1)$  and  $L_0$  separates  $v$  from  $v + (0, 1)$ . We define  $y$  as in Case 3. We want to show that  $(m, y) \in L$  is a Type 2 door.

Since we are in Case 4, the first coordinate of  $\Delta_+(v)$  lies in  $A\mathbf{Z}$ . The idea here is that  $\Delta_+(v)$  is equivalent mod  $(-A, A, 1)$  to a point whose first coordinate is either 0 or  $A$ . Hence

$$x = 2A(1 - m + n) - m \in A\mathbf{Z}.$$

Hence  $x/A \in \mathbf{Z}$ . Hence  $m/A \in \mathbf{Z}$ . Hence  $m = kp$ . By Lemma 14.7, the point  $(x, y)$  is a door.

Conversely, suppose that the point  $(kp, y)$  is door contained in  $L_0$ . Let  $n = \underline{y}$ . Then  $(kp, n) \in \Sigma(0, 1)$  and the first coordinate of  $\Delta_+(kp, n)$  lies in the set  $A\mathbf{Z}$ . Also,  $\Delta_+(kp, n) \in \Pi(0, 2A)$ . Hence,  $(kp, n)$  satisfies Case 4 above. Hence  $(kp, n)$  is critical for either  $(0, 1)$  or  $(-1, 0)$ . In either case,  $(kp, n)$  is a vertex of a crossing cell.

## 16.7 The Pattern of Crossing Cells

Our proof of the Hexagrid Theorem is done, but we can say more about the nature of the crossing cells. First of all, there are two crossing cells consisting of edges of slope  $\pm 1$ . These crossing cells correspond to the black and grey corner dots in Figure 16.6.

The remaining crossing cells involve either vertical or horizontal edges. These crossing cells correspond to the interiors of the segments in Figures 16.5 and 16.6. Let  $v = (m, n)$  be the critical vertex associated to the door  $(m, y)$ . Then  $v$  is critical either for  $(0, 1)$  or  $(-1, 0)$ . In the former case, the crossing cell associated to  $v$  is vertical, and in the latter case it is horizontal. Looking at the way Figure 16.5 is labelled, we see that

- The crossing cell is vertical if  $y - \underline{y} > 1/2$ .
- The crossing cell is horizontal if  $y - \underline{y} < 1/2$ .

The case  $y - \underline{y} = 1/2$  does not occur, by lemma 14.6.

There are exactly  $p + q$  crossing cells mod  $\Theta$ . These cells are indexed by the value of  $y - n$ . The possible numbers are

$$\left\{0, \frac{1}{p}, \dots, \frac{p-1}{p}, \frac{1}{q}, \dots, \frac{q-1}{q}, 1\right\}.$$

In all cases we have  $y - n = y - \underline{y}$ , except when  $n = y - 1$ .

Figure 16.7 shows, for the case  $p/q = 3/5$ , the images of the critical vertices, on one fundamental domain for Figure 16.6. (The fundamental domain here is nicer than the one in Figure 16.5.) We have labelled the image points by the indices of the corresponding crossing cells. The lines inside the dots show the nature of the crossing cell. The dashed grid lines in the figure are present to delineate the structure. The lines inside the dots show the nature of the crossing cell.

One can think of the index values in the following way. Sweep across the plane from right to left by moving a line of slope  $-5/3$  parallel to itself. (The diagonal line in Figure 16.7 is one such line.) The indices are ordered according to how the moving line encounters the vertices. The lines we are using correspond to the lines in  $\Pi$  that are parallel to the vector  $\zeta$ .

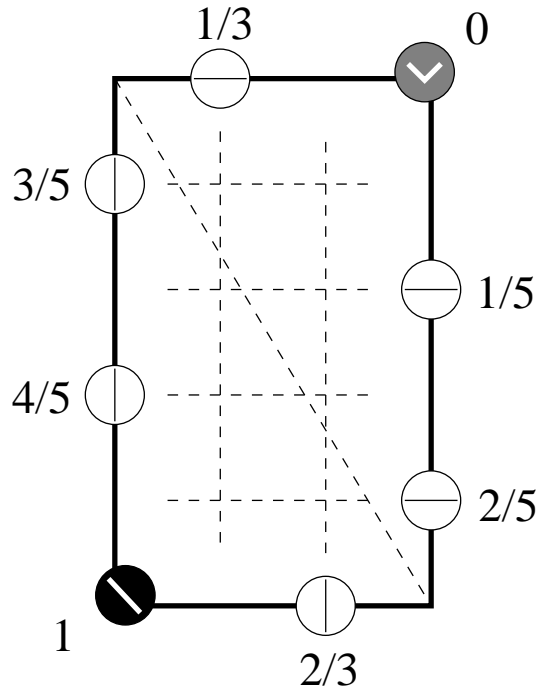


**Figure 16.7:** Images of the critical points

Figure 16.7 is representative of the general case. It is meant to suggest the general pattern. We hope that the pattern is clear.

## 16.8 The Even Case

When  $p/q$  is an even rational, all the constructions in this chapter go through word for word.

It appears that we used the fact that  $p/q$  is odd in Cases 3 and 4 in the last section, but this isn't so. We only used the fact that Corollary 14.6 was true, and that Lemma 14.7 was true. At the time, we had only proved these results in the odd rational case. However, since these results hold in the even case, the arguments for Cases 3 and 4 go through word for word.

A final remark on Case 3: Case 3 required us to use Corollary 14.6 to rule out the possibility that the point  $(m, n)$  is equivalent mod  $\Lambda$  to the points  $(A, 0, 0)$ . This can happen in the even case, and indeed it happens when  $(m, y)$  is a crossing of the kind we are no longer calling a door. In other words, this does not happen for a *door* because we have forced the situation.

## 17 The Barrier Theorem

We remind the reader that we don't need the material in this chapter until Part VI.

### 17.1 The Result

Let  $A = p/q$  be an even rational. All the components of  $\hat{\Gamma} = \hat{\Gamma}(A)$  are embedded polygons. Say that a *low component* is one that contains a low vertex. The component  $\Gamma$  containing  $(0, 0)$  is a distinguished low component. The infinite set of components  $\Gamma + kV$ , with  $k \in \mathbf{Z}$  are translates of  $\Gamma$ . Here  $V = (q, -p)$  as usual. We call these components *major* components. We call the remaining low components *minor* components.

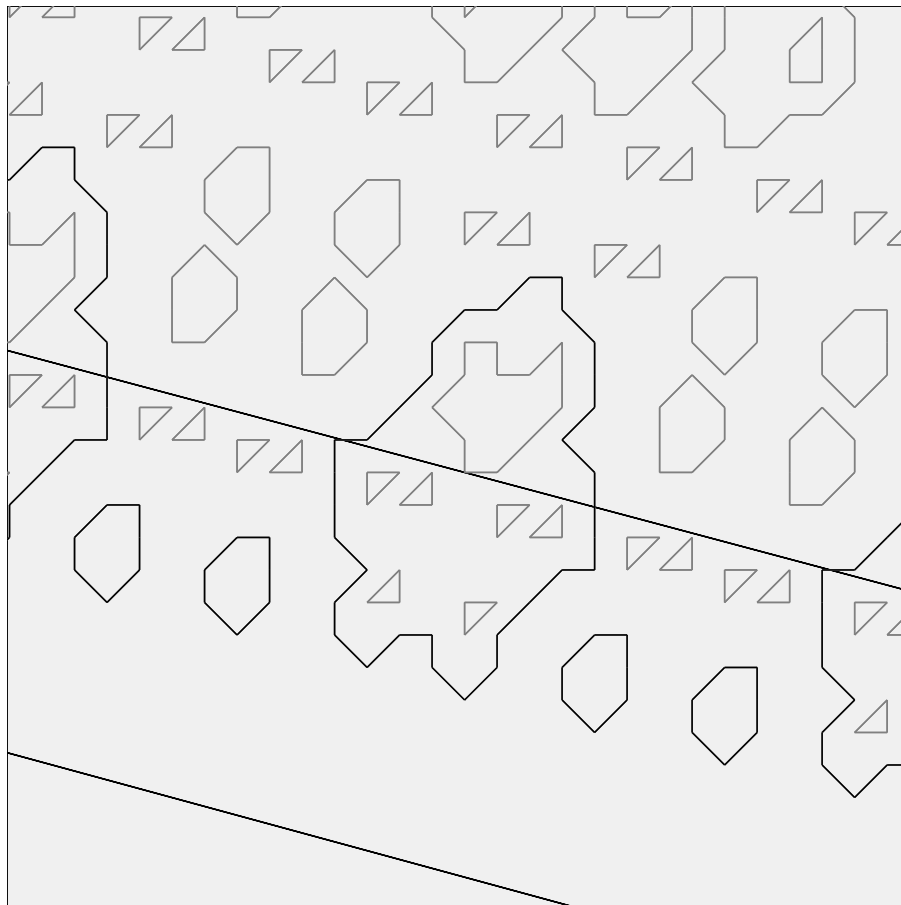


Figure 17.1: Components of  $\hat{\Gamma}(4/15)$  and a barrier.

Figure 17.1 shows some of  $\widehat{\Gamma}(4/15)$ . The three biggest polygons are major components, and the little polygons along the bottom are minor components. Figure 17.1 also shows a barrier, parallel to the baseline, which is only crossed by the major components. The Barrier Theorem describes this barrier and establishes its basic properties.

Referring to Equation 27, one of the two rationals  $p_{\pm}/q_{\pm}$  is even and one is odd. Let  $p'/q'$  denote whichever of these rationals is odd. We call  $p'/q'$  the *odd predecessor* of  $p/q$ . We say that the *barrier* is the line parallel to  $V$  that contains the point

$$\left(0, \frac{p' + q'}{2}\right) \tag{189}$$

**Theorem 17.1 (Barrier)** *Modulo translation by  $V$ , only 2 edges of  $\widehat{\Gamma}$  cross the barrier, and these lie on major components. Hence, no minor component of  $\widehat{\Gamma}$  crosses the barrier.*

One could think of the Barrier Theorem as an improvement of Statement 1 of the Hexagrid Theorem. Statement 1 of the Hexagrid Theorem bounds the distance that any low component can rise above the baseline. The Barrier Theorem gives a bound that is at least twice as good for all the minor components.

We have stated the precise version of the Barrier Theorem that we need for our applications, but the Barrier Theorem is really part of a more robust general theorem. If  $A^*$  is a parameter that is close to  $A$  in the sense of Diophantine approximation, then the line  $\Lambda^*$  parallel to  $V$  and containing the point

$$\left(0, \frac{p^* + q^*}{2}\right) \tag{190}$$

is not frequently crossed by  $\widehat{\Gamma}$ . The basic reason is that  $\Lambda^*$  serves as a kind of memory of the Hexagrid Theorem for the parameter  $A^*$ . The two graphs  $\widehat{\Gamma}$  and  $\widehat{\Gamma}^*$  mainly agree along  $\Lambda^*$ , and the only crossings take places at the few mismatches in the graphs.

We will prove the Barrier Theorem using the same ideas that we used to prove Statement 1 of the Hexagrid Theorem. Mainly we shall be interested in the differences between the Barrier Theorem and Statement 1 of the Hexagrid Theorem.

## 17.2 Review of the Hexagrid Proof

Let us recall the idea behind the proof of Statement 1 of the Hexagrid Theorem, given in §15. Our main idea was to analyze points just above the floor line and observe that no such point contained an edge of  $\widehat{\Gamma}$  that crossed the floor line. Given the Master Picture Theorem, this amounted to checking that the image of such points never landed in a “bad polygon” of the partition – one that would assign to the vertex a crossing edge. Here were the 3 main ideas.

1. In Lemma 15.1, we computed that  $M_-$  (one of the two classifying maps from the Master Picture Theorem) maps each floor line to a point of the form  $(\beta, 0, 0) \in \mathbf{R}^3/\Lambda$ .
2. In Lemma 15.2 we deduced from Lemma 15.1 that  $M_{\pm}$  mapped lattice points just above the floor line into a plane  $\Pi_{\pm}$ . Both planes were translates of the plane  $\Pi$  containing  $(1, 0, 0)$  and  $(1, 1, 1)$ . The relevant lattice points were contained in the strips  $\Sigma(\epsilon_1, \epsilon_2)$  for various choices of  $\epsilon_1, \epsilon_2 \in \{-1, 0, 1\}$ .
3. We sliced our partition  $\mathcal{P}_{\pm}$  by the planes  $\Pi_{\pm}$  and simply checked that no relevant vertex landed in a bad polygon. Figures 15.1 and 15.2 showed the relevant picture for  $A = 1/3$ . The relevant vertices are contained in the strips  $\Sigma(\epsilon_1, \epsilon_2)$  for various choices of  $\epsilon_1, \epsilon_2 \in \{-1, 0, 1\}$  and the relevant domains were strips  $\Pi_{\pm}(0, \lambda(\epsilon_1, \epsilon_2)) \subset \Pi_{\pm}$ . See Lemma 15.3.

Now we explain the change that occurs when we pass to the present situation. Let  $\Lambda$  be the barrier line.

**Lemma 17.2** *There is some real  $\beta$  such that*

$$M_-(\Lambda) = \left( \beta, \pm \frac{1}{q}, 0 \right) \tag{191}$$

**Proof:** We think of  $M_-$  as acting on all of  $\mathbf{R}^2$ . Then  $M_-$  is constant along  $\Lambda$ . If we use the map  $M'$ , relative to  $A'$ , then we get a point  $(\beta', 0, 0)$  by the previous calculation. But  $M(m, n) - M(m, n) = (\pm 2/q, 0)$ . But  $M_- = \mu_- \circ M$ , where  $\mu_-(2t) = (t - 1, t, t) \bmod \Lambda$ . Putting these two facts together gives the proof. ♠

### 17.3 Proof of the Barrier Theorem

We will suppose that  $A' < A$  until the end of the section. When  $A' > A$ , the (+) option in Equation 191 is taken.

The maps  $M_{\pm}$  map  $\Lambda$  into planes  $\Pi'_{\pm}$  that are obtained by translating  $\Pi_{\pm}$  in the  $y$  direction by  $1/q$ . The same argument as in Lemma 15.2 shows that  $M_{\pm}$  maps the relevant lattice points – namely those in the strips  $\Sigma(\epsilon_1, \epsilon_2)$  – into the regions  $\Pi'_{\pm}(0, \lambda)$ . Here  $\Pi'_{\pm}(0, \lambda) \subset \Pi'$  is a translate of the strip considered in Lemma 15.3.

The planes  $\Pi_{\pm}$  are transverse to the walls defining our partition. When we translate  $\Pi_{\pm}$  off itself by  $(0, 1/q, 0)$ , the intersections we see are practically the same. Note that  $\Pi_{\pm}$  is not transverse to the partition itself, just to the walls. When we translate, some new regions pop into view. Figure 17.2 shows one period of the exact picture for  $\Pi_+$  relative to the parameter  $4/15$ . The little lines in the middle refer to similar lines drawn in Figure 15.1.

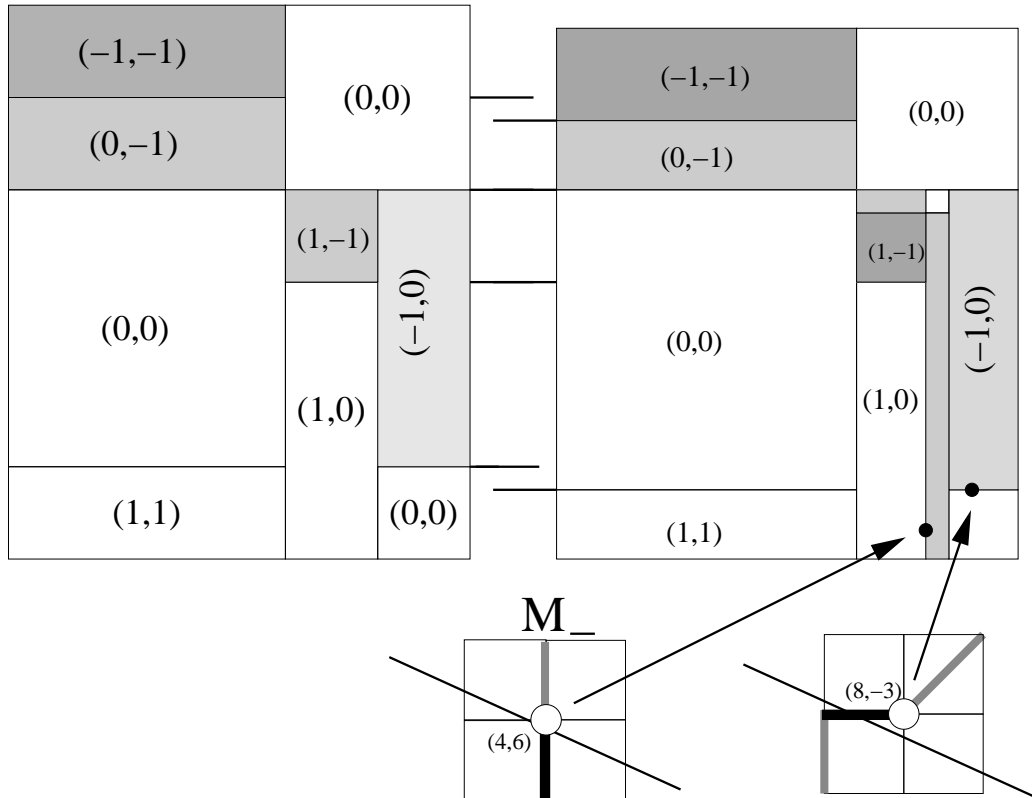


Figure 17.2: The slices  $\Pi_-$  and  $\Pi'_-$ .

The left hand side shows the slice  $\Pi_-$ . The right hand side shows the slice  $\Pi'_-$ . The point on the right is  $M(-3, 8)$ , the image of a vertex above the barrier incident to one of the crossing edges. The lightly shaded region above the point assigns the edge  $(-1, 0)$  to  $M_-(-3, 8)$ , and this edge crosses the barrier. The bottom of the figure shows this. Likewise, the skinny rectangle assigns the edge  $(0, -1)$  to  $M_-(4, 6)$ . This is also shown at the bottom of the figure. Were we to analyze the picture relative to the parameter  $A' = 3/11$ , these offending points would get assigned non-crossing edges.

In the new setting, our analysis for Statement 1 of the Hexagrid Theorem does not *completely succeed* for two potential reasons.

1. The image of a relevant vertex might lie in one of the newly appearing regions. These regions all have width  $1/q$ .
2. The image of a relevant vertex might lie in a different one of the old regions because the region has a slightly different rectangle and/or location in the new slice. This is what happens in our example. In this case, the change in each edge is at most  $1/q$ .

The bounds on the changes come from the equations for the walls defining our partitions.

Now we make an analysis of how many crossings one can get in Figure 17.2. The images of the relevant vertices all lie on a diagonal line of slope 1. This line starts on the bottom edge (on the right hand figure.) The difference in the coordinates between successive points is  $1/q$ . Thus, each modified rectangle can give rise to one new crossing. Likewise, each new rectangle can give rise to one new crossing. This implies that there are at most 5 crossings entailed by the picture.

We can reduce this number by looking more closely. The rectangle labelled  $(0, -1)$  remains out of range of the image  $M_-(\Sigma(0, -1))$ . The same argument as in the Hexagrid Theorem I applies here. Thus, this rectangle entail no crossings. This gets us down to 4. Here is a trick to get down to 2. Figure 17.3 shows 3 of the relevant rectangles.

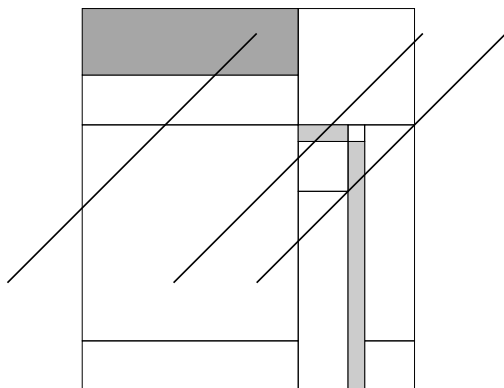


**Figure 17.3:** The bottom row of  $\Pi_+$  and  $\Pi'_+$ .

Note that any diagonal line intersects at most one of the 3 relevant rectangles. Therefore, what seems like 3 potential crossings is just 1. All in all, there are 2 potential crossings created by our perturbation. This estimate is sharp. The 2 crossings can happen.

The picture for  $\Pi_+$  is easier to analyze. Recall from the proof of the Hexagrid Theorem that all the relevant rectangles were well above the range of the corresponding vertices. See Figure 15.2. Thus, we only have to worry about the emergence of new rectangles. The only new rectangle to emerge within range is a rectangle labelled  $(-1, 0)$  that emerges at the very bottom. Hence, there is at most 1 crossing.

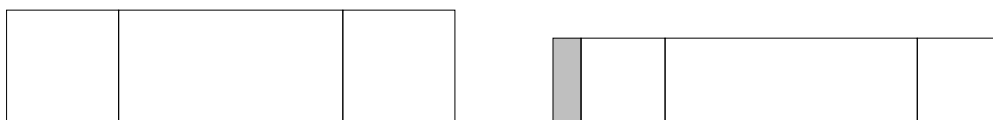


**Figure 17.4:** The bottom row of  $\Pi_+$  and  $\Pi'_+$ .

All in all, there are at most 3 barrier crossings within one period. Also, the number of barrier crossings is even because every component is a polygon. Hence there are exactly 2 barrier crossings. The major components do cross the barrier, and hence this accounts for the 2 crossings.

**Remark:** As in the proof of the Hexagrid Theorem, the pictures we drew above look somewhat different for other parameters. However, the main point of these pictures is depict the relative changes between the two pictures. This works the same for any parameter. The reader can see the picture for any

parameter using Billiard King.

Now we consider the case when  $A' < A$ . We can analyze this case just as above, though the details are somewhat trickier. The (+) slice still entails only one crossing. However, just from looking at the pictures, we cannot easily rule out the possibility that the (-) slice entails 3 crossings. This gives us a bound of 4 crossings, which is not quite good enough. A more subtle analysis of the picture could get us down to 2 crossings, but we prefer to take a different approach.

We will use symmetry. Let  $\Lambda_+$  denote the barrier line. There is nothing special about the fact that  $\Lambda_+$  lies above the baseline. We could consider the corresponding line  $\Lambda_-$  below the baseline. Here  $\Lambda_-$  is parallel to  $V$  and contains

$$P_- = \left(0, \frac{-p' + q'}{2}\right) \quad (192)$$

Actually, to get things exactly right, we think of  $\Lambda_+$  and  $\Lambda_-$  lying infinitesimally near, but below, the lines we have defined. This, in particular,  $P_-$  lies above  $\Lambda_-$ .

We compute that

$$M(P_-) = \left(\beta + \frac{1}{q}, 0, 0\right)$$

for some  $\beta \in \mathbf{R}$ . Thus, by considering  $\Lambda_-$  in place of  $\Lambda_+$ , we are back in the case we have already analyzed. But now we can apply the rotational symmetry  $\iota$  considered in §13.2. Assuming that  $\iota(\Lambda_-) = \Lambda_+$ , the result for  $\Lambda_+$  follows from the result for  $\Lambda_-$ .

It is not quite true that  $\iota(\Lambda_-) = \Lambda_+$ . In fact,  $\iota(\Lambda_-)$  is parallel to  $\Lambda_+$  and exactly  $1/q$  vertical units beneath  $\Lambda_-$ . Thus, we have actually proved the Barrier Theorem for a barrier that is lower by a tiny bit. This result suffices for all our purposes.

To get the stated result right on the nose, we note that  $P_-$  is the only point adversely effected:  $\iota(P_-)$  lies beneath  $\Lambda_+$  whereas  $P_-$  lies on  $\Lambda_-$ . However, recall that we consider our lines to be infinitesimally beneath the lines through integer points. Thus, as we mentioned above,  $P_-$  lies above  $\Lambda_-$ . So, even though  $\iota(\Lambda_-) \neq \Lambda_+$ , all the relevant lattice points lie on the correct sides.

This completes the proof of the Barrier Theorem.

# Part IV

Here is an overview of this part of the monograph.

- In §18 we prove the Superior Sequence Lemma from §4. The analysis here, especially Lemma 18.2, is central to all our arguments in this part. In §18.4 we introduce a function  $\Omega$ , closely related to our sequences, that plays an important role in subsequent chapters. We call  $\Omega$  the *Diophantine constant*. The reader interested mainly in Lemma 4.3 can skip everything in this chapter except §18.4.
- In §19 we prove the Diophantine Lemma. This result is the source of most of our period copying results.
- In §20 we prove Lemma 4.3 and Lemma 4.2. Lemma 4.2 is the final ingredient in the proof of the Erratic Orbits Theorem. Lemma 4.3 is an easier result that is the final ingredient in our proof of the Erratic Orbits Theorem for almost all parameters. The reader who is satisfied with the Erratic Orbits Theorem for almost all parameters can stop reading the monograph after §20.1.
- In §21 we prove the Decomposition Theorem, stated in §4.4. Our proof Lemma 4.2 relies on one case of the Decomposition Theorem, namely Lemma 21.5, which we prove in §21.3. The reader who is satisfied with the Erratic Orbits Theorem can stop reading the monograph after §21.3.

## 18 Proof of the Superior Sequence Lemma

### 18.1 Existence of the Inferior Sequence

We will give a hyperbolic geometry construction of the inferior sequence. Our proof is similar to what one does for ordinary continued fractions. Our model for the hyperbolic plane is the upper halfplane  $\mathbf{H}^2 \subset \mathbf{C}$ . The group  $SL_2(\mathbf{R})$  of real  $2 \times 2$  matrices acts isometrically by linear fractional transformations. The geodesics are vertical rays or semicircles centered on  $\mathbf{R}$ . See [B].

The *Farey graph* is a tiling of  $\mathbf{H}^2$  by ideal triangles. We join  $p_1/q_1$  and  $p_2/q_2$  by a geodesic iff  $|p_1q_2 - p_2q_1| = 1$ . The resulting graph divides the hyperbolic plane into an infinite symmetric union of ideal geodesic triangles. The Farey graph and the associated triangulation is one of the most beautiful pictures in all of mathematics.

We modify the Farey graph by erasing all the lines that connect even fractions to each other. The remaining edges partition  $\mathbf{H}^2$  into an infinite union of ideal squares. The subgroup  $\Gamma_2 \subset SL_2(\mathbf{R})$ , consisting of matrices congruent to the identity mod 2, acts in such a way as to preserve the tiling by ideal squares.

We say that a *basic square* is one of these squares that has all vertices in the interval  $(0, 1)$ . Each basic square has two opposing vertices that are labelled by positive odd rationals,  $p_1/q_1$  and  $p_2/q_2$ . These odd rationals satisfy  $|p_1q_2 - p_2q_1| = 2$ . Ordering so that  $q_1 < q_2$ , we call  $p_1/q_1$  the *head* of the square and  $p_2/q_2$  the *tail* of the square. We draw an arrow in each odd square that points from the tail to the head. That is  $p_1/q_1 \leftarrow p_2/q_2$ . We call the odd square *right biased* if the rightmost vertex is an odd rational, and *left biased* if the leftmost vertex is an odd rational.

The general form of a left biased square is

$$\frac{a_1}{b_1}; \quad \frac{a_1 + a_2}{b_1 + b_2}; \quad \frac{a_1 + 2a_2}{b_1 + 2b_2}; \quad \frac{a_2}{b_2}. \quad (193)$$

The leftmost vertex in a left-biased square is the head, and the rightmost vertex in a right-biased square is the head. One gets the equation for a right-biased square just by reversing Equation 193.

For an irrational parameter  $A$ , we simply drop the vertical line down from  $\infty$  to  $A$ , and record the sequence of basic squares we encounter. To form the inferior sequence, we list the heads of the encountered squares and weed out repeaters. The nesting properties of the squares guarantees convergence.

## 18.2 Structure of the Inferior Sequence

Now suppose that  $\{p_n/q_n\}$  is the inferior sequence approximating  $A$ . Referring to Equation 27, we write  $A_n = p_n/q_n$  and  $(A_n)_\pm = (p_n)_\pm/(q_n)_\pm$ . We have  $(A_n)_- < A_n < (A_n)_+$ , and these numbers form 3 vertices of an ideal square.  $A_n$  is the tail of the square.

**Lemma 18.1** *The following is true for all indices  $m$ .*

1. Let  $N > m$ . Then  $A_{m-1} < A_m$  iff  $A_{m-1} < A_N$ .
2. If  $A_{m-1} < A_m$  then  $(q_m)_- = q_{m-1} + (q_m)_+$ .
3. If  $A_{m-1} > A_m$  then  $(q_m)_+ = q_{m-1} + (q_m)_-$ .
4. Either  $A_m < A < (A_m)_+$  or  $(A_m)_- < A < A_m$ .

**Proof:** Statement 1 follows from the nesting properties of the ideal squares encountered by the vertical geodesic  $\gamma$  as it converges to  $A$ .

For Statement 2, note that  $A_{m-1} < A_m$  iff these two rationals participate in a left-biased basic square, which happens iff  $(q_m)_+ < (q_m)_-$ . By definition  $q_{m-1} = |(q_m)_- - (q_m)_+|$ . When  $(q_m)_+ < (q_m)_-$ , we can simply remove the absolute value symbol and solve for  $(q_m)_-$ . Statement 3 is similar.

For Statement 4, we will consider the case when  $A_m < A_{m-1}$ . The other case is similar. At some point  $\gamma$  encounters the basic square with vertices

$$(A_m)_- < A_m < (A_m)_+ < A_{m-1}.$$

If  $A_{m+1} < A_m$ , then  $\gamma$  exits  $S$  between  $(A_m)_-$  and  $A_m$ . So,  $(A_m)_- < A < A_m$ . If  $A_{m+1} > A_m$ , then  $\gamma$  exits  $S$  to the right of  $A_m$ . If  $\gamma$  exits  $S$  to the right of  $(A_m)_+$ , then  $\gamma$  next encounters a basic square  $S'$  with vertices

$$(A_m)_+ < O < E < A_{m-1},$$

where  $O$  and  $E$  are odd and even rationals. But then  $A_m$  would not be the term in our sequence after  $A_{m-1}$ . The term after  $A_{m-1}$  would lie in the interval  $[O, A_{m-1})$ . This is a contradiction. ♠

Let  $[x]$  denote the floor of  $x$ . Let  $d_n$  be as in Equation 31. Relatedly, define

$$\delta_0 = q_1 - 1; \quad \delta_n = \left\lceil \frac{q_{n+1}}{q_n} \right\rceil; \quad n = 1, 2, 3... \quad (194)$$

Now we come to our main structural result about the inferior sequence.

**Lemma 18.2** *The following is true for any index  $m \geq 1$ .*

1. *If  $A_{m-1} < A_m < A_{m+1}$  then*

- $\delta_m$  is odd;
- $(q_m)_+ < (q_m)_-$ ;
- $(q_{m+1})_+ = d_m q_m + (q_m)_+$ ;
- $(q_{m+1})_- = (d_m + 1)q_m + (q_m)_+$ .

2. *If  $A_{m-1} > A_m < A_{m+1}$  then*

- $\delta_m$  is even;
- $(q_m)_- < (q_m)_+$ ;
- $(q_{m+1})_+ = d_m q_m - (q_m)_-$ ;
- $(q_{m+1})_- = d_m q_m + (q_m)_+$ .

3. *If  $A_{m-1} > A_m > A_{m+1}$  then*

- $\delta_m$  is odd;
- $(q_m)_- < (q_m)_+$ ;
- $(q_{m+1})_+ = (d_m + 1)q_m + (q_m)_-$ ;
- $(q_{m+1})_- = d_m q_m + (q_m)_-$ .

4. *If  $A_{m-1} < A_m > A_{m+1}$  then*

- $\delta_m$  is even;
- $(q_m)_+ < (q_m)_-$ ;
- $(q_{m+1})_+ = d_m q_m + (q_m)_-$ ;
- $(q_{m+1})_- = d_m q_m - (q_m)_+$ .

**Remarks:**

(i) Here  $A_{m-1} < A_m > A_{m+1}$  means that  $A_{m-1} < A_m$  and  $A_m > A_{m+1}$ .

(ii) There is a basic symmetry in this result. We we swap all inequalities, then the signs (+) and (-) all switch. This symmetry swaps Cases 1 and 3, and likewise swaps Cases 2 and 4.

(iii) The same result holds for  $p$  in place of  $q$ . We used  $q$  just for notational convenience.

**Proof:** Cases 3 and 4 follow from Cases 1 and 2 by symmetry: Whatever argument we would give for Cases 1 and 2, we would just switch all the (+) signs to (−) signs and reverse all the inequalities to prove the corresponding statement for Cases 3 and 4. Thus, it suffices to consider Cases 1 and 2. We will consider Case 1 in detail, and only treat Case 2 briefly at the end.

In Case 1, the vertical geodesic  $\gamma$  to  $A$  passes through the basic square  $S$  with vertices

$$A_{m-1} < (A_m)_- < A_m < (A_m)_+.$$

Since  $A_n < A_{m+1}$ , the geodesic  $\gamma$  next crosses through the geodesic  $\alpha_m$  connecting  $A_m$  to  $(A_m)_+$ . Following this,  $\gamma$  encounters the basic squares  $S'_k$  for  $k = 0, 1, 2, \dots$  until it crosses a geodesic that does not have  $A_m$  as a left endpoint. By Equation 193 and induction, we get the following list of vertices for the square  $S'_k$ :

$$\frac{p_m}{q_m} < \frac{(k+1)p_m + (p_m)_+}{(k+1)q_m + (q_m)_+} < \frac{(2k+1)p_m + 2(p_m)_+}{(2k+1)q_m + 2(q_m)_+} < \frac{kp_m + (p_m)_+}{kq_m + (q_m)_+}. \quad (195)$$

Here  $S'_k$  is a left-biased square. But then there is some  $k$  such that

$$\frac{p_{m+1}}{q_{m+1}} = \frac{(2k+1)p_m + 2(p_m)_+}{(2k+1)q_m + 2(q_m)_+}, \quad \frac{(p_{m+1})_+}{(q_{m+1})_+} = \frac{kp_m + (p_m)_+}{kq_m + (q_m)_+} \quad (196)$$

Since  $(q_m)_+ < (q_m)_-$ , we have  $2(q_m)_+ < q_m$ . Since  $2(q_m)_+ < q_m$ , we have

$$\frac{p_{m+1}}{q_{m+1}} - \frac{p_m}{q_m} = \frac{2}{(2k+1)q_m^2 + 2q_m(q_m)_+} \in \left( \frac{2}{(2k+2)q_m^2}, \frac{2}{(2k+1)q_m} \right). \quad (197)$$

Hence  $\delta_m = (2k+1) \equiv 1 \pmod{2}$ . Here  $k = d_m$ . This takes care of the second implication. Equation 196 gives the formula for  $(q_{m+1})_+$ . Lemma 18.1 now gives the formula for  $(q_{m+1})_-$ .

In Case 2, the vertical geodesic  $\gamma$  again encounters the basic square  $S$ . This time,  $\gamma$  exits  $S$  through the geodesic joining  $(A_m)_-$  to  $A_m$ . This fact follows from the inequality  $A_m > A_{m-1} > (A_m)_-$ , a result of Lemma 18.1. Following this,  $\gamma$  encounters the basic squares  $S''_k$  for  $k = 0, 1, 2$  until it crosses a geodesic that does not have  $A_m$  as a right endpoint. The coordinates for the vertices of  $S''_k$  are just like those in Equation 196, except that all terms have been reversed and each  $(\cdot)_+$  is switched to  $(\cdot)_-$ . The rest of the proof is similar. ♠

### 18.3 Existence of the Superior Sequence

The following result completes the proof of the Superior Sequence Lemma.

**Lemma 18.3**  $d_m \geq 1$  infinitely often.

**Proof:** We can sort the indices of our sequence into 4 types, depending on which case holds in Lemma 18.2. If this lemma is false, then  $n$  eventually has odd type. But, it is impossible for  $n$  to have Type 1 and for  $n + 1$  to have Type 3. Hence, eventually  $n$  has constant type, say Type 1. (The Type 3 case has a similar treatment.) Looking at the formula in Case 1 of Lemma 18.2, we see that the sequence  $\{(q_n)_+\}$  is eventually constant. But then

$$r = \lim_{n \rightarrow \infty} \frac{(q_n)_+ p_n}{q_n}$$

exists. Since  $(q_n)_+ p_n \equiv -1 \pmod{q_n}$  and  $q_n \rightarrow \infty$ , we must have  $r \in \mathbf{Z}$ . But then  $\lim p_n/q_n \in \mathbf{Q}$ , and we have a contradiction. ♠

**Lemma 18.4** If  $d_m \geq 1$  then

$$\left| \frac{p_N}{q_N} - \frac{p_m}{q_m} \right| < \frac{2}{d_m q_m^2} \quad \forall N > m; \quad \left| A - \frac{p_m}{q_m} \right| \leq \frac{2}{d_m q_m^2}$$

**Proof:** The first conclusion implies the second. We will consider the case when  $A_m < A_{m+1}$ . By Lemma 18.1, we have

$$|A_N - A_m| \leq |(A_{m+1})_+ - A_m| = \frac{1}{q_m (q_{m+1})_+}. \quad (198)$$

If  $m$  is an index of Type 1, then

$$(q_{m+1})_+ = d_m q_m + (q_m)_+ > d_m q_m. \quad (199)$$

if  $m$  is an index of Type 2, then Lemma 18.2 tell us that

$$(q_{m+1})_+ = (q_{m+1})_- - q_m = d_m q_m + (q_m)_+ - q_m > \left(d_m - \frac{1}{2}\right) q_m \geq \frac{1}{2} d_m q_m. \quad (200)$$

Combining Equations 198,199, and 200 we get our result. ♠

## 18.4 The Diophantine Constant

We have two odd rationals  $A_1 = p_1/q_1$  and  $A_2 = p_2/q_2$ . We define the real number  $a = a(A_1, A_2)$  by the formula

$$\left| \frac{p_1}{q_1} - \frac{p_2}{q_2} \right| = \frac{2}{aq_1^2}. \quad (201)$$

We call  $(A_1, A_2)$  *admissible* if  $a(A_1, A_2) > 1$ .

Define

$$\lambda_1 = \frac{(q_1)_+}{q_1} \in (0, 1). \quad (202)$$

If  $A_1 < A_2$  we define

$$\Omega = \text{floor}\left(\frac{a}{2} - \lambda_1\right) + 1 + \lambda_1. \quad (203)$$

if  $A_1 > A_2$  we define

$$\Omega = \text{floor}\left(\frac{a}{2} + \lambda_1\right) + 1 - \lambda_1. \quad (204)$$

Here we explain the geometric meaning of the Diophantine Constant. For ease of exposition, assume that  $A_1 < A_2$ . Assume also that  $(A_1, A_2)$  is admissible. Let  $\epsilon$  denote an infinitesimally small negative number. Consider two infinite rays  $R_1$  and  $R_2$  starting at  $(0, \epsilon)$ . Let  $R_j$  have slope  $-A_j$ . Thus,  $R_j$  is contained in the baseline of the arithmetic graph associated to  $A_j$ . Then there is no lattice point between  $R_1$  and  $R_2$  whose first coordinate lies in  $(0, \Omega q_1)$ . Compare Lemma 19.4 from the next chapter. Typically there is such a lattice point with first coordinate exactly  $\Omega q_1$ . (We think that this is always the case, but we did not try to prove it.)

### Remarks:

(i) We have formulated our description in terms of an infinitesimal number because e.g. the lattice point  $(q_1, -p_1)$  is closer to the origin and lies on the line of slope  $-A_1$  through the origin. However, this lattice point lies above both rays  $R_1$  and  $R_2$ , on account of the infinitesimal downward push we have given these rays. This is the same bit of silliness we dealt with when defining the baseline of the arithmetic graph.

(ii) The only fact relevant for Lemma 4.3 is that  $a > 4$  implies that  $\Omega > 2$ . The reader who cares mainly about Lemma 4.3 can skip the rest of this chapter.

## 18.5 Structure of the Diophantine Constant

Let  $A = p/q$  be an odd rational. We say that  $A'$  is a *near predecessor* of  $A$  if  $A'$  precedes  $A$  in the inferior sequence, but does not precede the superior predecessor of  $A$ . The inferior and superior predecessors of  $A$  are the two extreme examples of near predecessors of  $A$ . Here is nice characterization of the Diophantine constant for these pairs of rationals.

**Lemma 18.5** *If  $A'$  is a near predecessor of  $A$  then the following is true.*

1. *If  $A' < A$  then  $\Omega q' = q' + q_+$ .*
2. *If  $A' > A$  then  $\Omega q' = q' + q_-$ .*

**Proof:** There is a finite chain

$$A' = A_1 \dots \leftarrow \dots \leftarrow A_m = A. \quad (205)$$

Referring to Equation 31, we have  $d_1 \geq 0$  and  $d_2 = \dots = d_{m-1} = 0$ . By Lemma 18.1,  $A_1 < A_2$  iff  $A' < A$ . We will consider the case when  $A_1 < A_2$ . The other case is similar. Recall that

$$A - A' = \frac{2}{a(q')^2}; \quad \Omega = \text{floor}\left(\frac{a}{2} - \lambda\right) + 1 + \lambda; \quad \lambda = \frac{q'_+}{q'}. \quad (206)$$

Hence

$$\Omega q' = q'(N + 1) + q'_+; \quad N = \text{floor}\left(\frac{a}{2} - \lambda\right) \quad (207)$$

There are two cases to consider, depending on whether  $\delta_1$  is odd or even. Here  $\delta_1$  is as in Equation 194. If  $\delta_n$  is odd then we have Case 1 of Lemma 18.2. In this case, we will show below that  $d_1 = N$ . By Case 1 of Lemma 18.2, we get

$$(q_2)_+ = d_1 q_1 + (q_1)_+ = N q_1 + (q_1)_+. \quad (208)$$

If  $\delta_n$  is even then we show below that  $d_1 = N + 1$ . By Case 2 of Lemma 18.2, we have

$$(q_2)_+ = d_1 q_1 - (q_1)_- = (d_1 - 1)q_1 + q_+ = N q_1 + (q_1)_+. \quad (209)$$

We get the same result in both cases.

Repeated applications of Lemma 18.2, Case 1, give us

$$q_+ = (q_m)_+ = \dots = (q_2)_+ = N q' + q'_+ = (N + 1)q' - q' + q'_+ = \Omega q' - q'. \quad (210)$$

Rearranging this gives Statement 1. ♠

**Lemma 18.6** *If  $A_1 < A_2$  and  $\delta_1$  is odd, then  $d_1 = N$ .*

**Proof:** Rearranging the basic definition of  $a(A', A)$ , and using  $A' = A_1$  and  $A = A_m$  in equation 205, we have

$$\frac{a}{2} = \frac{1}{q_1^2 |A_1 - A_m|}.$$

By Lemma 18.1 and monotonicity, we have

$$\frac{1}{q_1^2 |A_1 - (A_2)_+|} < \frac{a}{2} < \frac{1}{q_1^2 |A_1 - A_2|}. \quad (211)$$

After some basic algebra, we get

$$d_1 + \lambda_1 =^* \frac{(q_2)_+}{q_1} < \frac{a}{2} < \frac{q_2}{2q_1}. \quad (212)$$

The starred inequality is Case 1 of Lemma 18.2. The lower bound gives us

$$d_1 < \frac{a}{2} - \lambda_1 \quad (213)$$

Here  $\lambda_1$  is the same as  $\lambda$  in Equation 206. Since  $d_1 \in \mathbf{Z}$ , we get  $d_1 \leq N$ . On the other hand, the upper bound gives us

$$N = \text{floor}\left(\frac{a}{2} - \lambda_1\right) \leq \text{floor}\left(\frac{q_2}{2q_1} - \lambda_1\right) \leq d_1. \quad (214)$$

In short,  $N \leq d_1$ . Combining the two halves gives  $N = d_1$ . ♠

**Lemma 18.7** *If  $A_1 < A_2$  and  $\delta_1$  is even, then  $d_1 = N + 1$ .*

**Proof:** The proof is very similar to what we did in the other case. Here we mention the 2 changes. The first change is that  $(d_1 - 1) + \lambda_1$  occurs on the left hand side of Equation 212, by Case 2 of Lemma 18.2. This gives us  $d_1 \leq N + 1$ . The second change occurs on the right hand side of Equation 214. By Case 2 of Lemma 18.2, we know that  $\text{floor}(q_2/q_1)$  is even. Hence  $q_2/(2q_1)$  has fractional part less than  $1/2$ . But, also by Case 2 of Lemma 18.2,  $\lambda_1$  has fractional part greater than  $1/2$ . Hence

$$\text{floor}\left(\frac{q_1}{2q_1} - \lambda_1\right) = \text{floor}\left(\frac{q_1}{2q_1}\right) - 1 \leq d_1 - 1.$$

This gives us the bound  $N \leq d_1 - 1$ , or  $N + 1 \leq d_1$ . Putting the two halves together, we get  $d_1 = N + 1$ . ♠

## 19 The Diophantine Lemma

### 19.1 Three Linear Functionals

Let  $p/q$  be an odd rational.

Consider the following linear functionals.

$$F(m, n) = \left(\frac{p}{q}, 1\right) \cdot (m, n) \quad (215)$$

$$G(m, n) = \left(\frac{q-p}{p+q}, \frac{-2q}{p+q}\right) \cdot (m, n). \quad (216)$$

$$H(m, n) = \left(\frac{-p^2 + 4pq + q^2}{(p+q)^2}, \frac{2q(q-p)}{(p+q)^2}\right) \cdot (m, n). \quad (217)$$

We have  $F = (1/2)M$ , where  $M$  is the fundamental map from Equation 19. We can understand  $G$  and  $H$  by evaluating them on a basis:

$$H(V) = G(V) = q; \quad H(W) = -G(W) = \frac{q^2}{p+q}. \quad (218)$$

Here  $V = (q, -p)$  and  $W$  are the vectors from Equation 21. We can also understand  $G$  by evaluating on a simpler basis.

$$G(q, -p) = q; \quad G(-1, -1) = 1. \quad (219)$$

We can also (further) relate  $G$  and  $H$  to the hexagrid from §3. A direct calculation establishes the following result.

**Lemma 19.1** *The fibers of  $G$  are parallel to the top left edge of the arithmetic kite. The fibers of  $H$  are parallel to the top right edge of the arithmetic kite. Also  $\|\nabla G\| \leq 3$  and  $\|\nabla H\| \leq 3$ .*

Here  $\nabla$  is the gradient.

Given any interval  $I$ , define

$$\Delta(I) = \{(m, n) \mid G(m, n), H(m, n) \in I\} \cap \{(m, n) \mid F(m, n) \geq 0\}. \quad (220)$$

This set is a triangle whose bottom edge is the baseline of  $\Gamma(p/q)$ .

## 19.2 The Main Result

**Lemma 19.2 (Diophantine)** *Let  $(A_1, A_2)$  be an admissible pair of odd rationals.*

1. *If  $A_1 < A_2$  let  $I = [-q_1 + 2, \Omega q_1 - 2]$ .*
2. *If  $A_1 > A_2$  let  $I = [-\Omega q_1 + 2, q_1 - 2]$ .*

*Then  $\hat{\Gamma}_1$  and  $\hat{\Gamma}_2$  agree on  $\Delta_1(I) \cup \Delta_2(I)$ .*

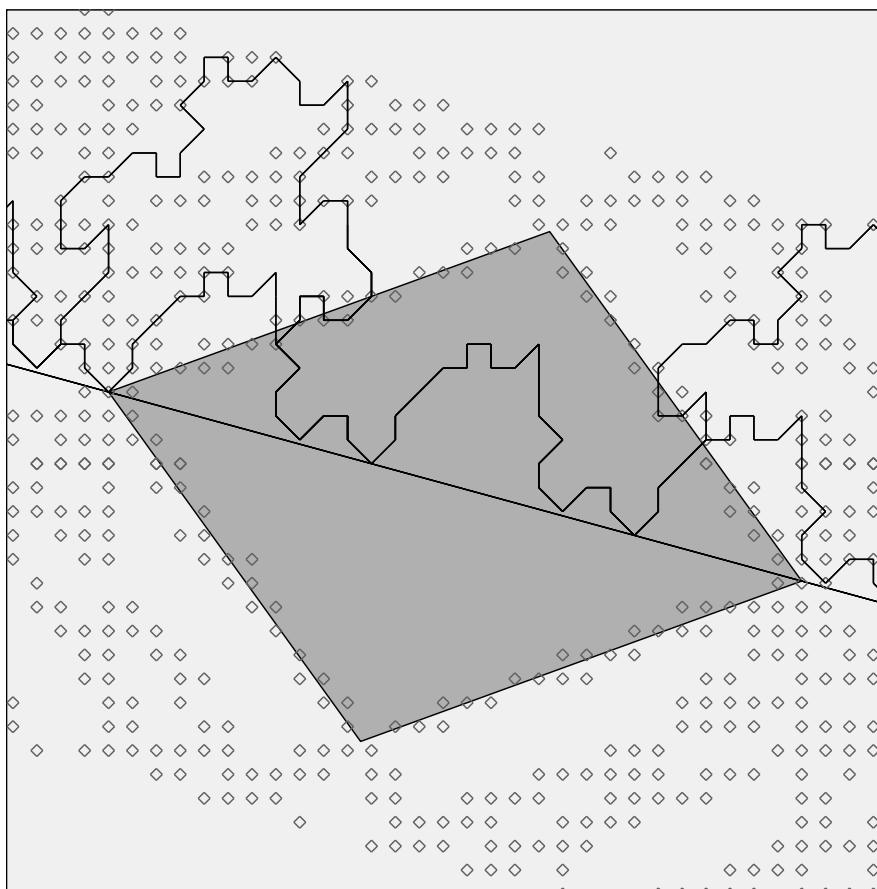


**Figure 19.1:** The Diophantine Lemma in action.

Figure 19.1 illustrates our result for  $A_1 = 3/11$  and  $A_2 = 7/25$ . The portion of the shaded parallelogram above the baseline is  $\Delta_1(-q_1, \Omega q_1)$ , a set slightly larger than  $\Delta_1(I)$ . The sets  $\Delta_1(I)$  and  $\Delta_2(I)$  are almost identical.

**Remarks:**

(i) The Diophantine Lemma also works for points below the baseline, but for technical reasons we ignore these points. We plot the points near  $\Delta$  where  $\widehat{\Gamma}_1$  and  $\widehat{\Gamma}_2$  disagree. Starting from  $(0,0)$  and tracing  $\Gamma_1$  and  $\Gamma_2$  in either direction, we get agreement until we nearly hit the edges of  $\Delta$ .

(ii) The Diophantine Lemma is quite nearly sharp. We think that the sharp version runs as follows. The two arithmetic graphs agree at any point in  $\Delta_1(-q_1, \Omega q_1)$  that is not adjacent to a point that lies outside of  $\Delta_1(-q_1, \Omega q_1)$ . One can see this structure plotting pictures on Billiard king.

(iii) The Diophantine Lemma is defined in terms of somewhat complicated formulas, but the domains involved have simple geometric descriptions. Consider the two triangles  $\Delta_1(-q_1, \Omega q_1)$  and  $\Delta_2(-q_1, \Omega q_1)$ . The bases of these two nearly identical triangles have no lattice points between them. The triangles are then constructed from the bases by extending lines parallel to the top edges of the arithmetic kites. Since  $A_1$  and  $A_2$  are nearby rational parameters, the two kites have about the same shape, and so do the two triangles.

Here we outline the proof of the Diophantine Lemma. We will establish the case when  $A_1 < A_2$ . The other case has a nearly identical proof.

We say that an integer  $\mu$  is *good* if  $\mu A_1$  and  $\mu A_2$  have the same floor. We call  $\mu$  *1-good* if  $\mu + \epsilon$  is good for all  $\epsilon \in \{-1, 0, 1\}$ . We can subject a lattice point  $(m, n)$  to the reduction algorithm from §11.2. For  $\theta \in \{1, 2\}$ , we perform the algorithm relative to the parameter  $A_\theta$ . This produces integers  $X_\theta$  and  $Y_\theta$  and  $Z_\theta$ . Below we prove the following result.

**Lemma 19.3 (Agreement)** *Suppose, for at least one choice of  $\theta \in \{1, 2\}$ , that  $m$  and  $m - X_\theta$  and  $m - Y_\theta$  and  $m + Y_\theta - X_\theta$  are all 1-good. Then  $\widehat{\Gamma}_1$  and  $\widehat{\Gamma}_2$  agree at  $(m, n)$ .*

Next, we give a criterion for an integer to be good.

**Lemma 19.4 (Goodness)** *If  $\mu \in (-q_1, \Omega q_1) \cap \mathbf{Z}$  then  $\mu$  is a good integer.*

Finally, we show that  $(m, n) \in \Delta_1(I) \cup \Delta_2(I)$  implies that the integers in the Agreement Lemma satisfy the criterion in the Goodness Lemma. This completes the proof.

### 19.3 Proof of the Agreement Lemma

In our technical lemmas, we will use integers  $\mu$  and  $\nu$  roughly in place of  $m$  and  $n$ . Sometimes  $\mu$  and  $\nu$  will take on values other than  $m$  and  $n$ , however.

**Lemma 19.5** *Let  $\mu, \nu, N_j \in \mathbf{Z}$  and*

$$N_j = \text{floor}\left(\frac{\mu A_j + \nu}{1 + A_j}\right).$$

*Suppose, for at least one choice of  $\theta \in \{1, 2\}$  that both  $\mu - N_\theta$  and  $\mu - N_\theta + 1$  are good. Then  $N_1 = N_2$ .*

**Proof:** For the sake of contradiction, assume w.l.o.g. that  $N_1 < N_2$ . Then

$$\begin{aligned} \mu A_1 + \nu &< N_2(A_1 + 1); & (\mu - N_2)A_1 &< N_2 - \nu \\ N_2(A_2 + 1) &\leq \mu A_2 + \nu; & N_2 - \nu &\leq (\mu - N_2)A_2. \end{aligned}$$

The first equation implies the second in each case. The second items imply that  $\mu - N_2$  is not good. On the other hand, we have

$$\begin{aligned} \mu A_1 + \nu &< (N_1 + 1)(A_1 + 1); & A_1(m - N_1 + 1) &< N_1 + 1 - n. \\ (N_1 + 1)(1 + A_2) &\leq \mu A_2 + \nu; & A_2(m - N_2 + 1) &\geq N_1 - 1 + n. \end{aligned}$$

The first equation implies the second in each case. The second items imply that  $\mu - N_1 + 1$  is not good. Now we have a contradiction. ♠

**Corollary 19.6** *Let  $(X_\theta, Y_\theta, Z_\theta)$  be as in the Agreement Lemma. Under the hypotheses of the Agreement Lemma, we have  $(X_1, Y_1, Z_1) = (X_2, Y_2, Z_2)$ .*

**Proof:** We go through the reduction algorithm. First we deal with  $(-)$  case.

1. Let  $z_j = A_j m + n$ .
2. Let  $Z_j = \text{floor}(z_j)$ . Since  $m$  is good, we have  $Z_1 = Z_2$ . Call this common integer  $Z$ .
3.  $y_j = z_j + Z_j = z_j + Z$ . Hence  $y_j = mA_j + n'$  for some  $n' \in \mathbf{Z}$ .

4. Recall that  $Y_j = \text{floor}(y_j/(1+A))$ . To see that  $Y_1 = Y_2$  we apply Lemma 19.5 to  $(\mu, \nu, N_j) = (m, n', Y_j)$ . Here we use the fact that  $m - Y_\theta$  and  $m - Y_\theta + 1$  are good. We set  $Y = Y_1 = Y_2$ .
5. Let  $x_j = y_j - Y(1 - A_j) - 1$ . Hence  $x_j = (m + Y)A_j + n''$ .
6. Recall that  $X_j = \text{floor}(x_j/(1 + A))$ . To see that  $X_1 = X_2$  we apply Lemma 19.5 to  $(\mu, \nu, N_j) = (m + Y, n'', X_j)$ . Here we use the fact that  $m + Y - X_\theta$  and  $m + Y - X_\theta + 1$  are good integers. We set  $X = X_1 = X_2$ .

Now we deal with the (+) case. The only difference is that

$$y_j = z_j + Z + 1.$$

This time we have  $y_j = mA_j + n' + 1$ , and the argument works exactly the same way. We apply Lemma 19.5 to  $(\mu, \nu, N_j)$  to  $(m, n' + 1, Y_j)$ . ♠

In the next result, all quantities except  $A_1$  and  $A_2$  are integers.

**Lemma 19.7** *If  $\mu - dN - \epsilon_1$  is good, then the statement*

$$(\mu A_j + \nu) - N(dA_j + 1) < \epsilon_1 A_j + \epsilon_2$$

*is true or false independent of  $j = 1, 2$ .*

**Proof:** Assume w.l.o.g. that the statement is true for  $j = 1$  and false for  $j = 2$ . Then

$$(\mu - dN - \epsilon_1)A_1 < \epsilon_2 + N - \nu \leq (\mu - dN - \epsilon_1)A_2,$$

a contradiction. ♠

Now we finish the proof of the Agreement Lemma. Let  $M_+$  and  $M_-$  be as in §6.6.3. By the Master Picture Theorem, it suffices to show that the two images  $M_+(m, n)$  and  $M_-(m, n)$  land in the same polyhedra for both  $A_1$  and  $A_2$ . We have already seen that the basic integers  $(X, Y, Z)$  are the same relative to both parameters. It remains to locate the relevant points inside our tori  $\mathbf{R}^3/\Lambda_1$  and  $\mathbf{R}^3/\Lambda_2$ . The polyhedra of interest to us are cut out by the following partitions.

- $\mathcal{Z}$ , the union  $\{z = 0\} \cup \{z = A\} \cup \{z = 1 - A\} \cup \{z = 1\}$ .
- $\mathcal{Y}$ , the union  $\{y = 0\} \cup \{y = A\} \cup \{y = 1\} \cup \{y = 1 + A\}$ .
- $\mathcal{X}$ , the union  $\{x = 0\} \cup \{x = A\} \cup \{x = 1\} \cup \{x = 1 + A\}$ .
- $\mathcal{T}$ , the union  $\{x + y - z = A + j\}$  for  $j = -2, 1, 0, 2, 1$ .

Letting  $\mathcal{S}$  stand for one of these partitions, we say that  $\mathcal{S}$  is *good* if the points  $M_+(m, n)$  land in the same component of  $R_+ - \mathcal{S}$  for both parameters  $A_1$  and  $A_2$ , and likewise the points  $M_-(m, n)$  land in the same component of  $R_- - \mathcal{S}$  for both parameters  $A_1$  and  $A_2$ . Here  $R_\pm = \mathbf{R}^3/\Lambda$ , the domain of the maps  $M_\pm$ . This domain depends on the parameter. By the Master Picture Theorem,  $\Gamma_1$  and  $\Gamma_2$  agree at  $(m, n)$  provided all the partitions are good. The proof works the same for the (+) and the (-) case.

- For  $\mathcal{Z}$ , we apply Lemma 19.7 to  $(\mu, \nu, d, N) = (m, n, 0, Z)$  to show that the statement  $z_j - Z < \epsilon_1 A_j + \epsilon_2$  is true independent of  $j$ , for  $\epsilon_1 \in \{-1, 0, 1\}$  and  $\epsilon_2 \in \{0, 1\}$ . The relevant good integers are  $m - 1$  and  $m$  and  $m + 1$ .
- For  $\mathcal{Y}$ , we apply Lemma 19.7 to  $(\mu, \nu, d, N) = (m, n', 1, Y)$  to show that the statement  $z_j - Z < \epsilon_1 A_j + \epsilon_2$  is true independent of  $j$ , for  $\epsilon_1 \in \{0, 1\}$  and  $\epsilon_2 \in \{0, 1\}$ . The relevant good integers are  $m - Y$  and  $m - Y - 1$ .
- For  $\mathcal{X}$ , we apply Lemma 19.7 to  $(\mu, \nu, d, N) = (m + Y, n'', 1, X)$ . The relevant good integers are  $m + Y - X$  and  $m + Y - X - 1$ .
- For  $\mathcal{T}$ , we define

$$\sigma_j = (x_j - X(1 + A_j)) + (y_j - Y(1 + A_j)) - (z_j - Z).$$

We have  $\sigma_j = (m - X)A_j + n'''$  for some  $n''' \in \mathbf{Z}$ . Let  $h \in \mathbf{Z}$  be arbitrary. To see that the statement  $\sigma_j < A_j + h$  is true independent of  $j$  we apply Lemma 19.7 to  $(\mu, \nu, d, N) = (m - X, n''', 1, 0)$ . The relevant good integer is  $m - X - 1$ .

**Remark:** Our proof does not use the fact that  $m - X + 1$  is a good integer. This technical detail is relevant for Lemma 19.12.

## 19.4 Proof of the Goodness Lemma

We prove the Goodness Lemma in two steps. The first step takes care of the lower bound and the second step takes care of the upper bound. Before we start our proof, we note that the Goodness Lemma is the result that justifies out claims, made in §18.4, about the geometric meaning of the Diophantine constant  $\Omega$ .

**Lemma 19.8** *If  $\mu \in (-q_1, 0)$ , then  $\mu$  is good.*

**Proof:** Since  $q_1$  is odd, we have unique integers  $j$  and  $M$  such that

$$\mu A_1 = M + \frac{j}{q_1}; \quad |j| < \frac{q_1}{2}. \quad (221)$$

By hypotheses,  $a > 1$ . Hence

$$|A_2 - A_1| < 2/q_1^2 \quad (222)$$

in all cases. If this result is false, then there is some integer  $N$  such that

$$\mu A_2 < N \leq \mu A_1. \quad (223)$$

Referring to Equation 221, we have

$$\frac{|j|}{q_1} < \mu A_1 - N \leq \mu A_1 - \mu A_2 < \frac{2|\mu|}{q_1^2} < \frac{2}{q_1}. \quad (224)$$

If  $j = 0$  then  $q_1$  divides  $\mu$ , which is impossible. Hence  $|j| = 1$ . If  $j = -1$  then  $\mu A_1$  is  $1/q_1$  less than an integer. Hence  $\mu A_1 - N \geq (q_1 - 1)/q_1$ . This is false, so we must have  $j = 1$ .

From the definition of  $\lambda_1$ , we have the following implication.

$$\mu \in (-q_1, 0) \quad \text{and} \quad \mu p_1 \equiv 1 \pmod{q_1} \quad \implies \quad \mu = -\lambda_1 q_1. \quad (225)$$

Equation 221 implies

$$\frac{\mu p_1}{q_1} - \frac{1}{q_1} \in \mathbf{Z}.$$

But then  $\mu p_1 \equiv 1 \pmod{q_1}$ . Equation 225 now tells us that  $\mu = -\lambda_1 q_1$ . Hence  $|\mu| < q_1/2$ . But now Equation 224 is twice as strong and gives  $|j| = 0$ . This is a contradiction. ♠

**Lemma 19.9** *If  $\mu \in (0, \Omega q_1)$  then  $\mu$  is good.*

**Proof:** We observe that  $\Omega < a$ , by Equation 203. If this result is false, then there is some integer  $N$  such that  $\mu A_1 < N \leq \mu A_2$ . If  $\mu A_2 = N$ . Then  $q_2$  divides  $\mu$ . But then,

$$\mu \geq q_2 \geq a q_1 > \Omega q_1.$$

This is a contradiction. Hence

$$\mu A_1 < N < \mu A_2. \quad (226)$$

Referring to Equation 221, we have

$$\frac{|j|}{q_1} \leq N - \mu A_1 < \mu(A_2 - A_1) = \frac{2\mu}{a q_1^2} < \frac{2}{q_1}. \quad (227)$$

Suppose that  $j \in \{0, 1\}$  in Equation 221. Then

$$1 - \frac{1}{q_1} \leq N - \mu A_1 \leq \mu A_2 - \mu A_1 < \frac{1}{q_1},$$

a contradiction. Hence  $j = -1$ . Hence  $\mu > a q_1 / 2$ .

Since  $j = -1$ , Equation 221 now tells us that  $\mu p_1 + 1 \equiv 0 \pmod{q_1}$ . But then

$$\mu = k q_1 + (q_1)_+, \quad (228)$$

for some  $k \in \mathbf{Z}$ . On the other hand, from Equation 203 and the fact that  $\mu < \Omega q_1$ , we have

$$\mu < k' q_1 + (q_1)_+; \quad k' = (\text{floor}(a/2 - \lambda_1) + 1). \quad (229)$$

Comparing the last two equations, we have  $k \leq k' - 1$ . Hence

$$k \leq (\text{floor}(a/2 - \lambda_1)). \quad (230)$$

Therefore

$$\mu \leq (\text{floor}(a/2 - \lambda_1)) q_1 + \lambda_1 q_1 \leq a q_1 / 2.$$

But we have already shown that  $\mu > a q_1 / 2$ . This is a contradiction. ♠

## 19.5 The End of the Proof

We will assume that  $(m, n) \in \Delta_\theta(I)$ , for one of the two choices  $\theta \in \{1, 2\}$ . Here  $I$  is as in the Diophantine Lemma. Our proof works the same for  $\theta = 1$  and  $\theta = 2$ . We set  $p = p_\theta$  and  $q = q_\theta$ , etc.

We will show that all the integers that arise in our proof of Lemma 19.3 lie in  $(-q_1, \Omega q_1)$ . These integers have the form  $N + \epsilon$  for  $\epsilon \in \{-1, 0, 1\}$ . We will show, for all relevant integers (except one), that  $N \in J := (-q_1 + 1, \Omega q_1 - 1)$ . For the exceptional case, see the remark after Lemma 19.12.

**Lemma 19.10**  $m \in J$ .

**Proof:** We have  $z = Am + n \geq 0$ . We compute

$$-q_1 + 2 \leq G(m, n) = m - \frac{2z}{1+A} \leq m. \quad (231)$$

$$\Omega q_1 - 2 \geq H(m, n) = m + \frac{2z(1-A)}{(1+A)^2} \geq m. \quad (232)$$

These inequalities establish that  $m \in J$ . ♠

**Lemma 19.11**  $m - Y \in J$ .

**Proof:** We have  $Y \geq 0$ . Hence  $m - Y \leq m \leq \Omega q_1 - 2$ . We just need the lower bound. worry about the lower bound on  $m - Y$ . We first deal with the algorithm in §11.2 for the  $(-)$  case. Let  $G = G(m, n)$ . We have  $y = z + Z \leq 2z$ . By definition of  $Y$ , we have

$$Y \leq \frac{y}{1+A} \leq \frac{2z}{1+A}; \quad Y < \frac{2z}{1+A}. \quad (233)$$

At least one of the first two inequalities is sharp. This gives us the second inequality. Now we know that

$$m - Y > m - \frac{2z}{1+A} = G \geq -q_1 + 2. \quad (234)$$

The last equality comes from Equation 231. In the  $(+)$  case we add 1 to  $Y$ , giving us  $m - Y > -q_1 + 1$ . ♠

**Lemma 19.12**  $m - X \in J \cup \{\Omega q_1 - 1\}$ .

**Proof:** The condition that  $F(m, n) \geq 0$  implies that  $y \geq Y \geq 0$ . Hence

$$x = y - Y(1 - A) - 1 \in [-1, y - 1]. \quad (235)$$

Hence  $X \in [-1, Y - 1]$ . Hence

$$m - X \in [m - Y + 1, m + 1] \subset J \cup \{\Omega q_1 - 1\},$$

by the two previous results. ♠

**Remark:** As we remarked at the end of the proof of Lemma 19.3, the integer  $m - X + 1$  does not arise in our proof of Lemma 19.3. The relevant integers  $m - X$  and  $m - X - 1$  are good, by the result above.

**Lemma 19.13**  $m + Y - X \in J$ .

**Proof:** Our proof works the same in the (+) and (-) cases. Lemma 19.12 gives us  $Y - X \geq 0$ . Hence

$$m + Y - X \geq m > -q_1 + 1.$$

This takes care of the lower bound. Now we treat the upper bound. We have

$$Y = \text{floor}\left(\frac{y}{1 + A}\right) \leq \frac{y}{1 + A}; \quad 1 + X = \text{floor}\left(1 + \frac{x}{1 + A}\right) \geq \frac{x}{1 + A}.$$

Hence

$$\begin{aligned} Y - X - 1 &\leq \frac{y - x}{1 + A} \stackrel{1}{=} Y \frac{1 - A}{1 + A} + \frac{1}{1 + A} <^* \\ 2z \frac{1 - A}{(1 + A)^2} + \frac{1}{1 + A} &\stackrel{2}{=} H - m + \frac{1}{1 + A} < H - m + 1. \end{aligned}$$

The first equality comes from Equation 235. The second equality comes from Equation 232. The starred inequality comes from the upper bound in Equation 233. Adding  $m$  to both sides, we get

$$m + Y - X < H + 1 \leq \Omega q_1 - 1.$$

This completes the proof. ♠

## 20 Existence of Strong Sequences

### 20.1 Proof of Lemma 4.3

We will prove the result when  $A_1 < A_2$ . The other case is similar. By hypotheses, we have  $a(A_1, A_2) > 4$ . From Equation 203, we get  $\Omega > 2$ . Let  $R_1 = R(A_1)$  be the parallelogram from the room lemma. Let

$$u = W_1; \quad w = V_1 + W_1 \quad (236)$$

denote the top left and right vertices of  $R_1$ . We compute

$$G_1(u) = -\frac{q_1^2}{p_1 + q_1} > -q_1 + 2; \quad H_1(w) = \frac{q_1^2}{p_1 + q_1} + q_1 < \Omega q_1 - 2. \quad (237)$$

The inequalities hold once  $p_1$  is sufficiently large. Given the description of the fibers of  $G$ , we have

$$G(u) \leq G(v) \leq H(v) \leq H(w); \quad \forall v \in R_1. \quad (238)$$

The middle inequality uses the fact that  $F(v) \geq 0$ . In short, we have made the extremal calculations. The extremal calculation shows that  $v \in \Delta_1(I)$  for all  $v \in R_1$ . The Diophantine Lemma now shows that  $\Gamma_1$  and  $\Gamma_2$  agree in  $R_1$ .

When  $v$  lies in the bottom edge of  $R_1$  we have

$$G_1(v), H_1(v) \in [0, q_1]. \quad (239)$$

Given our gradient bounds  $\|\nabla G_1\| \leq 3$  and  $\|\nabla H_1\| \leq 3$ , we see that

$$G_1(v), H_1(v) \in [-q_1 + 2, \Omega q_1 + 2] \quad (240)$$

provided that  $v$  is within  $q_1/4$  from the bottom edge of  $R_1$ . Hence  $\Gamma_1$  and  $\Gamma_2$  agree in the  $q_1/4$  neighborhood of the bottom edge of  $R_1$ .

By the Room Lemma,  $\Gamma_1^1 \subset R_1$ . Hence  $\Gamma_1^1 \subset \Gamma_2$ . Our calculation involving the bottom edge of  $R_1$  shows that  $\Gamma_1^{1+\epsilon} \subset \Gamma_2$  for  $\epsilon = 1/4$ . Since the right endpoint of  $\Gamma_2^1$  is far to the right of any point on  $\Gamma_1^{1+\epsilon}$ , we have  $\Gamma_1^{1+\epsilon} \subset \Gamma_2^1$ , as desired.

**Remark:** We proved Lemma 4.3 for  $\epsilon = 1/4$  rather than  $\epsilon = 1/8$ , which is what we originally claimed. We don't care about the value of  $\epsilon$ , as long as it is positive.

## 20.2 Proof of Lemma 4.2

The Decomposition Theorem is stated in §4.4. Our proof requires a limited version of this result. Define the complexity of an odd rational to be the number of terms preceding it in the superior sequence.

**Lemma 20.1** *The Decomposition Theorem holds for all  $A$  having sufficiently large complexity.*

**Proof:** This is an immediate consequence of Lemma 21.5, proved in §21.3. ♠

Let  $A$  be any irrational parameter. Let  $\{p_n/q_n\}$  denote the superior sequence associated to  $A$ . Let  $\mathcal{S}$  be a monotone subsequence of the superior sequence. We will treat the case when  $\mathcal{S}$  is monotone increasing. If necessary, we cut off the first few terms of  $\mathcal{S}$  so that Lemma 20.1 holds for all terms.

For any odd rational  $p/q$ , let  $R^*(p/q)$  denote the rectangle with vertices

$$-\frac{V}{2}; \quad -\frac{V+W}{2}; \quad \frac{V+W}{2}; \quad \frac{V}{2}. \quad (241)$$

Here  $V$  and  $W$  are as in Equation 21. The parallelogram  $R^*$  is just as wide as  $R$  but half as tall. Also, the bottom edge of  $R^*$  is centered on the origin.

**Lemma 20.2** *If  $A_1 \leftarrow A_2$  and  $p_1$  is sufficiently large, then  $\Gamma_1$  and  $\Gamma_2$  agree in  $A_1$ . Moreover,  $\Gamma_1$  and  $\Gamma_2$  agree in the  $q_1/8$  neighborhood of the bottom edge of  $R_1^*$ .*

**Proof:** The proof works the same way regardless of the sign of  $A_1 - A_2$ . The main point is that  $\Omega > 1$ . Note that  $(A_1, A_2)$  is admissible. We use the linear functionals  $G_1$  and  $H_1$  associated to  $A_1$ . Let

$$u = \frac{-V+W}{2}; \quad w = \frac{V+W}{2}$$

denote the top left and right vertices of  $R_1^*$  respectively. We compute

$$-G_1(u) = H_1(w) = \frac{q_1(p_1 + 2q_1)}{2p_1 + 2q_1} < q_1 - 2 < \Omega q_1 - 2. \quad (242)$$

The same argument as in Lemma 4.3 now finishes the proof. ♠

**Lemma 20.3** *Suppose that  $A_1 < A_2$  and  $A_1$  is the superior predecessor of  $A_2$ . If  $A_1$  has sufficiently large complexity, then  $\Gamma_1^{1+\epsilon} \subset \Gamma_2^1$ .*

**Proof:** If  $\Omega > 2$ , we have the same proof as in Lemma 4.3. Equation 203 does not allow  $\Omega = 2$ . We just need to consider the case  $\Omega < 2$ . By Equation 203, we must have  $\text{floor}(a/2 - \lambda_1) = 0$ . Since  $a > 1$ , we must have  $\lambda_1 > 1/2$ . Since  $\lambda_1 = (q_1)_+/q_1$  and  $q = q_+ + q_-$ , we must have  $(q_1)_- < (q_1)_+$ . This seemingly minor fact is crucial to our argument.

Now we really need to use Lemma 20.1. Let  $R(A_1)$  denote the parallelogram from the Room Lemma. In contrast, let  $R_1(A_1)$  and  $R_2(A_2)$  denote the smaller parallelograms from the Decomposition Theorem. Since  $(q_1)_- < (q_1)_+$ , we see that  $R_2(A_1)$  lies to the left of  $R_1(A_1)$ . By the Decomposition Theorem,

$$\Gamma_1 \cap R(A_1) \subset R_2(A_1) \cup (R_1(A_1) + V_1) \quad (243)$$

Figure 20.1 shows a schematic picture.

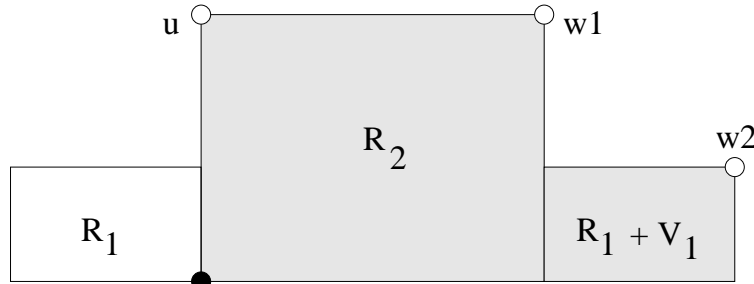


**Figure 20.1:**  $R_2(A_1)$  and  $R_1(A_1) + V_1$ .

The vertices shown in Figure 20.1 are

$$u = W_1; \quad w_1 \approx W_1 + \lambda_1 V_1; \quad w_2 \approx V_1 + \mu W_1. \quad (244)$$

Here  $\mu = q_0/q_1 < 1/2$ , where  $A_0 = p_0/q_0$  is the superior predecessor of  $A_1$ . Also,  $\lambda_1 = (q_1)_+/(q_1)$ , as in Equation 203.

The approximation sign means that the distance between the two points is at most 1 unit. For instance,  $w_1$  is the intersection of the line parallel to  $V_+$  and containing  $V_+$ , and the line parallel to  $V_1$  and containing  $W_1$ . The point  $V_+$  is  $O(q_1^{-2})$  of the point  $\lambda_1 V_1$ . Hence  $w_1$  is within  $O(q_1^{-2})$  of  $W_1 + \lambda_1 V_1$ . The argument for  $w_2$  is similar.

As in the proof of Lemma 4.3, we have  $G_1(u) > -q_1 + 2$  once  $p_1$  is large. The computations for  $H_1(w_1)$  and  $H_1(w_2)$  are the interesting ones. Case 1 of Lemma 18.2 gives  $(q_2)_+ \geq (q_1)_+$ . Hence, for  $p_1$  is sufficiently large, we get the following inequalities.

$$\begin{aligned} 2 + H_1(w_1) &\leq (2 + \|\nabla H\|) + H_1(W_1) + \lambda_1 H_1(V_1) \leq \\ 5 + \frac{q_1^2}{p_1 + q_1} + (q_1)_+ &< q_1 + (q_1)_+ \leq q_1 + (q_2)_+ = \Omega q_1. \end{aligned} \quad (245)$$

Here we use the bound  $\|\nabla H\| \leq 3$ . We already remarked that  $(q_2)_+ \geq (q_1)_+$ . We also know that  $(q_1)_+ > q_1/2$ . Hence

$$\Omega q_1 = q_1 + (q_2)_+ > (3/2)q_1. \quad (246)$$

For  $p_1$  large, we get

$$\begin{aligned} 2 + H_1(w_2) &\leq (2 + \|\nabla H\|) + H_1(V_1) + \mu H_1(W_1) < \\ 5 + H_1(V_1) + (1/2)H_1(W_1) &= 5 + q_1 + \frac{q_1^2}{2(p_1 + q_1)} < (3/2)q_1 < \Omega q_1. \end{aligned} \quad (247)$$

These arguments show that  $v \in \Delta_1(I)$  for all  $v \in \Gamma_1^1$ . The rest of the proof is just like the proof of Lemma 4.3. ♠

Suppose  $A'_1 < A'_2$  are two consecutive terms in  $\mathcal{S}$ , when we have a finite chain

$$A'_1 = A_1 \leftarrow A_2 \leftarrow \dots \leftarrow A_n = A'_2; \quad A_1 < A_n; \quad q_2 > 2q_1. \quad (248)$$

The following result finishes the proof of Lemma 4.2.

**Lemma 20.4**  $\Gamma_1^{n+\epsilon} \subset \Gamma_n^1$ .

**Proof:** We will change our notation slightly from the previous result. We let  $R_1 = R(A_1)$  denote the parallelogram from the Room Lemma. Likewise, let  $R_k^* = R^*(A_k)$ , the parallelogram from Lemma 20.2. For any parallelogram  $R_k$ , let  $XR_k$  denote the union of  $R$  with the points within  $q_k/8$  units from the bottom edge of  $R_k$ . Likewise define  $XR_k^*$ .

Since  $A_1 < A_n$ , we have  $A_1 < A_2$  by Lemma 18.1. We now have

$$\Gamma_1^{1+\epsilon} \subset \Gamma_1 \cap XR_1 \subset \Gamma_2. \quad (249)$$

The first containment comes from the Room Lemma and the definition of  $\Gamma_1^{1+\epsilon}$ . The second containment is Lemma 20.3. Lemma 20.2 gives us

$$\Gamma_k \cap XR_k^* \subset \Gamma_{k+1}. \quad k = 2, \dots, n-1. \quad (250)$$

Let us compare  $R_1$  and  $R_k^*$  for  $k \geq 2$ .

1. The sides of  $R_1$  have length  $O(q_1)$ .
2. The slope of each side of  $R_1$  is within  $O(q_1^{-2})$  of the slope of the corresponding side of  $R_k^*$ . This comes from Lemma 18.4.
3. Each side of  $R_1$  is less than half as long as the corresponding side of  $R_k^*$ . This follows from the first two facts, and from the fact that  $2q_1 < q_2 \leq q_k$ . Indeed, the quantity  $q_2 - 2q_1$  tends to  $\infty$  with the complexity of  $A_1$ .

These properties give us

$$XR_1 \subset XR_k^*; \quad k = 2, \dots, n-1. \quad (251)$$

Figure 20.2 shows a schematic picture.

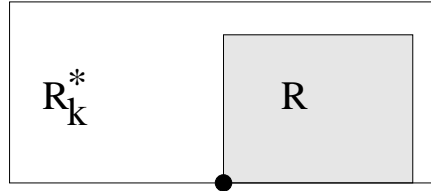


**Figure 20.2:**  $R_1$  and  $R_k^*$  for any  $k \geq 2$ .

We already know that  $\Gamma_1 \cap XR_1 \subset \Gamma_2$ . Suppose  $\Gamma_1 \cap XR_1 \subset \Gamma_k$  for some  $k \geq 2$ . Then

$$\Gamma_1 \cap XR_1 \subset \Gamma_k \cap XR_1 \subset \Gamma_k \cap XR_k^* \subset \Gamma_{k+1}. \quad (252)$$

Hence, by induction,  $\Gamma_1^{1+\epsilon} \subset \Gamma_n$ . The right endpoint of  $\Gamma_n^1$  lies far to the right of any point on  $\Gamma_1^{1+\epsilon}$ . Hence  $\Gamma_1^{1+\epsilon} \subset \Gamma_n^1$ . ♠

## 21 Proof of the Decomposition Theorem

### 21.1 Decomposition into Arcs

Let  $p/q$  be an odd rational in  $(0, 1)$ . There are 2 cases of the Decomposition Theorem, depending on whether  $q_- < q_+$  or  $q_+ < q_-$ . We will give our proofs mainly in the case when  $q_+ < q_-$ . This case relies on Statement 1 of the Diophantine Lemma. The other case relies on Statement 2.

Referring to §4.4, the lines  $L_j^+$  for  $j = 0, 1, 2$  are all parallel to the vector  $W$ . When  $q_+ < q_-$ , the line  $L_1^+$  contains  $V_+$  and the line  $L_2^+$  contains  $-V_-$ . By the Hexagrid Theorem,  $\Gamma$  only crosses  $L_0^+$  once, at the point  $(0, 0)$ .

**Lemma 21.1**  $\Gamma$  crosses each of  $L_1^+$  and  $L_2^+$  only once, and this crossing occurs within 1 unit of the baseline.

**Proof:** This result follows from symmetry and the Hexagrid Theorem. Our proof refers to Figure 21.1.

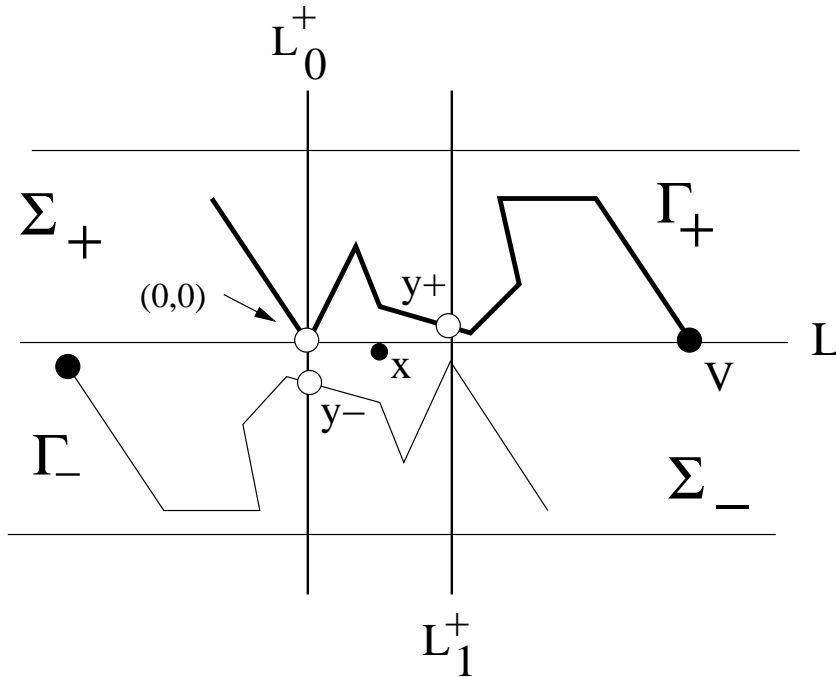


Figure 21.1: Rotating the graph

Let  $L$  denote the line of slope  $-A$  through the origin.  $\Sigma_+$  (respectively  $\Sigma_-$ ) is the infinite strip bounded by  $L$  and the first ceiling line above (respectively below)  $L$ . By Theorem 1.8, there is one infinite component of  $\widehat{\Gamma}$  in  $\Sigma_{\pm}$ . We call this component  $\Gamma_{\pm}$ . Here  $\Gamma_+ = \Gamma$  is the component of interest to us.

The point  $x = (1/2)V_+$  is the fixed point of  $\iota$ , the rotation from Equation 163. We have

$$\iota(L_0^+) = L_1^+; \quad \iota(\Gamma_-) = \Gamma_+; \quad \iota(L) \downarrow L. \quad (253)$$

Our last piece of notation means that  $\iota(L)$  lies (very slightly) beneath  $L$ .

By the Hexagrid Theorem,  $(0, 0)$  is the door corresponding to the point where  $\Gamma_+$  crosses  $L_0^+$  and *also* to the point  $y_-$  where  $\Gamma_-$  crosses  $L_0^+$ . This point is the intersection of  $L_0^+$  with the edge connecting  $(0, -1)$  to  $(-1, 0)$ . The image  $y_+ = \iota(y_-) \in \iota(L_0^+) = L^+$  is the only point where  $\iota(\Gamma_-) = \Gamma_+$  crosses  $L_+$ . This point is less than 1 unit from  $L$  because  $\iota(L)$  lies beneath  $L$ . This shows that  $\Gamma = \Gamma_+$  only crosses  $L^+$  once, within 1 units of  $L$ . Since  $L_1^+ = L_2^+ \pm V$ , and  $\Gamma$  is invariant under translation by  $V$ , it suffices to prove the result for one of the lines, as we have done. ♠

From this result we see that we can divide a period of  $\Gamma$  into the union of two connected arcs. One of the arcs lies in what we call  $R_0$  and the other arc lies in  $R_2$ . Each arc connects points near the bottoms of the boxes and otherwise does not cross the boundaries. Figure 21.1 shows a schematic picture. Here  $R_0$  is the union of the two shaded regions. Our main goal is to show that  $\Gamma \cap R_0 \subset R_1$ .

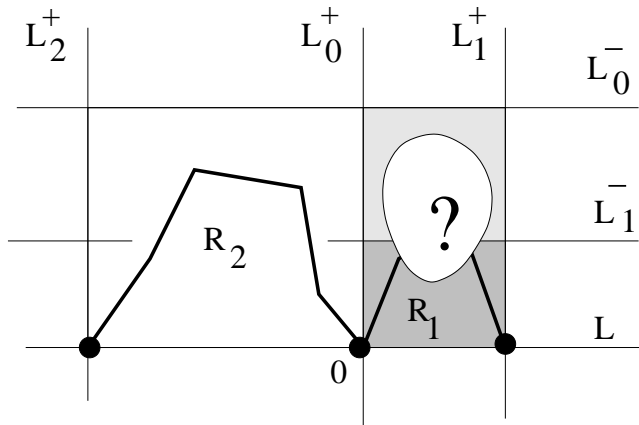


**Figure 21.2:** Dividing  $\Gamma^1$  into two arcs.

## 21.2 The Superior Predecessor

Let  $A' = p'/q'$  denote the superior predecessor of  $A$ . Let  $\Omega = \Omega(A', A)$ . We consider the case when  $A' < A$ .

**Lemma 21.2** *The second coordinate of any point in  $R_1$  lies in  $(0, \Omega q'_1 - 1)$ .*

**Proof:** By convexity, it suffices to consider the vertices of  $R_1$ . The bottom vertices of  $R_1$  have first coordinates 0 and  $q_+$ , whereas  $\Omega q' = q_+ + q'$ . This takes care of the bottom vertices. Let  $u = (u_1, u_2)$  be the top left vertex of  $R_1$ . Since  $R_1$  is a parallelogram, we can finish the proof by showing that  $u_1 \in (0, q' - 1)$ . Let  $y = (p' + q')/2 \leq q' - 1$ . Note that  $u$  lies on a line of slope in  $(1, \infty)$  through the origin. Since the top edge of  $R_1$  has negative slope and contains  $(0, y)$ , we get  $u_2 < y$ . Hence  $u_1 < y$  as well. ♠

**Lemma 21.3** *Let  $A'$  denote the superior predecessor of  $A$ . Suppose that  $A' \neq 1/1$ . Then  $\Gamma' \cap R_0 \subset R_1$ .*

**Proof:** Let  $\gamma = \Gamma' \cap R_0$ . Since  $\gamma$  starts out in  $R_1$  (at the origin), we just need to see that  $\gamma$  never cross the top edge of  $R_1$ . The top edge of  $R_1$  contained in the line  $\lambda = L_1^-$  of slope  $-A$  though the point  $X = (0, (p' + q')/2)$ . By the Room Lemma,  $\gamma$  does not cross the (nearly identical) line  $\lambda' = (L_0^-)'$  of slope  $-A'$  through  $X$ .

If  $\gamma$  crosses the top edge of  $R_1$ , then there is a lattice point  $(m, n)$  between  $\lambda$  and  $\lambda'$ , and within 1 unit of  $R_1$ . But then

$$\text{floor}(Am) \neq \text{floor}(A'm); \quad m \in (-1, q' + q_+) = (-q', \Omega q'). \quad (254)$$

The second equation comes from our previous result. Our last equations contradict Lemma 19.4. ♠

**Corollary 21.4** *Suppose that  $\Gamma$  and  $\Gamma'$  agree in  $R_1$ . Then The Decomposition Theorem holds for  $A$ .*

**Proof:** Let's trace  $\Gamma \cap R_0$  from left to right, starting at  $(0, 0)$ . By hypothesis, this arc does not cross the top of  $R_1$  until it leaves  $R_0$ . Once  $\Gamma \cap R_0$  leaves  $R_0$  from the right, it never re-enters. This is a consequence of Lemma 21.1. ♠

### 21.3 Most of the Parameters

Here we prove the Decomposition Theorem for most odd rationals. We deal with the exceptional cases in subsequent sections. Here is the result we prove.

**Lemma 21.5** *Let  $A' = p'/q'$  be the superior predecessor of  $A$ . Then the Decomposition Theorem holds for  $A$  as long as  $p' \geq 3$  and  $q' \geq 7$ .*

By Corollary 21.4, it suffices to prove that  $\Gamma'$  and  $\Gamma$  agree in  $R_1$ .

**Lemma 21.6**  *$\Gamma' \cap R_1$  and  $\Gamma \cap R_1$  have the same outermost edges.*

**Proof:** The leftmost edge of both arcs is the edge connecting  $(0, 0)$  to  $(1, 1)$ . Looking at the proof of Lemma 21.1, we see that the rightmost edge  $e$  of  $\Gamma \cap R_0$  connects  $V_+ + (0, 1)$  to  $V_+ + (1, 0)$ . Here  $V_+ = (q_+, -p_+)$ . Applying Lemma 21.1 to  $\Gamma'$ , we see that some edge  $e'$  of  $\Gamma'$  connects  $V'_+ + (0, 1)$  to  $V'_+ + (1, 0)$ . By repeated applications of Case 1 or Case 2 of Lemma 18.2 tell us that  $V_+ = V'_+ + dV'$  for some  $d \in \mathbb{Z}$ . Since  $\Gamma'$  is invariant under translation by  $V'$ , we see that  $e$  is also an edge of  $\Gamma'$ . ♠

**Adjacent Mismatch Principle:** Lemma 21.6 has the following corollary. If  $\Gamma'$  and  $\Gamma$  fail to agree in  $R_1$ , then there are two adjacent vertices of  $\Gamma' \cap R_1$  where our two arithmetic graphs  $\hat{\Gamma}$  and  $\hat{\Gamma}'$  do not agree. One can see this by tracing the two curves from left to right, starting at the origin. Once we get the first mismatch on  $\Gamma'$  our arc  $\Gamma$  has veered off, and the next vertex on  $\Gamma'$  is also a mismatch.

In our analysis below, we will treat the case when  $A' < A$ . The other case is similar. The bottom right vertex of  $R_1$  lies on a line of slope in  $(1, \infty)$  that contains the point  $V_+$ . The point  $V_+$  has the same first coordinate as the very nearby point

$$\tilde{V}_+ = \frac{q_+}{q} V. \quad (255)$$

Indeed, the two points differ by exactly  $1/q$ . Let  $\tilde{R}_1$  denote the slightly smaller parallelogram whose vertices are

$$(0, 0); \quad u; \quad \tilde{V}_+; \quad \tilde{w} =: u + \tilde{V}_+. \quad (256)$$

If the Decomposition Theorem fails for  $A$ , then at least one of the adjacent vertices of mismatch will lie in  $\tilde{R}_1$ . (There are not two adjacent vertices between the nearly identical right edges of  $R_1$  and  $\tilde{R}_1$ .)

As in the previous chapter, it suffices to make the extremal calculation

$$G(u) \geq -q' + 2; \quad H(\tilde{w}) \leq \Omega q' - 2 = q' + q_+ - 2. \quad (257)$$

The Diophantine Lemma then finishes the proof.

We first need to locate  $u$ . There is some  $r$  such that  $v_1 = rW$ . Letting  $M$  be the map from Equation 19, relative to the parameter  $A$ , we have

$$M(v_1) = M(rW) = p' + q'.$$

Solving for  $r$  gives

$$v_1 = \left( \frac{p' + q'}{p + q} \right) W. \quad (258)$$

We compute

$$G(u) = \frac{p' + q'}{p + q} G(W) = -\frac{p' + q'}{p + q} \times \frac{q^2}{p + q} = \frac{-(1 + A')q'}{(1 + A)^2} > \frac{-q'}{1 + A'}. \quad (259)$$

$$H(\tilde{w}) = H(u) + (q_+/q)H(V) = \frac{(1 + A')q'}{(1 + A)^2} + q_+ < \frac{q'}{1 + A'} + q_+. \quad (260)$$

Our last inequality in each case uses the fact that  $0 < A' < A$ . Notice the great similarity in these two calculations. One can ultimately trace this symmetry back to the affine symmetry of the arithmetic kite  $\mathcal{K}(A)$  defined in §3.

The conditions in Equation 257 are simultaneously met provided

$$\frac{-q'}{1 + A'} \geq -q' + 2; \quad \left( \iff \frac{1}{p'} + \frac{1}{q'} \leq \frac{1}{2} \right) \quad (261)$$

The equation on the right is equivalent to the one on the left. We see easily that it holds as long as  $p' \geq 3$  and  $q' \geq 7$ .

In the next two sections we will make a more detailed study of the few exceptions to Lemma 21.5. The reader mainly interested in the Erratic Orbits Theorem can stop reading here.

## 21.4 Some Tricks

Here we take care of some more cases of the Decomposition Theorem. We use the notation from the previous section. We assume that  $A' \neq 1/1$  is one of the rationals not covered by Lemma 21.5. In the previous section we used the linear functionals  $G$  and  $H$  defined relative to  $A$ . Given the statement of the Diophantine Lemma, we can try to use the linear functionals  $G'$  and  $H'$  for the same purpose. Here  $G'$  and  $H'$  are associated to  $A'$ . Before we begin our argument, we warn the reader that  $G'$  is not the derivative of  $G$ . We will denote the partial derivatives of  $G'$  by  $\partial_x G'$  and  $\partial_y G'$ .

**Lemma 21.7**  $G'(v) \geq -q' + 2$  for all  $v \in R_1$ .

**Proof:** We only have to worry about points near the top left corner of  $R_1$ . Such points lie on the first period of  $\Gamma'$  to the right of the origin. Call this period  $\beta'$ . When  $A' \in \{3/5, 3/7, 5/7\}$  we check this result explicitly for every point of  $\beta'$ . When  $A' = 1/q'$  we note that  $\partial_x G' > 0$  and  $\partial_y G' < 0$ . We also note that all points in  $R_1$  have positive first coordinate and second coordinate at most  $(q' - 1)/2$ . Thus, the point that minimizes  $G'$  is  $v = (1, (q' - 1)/2)$ . We compute

$$G'(v) + q - 2 = \frac{q' - 3}{q' + 1} \geq 0.$$

The extreme case occurs when  $q' = 3$ . ♠

$H'$  is tougher to analyze because the points of interest to us are near the top right corner of  $R_1$ , and this corner can vary drastically with the choice of  $A$ . We will use rotational symmetry to bring the points of interest back into view, so to speak. Let  $\iota$  be the isometric involution that swaps  $(0, 0)$  and  $V_+$ . Repeated applications of Lemma 18.2 show that  $V_+ = V'_+ + dV'$  for some  $d \in \mathbf{Z}$ . Hence  $\iota$  is a symmetry of  $\widehat{\Gamma}'$ . See the remark after Equation 164.

The infinite arc  $\iota(\Gamma')$  is the open component of  $\widetilde{\Gamma}'$  that lies just beneath the baseline. One period of  $\iota(\Gamma')$  connects the point  $(0, -1)$  to the point  $(q', -p' - 1)$ . Let's denote this period by  $\beta'$ . Compare the proof of Lemma 21.1. The points of  $R_1$  near the top right corner correspond to points on  $\beta'$ . To evaluate  $H'$  on the points near the top right corner of  $R_1$ , we evaluate  $H'$  on points of  $\beta'$  and then relate the results.

**Lemma 21.8** For any  $v \in \mathbf{R}^2$  we have

$$|H'(v) + H'(\iota(v)) - q_+| < \frac{2}{q'}.$$

**Proof:** Since  $H'$  is a linear functional, it suffices to prove our result for  $v = (0, 0)$ . In this case, we must show that  $|H'(V_+) - q_+| < 2/(q')$ . We have already remarked that  $V_+ = V'_+ + dV'$ . Hence  $q_+ = q'_+ + dq'$ . From Lemma 19.1, we get  $H'(dV') = dq'$ . Hence, our equality is equivalent to

$$|H'(V'_+) - q'_+| < \frac{2}{q'}. \quad (262)$$

The point  $V'_+$  lies on the same vertical line as the point  $u' = (q'_+/q')V'$ , and exactly  $1/q'$  units away. Equation 262 now follows from the next 3 facts.

$$H'(u') = q'_+; \quad |\partial_y H'| < 2; \quad \|u' - V'_+\| = \frac{1}{q'}. \quad (263)$$

The first fact comes from Lemma 19.1. The second fact is an easy calculus exercise. The third fact, already mentioned, is an easy exercise in algebra that uses  $|q'p'_+ - p'q'_+| = 1$ . ♠

The bound

$$H'(v) \leq \Omega q' - 2 = q' + q_+ - 2$$

only fails for points very near the top right vertex of  $R_1$ . Any such point has the form  $\iota(v)$  for some  $v \in \beta'$ . Thus, to establish the above bound, it suffices to prove that

$$H'(v) \geq -q' + 2 + \frac{2}{q'}. \quad (264)$$

This inequality can fail for very small choices of  $q'$ . However, from the Adjacent Mismatch Principle, the inequality must fail for at least 2 vertices on  $\beta'$ , and this does not happen.

We check all cases with  $q' \leq 7$  by hand. This leaves only  $A' = 1/q'$  for  $q' \geq 9$ . Reasoning as we did in Lemma 21.7, we see that the extreme point is  $v = (0, (1 - q)/2)$ . We compute

$$H'(v) - \left(-q' + 2 + \frac{1}{q'}\right) = \frac{2(q'^2 - 2q' - 1)}{(1 + q')^2} - \frac{2}{q'} > 0. \quad (265)$$

The last equation is an easy exercise in calculus. This completes our proof of the Decomposition Theorem for all parameters  $A$  such that  $A' \neq 1/1$ .

## 21.5 The End of the Proof

Now we deal with the case when  $A' = 1/1$  is the superior predecessor of  $A$ . We have the following structure

$$\frac{1}{1} \leftarrow A_1 = \frac{2k-1}{2k+1} \leftarrow \dots \leftarrow A_m = 1. \quad (266)$$

Here  $k \geq 1$ . For instance, when  $A = 17/21$ , we have  $1/1 \leftarrow 9/11 \leftarrow 17/21$ . Figure 21.3 shows  $\Gamma(17/21)$ . In this case  $\Gamma \cap R_1$  is the line segment connecting  $(0, 0)$  to  $(-5, 5) = (-k, k)$ . We will establish this structure in general.

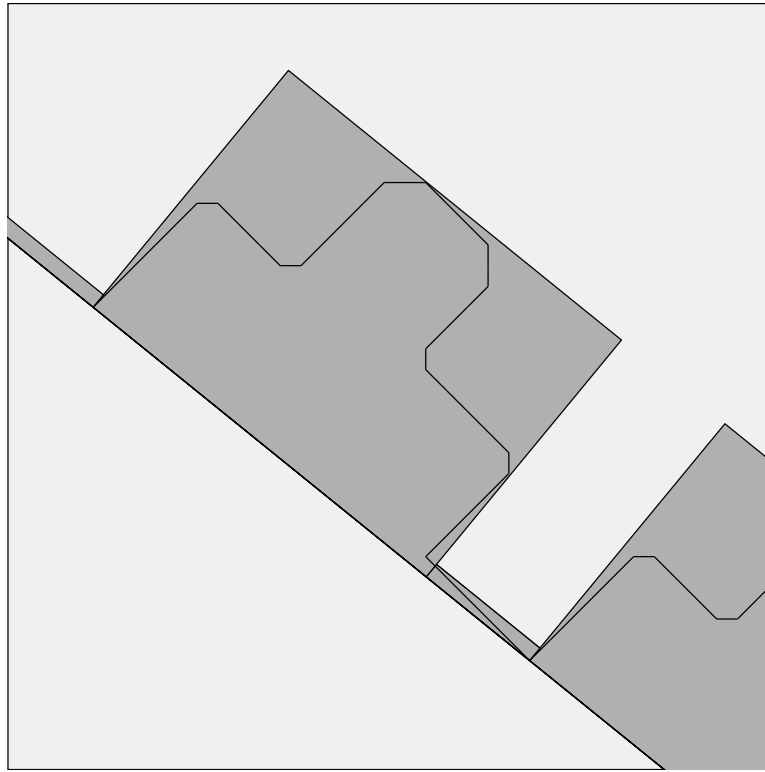


**Figure 21.3:**  $\Gamma(17/21)$

$R_1$  is the very short and squat parallelogram near the bottom right corner of Figure 21.3. This time  $R_1$  lies to the left of the origin. The left side of  $R_1$  lies in  $L_1^+$ . Repeated applications of Lemma 18.2 show that  $(-k, k-1) \in L_1^+$ . The right side of  $R_0$  lies in  $L_0^+$ , the parallel line through the origin. The top of  $R_1$  contains  $(0, 1)$  and is parallel to the baseline.

Let  $\gamma = \Gamma \cap R_0$ . The rightmost vertex of  $\gamma$  is  $(0, 0)$ , and the rightmost edge of  $\gamma$  connects  $(0, 0)$  to  $(-1, 1)$ . Compare the proof of the Room Lemma.

**Lemma 21.9** *The leftmost edge of  $\gamma$  connects  $(-k, k)$  to  $(-k + 1, k - 1)$ .*

**Proof:** By Lemma 21.1, there is a unique edge  $e$  of  $\Gamma$  that crosses  $L_1^+$ . Looking at the proof of Lemma 21.1 we see  $e = \iota(e')$ , where  $e'$  connects  $(0, -1)$  to  $(-1, 0)$  and  $\iota$  is order 2 rotation about the point

$$\left(\frac{-q_-}{2}, \frac{p_-}{2}\right) = \left(\frac{-k}{2}, \frac{k-1}{2}\right). \quad (267)$$

From this, we conclude that  $e$  connects  $(-k, k)$  to  $(-k + 1, k - 1)$ . The leftmost edge of  $\gamma$  crosses  $L_1^+$ . This edge must be  $e$ . ♠

**Lemma 21.10** *The line segment  $\gamma'$  connecting  $(0, 0)$  to  $(-k, k)$  lies beneath  $L_0^-$ . Hence  $\gamma' \cap R_0 \subset R_1$ .*

**Proof:** Letting  $F(m, n) = Am + n$ , we have  $F(0, 1) = 1$ . Hence  $F(x) = 1$  for all  $x \in L_0^-$ . On the other hand, we compute that  $F(0, 0) = 0$  and  $F(-k, k) = 2k/(2k + 1) < 1$ . By convexity,  $F(y) < 1$  for all  $y \in \gamma'$ . ♠

To finish our proof, we just have to show that  $\gamma' = \gamma$ . The first and last edges of  $\gamma$  and  $\gamma'$  agree, and these edges are  $\pm(1, -1)$ , with the sign depending on which way we orient our curves. Let  $p_j = (-j, j)$ , for  $j = 2, \dots, k - 1$ . By Lemma 18.1, we have

$$(A_1)_- = \left(\frac{k-1}{k}\right) < A < \left(\frac{k}{k+1}\right) = (A_1)_+; \quad \frac{1}{k+1} < 1 - A < \frac{1}{k} \quad (268)$$

The first equation implies the second. We compute

$$M_+(p_j) = (x_j, y_j, z_j) = j(1 - A, 1 - A, 1 - A) + (0, 1, 0); \quad \text{mod } \Lambda \quad (269)$$

Equation 268 combines with the fact that  $j \in \{1, \dots, k - 1\}$  to give

$$x_j = z_j \in [1 - A, A]; \quad x_j + y_j - z_j = y_j \in (1, 1 + A) \subset (A, 1 + A). \quad (270)$$

We check that these inequalities always specify the edge  $(-1, 1)$ . Hence  $\gamma'$  and  $\gamma$  are both line segments. Hence  $\gamma = \gamma'$ .

# Part V

- In §22 we prove some further results about the inferior and superior sequences. We list the basic results in the first section and then spend the rest of the chapter proving these results.
- In §23, we prove Theorem 1.9. We also build a rough model for the way the orbit  $O_2(1/q_n, -1)$  returns to the interval  $I = [0, 2] \times \{-1\}$ . Our work here depends on two technical results, the Copy Theorem and the Pivot Theorem, which we establish in Part VI.
- In §25 we prove Statements 2,3,4 of the Comet Theorem, modulo some technical details that we handle in Part VI. We defer the proof of Statement 1 of the Comet Theorem until Part VI.
- in §25 we deduce a number of dynamical consequences of the Comet Theorem, including minimality of the set of unbounded orbits. We also define the cusped solenoids and explain how the time-one map of their geodesic flow models the outer billiards dynamics.
- in §26 we analyze the structure of the Cantor set  $C_A$ . This chapter has a number of geometric results, such as a formula for  $\dim(C_A)$  when  $A$  is a quadratic irrational.

## 22 Odd Approximation Results

### 22.1 The Results

Let  $\{p_n/q_n\}$  be the inferior sequence associated to an irrational parameter  $A \in (0, 1)$ , and let  $\{d_n\}$  be sequence obtained from Equation 31. We call  $\{d_n\}$  the *inferior renormalization sequence*. We call the subsequence of  $\{d_n\}$  corresponding to the superior terms the *superior renormalization sequence* or just the *renormalization sequence*. Referring to the inferior sequences, we have  $d_n = 0$  if and only if  $n$  is not a superior term. In this case, we call  $n$  an *inferior term*. So, the renormalization sequence is created from the inferior renormalization sequence simply by deleting all the 0s.

For any odd rational  $p/q \in (0, 1)$ , define

$$p^* = \min(p_-, p_+); \quad q^* = \min(q_-, q_+). \quad (271)$$

Here  $p^*/q^*$  is one of the rationals  $p_{\pm}/q_{\pm}$ . It is convenient to define

$$\frac{p_0^*}{q_0^*} = \frac{1}{0}. \quad (272)$$

Given the superior sequence  $\{p_n/q_n\}$  we define

$$\lambda_n = |Aq_n - p_n|; \quad \lambda_n^* = |Aq_n^* - p_n^*|; \quad (273)$$

Note that

$$\lambda_0^* = 1. \quad (274)$$

For the purposes of making a clean statement, we define  $\lambda_{-1} = +\infty$ . All our results are meant to apply to the superior sequence, for indices  $n \geq 0$ .

$$d_n \lambda_n < 2q_n^{-1}; \quad (275)$$

$$q_{2n} > (5/4)^n D_{2n}. \quad (276)$$

$$\sum_{k=n}^{\infty} d_k \lambda_k = \lambda_n^* < \lambda_{n-1} \quad (277)$$

Note that Equation 275 is an immediate consequence of Lemma 18.4. The rest of the chapter is devoted to proving Equations 276 and 277.

## 22.2 The Growth of Denominators

Let  $\delta_n$  be as in Equation 194. By Lemma 18.2, the sequence  $\{\delta_n\}$  determines the sequence  $\{p_n/q_n\}$ . At each step,  $(q_{n+1})_{\pm}$  is a non-negative integer linear combination of  $(q_n)_{\pm}$ , and the precise linear combination is determined by  $\{\delta_n\}$ . Call this the *positivity property*. Call the sequence  $\{\delta_n\}$  the *inferior enhanced renormalization sequence*, or *IERS* for short. Call the subsequence corresponding to the superior indices the *enhanced renormalization sequence*. The reason for the terminology is that we can determine the inferior renormalization sequence from the IERS, but not *vice versa*.

Say that a parameter  $A$  is *superior to* the parameter  $A'$ , if the IERS for  $A'$  is obtained by inserting some 1s into the IERS for  $A$ . For instance,  $\sqrt{5}-2$  has IERS 2, 1, 2, 1... and  $\sqrt{2}-1$  has IERS sequence 2, 2, 2.... Hence  $\sqrt{2}-1$  is superior to  $\sqrt{5}-2$ .

**Lemma 22.1** *Suppose that  $A$  is superior to  $A'$ . Then  $q_n \leq q'_n$  for all  $n$ .*

**Proof:** Consider the operation of inserting a 1 into the  $m$ th position in IERS for  $A$  and recomputing  $\{A_n\}$ . Call this new sequence the  $A^*$ -sequence. We have  $(q_{m+1}^*)_{\pm} \geq (q_m)_{\pm}$ . By induction the positivity property, we get  $(q_{n+1}^*)_{\pm} \geq (q_n)_{\pm}$ . Now let's delete the  $(m+1)$ st term from the  $A^*$ -sequence. Call the new sequence the  $A'$ -sequence. We have  $q'_n \geq q_n$  for all  $n$ . Our result now follows from induction. ♠

Call  $A$  *superior* if the corresponding inferior sequence has no inferior terms. That is, the IERS has no 1s in it. For instance  $\sqrt{2}-1$  is a superior parameter. If we want to get a lower bound on the growth of denominators, it suffices to consider only the superior parameters. Equation 276 follows from induction and our next lemma.

**Lemma 22.2** *Suppose that  $A_1, A_2, A_3$  are 3 consecutive terms in the superior sequence. Let  $d_1, d_2, d_3$  be the corresponding terms of the renormalization sequence. Then  $q_3 > (5/4)(d_1+1)(d_2+1)q_1$ .*

**Proof:** It suffices to assume that  $A$  is a superior parameter, so that  $A_1, A_2, A_3$  are (also) 3 consecutive terms in the inferior sequence.

First of all, the estimates

$$q_{n+1} > 2d_n q_n; \quad q_{n+1} > \delta_n q_n; \quad (278)$$

follow directly from the definitions. Our notation is as in Lemma 18.2.

Suppose first that  $\min(d_1, d_2) \geq 2$ . Then

$$q_3 > 4d_1d_2q_1 > \frac{4}{3}(d_1 + 1)(d_2 + 1)q_1. \quad (279)$$

Now suppose that  $d_1 = d_2 = 1$  and  $\min(\delta_1, \delta_2) \geq 3$ . Then

$$q_3 > 6q_1 = \frac{3}{2}(d_1 + 1)(d_2 + 1)q_1. \quad (280)$$

Suppose finally that  $d_1 = d_2 = 1$  and  $\delta_1 = \delta_2 = 2$ . We will deal with the case that  $A_1 < A_2$ . The other case is similar. In this case, we must have

$$A_0 > A_1 < A_2 > A_3 \quad (281)$$

by Lemma 18.2.

By Case 2 of Lemma 18.2,

$$(q_2)_- = q_1 + (q_1)_+; \quad (q_2)_+ = (q_1)_+. \quad (282)$$

By Case 4 of Lemma 18.2,

$$(q_3)_+ = q_2 + (q_2)_-; \quad (q_3)_- = (q_2)_-. \quad (283)$$

Hence,

$$q_3 = (q_3)_+ + (q_3)_- = q_2 + 2(q_2)_- = jq_2 + 2q_1 + 2(q_2)_+. \quad (284)$$

The starred equality comes from Lemma 18.1, since  $A_1 < A_2$ .

Since  $A_0 > A_1$ , Lemma 18.2 says that

$$2(q_1)_+ > (q_1)_+ + (q_1)_- = q_1. \quad (285)$$

Combining Equations 282, 284, and 285, we have

$$q_3 = q_2 + 2q_1 + 2(q_1)_+ > q_2 + 3q_1 > 5q_1. \quad (286)$$

Hence

$$q_3 > \frac{5}{4}(d_1 + 1)(d_2 + 1)q_1. \quad (287)$$

This completes our proof. ♠

### 22.3 The Identities

We first verify the identity in Equation 277. In this identity, we sum over the superior indices. However, notice that we get the same answer if we sum over all indices. The point is that  $d_n = 0$  when  $n$  is an inferior index. So, for our derivation, we work with the inferior sequence. Let  $\{p_n/q_n\}$  be the inferior sequence associated to  $A$ . Define

$$\Delta(n, N) = |p_N q_n - q_N p_n|; \quad \Delta^*(n, N) = |p_N q_n^* - q_N p_n^*|; \quad N \geq n. \quad (288)$$

**Lemma 22.3**  $\Delta^*(n, N) - \Delta^*(n+1, N) = d_n \Delta(n, N)$ .

**Proof:** The quantities relevant to the case  $n = 0$  are

$$A_0 = \frac{1}{1}; \quad A_0^* = \frac{1}{0}; \quad A_1^* = \frac{d_0 - 1}{d_0} < A_1 = \frac{2d_0 - 1}{2d_0 + 1}.$$

In this case, a simple calculation checks the formula directly.

Now suppose  $n \geq 1$ . We suppose that  $A_{n-1} < A_n$ . The other case has a similar treatment. Let  $r$  stand for either  $p$  or  $q$ . There are two cases, depending on whether the index  $n$  has type 1 or type 4. When  $n$  has type 1, Lemma 18.2 gives

$$r_n^* = (r_n)_+; \quad r_{n+1}^* = (r_{n+1})_+; \quad r_n^* = d_n r_n - r_{n+1}^*. \quad (289)$$

We have  $\Delta^*(n, N) = |a_1 - a_2|$ , where

$$\begin{aligned} a_1 &= d_n p_N q_n - d_n q_N p_n = d_n \Delta(n, N); \\ a_2 &= p_N q_{n+1}^* - q_N p_{n+1}^* = -\Delta^*(n+1, N). \end{aligned} \quad (290)$$

The sign for  $a_1$  is correct because  $A_N > A_n$ . The sign for  $a_2$  is correct because, by Lemma 18.1, we have  $A_N < (A_{n+1})_+ = A_{n+1}^*$ . The identity in this lemma follows immediately.

When  $n$  has type 4, Lemma 18.2 gives

$$r_n^* = (r_n)_+; \quad r_{n+1}^* = (r_{n+1})_-; \quad r_n^* = d_n q_n - r_{n+1}^*.$$

Hence  $\Delta^*(n, N) = |a_1 + a'_2|$ , where  $a'_2 = -a_2$ . The sign changes for  $a'_2$  because  $A_N > (A_{n+1})_- = A_{n+1}^*$ . In this case, we get the same identity. ♠

Dividing the Equation in Lemma 22.3 by  $q_N$ , we get

$$|A_N p_n^* - q_n^*| - |A_N p_{n+1}^* - q_{n+1}^*| = d_n |A_N p_n - q_n|. \quad (291)$$

Taking the limit as  $N \rightarrow \infty$ , we get

$$\lambda_n^* - \lambda_{n+1}^* = d_n \lambda_n. \quad (292)$$

Summing this equation from  $n + 1$  to  $\infty$  gives the equality in Equation 277.

Now we verify the inequality in Equation 277.

**Lemma 22.4**  $\lambda_{n+1}^* < \lambda_n$ .

**Proof:** There are two cases to consider, depending on whether  $A_n < A$  or  $A_n > A$ . We will consider the case when  $A_n < A$ . The other case has a similar treatment. By Lemma 18.1, we have  $A_n < A_{n+1}$ . Therefore, by Lemma 18.2 (applied to  $m = n + 1$ ), we have  $(q_{n+1})_+ < (q_{n+1})_-$ . But this means that  $A_{n+1}^* = (A_{n+1})_+$ . By Lemma 18.1, we have

$$A_n < A < A_{n+1}^*. \quad (293)$$

Given the above ordering, we have

$$\lambda_n = |Aq_n - p_n| = Aq_n - p_n$$

and

$$\lambda_{n+1}^* = |Aq_{n+1}^* - p_{n+1}^*| = p_{n+1}^* - Aq_{n+1}^*.$$

Hence

$$\lambda_n - \lambda_{n+1}^* = A(q_n + q_{n+1}^*) - (p_n + p_{n+1}^*) \quad (294)$$

But

$$q_n + q_{n+1}^* = q_n + (q_{n+1})_+ = (q_{n+1})_- - (q_{n+1})_+ - (q_{n+1})_+ = (q_{n+1})_-.$$

Likewise

$$p_n + p_{n+1}^* = (p_{n+1})_-.$$

Combining these identities with Equation 294, we get

$$\lambda_n - \lambda_{n+1}^* = A(q_{n+1})_- - (p_{n+1})_- = (q_{n+1})_-(A - (A_{n+1})_-) > 0.$$

This completes the proof. ♠

## 23 The Fundamental Orbit

### 23.1 Main Results

We will assume that  $p/q = p_n/q_n$ , the  $n$ th term in a superior sequence. We call  $O_2(1/q_n, -1)$  the *fundamental orbit*. Let  $C_n$  denote the set from Theorem 1.9. Let

$$C'_n = O_2(1/q_n, -1) \cap I; \quad I = [0, 2] \times \{-1\}. \quad (295)$$

Theorem 1.9 says that  $C_n = C'_n$ . In this chapter we will prove Theorem 1.9, and establish a some geometric results about how the orbits return to  $C_n$ .

After we prove Theorem 1.9, we establish a coarse model for how the points of  $O_2(1/q_n)$  return to  $C_n$ . Statement 2 of the Comet Theorem is the “geometric limit” of the Discrete Theorem, and Statement 3 of the Comet Theorem is the “geometric limit” of the coarse model we build here.

Let  $\Pi_n$  denote the truncation of the space defined in Equation 5. Let  $\chi : \Pi_n \rightarrow C_n$  denote the mapping given in Theorem 1.9. We will describe the ordering on  $\Pi_n$  such that  $\chi(\kappa)$  returns to  $\chi(\kappa_+)$ , where  $\kappa_+$  is the successor of  $\kappa$  in the ordering.

Here we will define two natural orderings on the sequence space  $\Pi_n$  associated to  $p_n/q_n$ . Let  $\{d_n\}$  be the renormalization sequence.

**Reverse Lexicographic Ordering:** Given two finite sequences  $\{a_i\}$  and  $\{b_i\}$  of the same length, let  $k$  be the largest index where  $a_k \neq b_k$ . We define  $\{a_i\} \prec' \{b_i\}$  if  $a_k < b_k$ , and  $\{b_i\} \prec' \{a_i\}$  if  $a_k > b_k$ . This ordering is known as the *reverse lexicographic* ordering.

**Twist Automorphism:** Given a sequence  $\kappa = \{k_i\} \in \Pi_n$ , we define  $\tilde{k}_i = k_i$  if  $A_i < A_n$ , and  $\tilde{k}_i = d_i - k_i$  if  $A_i > A_n$ . We define  $\tilde{\kappa} = \{\tilde{k}_i\}$ . The map  $\kappa \rightarrow \tilde{\kappa}$  is an involution on  $\Pi_n$ . We call this involution the *twist involution*.

**Twirl Ordering:** Any ordering on  $\Pi_n$  gives an ordering on  $C_n$ , via the formula in Theorem 1.9. Now we describe the ordering that comes from the first return map. Given two sequences,  $\kappa_1, \kappa_2 \in \Pi_n$ , we define  $\kappa_1 \prec \kappa_2$  if and only if  $\tilde{\kappa}_1 \prec' \tilde{\kappa}_2$ . We call the ordering determined by  $\prec$  the *twirl ordering*. We think of the word “twirl” as a kind of acronym for *twisted reverse lexicographic*. We will give an example below.

**Lemma 23.1** *When  $C_n$  is equipped with the twirl order, each element of  $C_n$  except the last returns to its immediate successor, and the last element of  $C_n$  returns to the first.*

Our third goal is to understand  $O_2(1/q_n, -1)$  far away from  $I$ . Let  $h_1(\kappa)$  denote the maximum distance the forward  $\Psi$ -orbit of  $\chi(\kappa)$  gets from the kite vertex  $(0, 1)$  before returning as  $\chi(\kappa_+)$ . Let  $h_2(\kappa)$  denote the number of iterates it takes before the forward  $\Psi$ -orbit of  $\chi(\kappa)$  returns as  $\chi(\kappa_+)$ .

Let  $\sigma(\kappa)$  be the largest index  $k$  such that the sequences corresponding to  $\kappa$  and  $\kappa_+$  differ in the  $k$ th position. Here  $\sigma(\kappa) \in \{0, \dots, n-1\}$ . Finally, we define  $\sigma(\kappa) = n$  if  $\kappa$  is the last element of  $\Pi_n$ .

**Lemma 23.2** *Let  $m = \sigma(\kappa)$ . Then*

$$q_m/2 - 4 < h_1(\kappa) < 2q_m + 4; \quad h_2(\kappa) < 5q_m^2.$$

The table below encodes the example from the introduction:

$$\frac{p_0}{q_0} = \frac{1}{1} > \frac{1}{3} < \frac{5}{13} > \frac{19}{49} = \frac{p_3}{q_3}.$$

The first 3 columns indicate the sequences. The next column indicates the first coordinate of  $49\chi(\kappa)$ . The first point of  $C_3$  is  $(65/49, -1)$ . The next column shows  $(m) = \sigma(\kappa)$ . The last column shows  $q_m$ .

1	0	1	→	65	(0)	1
0	0	1	→	5	(1)	3
1	1	1	→	81	(0)	1
0	1	1	→	21	(1)	3
1	2	1	→	97	(0)	1
0	2	1	→	37	(2)	13
1	0	0	→	61	(0)	1
0	0	0	→	1	(1)	3
1	1	0	→	77	(0)	1
0	1	0	→	17	(1)	3
1	2	0	→	93	(0)	1
0	2	0	→	33	(3)	49

For instance, the the  $\Psi$  orbit of  $37/49$  wanders between  $13/2 - 4 = 5/2$  and  $2 * 13 + 4 = 30$  units away before returning to  $61/49$  in less than  $5 \times (13^2)$  steps. This is not such an inspiring result. We have included this small example just to show how the chart works. Larger examples would yield much more dramatic results.

## 23.2 The Copy and Pivot Theorems

Here we describe the technical results that we will establish in Part VI.

Relative to the parameter  $A$ , we associate a sequence of *pairs of points* in  $\mathbf{Z}^2$ . We call these points the *pivot points*. We make the construction relative to the inferior sequence.

Define  $E_0^\pm = (0, 0)$  and  $V_n = (q_n, -p_n)$ . Define

$$A_n < A_{n+1} \implies E_{n+1}^- = E_n^-; \quad E_{n+1}^+ = E_n^+ + d_n V_n \quad (296)$$

$$A_n > A_{n+1} \implies E_{n+1}^- = E_n^- - d_n V_n; \quad E_{n+1}^+ = E_n^+. \quad (297)$$

We have set  $A_n = p_n/q_n$ . Here is an example.

$$\frac{1}{1} \gtrless \frac{3}{5} \gtrless \frac{17}{29} \lesssim \frac{37}{63} \lesssim \frac{57}{97} \gtrless \frac{379}{645}$$

The inferior renormalization sequence is 2, 2, 1, 0, 3. We compute

- $E_1^+ = E_0^+ = (0, 0)$
- $E_2^+ = E_1^+ = (0, 0)$
- $E_3^+ = E_2^+ + 1(29, -17)$
- $E_4^+ = E_3^+ + 0(97, -57) = (29, -17)$
- $E^+(379/645) = E_5^+ = E_4^+$ .
- $E_1^- = E_0^- - 2(1, -1) = (-2, 2)$
- $E_2^- = E_1^- - 2(5, -3) = (-12, 8)$
- $E_3^- = E_2^- = (-12, 8)$
- $E_4^- = E_3^- = (-12, 8)$
- $E^-(379/645) = E_5^- = E_4^- - 3(97, -57) = (-303, 197)$ .

This procedure gives inductive way to define the pivot points to a pair of odd rationals. We define the *pivot arc*  $P\Gamma$  of  $\Gamma$  to be the arc whose endpoints are  $E^+$  and  $E^-$ . It turns out that the pivot arc is well-defined – this is something we will prove simultaneously with our Copy Theorem below. This is to say that  $E^+$  and  $E^-$  are both vertices of  $\Gamma$ . In Part VI we prove the following result.

**Theorem 23.3 (Copy)** *If  $A_1 \leftarrow A_2$  then  $P\Gamma_2 \subset \Gamma_1$ .*

Figures 22.1 and 22.2 together illustrate Theorem 23.3 for  $17/29 \leftarrow 57/97$ .

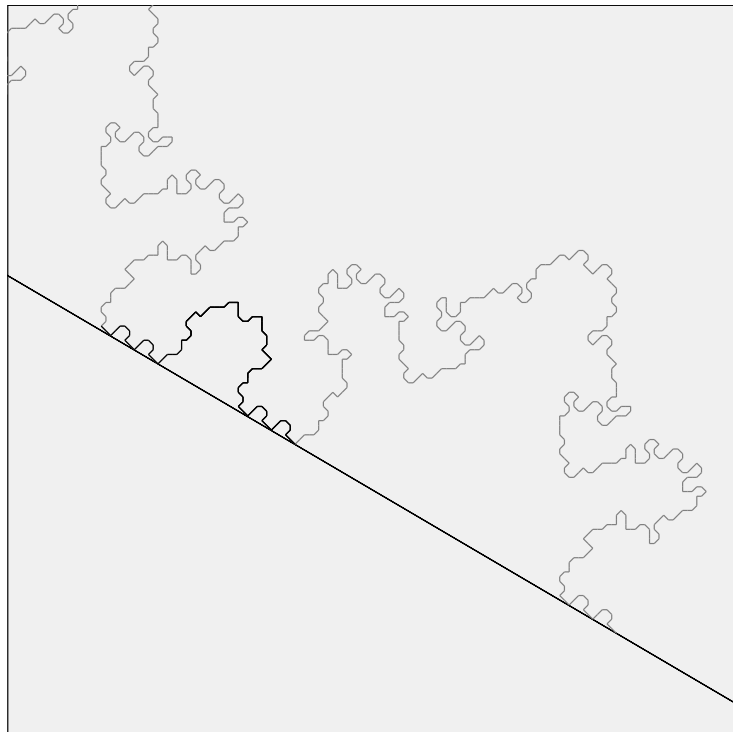


**Figure 23.1:**  $\Gamma(57/97)$  in grey and  $P\Gamma(57/97)$  in black.

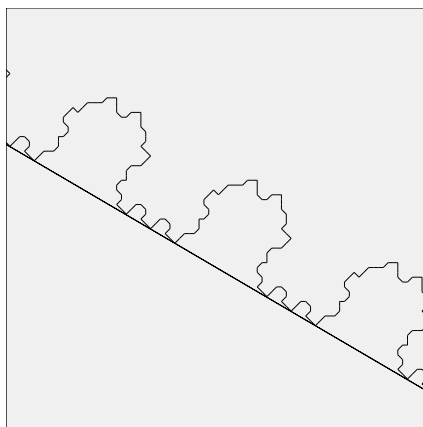


**Figure 23.2:**  $\Gamma(17/29)$

Now we turn to the statement of the Pivot Theorem. Given an odd rational parameter  $A = p/q$ , let  $V$  be the vector from Equation 21. Let  $ZV$  denote the group of integer multiples of  $V = (q, -p)$ . In Part VI we prove the following result.

**Theorem 23.4 (Pivot)** *Every low vertex of  $\Gamma$  is equivalent mod  $ZV$  to a vertex of  $P\Gamma$ . That is,  $P\Gamma$  contains one period's worth of low vertices on  $\Gamma$ .*

The Pivot Theorem makes a dramatic statement. Another way to state the Pivot Theorem is that there are no low vertices on the complementary arc  $\gamma - P\Gamma$ . Here  $\gamma$  is the arc just to the right of  $P\Gamma$  such that  $P\Gamma \cup \gamma$  is one full period of  $\Gamma$ . A glance at Figure 23.1 will make this clear. We will prove the Pivot Theorem in Part VI. We will also prove the following easy estimate.

**Lemma 23.5**

$$-\frac{q}{2} < \pi_1(E^-) < \pi_1(E^+) < \frac{q}{2}.$$

### 23.3 Half of Theorem 1.9

We will prove that  $C_n \subset C'_n$ . This almost an immediate consequence of the Copy Theorem. When  $1/1 \rightarrow A$ , the pivot arc  $P\Gamma$  contains the points

$$k\tilde{V}_1; \quad k = 0, \dots, d_1; \quad \tilde{V}_1 = (-1, 1). \quad (298)$$

This is a consequence of the argument in §21.5.

In general, suppose  $A_1 \leftarrow A_2$  are two parameters. Then, by construction, the pivot arc  $P\Gamma_2$  contains all points

$$v + k\tilde{V}_1 \quad k \in \{0, \dots, d\}; \quad d = \text{floor}(q_2/2q_1). \quad (299)$$

Here  $v$  is any vertex of  $P\Gamma_1$ . It now follows from induction that  $P\Gamma_n$  contains all points of the form

$$\sum_{j=0}^{n-1} k_j \tilde{V}_j; \quad k_j \in \{0, \dots, d_j\}. \quad (300)$$

Let  $M$  denote the map from Equation 19. Usually we take  $M$  so that  $M(0, 0) = 0$ , but for our proof here, we adjust so that  $M(0, 0) = (1/q_n, -1)$ .

(This makes no difference; see the discussion surrounding the definition of  $M$  in §2.6.) Call a lattice point even if the sum of its coordinates is even. Note that  $\tilde{V}_j$  is even for all  $j$ . Hence, all points in Equation 300 are even. The images of these points under  $M$  have second coordinate  $-1$ . We just have to worry about the first coordinate. We have

$$M(\tilde{V}_j) = \frac{1}{q_n} + 2|Aq_j - p_j| = \frac{1}{q_n} + \frac{1}{q_n}2|p_nq_j - q_np_j|. \quad (301)$$

The absolute value in our equation comes from the fact that  $\tilde{V}_j = (q_j, -p_j)$  iff  $p_j/q_j < A_j$ , and  $\tilde{V}_j = (-q_j, p_j)$  iff  $p_j/q_j > A_j$ .

For convenience, we recall the definition of  $C_n$ . Let  $\mu_i = |p_nq_i - q_np_i|$ .

$$C_n = \bigcup_{\kappa \in \Pi_n} (X_n(\kappa), -1); \quad X_n(\kappa) = \frac{1}{q_n} \left( 1 + \sum_{i=0}^{n-1} 2k_i \mu_i \right). \quad (302)$$

It now follows from the affine nature of  $M$  and from the definition of  $C_n$  that

$$C_n \subset O_2(1/q_n, -1). \quad (303)$$

It follows from the case  $n = 0$  of Equation 277, that  $C_n \subset [0, 2] \times \{-1\}$ .

## 23.4 The Inheritance of Low Vertices

The rest of Theorem 1.9 follows from the Pivot Theorem and from what we have done by applying the information contained in the Pivot Theorem to what we have already done in the previous section. To make the argument work, we first need to deal with a tedious technical detail. We take care of the detail in this section.

Let  $A_1 \leftarrow A_2$  be two odd rationals. Let  $\tilde{V}_1 = V_1$  if  $A_1 < A_2$  and  $\tilde{V}_1 = -V_1$  if  $A_1 > A_2$ . Let

$$d_1 = \text{floor}(q_2/2q_1). \quad (304)$$

Let  $v_1$  be a vertex on the pivot arc  $P\Gamma_1$ . Define

$$v_2 = v_1 + k\tilde{V}_1; \quad k \in \{0, \dots, d_1\}. \quad (305)$$

Notice that these were precisely the vertices that we considered in §23.3. Now we want to take a close look at these vertices. Here is the main result of this section.

**Lemma 23.6**  $v_1$  is low with respect to  $A_1$  iff  $v_2$  is low with respect to  $A_2$ .

**Proof:** There are two cases to consider, depending on whether  $A_1 < A_2$  or  $A_2 < A_1$ . We will consider the former case. The latter case has essentially the same treatment. In our case, we have  $\tilde{V}_1 = V_1$ . Let  $E_j^\pm$  be the pivot points for  $\Gamma_j$ . Say that a vertex is *high* if it is not low.

We will first suppose that  $v_1$  is low with respect to  $A_1$  and that  $v_2$  is high with respect to  $A_2$ . This will lead to a contradiction. We write  $v_j = (m_j, n_j)$ . Let  $M_j$  be the fundamental map from Equation 19. Since  $v_1$  is low and  $v_2$  is high, we have

$$\begin{aligned} 2A_1m_1 + 2n_1 + \frac{1}{q_1} &= M_1(v_1) \leq 2 - \frac{1}{q_1}; \\ 2A_2m_2 + 2n_2 + \frac{1}{q_2} &= M_2(v_2) \geq 2 + \frac{1}{q_2}. \end{aligned}$$

Rearranging terms,

$$2\left(\frac{p_2}{q_2}m_2 + n_2\right) - 2\left(\frac{p_1}{q_1}m_1 + n_1\right) \geq \frac{2}{q_1}. \quad (306)$$

Plugging in the relations  $m_2 = m_1 + kq_1$  and  $n_2 = n_1 - kp_1$  and simplifying, we get

$$\frac{(m_1 + kq_1)(p_2q_1 - p_1q_2)}{q_1q_2} \geq \frac{1}{q_1}. \quad (307)$$

Since  $A_1 \leftarrow A_2$  and  $A_1 < A_2$ , we have

$$p_2q_1 - p_1q_2 = 2. \quad (308)$$

Hence

$$m_1 + kq_1 \geq \frac{q_2}{2}. \quad (309)$$

Combining Equation 296 and Equation 309, we get

$$E_1^+(A_2) = E_1^+(A_1) + d_1q_1 \geq^* m_1 + kq_1 > \frac{q_2}{2} >^* E_1^+(A_2).$$

This is a contradiction. the first starred inequality comes from the Pivot Theorem and the fact that  $k \leq d_1$ . The second starred inequality comes from the Corollary 23.5.

Now we will suppose that  $v_1$  is high with respect to  $A_1$  and  $v_2$  is low with respect to  $A_2$ . This will also lead to a contradiction. Let  $M_1$  denote the first

coordinate of the fundamental map relative to the parameter  $A_1$ , adjusted so that  $M_1(0, 0) = 1/q_1$ . That is

$$M_1(m, n) = 2A_1m + 2n + \frac{1}{q_1}. \quad (310)$$

Since  $v_1$  is high, we have the following dichotomy.

$$M_1(v) \geq 2 + \frac{1}{q_1}; \quad M_1(v) > 2 + \frac{1}{q_1} \implies M_1(v) \geq 2 + \frac{3}{q_1}. \quad (311)$$

We will consider these two cases in turn.

**Case 1:** If  $M_1(v_1) = 2 + 1/q_1$ , then

$$M_1(m_1, n_1 - 1) = \frac{1}{q_1} = M_1(0, 0).$$

But then  $(m_1, n_1 - 1) = jV_1$  for some integer  $j$ . But then  $|m_1| \geq q_1$ . Since  $v_1 \in P\Gamma_1$ , this contradicts Corollary 23.5. Hence

$$v_1 = (0, 1); \quad v_2 = kV_1 + (0, 1).$$

If  $v_2$  is low then

$$0 = 2k(A_1q_1 - p_1) < 2k(A_2q_1 - p_1) = M_2(v_2) - M_2(0, 1) \leq 0.$$

This is a contradiction. The first inequality comes from  $A_1 < A_2$ .

**Case 2:** If  $M_1(v_1) \geq 2 + 3/q_1$ , then the same reasoning as in Equations 306, 307, and 308 (but with signs reversed) leads to

$$m_1 + kq_1 < -3q_2. \quad (312)$$

But then

$$\frac{-q_2}{2} < \frac{-q_1}{2} <^* m_1 \leq m_1 + kq_1 < -3q_2$$

The starred inequality comes from Corollary 23.5. Again we have a contradiction, this time by a wide margin. ♠

## 23.5 Proof of Theorem 1.9

Now we revisit the construction in §23.3 and show that actually  $C_n = C'_n$ . Let  $\Lambda_n$  denote the set of low vertices of  $P\Gamma_n$ . By the Pivot Theorem, every low vertex on  $P\Gamma_n$  is equivalent to a point of  $\Lambda_n$  modulo  $\mathbf{Z}V_n$ .

**Lemma 23.7** *For any  $n \geq 0$ , we have*

$$\Lambda_{n+1} = \bigcup_{k=0}^{d_n} (\Lambda_n + k\tilde{V}_n).$$

**Proof:** Induction. For  $n = 0$  we have  $E_1^- = (-d_0, d_0)$  and  $E_1^+ = (0, 0)$ . In this case, the right hand side of our equation precisely describes the set of points on the line segment joining the pivot points. The case  $n = 0$  therefore follows directly from the Pivot Theorem.

Let  $\Lambda'_{n+1}$  denote the right hand side of our main equation. Since  $\Gamma_n$  is invariant under translation by  $V_n$ , every vertex of  $\Lambda'_{n+1}$  is low with respect to  $A_n$ . Hence, by Lemma 23.6, every vertex of  $\Lambda'_{n+1}$  is low with respect to  $A_{n+1}$ . Combining this fact with Equation 299, we see that  $\Lambda'_{n+1} \subset \Lambda_{n+1}$ .

By Lemma 23.6 again, every  $v \in \Lambda_{n+1}$  is also low with respect to  $A_n$ . Hence

$$v = v' + k\tilde{V}_n; \quad k \in \mathbf{Z}. \quad (313)$$

for some  $v' \in \Lambda_n$ . If  $k \notin \{0, \dots, d_n\}$  then  $v$  either lies to the left of the left pivot point of  $\Gamma_{n+1}$  or to the right of the right pivot point of  $\Gamma_{n+1}$ . Hence  $k \in \{0, \dots, d_n\}$ . This proves that  $\Lambda_{n+1} \subset \Lambda'_{n+1}$ . Combining the two facts completes our induction step. ♠

We proved Lemma 23.7 with respect to the inferior sequence. However, notice that if  $d_n = 1$  then  $\Lambda_{n+1} = \Lambda_n$ . Thus, we get precisely the same result for consecutive terms in the superior sequence. We have shown that  $v \in \Gamma_n$  is low if and only if  $v \in \Lambda_n \bmod \mathbf{Z}V$ . But then

$$O_2(1/q_n, -1) \cap I = M(\Lambda_n); \quad I = [0, 2] \times \{-1\}. \quad (314)$$

Here  $M$  is the fundamental map. Recognizing  $\Lambda_n$  as the set from Equation 300, we get precisely the equality in Theorem 1.9. There is one last detail. One might worry that  $M$  maps some points of  $\Lambda_n$  to points on  $[0, 2] \times \{1\}$ , but all points in  $\Lambda_n$  have even parity. Hence, this does not happen.

This completes the proof of Theorem 1.9.

## 23.6 Proof of Lemmas 23.1 and 23.2

Let  $\Sigma_n$  denote the union of all points in Equation 300. Here  $M(\Sigma_n) = C_n$ . The ordering on  $\Sigma_n$  determines the ordering of the return dynamics to  $C_n$ . We set  $\Sigma_0 = \{(0, 0)\}$ , for convenience. We can determine the ordering on  $\Sigma_{n+1}$  from the ordering on  $\Sigma_n$  and the sign of  $A_{n+1} - A_n$ . When  $A_n < A_{n+1}$ , we can write the relation

$$\Sigma_n + kV_n \prec \Sigma_n + (k + 1)V_n; \quad k = 0, \dots, (d_n - 1). \quad (315)$$

to denote that each point in the left hand set precedes each point on the right hand set. Within each set, the ordering does not change. When  $A_n > A_{n+1}$ , we can write the relation

$$\Sigma_n - (k + 1)V_n \prec \Sigma_n - kV_n; \quad k = 0, \dots, (d_n - 1). \quad (316)$$

Lemma 23.1 follows from these facts, and induction.

Let  $\beta_n$  denote the arc of  $P\Gamma_n$ , chosen so that  $P\Gamma_n \cup \beta_n$  is one period of  $P\Gamma_n$ . Let  $L_n$  be the line of slope  $-A_n$  through the origin.

**Lemma 23.8** *No point of  $\beta_m$  lies more than  $q_m$  vertical units away from  $L_m$  and some point of  $\beta_m$  lies at least  $q_m/4$  vertical units away from  $L_m$ .*

**Proof:** By the Room Lemma,  $\beta_m \subset R(A_m)$ . The upper bound follows immediately from this containment. For the lower bound, recall from the Room Lemma that  $P\Gamma_m$  crosses the centerline  $L$  of  $R(A_m)$  once, and this crossing point lies at least  $(p_m + q_m)/4 > q_m/4$  vertical units from  $L_m$ . By Lemma 23.5 and symmetry, the left endpoint of  $\beta_m$  lies to the left of  $L$  and the right endpoint of  $\beta_m$  lies to the right of  $L$ . Hence,  $\beta_m$  contains the crossing point we have mentioned. For an alternative argument, we note that no point on the pivot arc crosses the line parallel to the floor and ceiling of  $R(A_m)$  and halfway between them, whereas the crossing point lies above this midline. ♠

Notice that the line  $L_n$  replaces the line  $L_m$  in our next lemma.

**Lemma 23.9** *Let  $m \leq n$  and  $q_m > 10$ . Then some point of  $\beta_m$  lies at least  $q_m/4 - 1$  vertical units from  $L_n$ . Moreover, no point of  $\beta_m$  lies more than  $q_m + 1$  vertical units away from  $L_n$ .*

**Proof:** Some point  $v$  of  $\beta_m$  at least  $q_m$  vertical units from  $L_m$  by the previous result. From Lemma 18.4, we have

$$|A_m - A_n| < \frac{2}{q_m^2}. \quad (317)$$

On the other hand, by the Room Lemma and by construction,  $P\Gamma_m$  is contained in two consecutive translates of  $R(A_m)$ , one of which is  $R(A_m)$  itself. Hence,  $P\Gamma_m$  lies entirely inside the ball  $B$  of radius  $4q_m$  about the origin. By Equation 317, the Hausdorff distance between the segments  $L_m \cap B$  and  $L_n \cap B$  is less than 1 once  $m > 10$ . By construction, the vertical line segment starting at  $v$  and dropping down  $q_m - 1$  units is disjoint from  $L_n \cap B$ . But this segment is disjoint from  $L_n - B$  as well. Hence  $v$  is at least  $q_m/2 - 1$  vertical units from  $L_n$ . The upper bound has a similar proof. ♠

**Lemma 23.10**  $\beta_m$  has length at most  $5q_m^2$ .

**Proof:**  $\beta_m$  is contained in one period of  $P\Gamma_m$ . Hence, it suffices to bound the length of any one period of  $P\Gamma_m$ . By the Room Lemma, one such period is contained in  $R(A_m)$ . We compute easily that the area of  $R(A_m)$  is much less than  $5q_m^2$ . Hence, there are less than  $5q_m^2$  vertices in  $R(A_m)$ . Hence, the length of one period of  $P\Gamma_m$  is less than  $5q_m^2$ . ♠

Suppose now that  $\kappa$  and  $\kappa_+$  are two consecutive points on  $\Sigma_n$ . We want to understand the arc of  $P\Gamma_n$  that joins these points. Suppose that  $\sigma(\kappa) = m$ . It follows from induction and from the Copy Theorem that there is some translation  $T$  such that  $T(\kappa)$  and  $T(\kappa_+)$  are the endpoints of the arc  $\beta_m$ . The arc joining  $\kappa$  to  $\kappa_+$  has the same length as  $\beta_m$ , and this length is less than  $5q_m^2$ . This gives us the estimate for  $h_2$ .

Now we deal with  $h_1$ . We check the result by hand for  $q_n < 10$ . So, suppose that  $q_n > 10$ . All the vertices  $\kappa$ ,  $\kappa_+$ ,  $T(\kappa)$ , and  $T(\kappa_+)$  lie within 1 vertical unit of the baseline  $L_n$ . We know that the vertical distance from some point of  $\beta_m$  to  $L_n$  is at least  $q_m/2 - 1$ . Hence, the vertical distance from some point on  $T(\beta_m)$  to  $L_n$  is at least  $q_m/2 - 2$ . Similarly, the vertical distance from any point of  $\beta_m$  to  $L_n$  is at most  $q_m + 2$ . If two points in  $\mathbf{Z}^2$  have vertical distance  $d$  then the images of these points under the fundamental map  $M_n$  have horizontal distance  $2d$ . In short, the fundamental map doubles the relevant distances. This fact gives us our estimate on  $h_1$ .

This completes the proof of Lemma 23.2.

### 23.7 Theorem 1.9 in the Even Case

Here we discuss Theorem 1.9 in the even case. For each even rational  $A_1 \in (0, 1)$  there is a unique odd rational  $A_2$  such that (in the language of Equation 27)  $A_1 = (A_2)_\pm$  and  $q_2 < 2q_1$ . In Lemma 28.2 we will show that  $\Gamma_1$  (a closed polygon) contains a copy of  $P\Gamma_2$ , and all low vertices of  $\Gamma_1$  lie on this arc. From this fact, we see that

$$O(1/q_1, -1) = M_1(\Sigma_1), \tag{318}$$

just as in the odd case. Here  $M_1$  is the fundamental map defined relative to the parameter  $A_1$  and  $\Sigma_1$  is the set of low vertices on  $P\Gamma_1$ .

Note that  $\Sigma_1 = \Sigma_2$ , where  $\Sigma_2$  is the set of low vertices on  $P\Gamma_2$ . The only difference between the two sets  $M_1(\Sigma_1)$  and  $M_2(\Sigma_2)$  is the difference in the maps  $M_1$  and  $M_2$ . Now we explain the precise form of Theorem 1.9 that this structure entails.

Switching notation, let  $A$  be an even rational. One of the two rationals  $A_\pm$  from Equation 27 is odd, and we call this rational  $A'$ . We can find the initial part of a superior sequence  $\{A_k\}$  such that  $A' = A_{n-1}$ . We set  $A = A_n$  even though  $A$  does not belong to this sequence. Referring to Theorem 1.9, we define  $\Pi_n$  exactly in the odd case, but for one detail. In case  $2q' > q$ , we simply ignore the  $n$ th factor of  $\Pi_n$ . That is, we treat  $q'$  as an inferior term. With these changes, Theorem 1.9 goes through word for word.

Here we give an example. Let  $A_1 = 12/31$ . Then  $A_2 = 19/49$ , exactly is in the introduction. We have  $n = 3$  and our sequence is

$$\frac{p_0}{q_0} = \frac{1}{1}, \frac{1}{3}, \frac{5}{13}, \frac{12}{31} = \frac{p_3}{q_3}.$$

All terms are superior, so this is also the superior sequence.  $n = 3$  in our example, and the renormalization sequence is 1, 2, 1. The  $\mu$  sequence is 19, 5, 1. The first coordinates of the 12 points of  $O_2(1/49) \cap I$  are given by

$$\bigcup_{k_0=0}^1 \bigcup_{k_1=0}^2 \bigcup_{k_2=0}^1 \frac{2(19k_0 + 5k_1 + 1k_2) + 1}{31}.$$

Writing these numbers in a suggestive way, the union above works out to

$$\frac{1}{31} \times (1 \ 3 \quad 11 \ 13 \quad 21 \ 23 \qquad 39 \ 41 \quad 49 \ 51 \quad 59 \ 61).$$

## 23.8 A Conjectural Extension

Let  $C_n$  be the set from Theorem 1.9. Each  $\xi \in C_n$  is the midpoint of a special interval, in the sense of §2.2. Call this interval  $J(\xi)$ . Define

$$\widehat{C}_n = \bigcup_{\xi \in C_n} J(\xi). \quad (319)$$

Figure 23.1 shows three examples. In the picture, we have thickened the intervals to get a better picture. We have also added in the white bars to clarify the spacing.

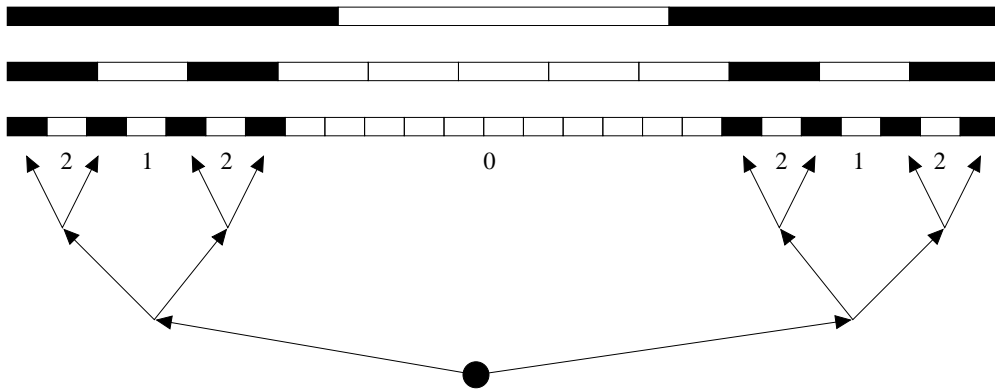


Figure 23.1:  $\widehat{C}(A)$  for  $A = 1/3$  and  $3/11$  and  $7/25$ .

The three rationals in Figure 30.1 are part of a superior sequence, one can see that each picture sort of refines the one above it. It is a consequence of Lemma 2.9 that, in the odd case, there is a gap between every pair of intervals in  $\widehat{C}(A)$ . In the even case, this need not be true. One can compute the positions of the intervals using the formula in Theorem 1.9.

Say that a *gap* is an maximal interval of  $I - \widehat{C}$ . For  $\widehat{C}(7/25)$  there are 7 gaps. Each gap has a *level*, as indicated in the figure. The levels go from 0 to  $n - 1$  in  $\widehat{C}_n$ . Informally, the gaps of level  $k \leq n - 2$  are inherited from simpler rationals, and the gaps of level  $n - 1$  are newly created with the new parameter. Generally speaking, the higher-level gaps are smaller, but this need not be the case. For  $\widehat{C}(7/25)$ , the gaps of level 1 and 2 have the same size.

Given this notion of levels there is a natural identification of  $C_n$  with the ends of a directed finite binary tree. The return map  $\Theta : C_n \rightarrow C_n$  comes from an automorphism of this tree. The union of all the gaps is bijective

with the forward cones of the tree. The automorphism of the tree induces a bijection on its forward cones.

**Conjecture 23.11** *The outer billiards map is entirely defined on the interior of any gap, and the return map to the interval  $I$  is naturally conjugate to the map on the forward cones induced by the tree automorphism.*

Some reflection will convince the reader that this is the simplest possible answer to the question of what happens in the gaps. Our Inheritance Lemma from §30 makes some progress in proving this conjecture, but it doesn't have quite enough juice in it.

## 24 Most of The Comet Theorem

### 24.1 Preliminaries

In this chapter we prove Statements 2,3,4 of the Comet Theorem. We defer the proof of Statement 1 until Part VI. Statement 4 assumes the truth of Statement 1, but our proof of Statement 1, given in Part VI, does not depend on Statement 4. (That is, our argument isn't circular.)

Suppose that  $\{A_n\}$  is the superior sequence approximating some irrational  $A$ . Let  $C_n$  be the set from Theorem 1.9. Let  $U_A$  and  $I$  be as in the Comet Theorem. We also prove the following result in Part VI.

**Theorem 24.1 (Period)** *For any  $\epsilon > 0$  there is an  $N > 0$  with the following property. If  $\zeta \in I$  is more than  $\epsilon$  units from  $C_n$ , then the period of  $\zeta$  is at most  $N$ . The constant  $N$  only depends on  $\epsilon$ .*

**Corollary 24.2**  $U_A \cap I \subset C_A$ .

**Proof:** We will suppose that  $U_A$  contains a point  $\zeta \notin C_A$  and derive a contradiction. By compactness, there is some  $\epsilon > 0$  such that  $\zeta$  is at least  $3\epsilon$  from any point of  $C_A$ . Since  $C_A$  is the geometric limit of  $C_n$ , we see that there is some  $N_1$  such that  $n > N_1$  implies that  $\zeta$  is at least  $2\epsilon$  from  $C_n$ .

Let  $\{\zeta_n\} \in I$  be a sequence of points converging to  $\zeta$ . We can choose these points so that the orbit of  $\zeta_n$  relative to  $A_n$  is well defined. There is a constant  $N_2$  such that  $n > N_2$  implies that  $\zeta_n$  is at least  $\epsilon$  from  $C_n$ . But then, by the Period Theorem, there is some  $N_3$  such that the period of  $\zeta_n$  is at most  $N_3$ .

On the other hand, by the Continuity Principle, the arithmetic graph  $\Gamma(\zeta_n, A_n)$  converges to the arithmetic graph  $\Gamma(\zeta, A)$ . In particular, the period of  $\Gamma(\zeta_n, A_n)$  tends to  $\infty$ . This is a contradiction. Hence,  $\zeta$  cannot exist.



Let  $\Pi_A$  be the sequence space from §5. Say that two sequences in  $\Pi_A$  are equivalent if they have the same infinite tail ends. Given the nature of the odometer map, we have the following useful principle.

**Odometer Principle:** Any two equivalent sequences are in the same orbit of the odometer map. Call this the *odometer principle*. We will use this principle several times in our proofs.

## 24.2 Overview of the Proof

We first prove a preliminary version of the Comet Theorem. Let

$$C'_A = C_A - (2\mathbf{Z}[A] \times \{-1\}). \quad (320)$$

**Theorem 24.3** *Let  $U_A$  denote the set of unbounded special orbits relative to an irrational  $A \in (0, 1)$ .*

1.  $C'_A \subset U_A$ .
2. The first return map  $\rho_A : C'_A \rightarrow C'_A$  is defined precisely on  $C'_A - \phi(-1)$ . The map  $\phi^{-1}$  conjugates  $\rho_A$  to the restriction of the odometer on  $\mathcal{Z}_A$ .
3. For any  $\zeta \in C'_A - \phi(-1)$ , the orbit-portion between  $\zeta$  and  $\rho_A(\zeta)$  has excursion distance in

$$\left[ \frac{d^{-1}}{2} - 4, 2d^{-1} + 20 \right]$$

and length in

$$\left[ \frac{d^{-2}}{32} - \frac{d^{-1}}{4}, 100d^{-3} + 100d^{-2} \right].$$

Here  $d = d(-1, \phi^{-1}(\zeta))$ .

### Remarks:

- (i) Our constants in Item 3 are not optimal; some tedious elementary arguments would improve them.
- (ii) Since  $d^{-1} \geq 1$ , the estimates in Item 3 above imply the less precise estimates in the Comet Theorem – once we establish that  $C_A^\# = C'_A$ .
- (iii) As we remarked after the Comet Theorem, the only non-sharp bound in Item 3 is the length upper-bound. For instance, our proof in [S1], which establishes a kind of coarse self-similarity structure, would give a better bound for  $A = \sqrt{5} - 2$  if carefully examined. We conjecture that  $-3$  is the best bound that works for all parameters at once.

Next, we prove a double identity.

**Lemma 24.4**  $U_A \cap I = C_A^\# = C_A - (2\mathbf{Z}[A] \times \{-1\})$ .

Statements 2 and 3 of the Comet Theorem follow from this result and Lemma 24.3. Lemma 24.4 also contains the first claim in Statement 4 of the Comet Theorem.

At the end of the chapter, we will prove the second claim made in Statement 4 of the Comet Theorem.

### 24.3 The Cantor Set

We first need to resolve the technical point that our set  $C_A$  is actually well defined. For convenience, we repeat the definition.

$$C_A = \bigcup_{\kappa \in \Pi} (X(\kappa), -1); \quad X(\kappa) = \sum_{i=0}^{\infty} 2k_i |Aq_i - p_i|. \quad (321)$$

**Lemma 24.5** *The infinite sums in Equation 321 converge. Hence  $C_A$  is well defined.*

**Proof:** Combining Equation 275 with the bound  $0 \leq k_n < d_n$ , we see that the  $n$ th term in the sum defining  $X(\kappa)$  is at most  $2q_n^{-1}$ . Given that  $2q_k < q_{k+1}$  for all  $k$ , we get  $2q_n^{-1} < 2^{-n+1}$ . The sequence defining  $X(\kappa)$  decays exponentially and hence converges. ♠

For the purposes of this section we equip the product space  $\Pi$  with the lexicographic ordering and the product topology.

**Lemma 24.6** *The map  $X : \Pi \rightarrow C_A$  is a homeomorphism that maps the lexicographic order to the linear order. Hence  $C_A$  is a Cantor set.*

**Proof:** We first show that the map  $X$  is injective. In fact, we will show that  $X$  is order preserving. If  $\kappa = \{k_i\} \prec \kappa' = \{k'_i\}$  in the lexicographic ordering, then there is some smallest index  $m$  such that  $k_i = k'_i$  for all indices  $i = 0, \dots, (m-1)$  and  $k_m < k'_m$ . Let  $\lambda_m = |Aq_m - p_m|$ , as in Equation 275. Then

$$X(\kappa') - X(\kappa) \geq 2\lambda_m - \sum_{k=m+1}^{\infty} 2d_k \lambda_k = \lambda_m - \lambda'_{m+1} > 0 \quad (322)$$

by Equation 277.

The map  $X : \Pi \rightarrow [0, 2]$  is continuous with respect to the topology on  $\Pi$ , because the  $n$ th term in the sum defining  $X$  is always less than  $2^{-n+1}$ . We also know that  $X$  is injective. Hence,  $X$  is bijective onto its image. Any continuous bijection from a compact space to a Hausdorff topological space is a homeomorphism. ♠

## 24.4 Convergence of the Fundamental Orbit

Let  $\{p_n/q_n\}$  denote the superior sequence associated to  $A$ . We use the notation from the previous chapter. Here  $\Gamma_n$  denotes the corresponding arithmetic graph and

$$C_n = \bigcup_{\kappa \in \Pi_n} (X_n(\kappa), -1); \quad X_n(\kappa) = \frac{1}{q_n} + \sum_{i=0}^{n-1} 2k_i |A_n q_i - p_i|. \quad (323)$$

We have already proved that  $C_n \subset O_2(1/q_n, -1)$ .

Let  $\kappa \in \Pi$  be some infinite sequence. Let  $\kappa_n \in \Pi_n$  be the truncated sequence. Let

$$\sigma_n = (X_n(\kappa_n), -1); \quad \sigma = (X(\kappa), -1) \quad (324)$$

Here is our basic convergence result.

**Lemma 24.7**  $\sigma_n \rightarrow \sigma$  as  $n \rightarrow \infty$ .

**Proof:** For  $i < n$ , let  $\tau_{i,n}$  denote the  $i$ th term in the sum for  $X_n(\kappa_n)$ . Let  $\tau_n$  be the corresponding term in the sum for  $X(\kappa)$ . When we construct the superior sequence, we will see that the sign of  $A - A_i$  is the same as the sign of  $A_n - A_i$ . Therefore

$$|\tau_n - \tau_{i,n}| = 2k |A - A_n| q_n < 2q_n^{-1} < 2^{-n+1}. \quad (325)$$

Therefore

$$\begin{aligned} |X(\kappa) - X(\kappa_n)| &= \sum_{i=0}^{n-1} |\tau_n - \tau_{i,n}| + \sum_{i=n}^{\infty} \tau_i < \\ &2 \sum_{i=0}^{n-1} 2^{-n} + 2 \sum_{i=n}^{\infty} 2^{-i} < 2^{n-3}. \end{aligned} \quad (326)$$

This completes the proof. ♠

## 24.5 All but the Last Sequence

We call the sequence  $\{k_i\}$  *first* if  $\tilde{k}_i = 0$  for all  $i$  and *last* if  $\tilde{k}_i = d_i$  for all  $i$ . The map  $\phi_2 : \Pi_A \rightarrow C_A$  is a homeomorphism. Using  $\phi_2$ , we transfer the notions of *first* and *last* to points of  $C_A$ .

Let  $\zeta \in C'_A$  denote a point that is not last. Let  $\kappa$  denote the corresponding sequence in  $\Pi_A$ . Say that two sequences in  $\Pi$  are *equivalent* if they have the same infinite tail end. We can define the reverse lexicographic order on any equivalence. Likewise we can extend the twirl order to any equivalence class. In particular, we extend the twirl order to the equivalence class of  $\kappa$ , the sequence currently of interest to us.

Since  $\kappa$  is not last, we can find some smallest index  $m = m(\zeta)$  such that where  $\tilde{k}_m < d_i$ . In other words,  $m$  is the smallest index such that  $\kappa$  differs from the last sequence in the  $m$ th spot.

The successor  $\kappa_+$  of  $\kappa$  is obtained by incrementing  $\tilde{k}_m$  by 1 and setting  $\tilde{k}_i = 0$  for all  $i < m$ . This notion of successor is compatible with the twirl ordering on the finite truncations  $\Pi_n$ . Define

$$\zeta_+ = (X(\kappa_+), -1); \quad (\zeta_n)_+ = (X(\kappa_n)_+, -1). \quad (327)$$

**Lemma 24.8** *Let  $\zeta \in C'_A$  be a point that is not last. Let  $m = m(\zeta)$ . The forward  $\Psi$  orbit of  $\zeta$  returns to  $C_A$  as  $\zeta_+$  in at most  $5q_m^2$  steps. Along the way, this portion of the orbit wanders between  $q_m/2 - 2$  units and  $2q_m + 2$  units away from  $(0, -1)$ .*

**Proof:** By Lemma 2.2, the orbit of  $\zeta$  is well-defined. Referring to the notation in Lemma 23.2, we get  $\sigma(\kappa_n) = m$  for  $n$  large enough. Hence the forward  $\Psi_n$  orbit of  $\zeta_n$  returns to  $(\zeta_n)_+$  after at most  $5q_m^2$  steps, moving away from  $(0, -1)$  by at least  $q_m/2 - 2$  units and at most  $2q_m + 2$  steps. Here  $m$  is independent of  $n$ . Since  $X$  is continuous, we have  $(\zeta_n)_+ \rightarrow \zeta_+$  as  $n \rightarrow \infty$ . The Continuity Principle implies that the forward  $\Psi$  orbit of  $\zeta$  returns as  $\zeta_+$  after at most  $5q_m^2$  steps, moving away from  $(0, -1)$  at least  $q_m/2 - 2$  units and at most  $2q_m + 2$  steps. ♠

There is an entirely analogous result for the backwards return map. This analogous result holds for all but the first point.

## 24.6 Statement 1 of Lemma 24.3

We call a sequence of  $\Pi_A$  *equivalent-to-first* if it differs from the first sequence in only a finite number of positions. We call a sequence *equivalent-to-last* if it differs from the last sequence in a finite number of positions. As in the previous section, we transfer these notions to  $C_A$ .

**Lemma 24.9** *No sequence in  $\Pi_A$  is both equivalent-to-first and equivalent-to-last.*

**Proof:** This is immediate from the definitions. ♠

Let  $\zeta$  be a point in  $C'_A$  that is not equivalent-to-last. We will show that the forwards orbit of  $\zeta$  is unbounded. Let  $m = m(\kappa)$  be as in the proof of Lemma 24.8. Lemma 23.2 says that the portion of the orbit between  $\zeta$  and  $\zeta_+$  wanders at least  $q_m/5$  from the origin. Since we can achieve any initial sequence we like with iterated successors of  $\kappa$ , we can find iterated successors  $\kappa'$  of  $\kappa$  such that  $m(\kappa')$  is as large as we like. But this shows that the forwards orbit of  $\zeta$  is unbounded. Here we are using the fact that  $\lim_{m \rightarrow \infty} q_m = \infty$ . This shows that  $\zeta$  has an unbounded forwards orbit.

Essentially the same argument works for the backwards orbit of points that are not equivalent-to-first. This establishes Statement 1.

## 24.7 Statement 2 of Lemma 24.3

The successor map on  $\Pi_A$  is defined except on the last sequence  $\kappa$  of  $\Pi_A$ . Referring to the homeomorphism  $\phi_1$  given in Equation 6, we have

$$\phi_1(-1) = \kappa.$$

Thus, the point  $\phi_2(\kappa) \in C_A$  corresponding to  $\kappa$  is precisely  $\phi(-1)$ . By Lemma 24.8, the return map  $\rho_A : C'_A \rightarrow C'_A$  is defined on  $C'_A - \phi(-1)$ .

The map  $\phi_1$  conjugates the odometer map on  $\mathcal{Z}_A$  to the successor map on  $\Pi_A$ . Combining this fact with Lemma 24.8, we see that  $\phi^{-1}$  conjugates  $\rho_A$  to the restriction of the odometer map on  $\mathcal{Z}_A$ .

It remains to understand what happens to the forward orbit of  $x = \phi(-1)$ , in case  $x \in C'_A$ . The following result completes the proof of Statement 2.

**Lemma 24.10** *If  $x \in C'_A$  then the forward orbit of  $x$  does not return to  $C'_A$ .*

**Proof:** Suppose that the forward orbit of  $x$  returns to  $C'_A$  after  $N$  steps. Since outer billiards is a piecewise isometry, there is some open neighborhood  $U$  of  $x$  such that every point of  $C'_A \cap U$  returns to  $C'_A$  in at most  $N$  steps. But there is some uniformly small  $m$  such that every point  $\zeta \in C'_A - U$  differs from the last sequence  $\kappa$  at or before the  $m$ th spot. Lemma 24.8 says that such points return to  $C'_A$  in a uniformly bounded number of steps. In short, all points of  $C'_A$  return to  $C'_A$  in a uniformly bounded number of steps. But then all orbits in  $C'_A$  are bounded. This is a contradiction. ♠

### 24.8 Statement 3 of Lemma 24.3

Let  $\zeta \in C'_A$ . Let  $O_\zeta$  denote the portion of the forward outer billiards orbit of  $\zeta$  between  $\zeta$  and  $\rho_A(\zeta)$ . We mean to use the original outer billiards map  $\psi'$  here. Let  $m$  be such that

$$d(\phi^{-1}(\zeta), -1) = q_m^{-1}. \quad (328)$$

By definition  $\phi^{-1}(\zeta)$  and  $-1$  disagree by  $\mathbf{Z}/D_{m+1}$ , but agree in  $\mathbf{Z}/D_k$  for  $k = 1, \dots, m$ . In case  $m = 0$ , the points  $\phi^{-1}(\zeta)$  and  $-1$  already disagree in  $\mathbf{Z}/D_1$ . Let  $\kappa \in \Pi_A$  denote the sequence corresponding to  $\zeta$ .

**Lemma 24.11**  $\sigma(\kappa) = m$ ,

**Proof:** Let  $\lambda$  be the sequence corresponding to  $\phi(-1)$ . Then  $\lambda$  is the last sequence in the twirl order. The sequences  $\kappa$  and  $\lambda$  agree in positions  $k = 0, \dots, m - 1$  but then disagree in position  $m$ . When  $m = 0$ , the sequences already disagree in position 0. This is to say that  $m$  is the first index where  $\kappa$  disagrees with the last sequence in the twirl order. But then,  $\kappa$  and  $\kappa_+$  disagree in positions  $0, \dots, m$  and agree in position  $k$  for  $k > m$ . ♠

**Lemma 24.12**  $O_\zeta$  has excursion distance between  $q_m/2 - 4$  and  $2q_m + 20$ ,

**Proof:** Lemma 24.8 tells us that the  $\Psi$ -orbit of  $\zeta$  between  $\zeta$  and  $\rho_A(\zeta)$  wanders between  $q_m/2 - 4$  and  $2q_m + 4$  units from the origin. Here are interested in the full outer billiards  $O_\zeta$ . Since the  $\Psi$  orbit of  $\zeta$  between  $\zeta$  and  $\rho_\zeta$  is a subset of  $O_\zeta$ , the lower bound on the excursion distance is an immediate corollary of the lower bound from Lemma 24.8.

The upper bound follows from a simple geometric analysis of the Pinwheel Lemma. Looking at the proof of the Pinwheel Lemma, we see the following geometry. Starting at a point on  $\Xi$  that is  $R$  units from the origin, the  $\psi$ -orbit remains within  $2R + 8$  units of the origin before returning to  $\Xi$ . Essentially, the  $\psi$ -orbit follows an octagon once around the kite before returning, as shown in Figure 7.3. The constant of 10 takes care of the small deviations from the path in Figure 7.3, as discussed in §7.7 and §7.8.

Recall that  $\psi$  is the square of the outer billiards map  $\psi'$ . Since  $\psi'$  is always reflection in a vertex that is within 1 unit of the origin, we see that the entire  $\psi'$  orbit of interest to us is at most  $2R + 12$  units from the origin. Hence, the portion of the outer billiards orbit of interest to us wanders at most  $2(q_m + 4) + 12 = 2q_m + 20$  units from the origin. ♠

**Lemma 24.13**  $O_\zeta$  has length at most  $100q_m^3 + 100q_m^2$ .

**Proof:** We know that the  $\Psi$  orbit of  $\zeta$  between  $\zeta$  and  $\rho_A(\zeta)$  has length at most  $5q_m^2$ . Examining the proof of the Pinwheel Lemma, we see that the a point on  $\Xi$  that is  $R$  units from the origin returns to  $\Xi$  in less than  $10R$  iterates. Given our bound of  $R = 2q_m + 2$ , we see that the orbit  $O_\zeta$  is at most  $20q_m + 20$  times as long as the corresponding  $\Psi$ -orbit. This gives us a length bound of  $100q_m^3 + 100q_m^2$ . ♠

**Lemma 24.14**  $O_\zeta$  has length at least  $q_m^2/32 - q_m/4$ .

**Proof:** Some point in the  $\Psi$ -orbit of  $\zeta$  between  $\zeta$  and  $\rho_A(\zeta)$  lies at least  $q_m/2 - 4$  vertical units from the origin. Consecutive iterates in the  $\Psi$ -orbit have vertical distance at most 4 units apart. Hence, there are at least  $q_m/8 - 1$  points in the  $\Psi$ -orbit that are at least  $q_m/4$  horizontal units from the origin. Inspecting the Pinwheel Lemma, we see that the length of the  $\psi'$ -orbit between two such points is at least  $q_m/4$ . Hence,  $O_\zeta$  has length at least  $q_m^2/32 - q_m/4$ . ♠

This completes the proof of Statement 3.

## 24.9 Proof of Lemma 24.4

**Lemma 24.15** *No point of  $C_A - C_A^\#$  has a well-defined orbit.*

**Proof:** Call a sequence in  $\Pi_A$  *equivalent-to-trivial* if either differs from the 0 sequence by a finite number of terms, or it differs from the sequence  $\{d_i\}$  by a finite number of terms. The homeomorphism  $\phi_2$  bijects the equivalent-to-trivial points in  $\Pi_A$  to  $C_A - C_A^\#$ .

Suppose first that the superior sequence for  $A$  is not eventually monotone. In this case, an equivalent-to-trivial sequence is neither equivalent-to-first nor equivalent-to-last. See §24.6 for definitions of these terms.

Suppose  $\sigma \in C_A - C_A^\#$  has a well-defined orbit. Let  $\kappa$  be the equivalent-to-trivial sequence corresponding to  $\sigma$ . By Lemma 24.8 and the analogue for the backwards orbit, both directions of the orbit of  $\sigma$  return infinitely often to  $C_A - C_A^\#$ . If  $\kappa$  is eventually 0, then by the Odometer Principle  $\kappa$  is in the same sequence orbit as the 0 sequence  $\kappa_0$ . But the point in  $C_A$  corresponding to  $\kappa_0$  is exactly the vertex  $(0, -1)$ . This vertex does not have a well defined orbit. This is a contradiction. If  $\kappa$  is such that  $k_i = d_i$  for large  $i$ , then by the Odometer Principle,  $\kappa$  is in the same orbit as the sequence  $\{d_i\}$ . By Equation 275, the corresponding point in  $C_A$  is  $(2, -1)$ . One checks easily that the orbit of  $(2, -1)$  is not defined after the second iterate. Again we have a contradiction.

Now suppose the superior sequence is eventually monotone. We will treat the case when  $A - A_n$  is eventually positive. In this case,  $\{A_n\}$  is eventually monotone increasing. Suppose that  $\kappa$  is equivalent to the 0-sequence. We can iterate backwards a finite number of times until  $\sigma$  returns as the first point of  $C_A$ . Hence, without loss of generality, we can assume that  $\kappa$  is the first sequence in  $\Pi_A$ . But now we can iterate forwards indefinitely, and we will reach every equivalent-to-zero sequence by the Odometer Principle. Eventually we reach the 0 sequence and get the same contradiction as above. If  $\kappa$  is such that  $k_i = d_i$  for large  $i$ , we run the same argument backwards. ♠

**Lemma 24.16** *No point of  $C_A^\#$  has first coordinate in  $2\mathbf{Z}[A]$ .*

**Proof:** Let  $\{A_n\}$  be the superior sequence approximating  $A$ . We assume that  $A_n < A$  infinitely often. The other case has the same treatment. Suppose that

$$\alpha = (2MA + 2N, -1) \in C^\#. \quad (329)$$

By Equation 277, the set  $C_A^\#$  is invariant under the map  $(x, -1) \rightarrow (2-x, -1)$ . Indeed, the twist automorphism of  $\Pi$  induces this map on  $C_A$ . From this symmetry, we can assume that  $M > 0$ .

Let  $P\Gamma_k$  denote the pivot arc. We claim that  $(M, N)$  is not a vertex of  $P\Gamma_k$  for any  $k$ . Here is the proof. Suppose that  $(M, N) \in P\Gamma_k$  for some  $k$ . Then  $2AM + 2N$  is a finite sum of terms  $\lambda_j = |2Aq_j - p_j|$ , by Theorem 1.9. But such points all lie in  $C_A - C_A^\#$ . To avoid a contradiction,  $(M, N) \notin P\Gamma_k$  for any  $k$ . This completes the proof of the claim.

Let  $P\Gamma_k^+$  denote the forwards portion of  $P\Gamma_k$ . From the definition of the pivot points, the length of  $P\Gamma_k^+$  tends to  $\infty$  with  $k$ . Hence  $\{\Gamma_k^+\}$  and  $\{P\Gamma_k^+\}$  have the same Hausdorff limit. We can choose  $k$  so large enough so that  $P\Gamma_k^+$  contains a low vertex  $(M', N')$  to the right of  $(M, N)$ . So,  $P\Gamma_k^+$  connects  $(0, 0)$  to  $(M', N')$  and skips right over  $(M, N)$ .

Since  $\alpha \in C_A^\#$ , we can find a sequence of points  $\{\alpha_n\} \in C_A^\# - \mathbf{Z}[A]$  such that the first coordinate of  $\alpha_n - \alpha$  is positive. Let  $\zeta_n = \alpha_n - \alpha$ . Note that  $\zeta_n \notin 2\mathbf{Z}[A]$ . Let  $\widehat{\Gamma}(\zeta_n, A)$  be the whole arithmetic graph corresponding to  $\zeta_n$ . Let  $\gamma_n = \Gamma(\zeta_n, A)$  be the component containing  $(0, 0)$ . By the Rigidity Lemma, the sequences  $\{\Gamma(\zeta_n, A_n)\}$  and  $\{\Gamma_n\}$  have the same Hausdorff limit. Hence  $P\Gamma_k^+ \subset \gamma_n$  once  $n$  is large. In particular, some arc of  $\gamma_n$  connects  $(0, 0)$  to  $(M', N')$  and skips over  $(M, N)$ . Call this the *barrier arc*.

Since  $\alpha_n - \zeta_n = \alpha \in 2\mathbf{Z}[A]$ , there is another component  $\beta_n \subset \widehat{\Gamma}(\zeta_n)$  that tracks the orbit of  $\alpha_n$ . One of the vertices of  $\beta_n$  is exactly  $(M, N)$ . The component  $\beta_n$  is unbounded in both directions, because all defined orbits in  $C_A^\#$  are unbounded. On the other hand  $\beta_n$  is trapped beneath the barrier arc. It cannot escape out either end, and it cannot intersect the barrier arc, by the Embedding Theorem. But then  $\beta_n$  cannot be unbounded in either direction. This is a contradiction. ♠

Corollary 24.2 and Lemma 24.15 show that  $U_A \cap I \subset C_A^\#$ . Lemma 24.16 shows that  $C_A^\# \subset C'_A$ . Lemma 24.3 shows that  $C'_A \subset U_A \cap I$ . Putting all this together gives Equation 24.4.

## 24.10 Statement 4 of the Comet Theorem

We have already established the first part of Statement 4. Now we prove the second part.

By Statements 1 and 2 of the Comet Theorem, it suffices to consider pairs of points in  $C_A^\#$ . (This is where we use the truth of Statement 1.) It follows

immediately from Equation 15 that two points of  $C_A^\#$  lie on the same orbit only if their first coordinates differ by an element of  $2\mathbf{Z}[A]$ . Our goal is to prove the converse.

**Lemma 24.17** *All but at most 2 orbits in  $C_A^\#$  are erratic.*

**Proof:** By Lemma 24.3 and Lemma 24.8, and the backwards analogue of Lemma 24.8, all orbits in  $C_A^\#$  are erratic except for those corresponding to the equivalent-to-first sequences and the equivalent-to-last sequences. By the Odometer Principle, all the points in  $C_A^\#$  corresponding to equivalent-to-first sequences lie on the same orbit. Likewise, all the points in  $C_A^\#$  corresponding to equivalent-to-last sequences lie in the same orbit. These two orbits are the only ones which can fail to be erratic. ♠

**Lemma 24.18** *Suppose that two points in  $C_A^\#$  have first coordinates that differ by  $2\mathbf{Z}[A]$ . Suppose also that at least one of the points has an erratic orbit. Then the two points lie on the same orbit.*

**Proof:** One direction follows immediately from Equation 15. For the converse, suppose that our two points have first coordinates that differ by  $2\mathbf{Z}[A]$ . The first coordinates of our points do not lie in  $2\mathbf{Z}[A]$ , by Lemma 24.16. Hence, one and the same arithmetic graph  $\hat{\Gamma}$  contains components  $\gamma_1$  and  $\gamma_2$  that respectively track our two orbits.

Since both orbits are dense in  $C_A^\#$ , we know that both orbits are erratic in at least one direction. Suppose first that  $\gamma_1$  is erratic in both directions. Since  $\gamma_2$  is erratic in one direction, we can find a low vertex  $v$  of  $\gamma_1$  that is not a vertex of  $\gamma_2$ . Since  $\gamma_2$  is erratic in both directions, we can find vertices  $w_1$  and  $w_2$  of  $\gamma_1$ , lying to the left and to the right of  $v$ . But then the arc of  $\gamma_1$  starting at  $v$  is trapped beneath the arc of  $\gamma_2$  connecting  $w_1$  to  $w_2$ . This contradicts the Embedding Theorem. In short,  $\hat{\Gamma}$  is not big enough to contain both components. ♠

It only remains to deal with the case when both points lie on orbits that are only erratic in one direction..

**Lemma 24.19** *Suppose that two points in  $C_A^\#$  have first coordinates that differ by  $2\mathbf{Z}[A]$ . Suppose also that neither point lies on an erratic orbit. Then the two points lie on the same orbit.*

**Proof:** Let  $\alpha \in C_A^\#$  (respectively  $\beta$ ) be the unique point such that the forwards (respectively backwards) first return map to  $C_A^\#$  at  $\alpha$  (respectively  $\beta$ ) does not exist. There are exactly 2 one-sided erratic orbits.  $\alpha$  is one orbit and  $\beta$  is on the other. It suffices to prove that  $\alpha - \beta \notin 2\mathbf{Z}[A] \times \{0\}$ . We will suppose the contrary, and derive a contradiction. Suppose that  $\alpha - \beta = (2Am + 2n, 0)$  for some  $(m, n) \in \mathbf{Z}^2$ .

$\alpha$  is the last point in the twirl order and  $\beta$  is the first point. In terms of sequences,  $\alpha$  corresponds to the sequence  $\{\tilde{d}_i\}$  and  $\beta$  corresponds to the sequence  $\{\tilde{0}_i\}$ . Let  $\{\alpha_j\}$  be a sequence of points in  $C_A^\#$  converging to  $\alpha$ , chosen so that the corresponding orbit is erratic. Define  $\beta_j = \alpha_j + (\beta - \alpha)$ . Then  $\alpha_j - \beta_j = (2Am + 2n, 0)$ . By the case we have already considered,  $\beta_j$  lies in the same orbit as  $\alpha_j$ .

For  $j$  large, the sequence corresponding to  $\alpha_j$  matches the terms of the sequence for  $\alpha$  for many terms. Likewise, the sequence corresponding to  $\beta_j$  matches the terms of the sequence for  $\beta$  for many terms. Hence, these two sequences disagree for many terms. Given that our return dynamics to  $C_A^\#$  is conjugate to the odometer map on the sequence space, we have

$$2Am + 2n = \pi_1(\alpha_j - \beta_j) = \sum_{i=0}^{N_j} a_{ji} \lambda_i; \quad |a_{ji}| \leq d_i. \quad (330)$$

Here  $N_j \rightarrow \infty$  as  $j \rightarrow \infty$ , and  $\pi_1$  denotes projection onto the first coordinate.

Let  $M$  be the map from Equation 19. We have

$$M(m, n) = \sum_{i=0}^{N_j} b_{ji} M(V_i); \quad |b_{ji}| \leq d_i. \quad (331)$$

Here  $b_{ji} = \pm a_{ji}$ , depending on the sign of  $A_i - A$ . Since  $A$  is irrational,  $M$  is injective. Therefore, setting  $N = N_j$  for ease of notation, we have

$$(m, n) = \sum_{i=0}^N b_{ji} V_i = b_{N_i} V_N + \sum_{i=0}^{N-1} b_{ji} V_i. \quad (332)$$

Looking at the second coordinates, we see that

$$q_N - \sum_{i=0}^{N-1} d_i q_i \leq \left| b_{N_i} q_N - \sum_{i=0}^{N-1} b_{ji} q_i \right| = |n|. \quad (333)$$

However, it follows fairly easily from Equation 276 that the left hand side tends to  $\infty$  as  $N_j \rightarrow \infty$ . This contradiction finishes the proof. ♠

## 25 Dynamical Consequences

In this chapter we discuss some dynamical consequences of the Comet Theorem.

### 25.1 Minimality and Homogeneity

Now we deduce some consequences of the Comet Theorem. Let  $U_A$  denote the set of unbounded special orbits. Since every orbit in  $U_A$  intersects  $C_A^\#$ , it suffices to prove that every point of  $C_A^\#$  lies on an orbit that is either forwards dense in  $U_A$  or backwards dense or both.

Let  $\zeta \in C_A^\#$  be our point. By the Comet Theorem, the orbit of  $\zeta$  is either forwards dense in  $C_A^\#$ , or backwards dense in  $C_A^\#$ , or both. Assume that  $\zeta$  lies on an orbit that is forwards dense in  $C_A^\#$ . The case of backwards dense orbits has a similar treatment.

Let  $\beta \in U_A$  be some other point. Some point  $\alpha \in C_A^\#$  lies in the orbit of  $\beta$ . Hence,  $(\psi')^k(\alpha) = \beta$  for some  $k$ . Here  $\psi'$  is the outer billiards map. But  $(\psi')^k$  is a piecewise isometry. Hence,  $(\psi')^k$  maps small intervals centered at  $\alpha$  isometrically to small intervals centered at  $\beta$ . The forwards orbit of  $\zeta$  enters any interval about  $\alpha$  infinitely often. Hence, the forwards orbit of  $\zeta$  enters every interval about  $\beta$  infinitely often.

Say that a subset  $S \subset \mathbf{R}^2$  is *locally homogeneous* if every two points of  $S$  have arbitrarily small neighborhoods that are translation equivalent. Note that the points themselves need not sit in the same positions within these sets.

**Lemma 25.1** *For any irrational  $A$ , the set  $U_A$  is locally homogeneous.*

**Proof:** For any  $p \in U_A$ , there is some integer  $k$  such that  $(\psi')^k(p) \in C_A^\#$ . Here  $\psi'$  is the outer billiards map. But  $\psi^k$  is a local isometry. Hence, there are arbitrarily small neighborhoods of  $p$  that are isometric to neighborhoods of points in  $C_A^\#$ .

Hence, it suffices to prove that  $C_A^\#$  is locally homogeneous. Let  $\{d_k\}$  denote the renormalization sequence. The set  $C_A$  breaks into  $d_0 + 1$  isometric copies of a smaller Cantor set. Each of these breaks into  $d_1 + 1$  isometric copies of still smaller Cantor sets. And so on. From this we see that both  $C_A$  and  $C_A^\#$  are locally homogeneous. ♠

## 25.2 Tree Interpretation of the Dynamics

Let  $A$  be an irrational kite parameter. We can illustrate the return dynamics to  $C_A^\#$  using infinite trees. The main point here is that the dynamics is conjugate to an odometer. The conjugacy is given by the map  $\phi : \mathcal{Z}_A \rightarrow C_A$  from the Comet Theorem. Our pictures encode the structure of  $\phi$  graphically.

We think of  $C_A$  as the ends of a tree  $T_A$ . We label  $T_A$  according to the sequence of signs  $\{A - A_n\}$ . Since  $A - A_0$  is negative, we label the level 1 vertices  $0, \dots, d_0$  from right to left. Each level 1 vertex has  $d_1$  downward vertices. We label all these vertices from left to right if  $A - A_1 > 0$  and from right to left if  $A - A_1$  is negative. And so on. This business of switching left and right according to the sign of  $A - A_k$  corresponds precisely to our method of identification in Equations 6 and 7. Figure 25.1 shows the example for the renormalization sequence  $\{1, 3, 2\}$  and the sign sequence  $-, +, -$ .

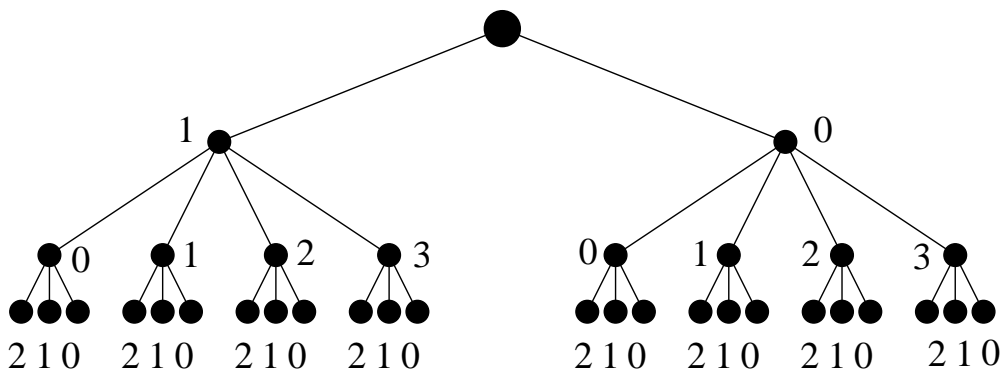


Figure 25.1: Tree Labelling

We have the return map

$$\rho_A : C_A^\# - \phi(-1) \rightarrow C_A^\# - \phi(-1),$$

and this map is conjugate to the restriction of the odometer on  $\mathcal{Z}_A$ . Accordingly, we can extend  $\rho_A$  to all of  $C_A$ , even though the extension no longer describes outer billiards dynamics on the extra points. Nonetheless, it is convenient to have this extension.

To see what  $\rho_A$  does, we write the code for a given end. Then we add 1, carrying to the right. Referring to our example above, we have  $000\dots \rightarrow 100\dots$  and  $130\dots \rightarrow 001\dots$ . This map is exactly what is called an odometer.

### 25.3 Periodic Orbits

One might wonder about the other orbits in the interval  $I$ . First of all, we have the following result.

**Theorem 25.2** *Any defined orbit in  $I - C_A$  is periodic. There is a uniform bound on the period, depending only on the distance from the point to  $C_A$ .*

**Proof:** The Comet Theorem combines with the Dichotomy Theorem to prove any defined orbit in  $I - C_A$  is periodic. The period bound comes from taking a limit of the Period Theorem as  $n \rightarrow \infty$  in our rational approximating sequence. In other words, if this result was false, then we could contradict the Period Theorem using our Continuity Principle. ♠

In the next chapter we will prove that  $C_A$  has length 0. See Lemma 26.1. By the local homogeneity,  $U_A$  also has length 0. Hence, by the Dichotomy Theorem, almost all special orbits are periodic.

**A Conjectural Picture:** If we knew Conjecture 23.11, we could give a very nice account of what happens. We now describe this conjectural picture.

We can naturally identify  $C_A$  with the ends of an infinite directed tree  $T_A$ . Using the homeomorphism  $\phi : \mathcal{Z}_A \rightarrow C_A$ , we can formally extend the return map on  $C_A^\# - \phi(-1)$  to all of  $C_A$ , even though the extended return map does not correspond to the outer billiards dynamics on the extra points. This is exactly what we did in §25.2 above.

The extended return map to  $C_A$  induced by an automorphism

$$\Theta_A : T_A \rightarrow T_A \tag{334}$$

as discussed in §25.2. The complementary open intervals in  $I - C_A$  – the *gaps* – are naturally in bijection with the forward cones of  $T_A$ .

**Conjecture 25.3** *The outer billiards map is entirely defined on a gap. The return map to  $I - C_A$  permutes the gaps according to the action of  $\Theta_A$  on the forward cones of  $T_A$ .*

## 25.4 Proper Return Models and Cusped Solenoids

Here we will describe the sense in which the Comet Theorem allows us to combinatorially model the dynamics on  $U_A$ . The results in this section are really just a repackaging of some of the statements of the Comet Theorem.

Let  $X$  be an unbounded metric space and let  $f : X \rightarrow X$  be a bijection. We assume that  $f^2$  moves points by a small amount. That is, there is a universal constant  $C$  such that

$$d(x, f^2(x)) < C \quad \forall x \in X. \quad (335)$$

The example we have in mind, of course, is the outer billiards map

$$\psi' : U_A \rightarrow U_A. \quad (336)$$

The square map  $\psi$  moves points by at most 4 units.

We say that a compact subset  $X_0 \subset X$  is a *proper section* for  $f$  if for every  $N$  there is some  $N'$  such that  $d(x, X_0) < N$  implies that  $f^k(x) \in X_0$  for some  $|k| < N'$ . In particular, every orbit of  $f$  intersects  $X_0$ . This condition is just the abstract version of Statement 1 of the Comet Theorem. Informally, all the orbits either head directly to  $X_0$  or directly away from  $X_0$ .

Let  $f_0 : X_0 \rightarrow X_0$  be the first return map. This is a slight abuse of notation, because  $f_0$  might not be defined on all points of  $X_0$ . Some points might exit  $X_0$  and never return. We define two functions  $e_1, e_2 : X_0 \rightarrow (0, \infty]$ . The function  $e_1(x)$  is the maximum distance the forward orbit of  $x$  gets away from  $X_0$  before returning as  $f_0(x)$ . The function  $e_2(x)$  is the length of this same portion of the orbit. If  $f_0$  is not defined on  $x$  then obviously  $e_2(x) = \infty$ . The proper section condition guarantees that  $e_1(x) = \infty$  as well.

The condition that  $X_0$  is a proper section guarantees that  $e_1$  and  $e_2$  are proper functions of each other. That is, if  $\{x_n\}$  is a sequence of points in  $X_0$ , then  $e_1(x) \rightarrow \infty$  if and only if  $e_2(x) \rightarrow \infty$ . This observation includes the statement that  $e_1(x) = \infty$  iff  $e_2(x) = \infty$  iff  $f_0$  is not defined on  $x_0$ . For the purposes of getting a rough qualitative picture of the orbits, we just consider the function  $e_1$ . We set  $e = e_1$ , and call  $e$  the *excursion function*.

Suppose now that  $f' : X' \rightarrow X'$  is another bijection, and  $X'_0$  is a proper section. Let  $e' : X'_0 \rightarrow (0, \infty]$  denote the excursion function for this system. We say that  $(X, X_0, f)$  is *properly equivalent* to  $(X', X'_0, f')$  if there is a homeomorphism  $\phi : X \rightarrow X'$  such that

- $\phi$  conjugates  $f_0$  to  $f'_0$ .

- $e' \circ \phi$  and  $e$  are proper functions of each other on  $X_0$ .

These conditions guarantee that  $\phi$  carries the points where  $f_0$  is not defined to the points where  $f'_0$  is not defined.

The notion of proper equivalence turns out to be a tiny bit too strong for our purposes. We say that  $(X, X_0, f)$  and  $(X', X'_0, f')$  are *essentially properly equivalent* if  $\phi$  has all the above properties but is only defined on the complement of a finite number of orbits of  $X_0$ . In this case, the inverse map will have the same property: It will be well defined on all but a finite number of orbits of  $X'_0$ . In other words, an essential proper equivalence is a proper equivalence provided that we first delete a finite number of orbits from our spaces. We call  $(X, X_0, f)$  an *essentially proper model* for  $(X', X'_0, f')$ .

Statement 1 of the Comet Theorem says that  $C_A^\#$  is a proper section for the map in Equation 336. Now we can describe our proper models for the triple  $(U_A, C_A^\#, \psi')$ . Statements 2 and 3 in particular describe the excursion function up to a b-lipschitz constant. Here we convert this information into a concrete essentially proper model for this dynamics.

Let  $\mathcal{Z}_A$  denote the metric abelian group from the Comet Theorem. For convenience, we recall the definition of the metric  $d$  here.  $d(x, y) = q_n^{-1}$ , where  $n$  is the smallest index such that  $[x]$  and  $[y]$  disagree in  $\mathbf{Z}/D_n$ . Here  $\{p_n/q_n\}$  is the superior sequence approximating  $A$ .

We denote the odometer map on  $\mathcal{Z}_A$  by  $f_0$ . That is,  $f_0(x) = x + 1$ . Topologically, the *solenoid* based on  $\mathcal{Z}_A$  is defined as the mapping cylinder

$$\mathcal{S}_A = \mathcal{Z}_A \times [0, 1] / \sim; \quad (x, 1) \sim (x + 1, 0). \quad (337)$$

This is a compact metric space.

We now modify this space a bit. First of all, we remove the point

$$(-1, 1/2)$$

from  $\mathcal{S}_A$ . This deleted point, our cusp, lies halfway between  $(-1, 0)$  and  $(0, 0)$ . We now change the metric on our space by declaring the length of the segment between  $(x, 0)$  and  $(x, 1)$  to be

$$\frac{1}{d(x, -1)}$$

Metrically, we simply rescale the length element on each interval by the appropriate amounts. We call the resulting space  $\mathcal{C}_A$ . We call  $\mathcal{C}_A$  the *cusped solenoid* based on  $A$ .

We define  $f : \mathcal{C}_A \rightarrow \mathcal{C}_A$  to be the map such that

$$f(x, t) = \left( x, \frac{t}{d(x, -1)} \right) \quad (338)$$

From the way we have scaled the distances,  $f$  maps each point by 1 unit. Indeed, some readers will recognize  $f$  as the time-one map of the geodesic flow on  $\mathcal{C}_A$ . The original set  $\mathcal{Z}_A$  is a proper section for the map, and the return map is precisely  $f_0$ . Put another way,  $f$  is a suspension flow over  $f_0$ . Note that  $f$  also depends on  $A$ , but we suppress this from our notation.

**Theorem 25.4** *The triple  $(\mathcal{C}_A, \mathcal{Z}_A, f)$  is an essentially proper model for  $(U_A, C_A^\#, \psi')$ .*

**Proof:** This is just a repackaging (and weakening) of Statements 2 and 3 of the Comet Theorem. ♠

**Remarks:**

- (i) Our model forgets the linear ordering on  $C_A^\#$  that comes from its inclusion in  $I$ , but one can recover this from the discussion in §25.2.
- (ii) In a certain sense, the triple  $(\mathcal{C}_A, \mathcal{Z}_A, f)$  provides a *bi-lipschitz model* for the nature of the unboundedness of the orbits in  $U_A$ . However, it would be misleading to call our model an actual bi-lipschitz model for the dynamics on  $U_A$  because we are not saying much about what happens to the orbits in the two systems after they leave their proper section. For instance, the excursion times could be wildly different from each other, even though they are proper functions of each other.

Here is a universality result.

**Theorem 25.5** *The time-one map of the geodesic flow on any cusped solenoid serves as an essentially proper model for the dynamics of the special unbounded orbits relative to uncountably many different parameters.*

**Proof:** Up to a proper change of the excursion function, our model only depends on the renormalization sequence, and there are uncountably many parameters realizing any renormalization sequence. ♠

## 25.5 Equivalence and Universal Behavior

To each parameter  $A$ , we associate the renormalization sequence  $\{d_n\}$ . We then associate the sequence  $\{D_n\}$ , where

$$D_n = \prod_{i=0}^{n-1} (d_i + 1). \quad (339)$$

We call  $A$  and  $A'$  *broadly equivalent* iff for each  $m$  there is some  $n$  such that  $D_m$  divides  $D'_n$  and  $D'_m$  divides  $D_n$ . Each broad equivalence class has uncountably many members.

**Lemma 25.6** *If  $A$  and  $A'$  are broadly equivalent then there is a homeomorphism from  $\mathcal{Z}_A$  to  $\mathcal{Z}_{A'}$  that conjugates the one odometer to the other.*

**Proof:** Each element of  $\mathcal{Z}_A$  is a compatible sequence  $\{a_m\}$  with  $a_m \in \mathbf{Z}/D_m$ . Using the divisibility relation, this element determines a corresponding sequence  $\{a'_m\}$ . Here  $a'_m$  is the image of  $a_n$  under the factor map  $\mathbf{Z}/D_n \rightarrow \mathbf{Z}/D'_m$ , where  $n$  is such that  $D'_m$  divides  $D_n$ . One checks easily that this map is well defined and determines the desired homeomorphism. ♠

**Theorem 25.7** *If  $A$  and  $B$  are broadly equivalent then there is an essentially proper equivalence between  $(U_A, C_A^\#, \psi'_A)$  and  $(U_B, C_B^\#, \psi'_B)$ . In particular, the return maps to  $C_A$  and  $C_B$  are topologically conjugate modulo countable sets.*

**Proof:** The homeomorphism from  $\mathcal{Z}_A$  to  $\mathcal{Z}_B$  maps  $-1$  to  $-1$ . By construction, this homeomorphism sets up a proper equivalence between  $(C_A, \mathcal{Z}_A, f_A)$  and  $(C_B, \mathcal{Z}_B, f_B)$ . This result now follows from Theorem 25.4. ♠

One might wonder about the nature of the topological equivalence between the return maps to  $C_A^\#$  and  $C_B^\#$ . One can reconstruct the conjugacy from the tree labellings given in §25.2. The conjugacy is well defined for all points of  $C_A$  and  $C_B$ , but we typically have to ignore the countable sets of points on which the relevant return maps are not defined. This accounts for the precise statement of our theorem above.

Let  $\mathcal{Z}$  denote the inverse limit over all finite cyclic groups. The map  $x \rightarrow x + 1$  is defined on  $\mathcal{Z}$ . This dynamical system is called the *universal odometer*. Sometimes  $\mathcal{Z}$  is called the *profinite completion* of  $\mathbf{Z}$ .

We call  $A$  *universal* if every  $k \in \mathbf{N}$  divides some  $D_n$  in the sequence. If  $A$  is universal, then there is a group isomorphism from  $\mathcal{Z}$  to  $\mathcal{Z}_A$  that respects the odometer maps. In short, when  $A$  is universal,  $\mathcal{Z}_A$  is the universal odometer. See [H, §5] for a proof of this fact – stated in slightly different terms – and for a detailed discussion of the universal odometer.

**Lemma 25.8** *Almost every parameter is universal.*

**Proof:** A sufficient condition for a parameter to be universal is that every integer appears in the renormalization sequence. We can express the fact that a certain number appears in the renormalization sequence as a statement that a certain combination appears in the continued fraction expansion of  $A$ . Geometrically, as one drops a geodesic down from  $\infty$  to  $A$ , the appearance of a certain pattern of geodesics in the Farey graph forces a certain number in the renormalization sequence. As is well known, the continued fraction expansion for almost every number in  $(0, 1)$  contains every finite string of digits. ♠

**Theorem 25.9** *For almost every  $A \in (0, 1)$ , the triple  $(U_A, C_A^\#, \psi')$  is properly modelled by the time-one map of the geodesic flow on the universal cusped solenoid. In particular, the return map to  $C_A^\#$  is topologically conjugate to the universal odometer, modulo a countable set.*

**Proof:** This is an immediate consequence of the previous result and Theorem 25.4. ♠

One might wonder if there is a concrete parameter that exhibits this universal behavior. Here we give an example. Let  $A$  be the parameter whose inferior sequence satisfies

$$\frac{1}{1} \leftarrow \frac{5}{7} \leftarrow \frac{51}{71} \leftarrow \frac{719}{1001} \dots; \quad r_{n+1} = (4n + 2)r_n + r_{n-1}$$

$r$  stands for either  $p$  or  $q$ . All terms are superior. The renormalization sequence is 3, 5, 7, 9... Hence

$$D_0 = 4; \quad D_1 = 4 \times 6; \quad D_2 = 4 \times 6 \times 8 \dots$$

One can see easily in this example that  $\Sigma(A) = \mathbf{N}$ . Hence  $A$  is universal. Let  $E = A + 2$ . It seems that  $E = e$ , the base of the natural log. We didn't work out a proof, but this should follow from the famous continued fraction expansion  $e = [2; 1, 4, 1, 1, 6, 1, 1, 8, \dots]$ . In short,  $e - 2$  is universal.

## 25.6 Some other Equivalence Relations

Call  $A$  and  $B$  *narrowly equivalent* if they have the same renormalization sequence and if the sign of  $A - A_j$  is the same as the sign of  $B - B_j$  for all  $j$ . Here  $\{A_j\}$  and  $\{B_j\}$  are the superior sequences approximating  $A$  and  $B$  respectively. Referring to Equation 7, the definition of  $\tilde{k}_j$  relative to the narrowly equivalent parameters is the same for every index. Each narrow equivalence class again has uncountably many members.

**Theorem 25.10** *If  $A$  and  $B$  are narrowly equivalent then there is an order-preserving homeomorphism from  $I$  to  $I$  that conjugates the return map on  $C_A^\#$  to the return map on  $C_B^\#$ . This map is a proper equivalence from  $(U_A, C_A^\#, \psi'_A)$  to  $(U_B, C_B^\#, \psi'_B)$  to*

**Proof:** The two spaces  $\Pi_A$  and  $\Pi_B$  are exactly the same, and the extended twirl orders on the (equivalence classes) of these spaces are the same. Thus, the successor maps on the two spaces are identical. The map  $h = \phi'_2 \circ \phi_2^{-1}$  is a homeomorphism from  $C_A$  to  $C_B$  that carries  $C_A^\#$  and  $C_B^\#$  and conjugates the one return dynamics to the other. By construction,  $h$  preserves the linear ordering on  $I$ , and we can extend  $h$  to the gaps of  $I - C_A$  in the obvious way. By construction, this map carries  $\phi_A(-1)$  to  $\phi_B(-1)$  and is continuous. Hence, it is a proper equivalence in the sense discussed above. ♠

The *first renormalization* of the odometer map  $x \rightarrow x + 1$  on the inverse system

$$\dots \rightarrow \mathbf{Z}/D_3 \rightarrow \mathbf{Z}/D_2 \rightarrow \mathbf{Z}/D_1 \quad (340)$$

is the  $D_1$ st power of the map. This corresponds to the map  $x \rightarrow x + 1$  on the inverse system

$$\dots \rightarrow \mathbf{Z}/D'_3 \rightarrow \mathbf{Z}/D'_2 \rightarrow \mathbf{Z}/D'_1; \quad D'_n = D_{n+1}/D_1. \quad (341)$$

As in the Comet Theorem, each  $D_n$  divides  $D_{n+1}$  for all  $n$ , so the construction makes sense. In terms of the symbolic dynamics on the sequence space  $\Pi$ , the renormalization consists of the first return map to the subspace

$$\Pi' = \{\kappa \in \Pi \mid k_0 = 0.\} \quad (342)$$

In terms of the dynamics on  $C_A$ , the first renormalization is the first return map to the Cantor subset corresponding to  $\Pi'$ . The *second renormalization* is the first renormalization of the first renormalization. And so on.

Let  $\Gamma_2 \subset SL_2(\mathbf{Z})$  denote the subgroup of matrices congruent to the identity mod 2. Then  $\Gamma_2$  acts on  $\mathbf{Q} \cup \infty$  by linear fractional transformations. The action preserves the parity of the rationals. Even though  $\Gamma_2$  does not preserve the parameter interval  $(0, 1)$ , it still makes sense to say that  $A \sim B$  mod  $\Gamma_2$ . This is to say that

$$B = \frac{aA + b}{cA + d}; \quad \begin{bmatrix} a & b \\ c & d \end{bmatrix} \in \Gamma_2. \quad (343)$$

Here we recall our construction of the inferior sequence for  $A$ . Our construction is based on the graph in the hyperbolic plane obtained from the Farey graph by deleting the edges connecting even rationals to each other. The result is the 1-skeleton of a tiling by ideal squares.  $\Gamma_2$  preserves this tiling. We construct the inferior sequence by dropping a vertical geodesic down to  $A$  and recording the sequence of ideal squares the geodesic enters as it limits to  $A$ . From this description, we see that the renormalization and sign sequences for  $A$  and  $B$  are eventually the same. This gives us the following result.

**Corollary 25.11** *Suppose that  $A$  and  $B$  are equivalent under  $\Gamma_2$ . Then the return maps to  $C_A^\#$  and  $C_B^\#$  have a common renormalization. The conjugacy between the one renormalization to the other is implemented by a homeomorphism that preserves the order on the interval  $I$ .*

## 26 Geometric Consequences

### 26.1 Hausdorff Dimension

In this chapter we study the structure of  $C_A$ .

We first review some basic properties of the Hausdorff dimension, including its definition.

**Basic Definition:** Given an interval  $J$ , let  $|J|$  denote its length. Let  $I = [0, 2] \times \{-1\}$  be our usual interval. Given a subset  $S \subset I$ , and  $s \in [0, 1]$ , and some  $\delta > 0$ , we define

$$\mu(S, s, \delta) = \inf \sum |J_n|^s \quad (344)$$

The infimum is taken over all countable covers of  $S$  by intervals  $\{J_n\}$  such that  $\text{diam}(J_n) < \delta$ . Next, we define

$$\mu(S, s) = \lim_{\delta \rightarrow 0} \mu(S, s, \delta) \in [0, \infty]. \quad (345)$$

This limit exists because  $\mu(S, s, \delta)$  is a monotone function of  $\delta$ . Note that  $\mu(S, 1) < \infty$  because  $I$  has finite total length. Finally,

$$\dim(S) = \inf \{s \mid \mu(S, s) < \infty\}. \quad (346)$$

The number  $\dim(S)$  is called the *Hausdorff dimension* of  $S$ .

**Bi-Lipschitz Invariance:** Let  $f : \mathbf{R} \rightarrow \mathbf{R}$  be a map.  $f$  is called *K-bi-lipschitz* if

$$K^{-1}\|x - y\| < \|\phi(x) - \phi(y)\| < K\|x - y\| \quad (347)$$

$f$  is called *bi-lipschitz* if it is *K-bi-lipschitz* for some  $K$ . It follows easily from the definitions that  $\dim(S) = \dim(S')$  if  $f(S) = S'$  for some bi-lipschitz function  $f$ .

**Borel Slicing Property:** Let  $S \subset [0, 1]^2$  be a Borel subset. Let  $S_A$  denote the intersection of  $S$  with the line  $\{y = A\}$ . Let  $f(A) = \dim(S_A)$ . It is known that  $f$  is a Borel measurable function. See [MM]. In our application, we shall apply this criterion to the set  $C$  from Equation 11. This is a very explicit example of a Borel measurable set.

## 26.2 Ubiquity of Periodic Orbits

**Lemma 26.1**  $C_A$  has length 0.

**Proof:** Let  $\lambda_n = |Aq_n - p_n|$ , as in Equation 275. We define

$$G_n = \sum_{k=n+1}^{\infty} 2\lambda_k d_k. \quad (348)$$

Then

$$C_A \subset \sum_{\kappa \in \Pi_n} (I_n + X(\kappa)). \quad (349)$$

Here  $I_n$  is the interval with endpoints  $(0, 1)$  and  $(G_n, 1)$ . In other words,  $C_A$  is contained in  $D_n$  translates of an interval of length  $G_n$ . We just need to prove that  $D_n G_n \rightarrow 0$ . It suffices to prove this when  $n$  is even. By Equation 276,

$$D_n < \epsilon^{-n} q_n; \quad \epsilon = \sqrt{5/4}. \quad (350)$$

By Equation 275 we have

$$G_n < 2 \sum_{k=n+1}^{\infty} q_k^{-1} < 2q_n^{-1} \sum_{k=1}^{\infty} 2^{-k} < 2q_n^{-1}. \quad (351)$$

Here we have used the trivial bound that  $q_m/q_n < 2^{n-m}$  when  $m > n$ . Therefore

$$D_n G_n < 2\epsilon^{-n}. \quad (352)$$

This completes the proof. ♠

**Theorem 26.2** *Relative to any irrational parameter, almost every point on  $\mathbf{R} \times \mathbf{Z}_{\text{odd}}$  has a periodic outer billiards orbit.*

**Proof:** Since  $U_A$  is locally homogeneous and  $C_A^\#$  has length 0, the set  $U_A$  has length 0. The point here is that  $U_A$  cannot have any points of Lebesgue density. There are only countably many points in  $\mathbf{R} \times \mathbf{Z}_{\text{odd}}$  with undefined orbits, and the rest are periodic by the Dichotomy Theorem. ♠

### 26.3 A Dimension Formula

Now we prove the following result.

**Theorem 26.3** *Let  $A$  be an irrational parameter. Let  $\{p_n/q_n\}$  be the superior sequence associated to  $A$ . Suppose that  $q_{n+1} < Cq_n$  for some constant  $C$  that is independent of  $n$ . Then*

$$u(A) = \frac{D}{Q}; \quad D = \lim_{n \rightarrow \infty} \frac{\log(D_n)}{n}; \quad Q = \lim_{n \rightarrow \infty} \frac{\log(q_n)}{n},$$

*provided that these limit exist. Limits are taken with respect to the superior terms.*

We call  $A$  *tame* if  $A$  satisfies the hypotheses of Theorem 26.3. We leave it as an exercise to the interested reader to show that all quadratic irrational parameters are tame.

**Lemma 26.4** *Suppose  $A$  is a tame parameter. Let  $\{p_n/q_n\}$  be the associated superior sequence. Then  $\lambda_n \in [C_1, C_2]q_n^{-1}$  for positive constants  $C_1, C_2$ .*

**Proof:** For tame parameters, the renormalization sequence  $\{d_n\}$  is bounded. We have

$$\lambda_n = q_n|A - A_n| < 2d_n^{-1}q_n^{-1} < C_2q_n^{-1}$$

by Lemma 18.4. For the lower bound note first that  $\lambda_{n+1} < \lambda'_{n+1} < \lambda_n$ , by Equation 277. By the triangle inequality

$$|A - A_n| + |A - A_{n+1}| \geq |A_n - A_{n+1}| \geq \frac{2}{q_n q_{n+1}}.$$

Hence

$$\begin{aligned} 2\lambda_n &> \lambda_n + \lambda_{n+1} = q_n|A - A_n| + q_{n+1}|A - A_{n+1}| > \\ & q_n(|A - A_n| + |A - A_{n+1}|) \geq 2q_{n+1}^{-1} \geq 2C_1q_n^{-1}. \end{aligned}$$

This gives the lower bound. ♠

Now we derive our dimension formula for tame parameters  $A$ . The constants  $C_1, C_2, \dots$  denote positive constants that depend on  $A$ . Let  $\mathcal{C}_n$  be the covering constructed in the proof of Lemma 26.1. The intervals in  $\mathcal{C}_n$  are

pairwise disjoint and all have the same length. Each interval of  $\mathcal{C}_n$  contains  $(d_n + 1)$  evenly and maximally spaced intervals of  $\mathcal{C}_{n+1}$ . From these properties, it suffices to use the covers  $\mathcal{C}_n$  to compute  $u(A)$ .

There are  $D_n$  intervals in  $\mathcal{C}_n$ , all having length  $G_n$ . Choose any  $\epsilon > 0$ . For  $n$  large, we have

$$D_n \in \left( \exp(n(D - \epsilon)), \exp(n(D + \epsilon)) \right) \quad (353)$$

We have

$$G_n = 2\lambda_{n+1}^* \in [2\lambda_{n+1}, \lambda_n] \in [C_1 q_{n+1}^{-1}, C_2 q_n^{-1}] \in [C_3, C_2] q_n^{-1},$$

by the preceding lemma. Hence

$$G_n \in \left( \exp(-n(Q + \epsilon)), \exp(-n(Q - \epsilon)) \right). \quad (354)$$

From these estimates, we get  $u(A) \in [(D/Q) - \epsilon, (D/Q) + \epsilon]$ . But  $\epsilon$  is arbitrary. This establishes our dimension formula.

## 26.4 Modularity

The level 2 congruence subgroup  $\Gamma_2$  acts on  $\mathbf{R} \cup \infty$  by linear fractional transformations. To say that  $A$  and  $A'$  are in the same  $\Gamma_2$  orbit is to say that

$$A' = \frac{aA + b}{cA + d}; \quad \begin{bmatrix} a & b \\ c & d \end{bmatrix} \in \Gamma_2. \quad (355)$$

**Lemma 26.5** *If  $A$  and  $A'$  belong to the same  $\Gamma_2$ -orbit, then  $C_A$  and  $C_{A'}$  are asymptotically similar. In particular,  $\dim(C_A) = \dim(C_{A'}^\#)$ .*

**Proof:** Recall that  $C_A$  is defined by the formula

$$C_A = \bigcup_{\kappa \in \Pi} (X(\kappa), 1); \quad X(\kappa) = \sum_{i=0}^{\infty} 2k_i \lambda_i; \quad \lambda_i = |Aq_i - p_i|. \quad (356)$$

We say that two sequences  $\{\lambda_i\}$  and  $\{\lambda'_i\}$  are *asymptotically proportional* if there is an integer  $m$  and a constant  $C$  such that

$$\lim_{k \rightarrow \infty} \frac{\lambda'_k}{\lambda_{k+m}} = C \neq 0. \quad (357)$$

The integer  $m$  just serves to shift the terms appropriately.

**Lemma 26.6** *Suppose that  $A$  and  $A'$  are  $\Gamma_2$ -equivalent. Then the corresponding sequences  $\{\lambda_k\}$  and  $\{\lambda'_k\}$  are asymptotically proportional.*

**Proof:** Let  $T \in \Gamma$  be such that  $T(A) = A'$ , as in Equation 355. Let  $T'(A)$  be the derivative of  $T$  at  $A$ . Our construction of the inferior sequence is such that  $T(A_{m+k}) = A'_k$  for some  $m$  and all sufficiently large  $k$ . Therefore

$$\lim_{k \rightarrow \infty} \frac{q'_k \lambda'_k}{q_{k+m} \lambda_{k+m}} = \lim_{k \rightarrow \infty} \frac{\|T(A) - T(A_k)\|}{\|A_{k+m} - A\|} = \|T'(A)\|. \quad (358)$$

We compute

$$T(p/q) = \frac{ap + bq}{cp + dq}.$$

It is an exercise in modular arithmetic to show that the fraction on the right is already in lowest terms. Therefore

$$\lim_{k \rightarrow \infty} \frac{q'_k}{q_{k+m}} = \lim_{k \rightarrow \infty} \frac{cp_{m+k} + dq_{m+k}}{q_{k+m}} = cA + d. \quad (359)$$

Combining Equations 358 and 359, we get

$$\lim_{k \rightarrow \infty} \frac{\lambda'_k}{\lambda_{k+m}} = \frac{\|T'(A)\|}{cA + d} \quad (360)$$

This completes the proof. ♠

**Corollary 26.7** *If  $A$  and  $A'$  are  $\Gamma_2$ -equivalent, then  $C_A$  and  $C'_A$  are asymptotically similar.*

**Proof:** If  $A$  and  $A'$  are  $\Gamma_2$ -equivalent, then we have an obvious map

$$\sum_{i=k_0}^{\infty} k_{m+i} \lambda_{m+i} \rightarrow \sum_{i=k_0}^{\infty} k_i \lambda'_i, \quad (361)$$

which is defined if  $k_0$  is taken large enough. This map makes sense because the corresponding sequence spaces are the same. Given the asymptotic proportionality of the sequences, the map above is  $f(k_0)$ -bi-lipschitz. Here  $f(k_0)$  is a function that converges to 1 as  $k_0$  to  $\infty$ . ♠

**Lemma 26.8** *The function  $A \rightarrow \dim(C_A)$  is Borel measurable.*

**Proof:** When  $A = p/q$ , we define  $C_A = O_2(J) \cap I$ . Here  $J$  is the interval of length  $2/q$  in  $I$  whose left endpoint is  $(0, 1)$ . Thus,  $C_A$  is just a thickened version of part of the fundamental orbit. Having made this definition, we define  $C$  as in Equation 11. In the proof of Lemma 26.1 we produced a covering  $\mathcal{C}_n$  of  $C_A$  by intervals all having the same length. One can extend this definition to the rational case in a fairly obvious way. Let  $C_A^{(n)}$  denote the union of these intervals. Let  $C^{(n)}$  be the corresponding union, with  $C_A^{(n)}$  replacing  $C_A$  in Equation 11. The sizes and positions of the intervals in  $C_A^{(n)}$  vary with  $A$  in a piecewise continuous way. Hence  $C^{(n)}$  is a Borel set. Hence  $C = \bigcap C^{(n)}$  is a Borel set. Then  $C_A$  is obtained by intersecting a Borel subset of  $[0, 1]^2$  with the line  $\{y = A\}$ . By the Borel Slicing Property,  $u$  is Borel measurable. ♠

**Remark:** My website has a picture of the beautiful set  $C$ .

## 26.5 The Dimension Function

In this section we study the function  $u(A) = \dim(C_A) = \dim(U_A)$ .

**Lemma 26.9**  *$u$  is almost everywhere constant.*

**Proof:** We have already seen that  $u$  is constant on  $\Gamma_2$  orbits. Since  $\Gamma_2$  acts ergodically on  $\mathbf{R} \cup \infty$ , we see that  $u$  is almost everywhere constant. ♠

**Remarks:** We would guess that  $\dim(C_A) = 1$  for almost all  $A$ . We don't know.

Now we derive some corollaries of the dimension formula. Say that  $A$  is *superior* if all the terms in the inferior sequence are superior.

**Theorem 26.10** *Let  $A$  be a tame parameter. Let  $D = D_A$ . Then*

$$u(A) \leq \frac{D}{D + \log(\sqrt{5}/2)}.$$

*If  $A$  is also superior, then*

$$u(A) \geq \frac{D}{D + \log(2)}.$$

**Proof:** The upper bound follows from Equation 276 and our dimension formula. Now we prove the lower bound. Referring to the inferior sequence  $\{p_n/q_n\}$  and the inferior renormalization sequence  $\{d_n\}$ , we always have  $q_{n+1} < 2(d_n + 1)q_n$ . This bound directly applies to the superior sequence when  $A$  is superior. By induction,  $q_n \leq 2D_n$ . Hence  $Q \leq D + \log 2$ . Our bound follows immediately. ♠

**Lemma 26.11** *Let  $A$  be a superior parameter whose renormalization sequence  $\{d_n\}$  diverges to  $\infty$ . If  $d_{n+1}/d_n$  grows sub-exponentially,  $u(A) = 1$ .*

**Proof:** The same argument as in Lemma 26.4 shows that

$$\lambda_n > (h_n q_n)^{-1}. \quad (362)$$

Here  $h_n$  grows sub-exponentially. From Equation 277, we get

$$G_n = 2\lambda'_n > 2\lambda_n > 2(h_n q_n)^{-1}. \quad (363)$$

Therefore

$$\begin{aligned} \lim_{n \rightarrow \infty} \frac{\log(D_n)}{\log(G_n^{-1})} &\geq \lim_{n \rightarrow \infty} \frac{\log(D_n)}{\log(h_n q_n)} =^* \\ \lim_{n \rightarrow \infty} \frac{\log(D_n)}{\log(q_n)} &\geq \lim_{n \rightarrow \infty} \frac{\log(D_n)}{\log(D_n) + \log(2)} = 1. \end{aligned} \quad (364)$$

The starred equality comes from the sub-exponential growth of  $h_n$ . Essentially the same derivation as above now shows that  $u(A) \geq 1$ . But, of course  $u(A) \leq 1$  as well. Hence  $u(A) = 1$ . ♠

**Lemma 26.12**  *$u$  maps  $(0, 1) - \mathbf{Q}$  onto  $[0, 1]$ .*

**Proof:** By the previous result, we can get  $u(A) = 1$ . It is easy to get  $u(A) = 0$  by taking  $A$  so that the IERS is  $2, 0, \dots, 0, 2, 0, \dots, 0, \dots$  where the number of 0s grows rapidly enough. (See §22.2 for a definition of the IERS.)

Suppose we want find  $A$  such that  $u(A) = x \in (0, 1)$ . Let  $A$  be the parameter whose IERS is  $N, N, N, \dots$ . Here  $N$  must be even because the 0th term is even. Choosing  $N$  large enough, we can arrange that  $u(A) > x$ , by Lemma 26.10. Let  $B_m$  denote the parameter whose IERS is  $N, 0_m, N, 0_m, \dots$

Here  $0_m$  represents  $m$  zeros in a row. As  $m \rightarrow \infty$ , we have  $u(B_m) \rightarrow 0$ . Thus, we can find an integer  $m$  such that  $u(B_{m+1}) < \delta_0 < u(B_m)$ . (We're already done if we have equality on either side.)

Given a binary sequence  $\eta = \{\epsilon_k\}$  we define  $A(\eta) = N, 0_{m+\epsilon_1}, N, 0_{m+\epsilon_2}, \dots$ . The parameter  $A(\eta)$  is tame, and  $D(\eta) = \log N$ , independent of  $\eta$ . Letting  $\eta_0$  and  $\eta_1$  denote the 0 sequence and the 1 sequence, we have  $Q(\eta_0) < Dx$  and  $Q(\eta_1) > Dx$ . Essentially by the intermediate value theorem, we can adjust  $\eta$ , so that  $Q(\eta) = Dx$ . Then  $A(\eta)$  is the desired parameter. ♠

Since  $u$  is  $\Gamma_2$ -invariant, and  $\Gamma_2$  orbits are dense in  $(0, 1)$ , the function  $u$  maps any open subset of  $(0, 1) - \mathbf{Q}$  onto  $[0, 1]$ .

## 26.6 Example Calculations

**Example 1:** Let  $A = \sqrt{5} - 2$ , the Penrose kite parameter. The inferior sequence is

$$\frac{1}{1} \leftarrow \frac{1}{3} \leftarrow \frac{1}{5} \leftarrow \frac{3}{13} \leftarrow \frac{5}{21} \leftarrow \frac{13}{55} \leftarrow \frac{21}{89} \leftarrow \frac{55}{233} \leftarrow \frac{89}{377} \dots$$

The superior sequence is

$$\frac{1}{1}, \frac{1}{5}, \frac{5}{21}, \frac{21}{89} \dots \quad p_{n+1} = q_n; \quad q_{n+1} = 4q_n + p_n.$$

The inferior renormalization sequence is  $2, 0, 2, 0, \dots$ . The renormalization sequence is  $2, 2, 2, \dots$ . Hence  $D = \log(3)$ . The superior sequence satisfies the recurrence relation

$$p_{n+1} = q_n; \quad q_{n+1} = 4q_n + p_n.$$

This gives  $Q = \log(\phi^3)$ . Theorems 26.3 combines with the modularity to show that

$$\begin{bmatrix} a & b \\ c & d \end{bmatrix} \in \Gamma_2; \quad A = \frac{a\sqrt{5} + b}{c\sqrt{5} + d} \in (0, 1) \quad \implies \quad u(A) = \frac{\log(3)}{\log(\phi^3)}$$

**Example 2:** The renormalization sequence for the parameter  $A = E - 2$  considered at the end of §25.5 is  $3, 5, 7, 9, \dots$ . The example here satisfies Lemma 26.11. Therefore

$$\begin{bmatrix} a & b \\ c & d \end{bmatrix} \in \Gamma_2; \quad A = \frac{aE + b}{cE + d} \in (0, 1) \quad \implies \quad u(A) = 1. \quad (365)$$

Again, it seems that  $E = e$ .

## Part VI

- In §27 we prove the Copy Theorem from §23.2.
- In §28 we define what we mean by the pivot arc relative to an even rational kite parameter. Along the way we will prove another version of the Diophantine Lemma from §19.2. The Diophantine Lemma works for pairs of odd rationals, and the result here works for pairs of Farey-related rationals, even or odd.
- In §29 we prove the Pivot Theorem from §23.2. The Pivot Theorem works in both the even and the odd case, and is proved in an inductive way that requires both cases.
- In §30 we prove the Period Theorem.
- In §31 we prove Statement 1 of the Comet Theorem.

## 27 Proof of the Copy Theorem

### 27.1 A Formula for the Pivot Points

Let  $A$  be an odd rational. Let  $A_-$  be as in Equation 27. Let  $V_- = (q_-, -p_-)$ . Here we give a formula for the pivot points  $E^\pm$  associated to  $A$ .

**Lemma 27.1** *The following is true.*

- If  $q_- < q_+$  then  $E^+ + E^- = -V_- + (0, 1)$ .
- If  $q_+ < q_-$  then  $E^+ + E^- = V_+ + (0, 1)$ .

**Proof:** We will establish this result inductively. Suppose first that  $1/1 \leftarrow A$ . Then

$$A = \frac{2k-1}{2k+1}; \quad E^- = (-k, k); \quad E^+ = (0, 0); \quad V_- = (k, -k+1).$$

$$A_- = \frac{k-1}{k}; \quad q_- = k-1 < k = q_+.$$

The result works in this case.

In general, we have  $A = A_2$  and  $A_0 \leftarrow A_1 \leftarrow A_2$ . There are 4 cases, depending on Lemma 18.2. Here the index is  $m = 1$ . We will consider Case 1. The other cases are similar. By Case 1, we have  $(q_1)_+ < (q_1)_-$ . Hence, by induction

$$E_1^+ + E_1^- = (V_1)_+ + (0, 1).$$

Since  $A_1 < A_2$  we have

$$E_2^- = E_1^-; \quad E_2^+ = E_1^+ + d_1 V_1.$$

Therefore

$$E_2^+ + E_2^- = (V_1)_+ + d_1 V_1 + (0, 1) = (V_2)_+ + (0, 1).$$

The last equality comes from Case 1 of Lemma 18.2. As we remarked after stating Lemma 18.2, this result works for both numerators and denominators.) In Case 1, we have  $(q_2)_+ < (q_2)_-$ , so the result holds. ♠

**Lemma 27.2**  $E^-$  lies to the left of  $R_1$  and  $E^+$  lies to the right of  $R_1$ .

**Proof:** Let  $\pi_1$  denote the projection to the first coordinate. One or the other bottom vertices of  $R_1$  is  $(0, 0)$ . We will consider the case when the left bottom vertex is  $(0, 0)$ . In all cases one checks easily from our definitions that  $\pi_1(E^-) \leq -1$ . Hence  $E^-$  lies to the left of  $R_1$ .

Consider the right side. We have  $q_+ < q_-$  in our case. By Case 2 of Lemma 27.1, and the result for the left hand side, we have

$$\pi_1(E^+) \geq \pi_1(V_+) + 1.$$

But  $V_+$  lies on the line extending the bottom right edge of  $R_1$ , exactly  $1/q$  vertical units beneath the bottom edge of  $R_1$ . This right edge has slope greater than 1. Finally, the line connecting  $V_+$  to  $\pi_1(E^+)$  has nonpositive slope because  $E^+$  is a low vertex lying to the right of  $V_+$ . From all this geometry, we see that  $E_1^+$  lies to the right of  $R_1$ . ♠

While we are in the neighborhood, we clear up a detail from Part V.

**Proof of Lemma 23.2:** We will prove this result inductively. Suppose that  $A_1 \leftarrow A_2$ , and the result is true for  $A_1$ . We consider the case when  $A_1 < A_2$ . The case when  $A_1 > A_2$  has the same treatment. When  $A_1 < A_2$ , we have  $E_1^- = E_2^-$ , so certainly the bound holds for  $E_1^-$ . On the other hand, we have

$$\pi_1(E_2^+) = \pi_1(E_1^+) + d_1 q_1 \quad d_1 = \text{floor}\left(\frac{q_2}{2q_1}\right) \quad (366)$$

There are two cases to consider. Suppose first that  $\delta_1 = \text{floor}(q_2/q_1)$  is odd. In this case

$$(2d_1 + 1)q_1 < q_2; \quad \implies \quad d_1 q_1 < \frac{q_2}{2} - \frac{q_1}{2}.$$

The first equation implies the second. Hence, by induction

$$\pi_1(E_2^+) < \frac{q_1}{2} + \frac{q_2 - q_2}{2} < \frac{q_2}{2}.$$

Suppose that  $\delta_1$  is even. Then we have Case 2 of Lemma 18.2, applied to the index  $m = 1$ . This is to say that  $(q_1)_- < (q_1)_+$ . From our formula above, the first coordinate of  $E_2^- + E_2^+$  is negative. Hence

$$|\pi_1(E^-)| > |\pi_1(E^+)|.$$

This fact finishes the proof. ♠

## 27.2 Good Parameters

Our pivot points are well defined vertices, but so far, we don't know that the pivot arc is well defined. That is, we don't know that  $E^-$  and  $E^+$  are actually vertices of  $\Gamma$ . These points might be vertices of some other component of  $\tilde{\Gamma}$ . To start things off right, we deal with the base case.

**Lemma 27.3** *If  $1/1 \leftarrow A$ , then the pivot arc is well-defined relative to  $A$ .*

**Proof:** Here  $A = (2k - 1)/(2k + 1)$  for  $k \in \mathbf{N}$ . In §21.5, we showed that the line segment connecting  $(0, 0)$  to  $(-k, k)$  is contained in the arithmetic graph. So, the pivot arc is well defined. ♠

Now we consider the general case. Let  $A_1$  be an odd rational. For each integer  $\delta_1 \geq 1$ , there is a unique odd rational  $A_2 = A_2(\delta_1)$  such that  $A_1 \leftarrow A_2$  and

$$\delta_1 = \text{floor}\left(\frac{q_2}{q_1}\right).$$

Lemma 18.2 gives the recipe for how to construct  $A_2$ . As in Equation 31, we define

$$d_1 = \text{floor}\left(\frac{q_2}{2q_1}\right).$$

Recall that  $E_j^\pm$  are the pivot points associated to  $\Gamma_j$ . Let  $P\Gamma_1(\delta_1)$  denote the arc of  $\Gamma_1$  whose endpoints are  $E_2^-$  and  $E_2^+$ .

**Lemma 27.4**  *$P\Gamma_1(\delta_1)$  is a well defined arc of  $\Gamma_1$ .*

**Proof:** Suppose that  $A_1 < A_2$ . When  $A_2 < A_1$  the proof is similar. Then, by Equation 296, we have

$$E_2^- = E_1^-; \quad E_2^+ = E_1^+ + d_1 V_1; \quad V_1 = (q_1, -p_1).$$

But  $\Gamma_1$  is invariant under translation by  $V_1$ . Hence  $E_2^\pm$  is a vertex of  $\Gamma_1$ . ♠

Call  $A_1$  a *good parameter* if

$$P\Gamma_1 \subset \Delta_1(I). \tag{367}$$

Here  $\Delta_1(I)$  is the region from the Diophantine Lemma, defined relative to the pair  $(A_1, A_2(1))$ . We call  $I$  the *base interval*. We will give a formula below.

**Lemma 27.5** *If  $A_1$  is good, then the Copy Theorem holds for  $A_1$  and  $A_2(1)$ .*

**Proof:** Note that  $P\Gamma_1(1) = P\Gamma_1$ , the pivot arc of  $\Gamma_1$ . The pivot points do not change in this case:  $E_1^\pm = E_2^\pm$ . So, if  $A_1$  is good then the Diophantine Lemma immediately implies that  $P\Gamma_1(1) = P\Gamma_1 \subset \Gamma_2$ . But then, there is an arc of  $\Gamma_2$  that connects  $E_2^-$  to  $E_2^+$ , the two endpoints of  $P\Gamma_1(1)$ . This shows that the Pivot arc for  $A_2$  is well defined, and that this pivot arc is a subarc of  $\Gamma_1$ . ♠

**Lemma 27.6** *If  $A_1$  is good, then the Copy Theorem holds for  $A_1$  and  $A_2(3)$ .*

**Proof:** Let  $A_0$  be such that the sequence  $A_0 \leftarrow A_1 \leftarrow A_2(1)$  is a fragment of the inferior sequence. We will consider the case when  $A_0 < A_1$ . In this case  $A_1 < A_2(1)$  by Lemma 18.2. The base interval is given by

$$I = [-q_1 + 2, q_1 + (q_2)_+ - 2] = [-q_2 + 2, q_1 + (q_1)_+ - 2]. \quad (368)$$

The first equality is Lemma 18.5. The second equality is Case 1 of Lemma 18.2, with  $d_1 = 0$ .

Let  $R_j = R_j(A_1)$ , as in the Decomposition Theorem for  $A_1$ . As in Lemma 27.2, we know that  $R_1$  lies to the right of the origin and  $R_2$  to the left. (This is because  $(q_1)_+ < (q_1)_-$  in the case we are considering.) The arc  $P\Gamma_1(3)$  is obtained from  $P\Gamma_1(1)$  by concatenating one period of  $\Gamma_1$  to the right.

We claim that

$$P\Gamma_1(3) = P\Gamma_1 \cup \gamma \cup (P\Gamma_1 + V_1); \quad \gamma \in (R_2 + V_1). \quad (369)$$

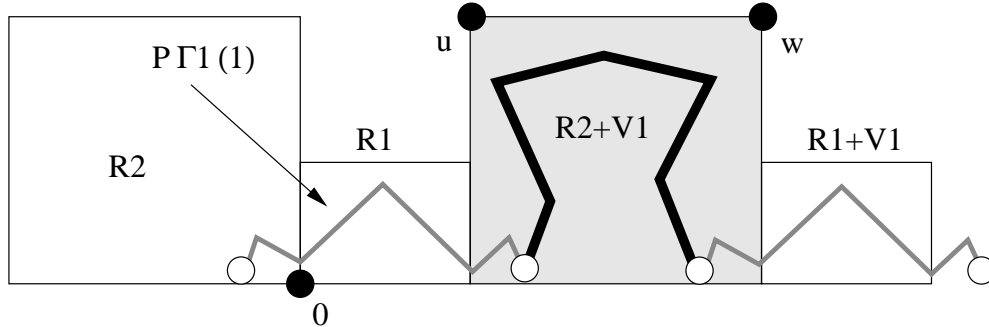


**Figure 27.1:** Decomposition of  $P\Gamma_1(3)$ .

Here is the proof. By Lemma 27.2, the arc  $P\Gamma_1$  completely crosses  $R_1$ . The left endpoint lies in  $R_2$  and the right endpoint lies in  $R_2 + V_1$ , the translate of  $R_2$  that lies on the other side of  $R_1$ . By symmetry, one endpoint of  $P\Gamma_1(1)$  enters  $R_2 + V_1$  from the left and one endpoint of  $P\Gamma_1(1) + V_1$  enters  $R_2 + V_1$  from the right. The arc  $\gamma$  joins two points already in  $R_2 + V_1$ . This arc cannot cross out of  $R_2 + V_1$ , by Lemma 21.1.

Now we know that Equation 369 is true. Let  $A_2 = A_2(1)$  and  $A_2^* = A_2(3)$ . We attach a  $(*)$  to objects associated to  $A_2^*$ . Let  $I$  be the base interval. Let  $I^*$  denote the interval corresponding to the pair  $(A_1, A_2^*)$ . By Lemma 18.2, we have  $(q_2^*)_+ = q_1 + (q_1)_+$ . Hence, by Lemma 18.5 and by definition,

$$I^* = [-q_1 + 2, 2q_1 + (q_1)_+ - 2] = [I_{\text{left}}, I_{\text{right}} + q_1]. \quad (370)$$

We have  $P\Gamma_1 \subset \Delta_1(I) \subset \Delta_2(I)$ . The first containment is the definition of goodness. Any  $v^* \in P\Gamma_1 + V_1$  has the form  $v + V_1$ , where  $v \in P\Gamma_1$ . By Lemma 19.1 we have

$$G_1(v^*) = G_1(v) + q_1; \quad H_1(v^*) = H_1(v) + q_1.$$

Hence  $v \in \Delta_1(I)$  implies  $v^* \in \Delta(I^*)$ . It remains to deal with the arc  $\gamma$ .

We will use the same argument that we used in §21.3. Let  $u$  and  $w$  respectively be the upper left and upper right vertices of  $R_2 + V_1$ . We have

$$u \approx W_1 + \frac{(q_1)_+}{q_1} V_1; \quad w = W_1 + V_1. \quad (371)$$

Here the vectors are as in Equation 21, as usual. The approximation is good to within  $1/q_1$ . To avoid approximations, we consider the very slightly altered parallelogram  $\tilde{R}_2 + V_1$ . The vertices are

$$(V_1)^+; \quad \tilde{u} = W_1 + \frac{(q_1)_+}{q_1} V_1; \quad V_1; \quad w = V_1 + W_1. \quad (372)$$

Each vertex of the new parallelogram is within  $1/q_1$  of the corresponding old parallelogram. Using the Adjacent Mismatch Principle, it suffices to do the calculation in  $\tilde{R}_2 + V_1$ . The following calculation combines with the Diophantine Lemma to show that  $\gamma \subset \Gamma_2(A_2^*)$ .

$$G_1(\tilde{u}) - (-q_1) = (2q_1 + q_+) - H_1(w) = q_1 + (q_1)_+ - \frac{q_1^2}{p_1 + q_1} \geq 2. \quad (373)$$

This completes the proof. ♠

**Lemma 27.7** *If  $A_1$  is good and  $\delta_1$  is odd, then the Copy Theorem holds for  $A_1$  and  $A_2(\delta_1)$ .*

**Proof:** Now consider the case when  $\delta_1 = 5$ . In this case,  $P\Gamma_1(5)$  is obtained by concatenating 2 periods of  $\Gamma_1$  to the right of  $P\Gamma_1(1)$ . We have decomposition of the form

$$P\Gamma_1(5) = P\Gamma_1(1) \cup \gamma \cup (P\Gamma_1(1) + 2V_1); \quad \gamma \subset (R_2 + V_1) \cup (R_2 + 2V_1). \quad (374)$$

Here  $\gamma$  is contained in a parallelogram that is twice as long as in the case  $\delta = 3$ . The calculations are exactly the same in this case. The key point is that  $I^* = [a, b + 2q_1]$ . The cases  $\delta = 7, 9, 11, \dots$  have the same treatment. ♠

**Lemma 27.8** *If  $A_1$  is good, then the Copy Theorem holds for  $A_1$  and  $A_2(2)$ .*

**Proof:** In this case,  $P\Gamma_1(2)$  is obtained from  $P\Gamma_1$  by concatenating one period of  $\Gamma_1$  to the left. See Figure 27.2 below. We have the decomposition

$$P\Gamma_1(2) = (P\Gamma_1(1) - V_1) \cup \gamma \cup P\Gamma_1(1); \quad \gamma \subset R_2. \quad (375)$$

The proof is the same as in Lemma 27.6.

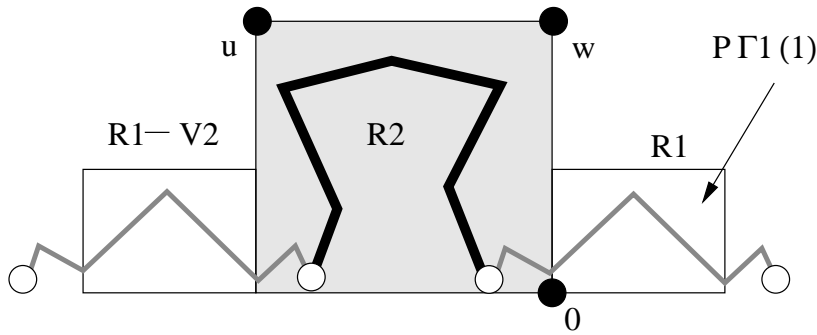


**Figure 27.2:** Decomposition of  $P\Gamma_1(2)$ .

We use the same notational conventions as in the odd case. The same argument as above works here, provided that we can get the right estimates on the top vertices  $u$  and  $w$  of  $R_2 = R_2(A_1)$ . Case 4 of Lemma 18.2 tells us that

$$(q_2^*)_- = q_1^-.$$

Combining this fact with Lemma 18.5, we get

$$I^* = [-q_1 - (q_2^*)_- + 2, q_1 - 2] = [-q_1 - (q_1)_- + 2, q_1 - 2]. \quad (376)$$

We have

$$u \approx \frac{-(q_1)_-}{q_1} V_1 + W_1; \quad w = W_1. \quad (377)$$

Again, the approximation holds up to  $1/q_1$ . To avoid approximations, we use the modified parallelogram  $\tilde{R}_2$  with vertices

$$\frac{-(q_1)_-}{q_1} V_1; \quad \tilde{u} = \frac{-(q_1)_-}{q_1} V_1 + W_1; \quad (0, 0); \quad w = W_1. \quad (378)$$

Again, this is justified by our Adjacent Mismatch Principle. The following estimate combines with the Diophantine Lemma to show that  $\gamma \subset \Gamma_2(A_2^*)$ .

$$G_1(\tilde{u}) - (-q_1 - (q_1)_-) = q_1 - H(w) = q_1 - \frac{q_1}{p_1 + q_1} \geq 2. \quad (379)$$

As in §21.3, this estimate holds as long as  $p_1 \geq 3$  and  $q_1 \geq 7$ . We handle the few exceptional cases as we did in §21.4. ♠

**Lemma 27.9** *If  $A_1$  is good and  $\delta_2$  is even, then the Copy Theorem holds for  $A_1$  and  $A_2(\delta_1)$  when  $\delta_1$ .*

**Proof:** The cases  $\delta_1 = 4, 6, 8, \dots$  relate to the case  $\delta_1 = 2$  exactly as the cases  $\delta_1 = 5, 7, 9, \dots$  relate to the cases  $\delta_1 = 3$ . ♠

### 27.3 The End of the Proof

It remains to show that any odd rational is good. We will give an inductive argument.

**Lemma 27.10** *If  $1/1 \leftarrow A$ , then  $A$  is good.*

**Proof:** In this case, Lemma 18.2 tells us that  $1/1 > A > \hat{A}$ . (The first inequality is obvious.) We have

$$A = \frac{2k-1}{2k+1}; \quad \hat{A} = \frac{4k-3}{4k+1}; \quad \hat{q}_- = k.$$

By Lemma 18.5, we have

$$I = [-q - q_- + 2, q - 2] = [-3k + 1, 2k - 1]$$

The left vertex of  $P\Gamma_1$  is  $u = (-k, k)$  and the right vertex is  $v = (0, 0)$ . We compute

$$G(u) = -k - 1 \geq -3k + 1; \quad H(w) = 0 \leq 2k - 1.$$

The extreme case happens when  $k = 1$ . ♠

**Lemma 27.11**  *$A = p/q$  is good if  $q < 20$  or if  $p = 1$ .*

**Proof:** We check the case  $q < 20$  by hand. If  $p = 1$ , the pivot arc is just the edge connecting  $(-1, 1)$  to  $(0, 0)$  whereas the interval  $I$  contains  $[-q, q]$ , a huge interval. This case is obvious. ♠

Now we establish the inductive step. Suppose that  $A_1 \leftarrow A_2$  and that  $A_1$  is good. Having eliminated the few exceptional cases by our result above, our argument in the previous section shows that  $P\Gamma_2 \subset \Delta_1(I_1)$ . Here  $I_1$  is the interval based on the constant  $\Omega(A_1, A_2)$ . This is the Diophantine constant defined in §18.4 relative to the pair  $(A_1, A_2)$ . To finish of the proof of the Copy Theorem, we just have to establish the following equation.

$$P\Gamma_2 \subset \Delta_2(I_2), \tag{380}$$

where  $I_2$  is the different interval based on the pair  $A_2 \leftarrow A_3$ , with  $\delta(A_2, A_3) = 1$ . Here we establish two basic facts.

**Lemma 27.12**  *$I_1 \subset I_2$ , and either endpoint of  $I_1$  is more than 1 unit from the corresponding endpoint of  $I_2$ .*

**Proof:** By Lemma 18.5, applied to both parameters, we have

$$I_1 \subset [-q_2 + 3, q_2 - 3] \subset [-q_2 - 2, q_2 - 2] \subset I_2.$$

This completes the proof. ♠

**Lemma 27.13**  $|G_1(v) - G_2(v)| < 1$  and  $|H_1(v) - H_2(v)| < 1$  for  $v \in \Delta_1(I_1)$ .

**Proof:** From Lemma 18.5 and a bit of geometry, we get the bound

$$(m, n) \in \Delta_1(I_1) \quad \implies \quad \max(|m|, |n|) \leq q_2. \quad (381)$$

Looking at Equation 216, we see that

$$\begin{aligned} G(m, n) &= \left( \frac{1-A}{1+A}, \frac{-2}{1+A} \right) \cdot (m, n) = (G_1, G_2) \cdot (m, n) \\ H(m, n) &= \left( \frac{1+4A-A^2}{(1+A)^2}, \frac{2-2A}{(1+A)^2} \right) \cdot (m, n) = (H_1, H_2) \cdot (m, n) \end{aligned} \quad (382)$$

A bit of calculus shows that

$$|\partial_A G_j| \leq 2; \quad |\partial_A H_1| \leq 6; \quad |\partial_A H_2| \leq 2. \quad (383)$$

Since  $A_1 \leftarrow A_2$ , we have

$$|A_1 - A_2| = \frac{2}{q_1 q_2}. \quad (384)$$

Putting everything together, and using basic calculus, we arrive at the bound

$$|G_1(v) - G_2(v)|, |H_1(v) - H_2(v)| < \frac{16}{q_1} < 1, \quad (385)$$

at least for  $q_1 > 16$ . ♠

We have already remarked, during the proof of the Decomposition Theorem, that no lattice point lies between the bottom of  $\Delta_2(I_2)$  and the bottom of  $\Delta_1(I_2)$ . Hence  $F_1(v) > 0$  iff  $F_2(v) > 0$ . Our two lemmas now show that  $\Delta_1(I_1) \subset \Delta_2(I_2)$ . This was our final goal, from Equation 380.

This completes the proof of the Copy Theorem.

## 28 Pivot Arcs in the Even Case

### 28.1 Main Results

Given two rationals  $A_1 = p_1/q_1$  and  $A_2 = p_2/q_2$ , we introduce the notation

$$A_1 \bowtie A_2 \iff |p_1q_2 - q_1p_2| = 1; \quad q_1 < q_2. \quad (386)$$

In this case, we say that  $A_1$  and  $A_2$  are *Farey related*. We sometimes call  $(A_1, A_2)$  a *Farey pair*.

We have the notions of *Farey addition* and *Farey subtraction*:

$$A_1 \oplus A_2 = \frac{p_1 + p_2}{q_1 + q_2}; \quad A_2 \ominus A_1 = \frac{p_2 - p_1}{q_2 - q_1}. \quad (387)$$

Note that  $A_1 \bowtie A_2$  implies that  $A_1 \bowtie (A_1 \oplus A_2)$  and that  $A_1$  is Farey related to  $A_2 \ominus A_1$ .

**Lemma 28.1** *Let  $A_1$  be an even rational. Then there is a unique odd rational  $A_2$  such that  $A_1 \bowtie A_2$  and  $2q_1 > q_2$ .*

**Proof:** Equation 27 works for both even and odd rationals. When  $A_1$  is even, exactly one of the rationals  $(A_1)_\pm$  is also even. Call this rational  $A'_1$ . Then  $A'_1 \bowtie A_1$ . We define  $A_2 = A_1 \oplus A'_1$ . If  $B_2$  was another candidate, then  $B_2 \ominus A'$  would be the relevant choice of  $(A_1)_\pm$ . Hence  $B_2 = A_2$ . ♠

We will write  $A_1 \bowtie! A_2$  to denote the relationship between  $A_1$  and  $A_2$  discussed in the previous result. We can think about this relation in a different way. Let  $A$  be an odd rational. Then either  $A_- \bowtie! A$  or  $A_+ \bowtie! A$  when  $A$  is an odd rational. If  $A_- \bowtie! A$  then we write  $A_+ \Leftarrow A$ . The relationship implies that  $2q_+ < q$ . Likewise we write  $A_- \Leftarrow A$  when  $2q_- < q$ . Here is an example: Let  $A = 3/7$ . Then

$$A_+ = 1/2 \Leftarrow 3/7; \quad A_- = 2/5 \bowtie! 3/7.$$

So far, we have defined pivot points and arcs for odd parameters. Now we define them for even parameters. We define

$$E^\pm(A_1) := E^\pm(A_2); \quad A_1 \bowtie! A_2. \quad (388)$$

This makes sense because we have already defined the pivot points in the odd case. We still need to prove that these vertices lie on  $\Gamma_1$ . We will do this below.

Assuming that the pivot points  $E_1^\pm$  are vertices of  $\Gamma_1$ , we define  $P\Gamma_1$  to be the lower arc of  $\Gamma_1$  that connects  $E_1^-$  to  $E_1^+$ . Since  $\Gamma_1$  is a polygon in the even case, it makes sense to speak of the lower arc. Figure 28.1 shows an example. Here  $P\Gamma_1 = P\Gamma_2$ . We will show that this always happens.

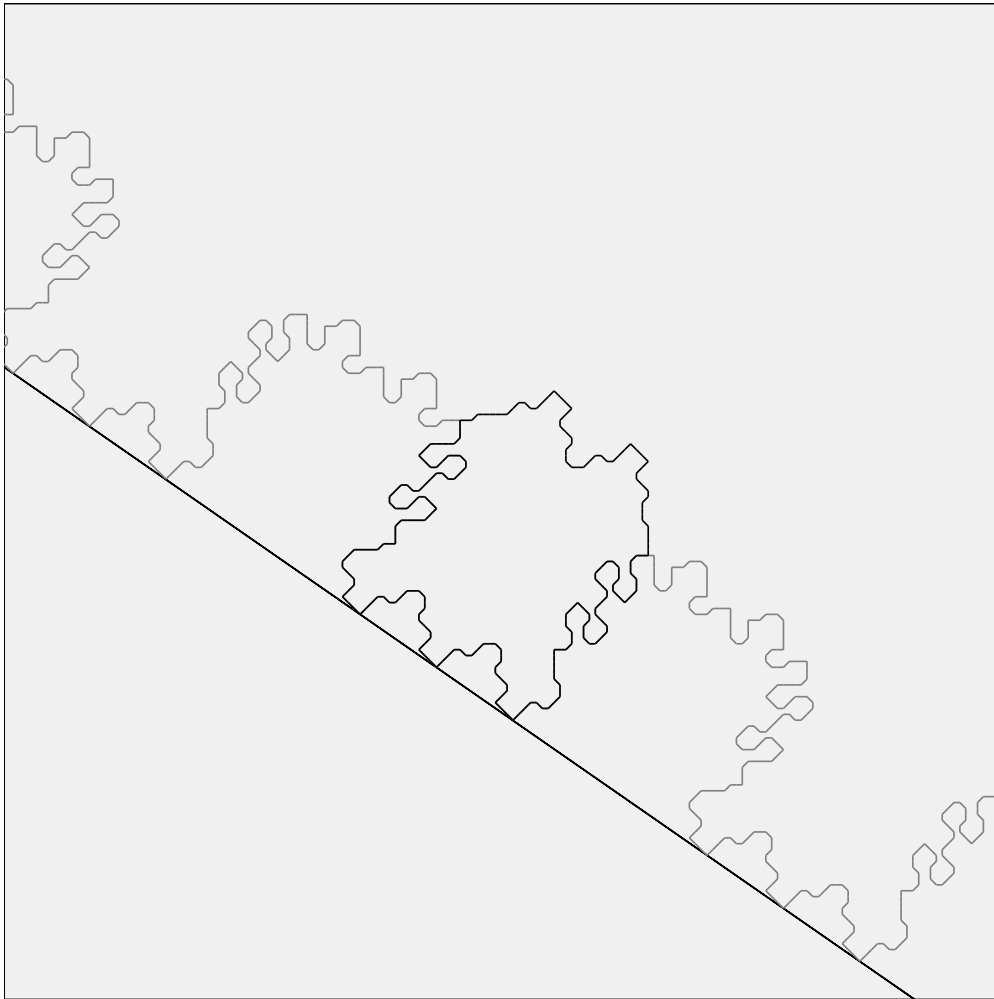


**Figure 28.1:**  $\Gamma(41/59)$  in grey and  $\Gamma(25/36)$  in black

In this chapter we prove the following results.

**Lemma 28.2** *Let  $A_1 \bowtie A_2$ . Then  $P\Gamma_1$  is well defined and  $P\Gamma_1 = P\Gamma_2$ .*

**Lemma 28.3 (Structure)** *The following is true.*

1. *If  $A_- \Leftarrow A$  then  $E^+(A) = E^+(A_-)$ .*
2. *If  $A_+ \Leftarrow A$  then  $E^-(A) = E^-(A_+)$ .*
3. *If  $A_- \Leftarrow A$  then  $E^-(A) + V = E^-(A_-) + kV_-$  for some  $k \in \mathbf{Z}$ .*
4. *If  $A_+ \Leftarrow A$  then  $E^+(A) - V = E^+(A_+) + kV_+$  for some  $k \in \mathbf{Z}$ .*

The Structure Lemma is of crucial importance in our proof of the Pivot Theorem and the Period Theorem. Here we illustrate its meaning and describe a bit of the connection to the Pivot Theorem.

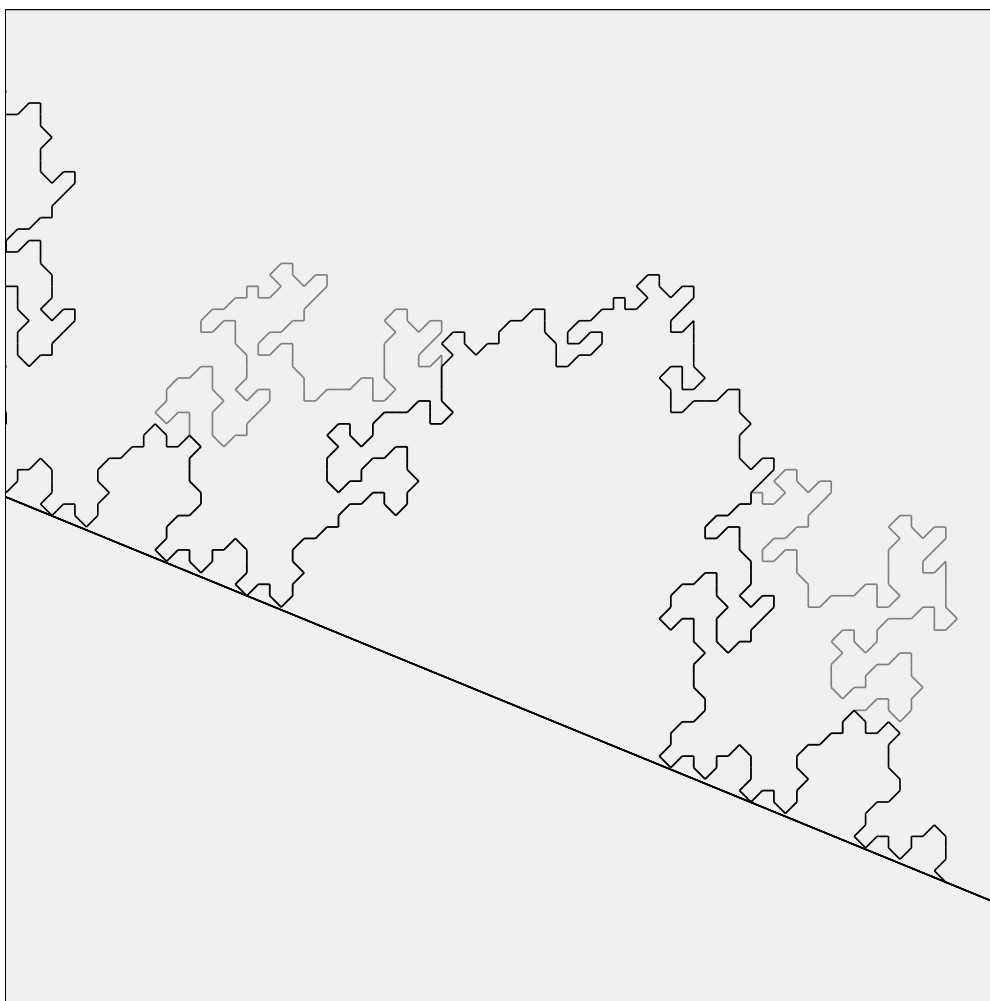


**Figure 28.2:**  $\Gamma(25/61)$  overlays several components of  $\hat{\Gamma}(9/22)$ .

Figure 28.2 shows slightly more than one period of  $\Gamma(25/61)$  in black. This black arc overlays  $\Gamma(9/22)$  on the left and

$$\Gamma(9/22) + 2V(9/22)$$

on the right. Call these two grey components *the eggs*. Here

$$9/22 \bowtie! 25/61.$$

The points

$$E^+(25/61); \quad E^-(25/61) + V(25/61)$$

are the left and right endpoints respectively of the big central hump of  $\Gamma(25/61)$ . Call this black arc *the hump*. The content of the Structure Lemma (in this case) is that the endpoints of the hump are simultaneously pivot points on the eggs. The reader can draw many pictures like this on Billiard King.

The content of the Pivot Theorem for  $25/61$  is that the hump has no low vertices except its endpoints. Note that the ends of the hump copy pieces of the eggs. If we already understand the behavior of the eggs – meaning how they rise away from the baseline – then we understand the behavior of the ends of the hump. The eggs are based on a simpler rational. In this way, the behavior of the arithmetic graph for a simpler rational gives us information about what happens for a more complicated rational. This is (some of) the strategy for our proof of the Pivot Theorem. In the first section of the next chapter we will have a long and somewhat informal discussion about the remainder of the strategy.

**Remarks:**

- (i) In §28.5 below we will give the precise relationship between the two pivot arcs in the cases of interest to us.
- (ii) Notice in Figure 28.2 that the grey curves lie completely above the black one, except for the edges where they coincide. There is nothing in our theory that explains such a clean kind of relationship, but it always seems to hold.
- (iii) The Structure Lemma has a crisp result, easy to check computationally for individual cases. However, as the reader will see, our proof is rather tedious. We wish we had a better proof.

## 28.2 Another Diophantine Lemma

Here we prove a copying lemma that helps with Lemma 28.2. Our result works for Farey pairs. Let  $\Delta_1(I)$  and  $\Delta_2(I)$  be the sets defined exactly as in the Diophantine Lemma. See §19.2. The result we prove here is actually more natural than our original result. However, the original result better suited our more elementary purposes.

**Lemma 28.4** *Suppose that  $A_1 \bowtie A_2$ .*

1. *If  $A_1 < A_2$  let  $I = [-q_1 + 2, q_2 - 2]$ .*
2. *If  $A_1 > A_2$  let  $I = [-q_2 + 2, q_1 - 2]$ .*

*Then  $\widehat{\Gamma}_1$  and  $\widehat{\Gamma}_2$  agree on  $\Delta_1(I) \cup \Delta_2(I)$ .*

**Proof:** We will consider the case when  $A_1 < A_2$ . The other case has a very similar treatment. In our proof of the Diophantine Lemma we only used the oddness of our rationals in Lemma 19.4. Once we prove the analogue of this result in the even setting, the rest of the proof works *verbatim*.

Recall that an integer  $\mu$  is *good* if  $\text{floor}(A_1\mu) = \text{floor}(A_2\mu)$ . The analogue of Lemma 19.4 is the statement that an integer  $\mu$  is good provided that  $\mu \in (-q_1, q_2)$ . We will give a geometric proof. Let  $L_1$  (respectively  $L_2$ ) denote the line segment of slope  $-A_1$  (respectively  $-A_2$ ) joining the two points whose first coordinates are  $-q_1$  and  $q_2$ . If we have a counterexample to our claim then there is a lattice point  $(m, n)$  lying between  $L_1$  and  $L_2$ .

If  $m < 0$ , we consider the triangle  $T$  with vertices  $(0, 0)$  and  $-V_1$  and  $(m, n)$ . Here  $V_1 = (q_1, -p_1)$ . The vertical distance between the left endpoints of  $L_1$  and  $L_2$  is  $1/q_2$ . By the base-times-height formula for triangles,  $\text{area}(T) < q_1/(2q_2) < 1/2$ . But this contradicts the fact that  $1/2$  is a lower bound for the area of a lattice triangle. If  $m > 0$  we consider the triangle  $T$  with vertices  $(0, 0)$  and  $V_1$  and  $(m, n)$ . The lattice point  $(m, n)$  is closer to the line containing  $L_1$  than is the right endpoint of  $L_2$ , namely  $(q_2, -p_2)$ . Hence,  $\text{area}(T) < \text{area}(T')$ , where  $T'$  is the triangle with vertices  $(0, 0)$  and  $V_1$  and  $V_2$ . But  $\text{area}(T') = 1/2$  because  $A_1$  and  $A_2$  are Farey related. We get the same contradiction as in the first case. ♠

### 28.3 Proof of Lemma 28.2

Suppose that  $A_1 \bowtie! A_2$ . To show that  $P\Gamma_1$  is well defined, we just have to show  $P\Gamma_2 \subset \Gamma_1$ . This simultaneously shows that  $P\Gamma_1 = P\Gamma_2$ , because the endpoints of these two arcs are the same by definition. We will consider the case when  $A_1 < A_2$ . The other case is similar. In this case, we have  $A_1 = (A_2)_-$ . To simplify our notation, we write  $A = A_2$ . Then  $A_1 = A_-$ .

By Lemma 28.4, it suffices to prove that

$$P\Gamma \subset \Delta(J); \quad J = [-q_- + 2, q - 2]. \quad (389)$$

We have actually already proved this, but it takes some effort to recognize the fact.

Let  $A' \leftarrow A$  denote the inferior predecessor of  $A$ . Since  $q_- > q_+$ , we have

$$A' = A_- \ominus A_+. \quad (390)$$

In the previous chapter, when we proved the Copy Theorem, we established (except for a few special cases)

$$P\Gamma \subset \Delta'(J'); \quad J' = [-q' + 2, q' + q_+ - 2]. \quad (391)$$

Here  $\Delta'$  is defined relative to the linear functionals  $G'$  and  $H'$ , which are defined relative to  $A'$ . The right endpoint in Equation 391 comes from Lemma 18.5. Now observe that

$$q' = q_- - q_+ < q_-; \quad q' + q_+ < (q_- - q_+) + q_+ = q_- < q. \quad (392)$$

These calculations show that  $J \subset J'$ . Usually  $J'$  is much larger.

The region  $\Delta(J)$  is computed relative to the parameter  $A$  whereas the region  $\Delta'(J')$  is computed relative to the parameter  $A'$ . The same argument as in Lemma 27.13 shows that

$$\Delta(J) \subset \Delta'(J') \quad (393)$$

except when  $q_2 < 20$ . The point is that the much larger size of  $J'$  compensates for any tiny difference between the pairs  $(G, G')$  and  $(H, H')$  defining the sets.

We check the remaining few cases by hand. This completes the proof.

**Remark:** By taking  $A_1 < A_2$  we omitted the case when  $B_1 = 1/(2k)$  and  $A_2 = 1/(2k + 1)$ . In this nearly trivial case,  $E^- = (-1, 1)$  and  $E^+ = (0, 0)$ .

## 28.4 Proof of the Structure Lemma

We will consider the case when  $A_- \leftarrow A$ . The other case is similar. Let  $B$  be the odd rational such that  $A_- \bowtie! B$ . Then  $P\Gamma(A_-) = P\Gamma(B)$  by definition.

**Lemma 28.5** *The Structure Lemma holds when  $1/1 \leftarrow A$ .*

**Proof:** In this case

$$A = \frac{2k-1}{2k+1}; \quad A_- = \frac{k-1}{k}; \quad B = \frac{2k-3}{2k-1}. \quad (394)$$

Then  $P\Gamma(A)$  is the line segment connecting  $(0,0)$  to  $(-k,k)$  and  $P\Gamma(B)$  is the line segment connecting  $(0,0)$  to  $(-k+1, k-1)$ . ♠

In all other cases, we have  $A' \leftarrow A$ , where  $A' \neq 1/1$ . As in Lemma 18.2, let

$$\delta = \delta(A', A) = \text{floor}\left(\frac{q'}{q}\right).$$

**Lemma 28.6** *If  $\delta = 1$  then the structure Theorem holds by induction.*

**Proof:** If  $\delta(A', A) = 1$  then  $d(A', A) = 0$ . If  $d(A', A) = 0$  then  $P\Gamma = P\Gamma'$  by the Copy Theorem and the definition of pivot arcs. At the same time, we can apply Lemma 18.2 to the pair  $A_m = A'$  and  $A_{m+1} = A$ . Since  $\delta(A', A) = 1$ , we must have Case 1 or Case 3. But we also have  $A_- < A_+$ . Hence, we have Case 3. But then  $A'_- = A_-$ . Hence, we can replace the pair  $(A_-, A)$  by the pair  $(A'_-, A')$ , and the result follows by induction on the size of the denominator of  $A$ . ♠

**Lemma 28.7** *Suppose that  $\delta = 2$ . Then  $A' = B$ .*

**Proof:**  $B$  is characterized by the property that  $A_-$  and  $B$  are Farey related, and

$$2q_- > \text{denominator}(B) > q_-.$$

We will show that  $A'$  has this same property. Note that  $A'$  and  $A_-$  are Farey related. The equations

$$2q' < q; \quad q = q_+ + q_-; \quad q' = q_+ - q_-$$

lead to

$$3q_- > q_+ \quad \implies \quad 2q_- > (q_+ - q_-) = q'.$$

This establishes the first property for  $A'$ . The fact that  $\delta = 2$  gives  $3q' > q$ . This leads to

$$q_+ > 2q_-; \quad \implies \quad q' = q_+ - q_- > q_-.$$

This is the second property for  $A'$ . ♠

**Lemma 28.8** *Suppose  $\delta \geq 3$ . Then  $A' \leftarrow B$ .*

**Proof:** There is some even rational  $C$  such that

$$B = A_- \oplus C \tag{395}$$

The denominator of  $C$  is smaller than the denominator of  $A_-$ , because of the fact that  $A_- \bowtie! B$ . The inferior predecessor of  $B$  is  $A_- \ominus C$ . At the same time,

$$A' = A_+ \ominus A_- \tag{396}$$

So, we are trying to show that  $A_+ \ominus A_- = A_- \ominus C$ . This is the same as showing that

$$C = D := A_- \oplus A_- \ominus A_+. \tag{397}$$

Since  $A_+$  and  $A_-$  are Farey-related,  $D$  and  $A_-$  are Farey related. We claim that

$$2q_- - q_+ = \text{denominator} \in (0, q_-). \tag{398}$$

The upper bound comes from the fact that  $q_+ > q_-$ . The lower bound comes from the fact that  $q_+ < 2q_-$ . To see this last equation, note

$$q = q_+ + q_-; \quad q' = q_+ - q_-; \quad 3q' < q.$$

But  $C$  is the only even rational that is Farey related to  $A_-$  and satisfies equation 398. Hence  $C = D$ . ♠

As we already proved, the case  $\delta = 1$  is handled by induction on the denominator of  $A$ . The case  $\delta = 2$  gives

$$P\Gamma_- = P\Gamma'.$$

In this case, the Structure Lemma follows from the definition of the pivot points.

When  $\delta \geq 3$ , the rational  $A'$  is a common inferior predecessor of  $A$  and  $B$ . Since  $A_+ = A' \oplus A_-$  and  $A_- < A_+$ , we have  $A' > A_+$ . Hence  $A' > A$ .

**Lemma 28.9**  $A' > B$ .

**Proof:** Lemma 28.8 gives

$$A' = A_- \ominus C; \quad A_+ = A' \oplus A_-; \quad A = A_+ \oplus A_-; \quad B = A_- \oplus C. \quad (399)$$

This gives us

$$A \ominus B = A_+ \ominus C = A' \oplus A_- \ominus C = A' \oplus A'.$$

Hence

$$A = B \oplus A' \oplus A'. \quad (400)$$

Since  $A_+ = A' \oplus A_-$  and  $A_- < A_+$ , we have  $A' > A_+$ . Hence  $A' > A$ . By Equation 400,  $A$  lies between  $A'$  and  $B$ . Hence  $B < A < A'$ . Hence  $A' > B$ . In short,  $A' > A$  and  $A' > B$ . ♠

Finally, from the definition of Pivot Points, we have  $E^+(A) = E^+(B)$ . This establishes Statement 1. Statement 2 has a similar proof.

Now for Statement 3. By Lemma 27.1,

$$E^+(A) + E^-(A) = -A_- + (0, 1); \quad E^+(B) + E^-(B) = -B_+ + (0, 1).$$

Since  $E^+(A) = E^+(B)$ , we have

$$E^-(B) - E^-(A) = A_- - B_+ = V(C) \quad (401)$$

Here  $V(C)$  is as in Equation 21 defined relative to  $C$ . We now have

$$\begin{aligned} E^-(A) + V - E^-(A_-) &= E^-(A) - E^-(B) + V = -V(C) + V(A) = \\ V(A_+ \oplus A_-) - V(A_+ \ominus A_-) &= 2V(A_-) \in \mathbf{Z}(V_-). \end{aligned} \quad (402)$$

This completes the proof of Statement 3. Statement 4 is similar.

## 28.5 The Decrement of a Pivot Arc

Here we work out the precise relationship between the pivot arcs in the Structure Lemma.

Let  $A$  be an odd rational, and let  $A'$  be the superior predecessor of  $A$ . By the Copy Theorem,  $P\Gamma$  contains at least one period of  $\Gamma'$ , starting from either end. Let  $\gamma'$  be one period of  $\Gamma'$  starting from the right endpoint of  $P\Gamma$ . We define  $DPT\Gamma$  by the following formula.

$$P\Gamma = DPT\Gamma * \gamma', \quad (403)$$

The operation on the right hand side of the equation is the concatenation of arcs. We call  $DPT\Gamma$  the *decrement* of  $P\Gamma$ .

The arc  $DPT\Gamma$  is a pivot arc relative to a different parameter. (See the next lemma.)  $DPT\Gamma$  is obtained from  $P\Gamma$  by deleting one period of  $\Gamma'$ . Now we give an *addendum* to the Structure Lemma.

**Lemma 28.10** *If  $B \Leftarrow A$  then  $P\Gamma(B) = DPT\Gamma(A)$ , up to translation.*

**Proof:** We will consider the case when  $A_- \Leftarrow A$ . The other case, when  $A_+ \Leftarrow A$ , has essentially the same proof. We re-examine Lemmas 28.7 and 28.8. In Lemma 28.7, we have

$$P\Gamma_- = P\Gamma'.$$

However, in this case,  $\delta(A, A') = 2$ , and from the definition of pivot points we see that  $P\Gamma$  is obtained from  $P\Gamma'$  by concatenating a single period of  $\Gamma'$ . This gives us what we want.

In Lemma 28.8, we have Equation 400, which implies

$$\text{denominator}(A) = \text{denominator}(B) + 2q'. \quad (404)$$

But this implies that  $d(A', A) = d(A', B) + 1$ . Applying the Copy Theorem to both pairs, we see that  $P\Gamma$  is obtained from  $P\Gamma'$  by concatenating  $d(A, B) + 1$  periods of  $\Gamma'$  where  $P\Gamma_-$  is obtained from  $P\Gamma'$  by concatenating  $d(A', B)$  periods of  $\Gamma'$ . This gives us the desired relationship. ♠

## 28.6 A Corollary of the Structure Lemma

For each even rational  $A_2 \in (0, 1)$  that is not of the form  $1/q_2$ , there is another even rational  $A_1 = p_1/q_1 \in (0, 1)$  such that  $q_1 < q_2$  and  $A_1 \bowtie A_2$ . In this section we prove that the Structure Lemma above implies the same result for  $A_1$  and  $A_2$ .

Consider Statement 1. Let  $A_3 = A_1 \oplus A_2$ . Then  $A_1 \Leftarrow A_3$  and  $A_2 \bowtie! A_3$ . Note that  $E_2^+ = E_3^+$  by definition. Also,  $E_1^+ = E_3^+$  by the Structure Lemma. Hence  $E_1^+ = E_2^+$ . This proves Statement 1 for the pair  $(A_1, A_2)$ . Statement 2 has the same kind of proof.

Consider Statement 3. We have  $E_2^- = E_3^-$  and

$$E_3^- - E_1^- + V_3 \in \mathbf{Z}V_1. \quad (405)$$

On the other hand

$$V_3 = V_2 + V_1; \quad \implies \quad E_3^- - E_1^- + V_2 \in \mathbf{Z}V_1. \quad (406)$$

The first equation implies the second. But  $E_3^- = E_2^-$ . This finishes the proof of Statement 3. Statement 4 has the same kind of proof.

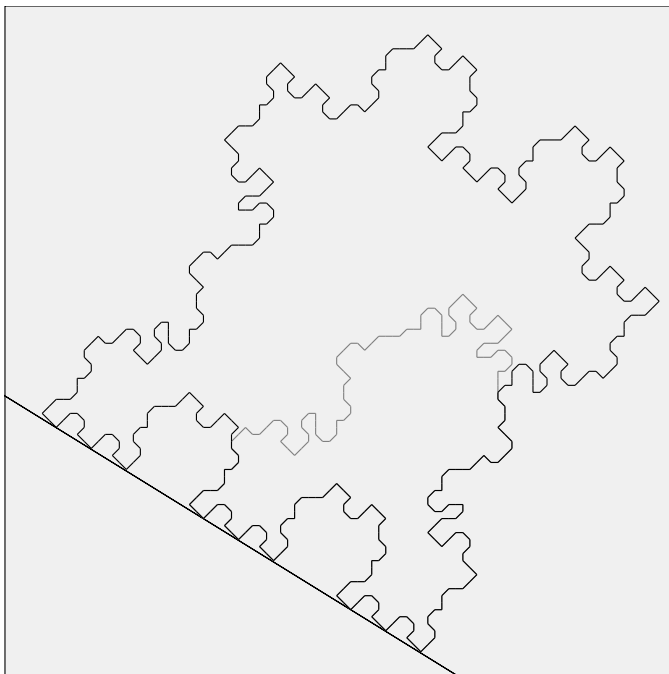


**Figure 28.3:**  $\Gamma(34/55)$  in black and  $\Gamma(21/34)$  in grey.

## 28.7 An Even Version of the Copy Theorem

Let  $A_2$  be an even rational. We write  $A_2 = A_0 \oplus A_1$  where  $A_0$  is odd and  $A_1$  is even.

**Lemma 28.11**  $P\Gamma_2 \subset \Gamma_0$ .

**Proof:** We have  $P\Gamma_2 = P\Gamma(A_3)$ , where  $A_3$  is the odd rational such that  $A_2 \bowtie A_3$ . Since  $A_1 \bowtie A_2$  and both  $A_1$  and  $A_2$  are even, we have  $A_3 = A_1 \oplus A_2$ . At the same time, we have  $A_0 = A_2 \ominus A_1$ . Hence  $A_0 \leftarrow A_3$ . But now we can apply the Copy Theorem to the pair  $(A_0, A_3)$  to conclude that  $P\Gamma_3 \subset \Gamma_0$ . But  $P\Gamma_3 = P\Gamma_2$ . ♠

## 29 Proof of the Pivot Theorem

### 29.1 An Exceptional Case

We first prove the Pivot Theorem for the parameter  $A = 1/q$ , with  $q \geq 2$  being either even or odd. This case does not fit the general pattern of proof.

Let  $\Gamma$  be the arithmetic graph associated to  $A = 1/q$ , and let  $P\Gamma$  denote the pivot arc. In all cases,  $P\Gamma$  contains the vertices  $(0, 0)$  and  $(-1, 1)$ . These vertices correspond to the two points

$$\left(\frac{1}{q}, -1\right); \quad \left(2 - \frac{1}{q}, -1\right) \quad (407)$$

These two points are the midpoints of the special intervals

$$I_1 = \left(0, \frac{2}{q}\right) \times \{-1\} \quad I_2 = \left(2 - \frac{2}{q}, 2\right) \times \{-1\}. \quad (408)$$

These intervals appear at either end of

$$I = [0, 2] \times \{-1\}. \quad (409)$$

When we say *special interval*, we refer to the discussion in §2.2. These special intervals are permuted by the outer billiards dynamics.

For any  $A < 1/2$ , our phase portrait in Figure 2.4 shows that the interval

$$I_3 = (2A, 2 - 2A) \times \{-1\} \quad (410)$$

returns to itself under one iterate of  $\Psi$ . When  $A = 1/q$ , we have

$$I - I_3 = I_1 \cup I_2. \quad (411)$$

But then the orbit of  $I_1$  only intersects  $I$  in  $I_1 \cup I_2$ . In terms of the arithmetic graph, this is to say that the only low vertices on  $\Gamma$  are equivalent to  $(0, 0)$  and  $(-1, 1)$  modulo translation by  $V = (-q, 1)$ . This establishes the Pivot Theorem for  $A = 1/q$ .

### 29.2 Discussion of the Proof

Now we consider the general case of the Pivot Theorem. We will consider the odd case until the last section of the chapter. At the end, we will explain the

minor differences in the even case. For any odd rational  $A_2 \neq 1/q_2$ , we have  $A_1 \Leftarrow A_2$ , where  $A_1 \in (0, 1)$  is an even rational. See §28.1. By induction, we can assume that the Pivot Theorem is true for  $A_1$ . Our discussion refers to Figure 29.1.

Lemma 28.4 gives a large region  $\Delta$  where  $\widehat{\Gamma}_1$  and  $\widehat{\Gamma}_2$  agree.  $\Delta$  is white in Figure 29.1. The arc  $\Gamma_2$  is drawn in black and the relevant components of  $\widehat{\Gamma}_1$  are drawn in grey. The black dots are the endpoints of the black arc. This black arc is “the hump” that we discussed in connection with the Structure Lemma in the previous chapter. Indeed, Figure 29.1 is a cartoon of Figure 28.2, with other relevant details added.

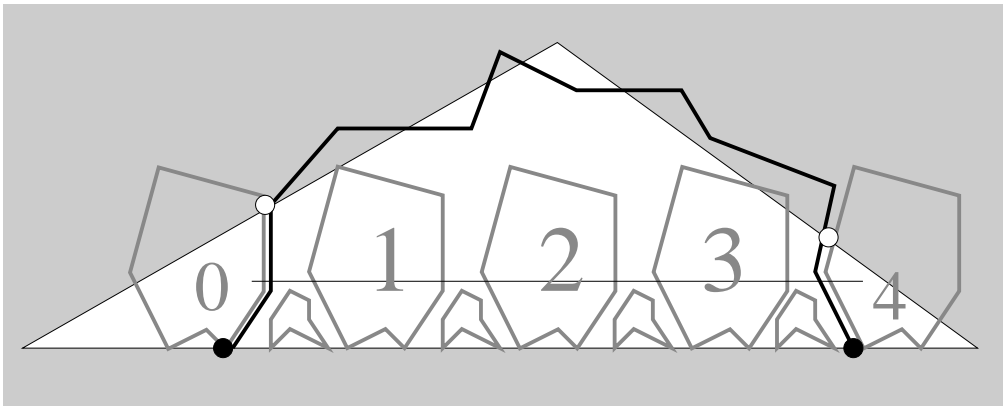


**Figure 29.1:** Cartoon view of the proof

We want to see that the black arc has no low vertices except for its endpoints. By the structure Lemma, the endpoints of the black arc are also endpoints of the pivot arcs of  $C_0$  and  $C_4$ . By induction, the only low vertices of  $C_0$  and  $C_4$  are contained on the pivot arcs. These pivot arcs are on the other sides of the endpoints we are considering. Hence there are no low vertices on the black arc as long as it coincides with either  $C_0$  or  $C_4$ .

There is one subtle point to our argument. When we refer to *low vertices* of the black arc, the vertices are low with respect to the parameter  $A_2$ . However, when we refer to low vertices of  $C_0$  and  $C_4$ , the vertices are low with respect to  $A_1$ . Will discuss this subtle point in the next section. What saves us is that the two notions of *low* coincide, due to the way in which  $A_1$  approximates  $A_2$ .

So, either end of our black arc starts out well: It rises away from the baseline. What could go wrong? One of the ends could dip back down into

$\Delta$  and (at the boundary) merge with a component of  $\widehat{\Gamma}_1$ . In other words, some component of  $\widehat{\Gamma}_1$  would have to stick out of  $\Delta$ .

There are two kinds of components of  $\widehat{\Gamma}_1$  we need to consider. First, there are the major components. Recall from §17.1 that these are the translates of  $\Gamma_1$  by vectors in  $\mathcal{Z}V_1$ . We have labelled these components  $C_1, C_2, C_3$ . Second, there are the minor components – the low components that are not major.

The components that seem to give us the most trouble are  $C_1$  and  $C_3$ . These come the closest to sticking out of  $\Delta$ . In fact, we will not be able to show that these components are contained in  $\Delta$ , even though experimentally it is always the case. However, Lemma 2.9 comes to the rescue. The low vertices on these components have odd parity, and the low vertices on the black arc (a subset of  $\widehat{\Gamma}_2$ ) have even parity. Hence, the black arc cannot merge with  $C_1$  and  $C_3$ . The parity argument steps in where our geometry fails.

The remaining major components are much farther inside  $\Delta$ , and do not pose a threat. We will give an explicit estimate to show that the other major components are contained entirely inside  $\Delta$ . In this case, we are referring to  $C_2$ , though in general there could be many such components.

This leaves the minor components. The Barrier Theorem from §17 handles these. The black horizontal line in Figure 29.1 represents the barrier, which no minor component can cross. Equipped with the Barrier theorem, we will be able to show that all minor components lie in  $\Delta$ .

This takes care of all the potential problems. Since the black arc can't merge with any of the grey components, it just skips over everything and has no low vertices, except for its endpoints. The rest of the chapter is devoted to making this cartoon description precise.

As with the proof of the Decomposition Theorem, the estimates we make are true by a wide margin when  $A_1$  is large. However, when  $A_1$  is small, the estimates are close and we need to deal with the situation in a case-by-case way. We hope that this fooling around with small cases doesn't obscure the basic ideas in the proof.

We close this section by remarking on a phenomenon that we cannot establish. Experimentally, we see that  $\widehat{\Gamma}_2$  copies all the low components of  $\widehat{\Gamma}_1$  beneath “the hump”. The interested reader can see this in action using Billiard King.

### 29.3 Confining the Arc

We continue with the notation from the previous section. For ease of exposition, we assume that  $A_1 < A_2$ . The other case is similar. For ease of notation, we set  $A = A_2$ . Until the end of this section, we only consider  $A$ . We write one period of  $\Gamma$  as  $P\Gamma \cup \gamma$ . Here  $P\Gamma$  is the pivot arc, and  $\gamma$  is the black arc considered in the previous section.

Let  $W$  be the vector from Equation 21. Let  $S$  be the infinite strip whose left edge is the line through  $(0, 0)$  parallel to  $W$  and whose right edge is the line through  $V_+$  and parallel to  $W$ . Here  $V_+ = (q_+, -p_+)$ , and  $p_+/q_+$  is as in Equation 27.

**Lemma 29.1**  *$\gamma$  does not cross the lines bounding  $S$ .*

**Proof:** The lines of  $S$  are precisely the extensions of the sides of  $R_2$ , the larger of the two parallelograms from the Decomposition Theorem. We know that  $\Gamma$  crosses these lines only once. The left crossing point is  $(0, 0) \in P\Gamma$ . Hence, the left crossing point is not a vertex of  $\gamma$ .

The right crossing point is  $x = V_+ + (0, 1)$ . Let  $\mathbf{J}$  be the symmetry from Lemma 13.5. Let  $\iota(v) = V_+ - v$ . Consider the map  $\phi = \iota \circ \mathbf{J}$ . On low vertices  $v$ , we have

$$\phi(v) = V_+ - v + (0, 1). \quad (412)$$

Hence  $\phi(0, 0) = x$ . By Lemma 27.1,  $\phi$  swaps the endpoint of  $\gamma$ . Moreover,  $\phi$  permutes the set of low vertices of  $\gamma$ .

Since  $V_+$  lies beneath the baseline,  $x$  is a low vertex. If  $x$  is a low vertex of  $\gamma$  then  $\phi(x) = (0, 0)$  is a low vertex of  $\gamma$ . This is a contradiction. Hence  $x$  is not a low vertex of  $\gamma$ . ♠

Now we can clear up the subtlety discussed in the previous section. We set  $S_2 = S$ , the strip defined relative to the odd rational  $A_2$ .

**Lemma 29.2** *A vertex in  $S_2$  is low with respect to  $A_1$  iff it is low with respect to  $A_2$ . Hence, a vertex of  $\gamma$  is low with respect to  $A_1$  iff it is low with respect to  $A_2$ .*

**Proof:** Let  $L_j$  denote the baseline with respect to  $A_j$ . The conclusion of this lemma is equivalent to the statement that there is no lattice point between  $L_1 \cap S$  and  $L_2 \cap S$ . This is a consequence of our proof of Lemma 28.4. ♠

## 29.4 A Topological Property of Pivot Arcs

Let  $A$  be a rational kite parameter, either even or odd. Let  $P\Gamma$  denote the pivot arc of  $\Gamma = \Gamma(A)$ . The two endpoints of  $P\Gamma$  are low vertices. Here we prove a basic structural result about  $P\Gamma$ .

**Lemma 29.3**  *$P\Gamma$  contains no low vertex to the right of its right endpoint. Likewise  $P\Gamma$  contains no low vertex to the left of its left endpoint.*

**Proof:** We will prove the first statement. The second statement has the same proof. We give an argument like the one in the proof of Lemma 2.9. Note that  $\Gamma$  right-travels at  $(0,0)$ . Hence  $P\Gamma$  right-travels at its right endpoint  $\rho$ . Suppose that  $P\Gamma$  contains a low vertex  $\sigma$  to the right of  $\rho$ . Then some arc  $\beta$  of  $P\Gamma$  connects  $\rho$  to  $\sigma$ . Since  $\Gamma$  right travels at  $\rho$ , some arc  $\gamma$  of  $\Gamma - P\Gamma$  enters into the region between  $\rho$  and  $\sigma$  and beneath  $\beta$ . But  $\gamma$  cannot escape from this region, by the Embedding Theorem. The point here is that  $\gamma$  cannot squeeze beneath a low vertex, because the only vertices below a low vertex are also below the baseline. Figure 29.2 shows the situation.

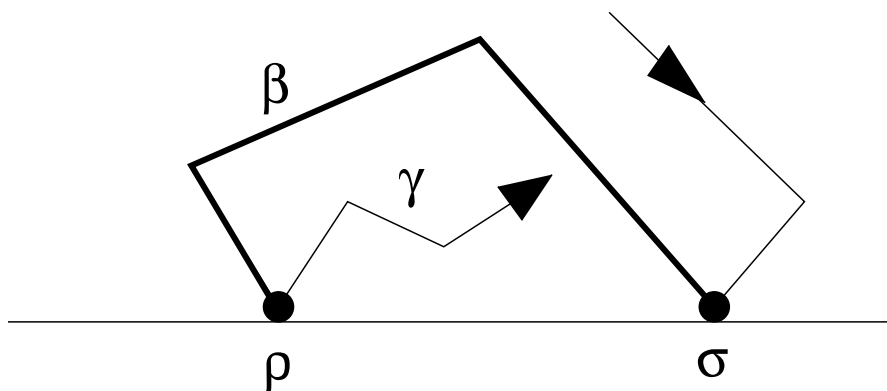


**Figure 29.2:**  $P\Gamma$  creates a pocket.

In the odd case we have an immediate contradiction. In the even case, we see that there must be a loop containing both  $\rho$  and  $\sigma$ . This loop must be a closed polygon, and a subset of  $P\Gamma$ . Since  $P\Gamma$  is also a closed (and embedded) polygon, we our loop must equal  $P\Gamma$ . But by definition,  $P\Gamma$  lies below  $\Gamma - P\Gamma$ . From Figure 29.3, we see that  $P\Gamma$  (which contains  $\beta$ ) in fact lies above  $\Gamma - P\Gamma$  (which contains  $\gamma$ .) This is a contradiction. ♠

## 29.5 Corollaries of the Barrier Theorem

Here we derive a few corollaries of the Barrier Theorem. See §17 for the statement.

**Corollary 29.4** *A minor component of  $\widehat{\Gamma}$  cannot cross the line through  $(0, 0)$  that is parallel to  $W$ .*

**Proof:** Our line is one of the lines in the Hexagrid Theorem. By the Hexagrid Theorem, only  $\Gamma$  crosses this line beneath the barrier, and the crossing takes place at  $(0, 0)$ . ♠

We are trying to construct a parallelogram that bounds the minor components. The baseline contains the bottom edge. The barrier contains the top edge. The line in Corollary 29.4 contains the left edge. Now we supply the right edge. Actually, there are many choices for this right edge.

**Lemma 29.5** *Let  $V_+ = (q_+, -p_+)$ . A minor component of  $\widehat{\Gamma}$  cannot cross the line through  $(0, 0)$  that is parallel to  $V_+ + kV$  for any  $k \in \mathbf{Z}$ .*

**Proof:** Since  $\widehat{\Gamma}$  is invariant under translation by  $V$ , it suffices to prove this result for  $k = 0$ . Let  $L$  be the line through  $V_+$  parallel to  $W$ . Our result really follows from the bilateral symmetry discussed in §13.3. Here we work out the details, using the rotational symmetry instead. (We made more precise statements about the rotational symmetry.)

Let  $\Lambda$  be the barrier. Consider the symmetry  $\iota$  defined in §13.2. The two lines  $\Lambda$  and  $\iota(\Lambda)$  are equally spaced above and below the baseline up to an error of at most  $1/q$ . Suppose that some minor component  $\beta$  crosses our line  $L$ . Then the component  $\iota(\beta)$  crosses the line  $\iota(L)$ . But  $\iota(L)$  is the line from Lemma 29.4. Inspecting the hexagrid, we see that  $\iota(L)$  contains the door  $(0, 0)$ , but no other door between the baseline and  $\iota(\Lambda)$ . Indeed, the doors above and below the baseline are just about evenly spaced away from  $(0, 0)$  going in either direction. See Figure 3.2, a representative figure. (In this figure, we are talking about the long axis of the kite, and  $(0, 0)$  is the bottom tip of the kite.)

The component  $\gamma'$  of  $\widehat{\Gamma}$  that crosses  $\iota(L)$  near  $(0, 0)$  has the same size as  $\Gamma$ . Hence, this component crosses through  $\iota(\Lambda)$ . Hence  $\iota(\gamma')$  is a major component. Hence  $\beta \neq \iota(\gamma')$ . Hence  $\iota(\beta) \neq \gamma$ . Hence  $\iota(\beta)$  does not cross  $\iota(L)$ . Hence  $\beta$  does not cross  $L$ . ♠

## 29.6 Juggling Two Parameters

In our proof of the Pivot Theorem, we have two parameters  $A_1 \Leftarrow A_2$ . As above, we focus our attention on the case when  $A_1 < A_2$ . The other case has a completely parallel discussion. See §31.2.3 for a brief discussion of the other case.

Lemma 29.5 applies to vectors defined in terms of  $A_1$ , but we would like to apply it to a special line defined partly in terms of  $A_2$ . Let  $(V_j)_+$  be as in §29.3. Then Lemma 29.5 applies to the vectors of the form  $(V_1)_+ + kV_1$ . However, we are also interested in the vector  $(V_2)_+$ .

**Lemma 29.6** *Suppose that  $A_1 < A_2$ . Then, there is some integer  $k$  such that  $(V_2)_+ = (V_1)_+ + kV_1$ .*

**Proof:** We set  $A = A_2$ . Then  $A_- = A_1$ . Let  $A_{-+}$  denote the parameter that relates to  $A_-$  in the same way that  $A_+$  relates to  $A$ . That is  $A_{-+} > A_-$  are Farey related and  $A_{-+}$  has smaller denominator than  $A_-$ . We want to prove that  $V_+ = V_{-+} + kV_-$  for some  $k$ . The rationals  $A_{-+}$  and  $A_-$  are Farey-related. Therefore, so are the parameters

$$A_-; \quad A_{-+} \oplus A_- \oplus \dots \oplus A_- \tag{413}$$

Here we are doing Farey addition. Conversely, if any rational  $A'$  is Farey related to  $A_-$ , and has bigger denominator, then the Farey difference  $A' \ominus A_-$  is also Farey related to  $A_-$ . Thus, the rationals in Equation 413 account for all the rationals  $A'$  with the properties just mentioned. But  $A_+$  is one such rational. Hence  $A_+$  has the form given in Equation 413. This does it. ♠

Let  $R$  denote the parallelogram defined by the following lines

- The baseline relative to  $A_1$ .
- The barrier for  $A_1$ .
- The line parallel to  $W_1$  through  $(0, 0)$ .
- The line parallel to  $W_1$  through  $(V_2)_+$ .

Then any minor component with one vertex in  $R$  stays completely in  $R$ . This is a consequence of the Barrier Theorem, its corollaries, and the lemma in this section. Modulo a tiny adjustment in the slopes, the left and right edges of  $R$  are contained in the left and right edges of the strip  $S$  considered in §29.3.

## 29.7 A Bound for Minor Components

Let  $A_1 \Leftarrow A_2$  be as above. Again, we assume that  $A_1 < A_2$  for ease of exposition. Define

$$\Delta = \Delta_1(I) \cup \Delta_2(I); \quad I = [-q_1 + 2, q_2 - 2]. \quad (414)$$

Here  $\Delta$  is as in Lemma 28.4. Let  $R$  be the parallelogram discussed in the previous section.

**Lemma 29.7** *Let  $\beta \subset \hat{\Gamma}_1$  be any component that is contained in  $R$ . Then  $\beta \subset \hat{\Gamma}_2$ .*

**Proof:** Our proof follows the same strategy as in the Decomposition Theorem. We will work with the functionals  $G_1$  and  $H_1$  defined relative to  $A_1$ .

Essentially, we want to show that  $R \subset \Delta$  and then apply Lemma 28.4. However, to avoid a messy calculation, we invoke the Adjacent Mismatch Principle, and replace  $R$  by the extremely nearby parallelogram  $\tilde{R}$  with vertices

$$(0, 0); \quad \lambda W_1; \quad (V_2)_+; \quad (V_2)_+ + \lambda W_1. \quad (415)$$

The constant  $\lambda$  has the following definition. The top left vertex of  $R$  lies on the line through  $(0, 0)$  and parallel to  $W_1$ , as we discussed above. Hence this vertex has the form  $\lambda W_1$ . We have

$$M_1(W_1) = M_1\left(0, \frac{p_1 + q_1}{2}\right) = p_1 + q_1; \quad M_1(\lambda W_1) = p'_1 + q'_1 < p_1 + q_1. \quad (416)$$

Here  $A'_1$  is the rational that appears in the Barrier Theorem. The point here is that the barrier contains the point  $(0, (p'_1 + q'_1)/2)$ . In particular,  $\lambda < 1$ .

Let  $u$  and  $w$  be the top left and top right vertices of  $R$ . As usual, it suffices to show that the quantities

$$G_1(u) - (-q_1 + 2); \quad (q_2 - 2) - H_1(w) \quad (417)$$

are both positive. In fact these quantities are equal. As in Equation 218, we compute

$$G_1(u) - (-q_1 + 2) = q_1 - \lambda \frac{q_1^2}{p_1 + q_1} - 2 \quad (418)$$

We will do the second calculation by symmetry. By Lemma 29.6, we have

$$(V_2)_+ + V_1 = (V_2)_+ + (V_2)_- = V_2.$$

Hence

$$V_2 - w = V_1 - \lambda W_1.$$

Hence

$$\begin{aligned} (q_2 - 2) - H_1(w) &= -2 + H_1(V_2 - w) = \\ -2 + H_1(V_1 - \lambda W_1) &= q_1 - \lambda \frac{q_1^2}{p_1 + q_1} - 2 \end{aligned} \quad (419)$$

We get exactly the same answer in both cases. This is a reflection of an underlying affine symmetry, as we remarked after Equations 259 and 260.

Since  $\lambda \leq 1$ , the quantities in Equation 417 are non-negative as long as  $p_1 \geq 3$  and  $q_1 \geq 7$ . This is exactly the same estimate as in Lemma 21.5. When  $p_1 = 2$  we see that

$$p'_1 = 1; \quad q'_1 = \frac{q_1 - 1}{2}.$$

Thus  $\lambda \approx 1/2$ , and we get a massive savings. When  $p_1 \geq 2$  and  $q_1 \leq 7$  we check the cases by hand, using the same trick as in §21.4.

It remains to consider the case  $p_1 = 1$ . In this case  $\widehat{\Gamma}_1$  has no minor components, as we saw in §29.1. ♠

## 29.8 A bound for Major Components

We keep the parameters  $A_1 \Leftarrow A_2$  as above, with  $A_1 < A_2$ . We have already defined the pivot points of  $\Gamma_1$ . We define the pivot points of the translates  $C_k = \Gamma_1 + kV_1$  in the obvious way, by translation.

By the Structure Lemma, there is some component  $C_k$  whose left pivot point is  $E_2^- + V_2$ , the right endpoint of the “hump” discussed in §29.2. The components  $C_0, \dots, C_k$  are exactly as in §29.2. By Lemma 2.9, the index  $k$  is even. More generally,  $C_j$  contains low vertices of even parity if and only if  $j$  is even.

As in §29.2 we are interested in bounding the components  $C_2, \dots, C_{k-2}$ . Actually, we only care about the even components, but our bound works equally well for the odd components between  $C_2$  and  $C_{k-2}$ . If  $k = 2$  one can just ignore the construction in this section.

By the Hexagrid Theorem,  $C_0$  is contained in the parallelogram  $R_0$  with vertices

$$-V_1; \quad -V_1 + 2W_1; \quad V_1 + 2W_1; \quad V_1. \quad (420)$$

This means that  $C_j$  is contained in translated parallelogram

$$R_j = R_0 + jV_1 \tag{421}$$

We choose  $j \in \{2, \dots, k - 2\}$ .

Here we describe some features of  $R_j$ , as well as a recipe for symmerizing it.

1. The bottom edge of  $R_j$  is contained in the line through  $(0, 0)$  and parallel to  $V_1$ —i.e. the baseline, as usual.
2. The top edge of  $R_j$  is contained in the line through  $2W_1$  and parallel to  $V_1$ . These lines are independent of  $j$ .
3. The left edge of  $R_j$  is parallel to, and to the right of, the line  $\Lambda$  parallel to  $W_1$  and containing  $V_1$ . When  $j = 2$  the left edge of  $R_j$  is contained in  $\Lambda$ .
4. The same symmetry argument as in Lemma 29.5 shows that  $C_2$  lies to the left of the line through the point  $(V_2)_+ - V_1$  and parallel to  $W_1$ . Referring to the symmetry  $\iota$  in Lemma 29.5, this is the line  $\iota(\Lambda)$ . In brief, if  $C_j$  crosses  $\iota(\Lambda)$ , then  $\iota(C_j)$  crosses  $\Lambda$ , and this contradicts the Hexagrid Theorem, applied below the baseline.

Let  $R$  be the parallelogram defined by the 4 lines above. By construction  $C_j \subset R$  for  $j \in \{2, \dots, k - 2\}$ .

**Lemma 29.8** *Let  $\beta \subset \Gamma_1$  be any component of  $\widehat{\Gamma}_1$  that is contained in  $R$ . Then  $\beta \subset \widehat{\Gamma}_2$ .*

**Proof:** The proof is exactly the same. Let  $u$  and  $w$  denote the top left and top right vertices of  $R$ . We get the same symmetry as in the previous bound, and so we just have to compute  $G_1(u) \geq -q_1 + 2$ . We compute

$$G_1(u) - (-q_2 + 2) = 2q_1 - \frac{2q_1^2}{p_1 + q_1} - 2. \tag{422}$$

This time we always get a positive number, though in small cases it is pretty close. ♠

## 29.9 Even implies Odd

Let  $P(A)$  be the statement that the Pivot Theorem is true for  $A$ .

**Lemma 29.9** *Let  $A_1 \Leftarrow A_2$ . Then  $P(A_1)$  implies  $P(A_2)$ .*

Our proof follows the format of the discussion in §29.2. As in §29.3, we define the *complementary arc*  $\gamma_2 \subset \Gamma$  to be the arc to the right of  $P\Gamma_2$  such that  $P\Gamma_2 \cup \gamma_2$  is one period of  $\Gamma_2$ . The endpoints of  $\gamma_2$  are

$$E_2^+; \quad E_2^- + V_2. \quad (423)$$

This is the “hump” we discussed in §29.2.

We say that a *spoiler* is a low vertex of  $\gamma_2$  that is not an endpoint of  $\gamma_2$ . The Pivot Theorem is equivalent to the statement that there are no spoilers.

Let  $L(\gamma_2)$  denote the left endpoint of  $\gamma_2$ . Likewise, let  $R(\gamma_2)$  denote the right endpoint of  $\gamma_2$ .

**Lemma 29.10** *Any spoiler lies between  $L(\gamma_2)$  and  $R(\gamma_2)$ .*

**Proof:** We will show that any spoiler lies to the right of  $L(\gamma_2)$ . The statement that any spoiler lies to the left of  $R(\gamma_2)$  is similar. By Lemma 29.1, all spoilers lie in the strip  $S_2$ . But  $P\Gamma_2$  crosses the left boundary of  $S_2$ . Any low vertices in  $S_2$  to the left of  $L(\gamma_2)$  either lie on  $P\Gamma_2$  or beneath it. By the Embedding Theorem,  $\gamma$  cannot contain these vertices. ♠

**Lemma 29.11**  *$\Delta$  contains all the spoilers.*

**Proof:** We will work with the linear functionals  $G_2$  and  $H_2$  defined relative to  $A_2$ . Thus, we are really showing that the smaller set  $\Delta_2(I)$  contains all the spoilers.

Let  $v = (m, n)$  be a spoiler. It suffices to prove that  $G_2(v) \geq -q_0 + 2$  and  $H_2(v) \leq q_2 - 2$ . We have  $m \geq 1$ . Since  $v$  is a low vertex, we have  $n \leq 0$ . We compute that  $\partial_y G_2 < 0$ . Hence

$$G_2(v) \geq G_2(m, 0) = m \frac{1 - A_2}{1 + A_2} > 0 \geq -q_1 + 2.$$

This takes care of  $G_2$ .

Let  $w = v - V_2 = (r, s)$ . By Lemma 19.1, it suffices to show  $H_2(w) \leq -2$ . We compute  $\partial_y H > 0$ . Since  $w$  lies at most one vertical unit above the line of slope  $-A_2$  through the origin, we have

$$H_2(w) \leq H_2(w'); \quad w' = (r, -A_2 r + 1). \quad (424)$$

We compute

$$H_2(w') = r + \frac{2(1 - A_2)}{(1 + A_2)^2} < r + 2. \quad (425)$$

This shows that  $H(w) < -2$  as long as  $r \leq -4$ . By Lemma 2.9, we have  $r + s$  even. We just have to rule out  $(-2, 2)$  and  $(-3, 1)$  as spoilers.

If  $A_2 < 1/2$  then  $(-2, 2)$  is not a low vertex. If  $A_2 > 1/2$  then

$$\frac{2k - 1}{2k + 1} \leftarrow \dots \leftarrow A_2$$

for some  $k \geq 2$ . In this case,  $E_2^-$  has first coordinate  $\leq -2$ . But then  $r \leq -3$ . This rules out  $(-2, 2)$ . We compute that  $H_2(-3, 1) < -2$  when  $A \geq 1/9$ . When  $A < 1/9$ , we use the phase portrait in §2.8 to check that  $\widehat{\Gamma}_2$  is trivial at  $(-3, 1)$ . This rules out  $(-3, 1)$ . ♠

Let  $v$  be a spoiler. By the previous result, there is some component  $\beta$  of  $\widehat{\Gamma}_1$  that has  $v$  as a vertex.

**Lemma 29.12**  *$\beta$  is not a subset of  $\widehat{\Gamma}_2$ .*

**Proof:** Let's start at  $v$  and trace  $\gamma_2$  in some direction. If the conclusion of this lemma is false, we remain simultaneously on  $\gamma_2$  and  $\beta$  until we loop around and return to  $v_2$  – because  $\beta$  is a closed polygon. This contradicts the fact that  $\gamma_2$  never visits the same vertex twice. ♠

Here is the end of the argument.  $\beta$  cannot be a minor component, given the bound in §29.7. Next,  $\beta \notin \{C_2, \dots, C_{k-2}\}$  given the bounds in §29.8. Next,  $\beta \notin \{C_1, C_{k-1}\}$  by Lemma 2.9. Next,  $\beta \neq C_0$ : By induction, all the low vertices of  $C_0$  lie on  $PC_0$ . By Lemma 29.3 these low vertices all lie to the left of the spoiler. Likewise  $\beta \neq C_k$ . We have exhausted all the possibilities.  $\beta$  cannot exist. Hence there is no spoiler. Hence  $P(A_2)$  holds.

## 29.10 A Decomposition in the Even Case

In this section we revisit the construction in §29.3, but for even parameters. Now  $A_1$  and  $A_2$  are both even parameters, with  $A_1 \bowtie A_2$ . We set  $A = A_2$  and just consider objects relative to  $A$ . We define the strip  $S$  exactly as in §29.3. This time we define

$$\gamma = (\Gamma \cup (\Gamma + V)) \cap S. \quad (426)$$

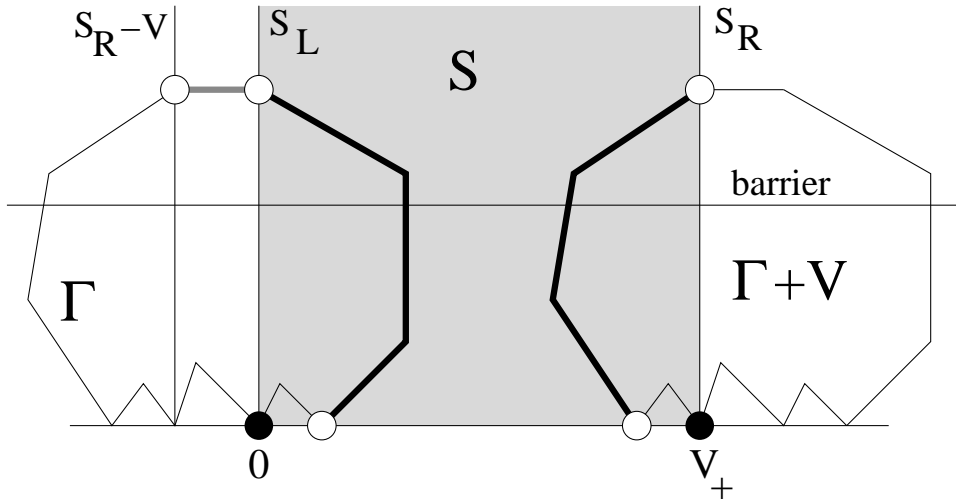


**Figure 29.3:** The even version of  $\gamma$ .

**Lemma 29.13**  $\gamma$  consists of two connected arcs. Any low vertex of  $\Gamma - P\Gamma$  is translation equivalent to a low vertex of  $\gamma$ .

**Proof:** By the Hexagrid Theorem  $\Gamma$  only crosses  $S_L$  once. The door on  $S_L$  lies above the barrier line. Hence, the crossing occurs above the barrier line. Likewise,  $\iota(\Gamma + V)$  only crosses  $S_L$  once. The relevant door lies below the image of the barrier line under  $\iota$ . Here  $\iota$  is as in the proof of Lemma 29.1. But then  $\Gamma + V$  only crosses  $S_R$  once, and the crossing occurs above the barrier line. Hence  $\gamma$  consists of 2 connected arcs.

The line  $S_R - V$  is parallel to  $S_L$  and lies to the left of  $S_L$ . By symmetry,  $\Gamma$  only crosses  $S_R - V$  once, and the crossing takes place above the barrier line. By the Barrier Theorem, the grey arc of  $\Gamma$  between  $S_L$  and  $S_R - V$  lies above the barrier line and hence has no low vertices. Finally, any vertex of  $\Gamma - P\Gamma$  not translation equivalent to a vertex of  $\gamma$  lies on the grey arc of  $\Gamma$  between  $S_L$  and  $S_R - V$ . ♠

## 29.11 Even implies Even

Let  $A_1 \bowtie A_2$  be a pair of even rationals as in §28.6. This pair exists as long as  $A_2 \neq 1/q_2$ . Referring to the terminology in Lemma 29.9, we prove the following result in this section.

**Lemma 29.14** *Let  $A_1 \Leftarrow A_2$ . Then  $P(A_1)$  implies  $P(A_2)$ .*

We have already taken care of the base case of our induction, the case  $A = 1/q$ . Lemma 29.14 and Lemma 29.9 then imply the Pivot Theorem by induction. The proof is essentially the same as in the odd case, once we see that the basic structural results hold. The result in §28.6 gives us the even/even version of the structure lemma.

We consider the case when  $A_1 < A_2$ . The other case is similar. We define spoilers just in the odd case. We just need to show that the arc  $\gamma_2$  defined in the previous section has no spoilers. The same argument as in the odd case shows that a spoiler must lie between  $L(\gamma_2)$  and  $R(\gamma_2)$ , the left and right endpoints.

Let  $\Delta$  be the region of agreement between  $\hat{\Gamma}_1$  and  $\hat{\Gamma}_2$  as above. The formulas are exactly the same. Here is the even version of Lemma 29.11.

**Lemma 29.15**  *$\Delta$  contains all the spoilers.*

**Proof:** The general argument in Lemma 29.11 works exactly the same here. It is only at the end, when we consider the vertices  $(2, -2)$  and  $(3, -1)$  that we use the fact that  $A_2$  is odd. Here we consider these special cases again. The argument for  $(-3, 1)$  does not use the parity of  $A_2$ . We just have to consider  $(-2, 2)$ .

If  $A_2 < 1/2$  then  $(-2, 2)$  is not a low vertex. We don't need to treat the extremely trivial case when  $A_2 = 1/2$ . When  $A_2 > 1/2$  we have  $A_1 > 1/2$  as well. The point is that no edge of the Farey graph crosses from  $(0, 1/2)$  to  $(1/2, 1)$ . Hence  $A_3 = A_1 \oplus A_2 > 1/2$  as well. But, by definition, the pivot points relative to  $A_2$  are the same as for  $A_3$ . This is as in §28.6. Hence, the same argument as in Lemma 29.11 now rules out  $(2, -2)$ . ♠

Essentially the same argument as in the odd case now shows that  $\gamma_2$  contains no spoilers.

## 30 Proof of the Period Theorem

### 30.1 Inheritance of Pivot Arcs

Let  $A$  be some rational parameter. For each polygonal low component  $\beta$  of  $\Gamma(A)$ , we define the pivot arc  $P\beta$  to be the lower arc of  $\beta$  that joins the two low vertices that are farthest apart. We say *lower arc* because all the components are closed polygons, and hence two arcs join the pivot points in all cases. When  $A$  is an even rational and  $\beta = \Gamma$ , this definition coincides with the definition of  $P\Gamma$ , by the Pivot Theorem. In general, we say that a pivot arc of  $\Gamma$  is a pivot arc of some low component of  $\widehat{\Gamma}$ . We call a pivot arc of  $\widehat{\Gamma}$  *minor* if it is not a translate of  $P\Gamma$ .

Here we recall the definitions of the odd and even predecessors of rationals in  $(0, 1)$ . Aside from a few trivial cases, the predecessors exist and are rationals in  $(0, 1)$ .

1. When  $A$  is odd,  $A'$  is as in the inferior sequence.
2. When  $A$  is odd,  $A''$  is as in the Structure Lemma and Lemma 29.9.
3. When  $A$  is even,  $A'$  is as in the Barrier Theorem.
4. When  $A$  is even,  $A''$  is as in Lemma 29.14.

It is worth mentioning another characterization of these numbers.

$$A \text{ even} \quad \implies \quad A = A' \oplus A''. \quad (427)$$

$$A \text{ odd} \quad \implies \quad A = A' \oplus A'' \oplus A''. \quad (428)$$

**Lemma 30.1 (Inheritance)** *Let  $A$  be any rational. Suppose that*

$$A' \leftarrow A; \quad A'' \leftarrow A.$$

*Then, every minor pivot arc  $\beta$  of  $\widehat{\Gamma}$  is either a minor pivot arc of  $\widehat{\Gamma}'$  or a pivot arc of  $\widehat{\Gamma}''$ . The set of low vertices of  $\beta$  is the same when considered either in  $A$  or in the relevant predecessor.*

We first prove the odd case and then we prove the even case. The proof is almost the same in both case.

**Proof in the Odd Case:** Recall that  $P\Gamma \cup \gamma$  is one period of  $\Gamma$ . There are two kinds of minor components of  $\widehat{\Gamma}$ .

1. Those pivot arcs that lie underneath  $P\Gamma$ .
2. Those pivot arcs that lie underneath  $\gamma$ .

We can push harder on Lemma 28.2. Since  $P\Gamma$  lies in the set  $\Delta$  from Lemma 28.4, so does every low component of  $\widehat{\Gamma}$  underneath  $P\Gamma$ . To see this, recall that our proof involved showing that  $P\Gamma \subset \Delta$ . But, if a point of  $P\Gamma$  lies in  $\Delta$ , then so does the entire line segment connecting this point to the baseline. Hence, all components of  $\widehat{\Gamma}$  beneath  $P\Gamma$  also belong to  $\Delta$ . Hence, the low components of  $\widehat{\Gamma}$  lying underneath  $P\Gamma$  coincide with the low components of  $\widehat{\Gamma}'$  lying underneath  $P\Gamma'$ . This takes care of the first case.

In the second case, our proof of Lemma 29.9 shows that every minor component of  $\widehat{\Gamma}''$  lying inside  $\Delta(A'', A)$  is contained in  $\widehat{\Gamma}$ . We showed the same result for every major component except the ones we labelled  $C_1$  and  $C_{k-1}$ . Note that the pivot arcs are subject to the Barrier Theorem. That is, the two crossings from the Barrier theorem occur on the upper arcs rather than on the pivot arcs. Hence, the pivot arcs behave exactly as the minor components. Hence, the pivot arcs of  $C_1$  and  $C_{k-1}$  are copied by  $\widehat{\Gamma}$ , even though the upper arcs might not be. By Lemma 29.11, every low vertex of  $\widehat{\Gamma}$  lying underneath  $\gamma$  lies on the pivot arcs of the components we have just considered. This takes care of the second case.

There is only one detail we need to take care of. A vertex of the kind we are considering is low relative to  $A'$  or  $A''$  is low if and only if it is low with respect to  $A$ . This follows from the basic property of  $\Delta$ . See our geometric proof of Lemma 28.4. Thus, every low component of  $\widehat{\Gamma}$  of the kind we have considered is also low relative to  $\widehat{\Gamma}'$  or  $\widehat{\Gamma}''$ , whichever is relevant. Likewise, the converse holds. ♠

**Proof in the Even Case:** The minor pivot arcs of  $\widehat{\Gamma}$  come in two kinds, those that lie underneath  $P\Gamma$  and those that do not. By the same argument as in the odd case, the pivot arcs of the first kind are all minor pivot arcs of  $\Gamma(A^*)$  where  $A^*$  is such that  $A \bowtie! A^*$ . But then  $A^* = A \oplus A''$ . Hence  $A'' \leftarrow A^*$ . At the same time,  $A' = A \ominus A''$ . Hence  $A' \leftarrow A^*$ . Applying the odd case of the Inheritance Lemma to the triple  $(A^*, A', A'')$ , we see that every pivot arc of  $\widehat{\Gamma}$  beneath  $P\Gamma$  is a pivot arc of either  $\widehat{\Gamma}'$  or  $\widehat{\Gamma}''$ . This takes care of the first case. The second case is just like the odd case. ♠

## 30.2 Freezing Numbers

Every rational parameter has an odd and an even predecessor. Starting with (say) an odd rational  $A$ , we can iterate the construction and produce a tree of simpler rationals. If  $B$  lies on this tree we write  $B \prec A$ . Here is an immediate corollary of the Inheritance Lemma.

**Corollary 30.2** *Every minor pivot arc of  $\widehat{\Gamma}(A)$  is a pivot arc of  $\widehat{\Gamma}(B)$  for some even  $B$  such that  $B \prec A$ .*

Let  $A$  be an odd rational. Let  $\beta$  be a minor component of  $\widehat{\Gamma}(A)$ . We define  $F(\beta, A)$  to be the smallest denominator of a rational  $B \prec A$  such that  $P\beta$  is a pivot arc of  $\widehat{\Gamma}(B)$ . We call  $F(\beta, A)$  the *freezing number* of  $\beta$ .

**Lemma 30.3** *The  $\Psi$ -period of a minor component  $\beta$  is at most  $20s^2$ , where  $s = F(\beta, A)$ .*

**Proof:** This is an immediate consequence of the Hexagrid Theorem, applied to the rational  $B = r/s$  such that  $\beta$  is a component of  $\widehat{\Gamma}(B)$ . The Hexagrid Theorem confines  $\beta$  to a parallelogram of area less than  $20s^2$ . ♠

Let  $x \in I$  correspond to a point not on  $C(A_n)$ . We let

$$F(x, n) = F(\beta_x, A_n),$$

where  $\beta_x$  is the component of  $\widehat{\Gamma}_n$  corresponding to  $x$ . We say that a *growing sequence* is a sequence  $\{x_n\}$  such that  $F(x_n, n) \rightarrow \infty$ . Recall that  $C_A$  is the Cantor set from the Comet Theorem.

**Lemma 30.4** *Suppose every growing sequence has  $(0, -1)$  as a limit point. Then the Period Theorem is true for  $A$ .*

**Proof:** If the Period Theorem is false, then we can find a sequence of points  $\{x_n\}$  in  $G_n$  such that the distance from  $x_n$  to  $C_n$  is uniformly bounded away from 0, and yet the period of  $x$  tends to  $\infty$ . But then Lemma 30.3 shows that  $\{x_n\}$  is a growing sequence. By construction  $\{x_n\}$  does not have a limit point on  $C_A$ . In particular,  $(0, -1)$  is not a limit point. ♠

### 30.3 A Weak Approximation Result

Let  $\{A_n\}$  be the odd sequence of rationals above. For each  $n$  we can form the tree of predecessors, as above. Suppose we choose some proper function  $m(n)$  such that  $B_m \prec A_n$  is some even rational in the tree for  $A_n$ .

**Lemma 30.5**  $\lim_{n \rightarrow \infty} B_m = A$ .

**Proof:** We consider the picture in the hyperbolic plane, relative to the Farey triangulation. See §18.1 for definitions. We consider the portion  $G$  of the Farey graph consisting of edges having both endpoints in  $[0, 1]$ . We direct each edge in  $G$  so that it points from the endpoint of smaller denominator to the endpoint of larger denominator. The two endpoints never have the same denominator, so our definition makes sense. Say that the *displacement* of a directed path in  $G$  is the maximum distance between a vertex of the path and its initial vertex.

Given and  $\epsilon > 0$  there are only finitely many vertices in  $G$  that are the initial points of directed paths having displacement greater than  $\epsilon$ . This follows from the nesting properties of the half-disks bounded by the edges in  $G$ , and from the fact that there are only finitely many edges in  $G$  having diameter greater than  $\epsilon$ .

Given the nature of the tree of predecessors, there is a directed path in  $G$  connecting  $B_m$  to  $A_n$ . The displacement of this path tends to 0 as  $n \rightarrow \infty$  because  $\{B_m\}$  is an infinite list of rationals with only finitely many repeaters. Also, the distance from  $A_n$  to  $A$  tends to 0. Hence, the distance from  $B_m$  to  $A$  tends to 0 by the triangle inequality. ♠

### 30.4 The End of the Proof

To finish our proof, we must show that every growing sequence has an accumulation point on  $C_A$ . We will prove this indirectly, using the Rigidity Lemma from §5.3. Let us first explain the input from the Rigidity Lemma.

Let  $\{B_m\}$  be any sequence of even rationals converging to the irrational parameter  $A$ . Then the Rigidity Lemma implies that the limits

$$\lim_{m \rightarrow \infty} \Gamma(A_m); \quad \lim_{m \rightarrow \infty} \Gamma(B_m) \quad (429)$$

agree. In other words, longer and longer portions of  $\Gamma(A_m)$  look like longer and longer pictures of  $\Gamma(B_m)$ . This is all we need to know from the Rigidity Lemma.

Now, let  $M_{m,A}$  be the fundamental map associated to  $A_m$ . This map is defined in Equation 19. In our proof of Theorem 1.5, we showed that

$$C_A = \lim_{m \rightarrow \infty} M_{m,A}(\Sigma(A_m)). \quad (430)$$

The limit takes place in the Hausdorff topology. Here  $\Sigma(A_m)$  is the set of low vertices on  $\Gamma_m$ . Given Equation 429, we get the analogous result

$$C_A = \lim_{n \rightarrow \infty} M_{n,B}(\Sigma(B_m)). \quad (431)$$

Let's generalize this result. For each  $m$  suppose there is some  $n \geq m$ . We also have

$$C_A = \lim_{m \rightarrow \infty} M_{n,A}(\Sigma(B_m)). \quad (432)$$

The reason is that the maps  $M_{m,A}$  and  $M_{n,B}$  converge to each other on any compact subset of  $\mathbf{R}^2$ , and compact pieces of our limit in Equation 429 determine increasingly dense subsets of  $C_A$ .

**Lemma 30.6** *Suppose that  $\Sigma_n \subset \widehat{\Gamma}(A_n)$  is a translate of  $\Sigma_m$ , consisting entirely of low vertices. Then*

$$C_A = \lim_{m \rightarrow \infty} M_{n,A}(\Sigma_n).$$

**Proof:** We have some vector  $U_m$  such that

$$\Sigma_n = \Sigma(A_m) + U_m. \quad (433)$$

Since  $M_{n,A}$  is affine, we have

$$M_{n,A}(\Sigma_n) = M_{n,A}\Sigma(A_m) + \lambda_m \quad (434)$$

Now we get to the moment of truth. Since  $\Sigma(B_m)$  consists entirely of low vertices, we have  $M_{A,n}(x) \in [0, 2]$  for all  $x \in \Sigma(B_m)$ . Since  $\Sigma_n$  consists entirely of low vertices, we have  $M_{A,n}(x) + \lambda_n \in [0, 2]$  as well. Putting  $t = M_{A,n}(x)$ , we have

$$t; \quad t + \lambda_m \in [0, 2]. \quad (435)$$

This last equation puts constraints on  $\lambda_m$ .

By the case  $n = 0$  of Equation 277, the set  $C_A$  contains both 0 and 2. Therefore, once  $m$  is large, we can choose  $x \in \Sigma(B_m)$  such that  $t = M_{A,n}(x)$  is very close to 0. But this forces

$$\liminf \lambda_m \geq 0.$$

At the same time, we can choose  $x$  such that  $M_{A,m}(x)$  is very close to 2. This shows that

$$\limsup \lambda_m \leq 0.$$

in short  $\lambda_m \rightarrow 0$ . ♠

We just have to tie the discussion above together with our notion of a growing sequence. Suppose that  $\{x_n\}$  is a growing sequence.

Let  $\beta_n$  denote the component of  $\widehat{\Gamma}_n$  corresponding to  $x_n$ . There is a proper function  $m = m_n$  such that the pivot arc  $P\beta_n$  is a translate of the major pivot arc  $P\Gamma(B_m)$ . Here  $\{B_m\}$  is a sequence of even rationals that satisfies the hypotheses of Lemma 30.5. Hence  $\{B_m\} \rightarrow A$ . Hence, the application of the Rigidity Lemma above applies.

Every low vertex on  $P\beta_n$  is a translate of a low vertex on  $P\Gamma(B_m)$ . By the Inheritance Lemma, every low vertex on  $P\beta_n$  relative to  $B_m$  is also low with respect to  $A_n$ . Thus, we have exactly the situation described in Lemma 30.6.

Let  $\Sigma_n$  denote the set of low vertices of  $P\beta_n$ . Then  $\Sigma_n$  is a translate of the set  $\Sigma(B_m)$  of low vertices on  $P\Gamma(B_m)$ , as in our lemma above. Since

$$x_n \in M_{A,n}(\Sigma_n) \tag{436}$$

we see that the Hausdorff distance from  $\{x\}$  to  $C_A$  tends to 0 as  $n$  (and  $m$ ) tends to  $\infty$ .

This completes the proof of the Period Theorem.

## 31 The End of the Comet Theorem

### 31.1 The Main Argument

In this chapter we finish the proof of the Comet Theorem by proving Statement 1. Our proof does not use any of the other statements of the Comet Theorem, so our proof is not circular. In this first section we give the main argument modulo several details. Following this section, we clear up the several details.

For each rational  $B$ , we form the depth-2 tree by considering the two predecessors of  $B$ , and their two predecessors. We define the complexity of  $B$  to be the minimum value of all the numerators of the rationals involved in this list of 7 rationals. The point is this definition is that these are the only rationals that arise in the geometric constructions we make in this chapter.

Let  $A \in (0, 1)$  be irrational. In this section we consider a sequence  $\{B_n\}$  of rationals that converges to  $A$ . In our applications, this sequence is the superior sequence, but our results hold more generally. Recall that any rational parameter  $B$  has its tree  $T(B)$  of predecessors. We can consider  $T(B_n)$  for each parameter  $B_n$  in our sequence.

**Lemma 31.1** *Let  $N$  be any integer. Then there are only finitely many rationals in the union*

$$\bigcup_{n=1}^{\infty} T(B_n)$$

*having complexity less than  $N$ .*

**Proof:** We will argue as in the proof of Lemma 30.5. Suppose  $C = r/s$  is a rational in the tree  $T(B_n)$  such that  $r$  is small and  $s$  and  $n$  are large. Then the directed Farey path connecting  $C$  to  $B_n$  has tiny displacement, and  $|B_n - A|$  is small. Hence  $|C - A|$  is small. Also,  $C$  is near 0. Hence  $A$  is near 0. This is a contradiction once  $s$  and  $n$  are large enough. Hence, there is some function  $f$ , depending on the sequence, such that  $s < f(r)$ . Hence, our union only contains finitely many rationals having numerator less than  $N$ . Our result follows from this fact. ♠

Let  $\beta$  be a component of the arithmetic graph. We call  $\beta$  a *hovering component* if it has no low vertices. More specifically, we call  $\beta$  a *D-hovering component* of  $\widehat{\Gamma}(A)$  if  $\beta$  has no low vertices, and if  $\beta$  contains a vertex with

is within  $D$  vertical units of the baseline. Here  $D \geq 2$  is an integer. We use this name because we think of  $\beta$  as hovering somewhere above the baseline without coming really close.

Below we prove the following result.

**Lemma 31.2** *Let  $A_2$  be any rational, having the predecessors  $A_0 \leftarrow A_2$  and  $A_1 \leftarrow A_2$ . Let  $\beta$  be a  $D$ -hovering component of  $\widehat{\Gamma}(A)$ . Assuming that  $A_2$  has sufficiently high complexity,  $\beta$  is either a translate of a  $D$ -hovering component of  $\widehat{\Gamma}_0$  or a translate of a  $D$ -hovering component of  $\widehat{\Gamma}_1$ .*

**Corollary 31.3** *Let  $\{A_n\}$  be the superior sequence approximating  $A$ . Let  $D$  be fixed. Then there is a constant  $D'$  with the following property. If  $n$  is sufficiently large, then  $\widehat{\Gamma}_n$  has no  $D$ -hovering components having diameter greater than  $D'$ . Here  $D'$  is independent of  $n$ .*

**Proof:** Applying Lemma 30.1 recursively, we see that  $\beta$  is the translate of a  $D$ -hovering component of  $\widehat{\Gamma}(C_n)$ , where  $C_n$  belongs to the tree of predecessors of  $A_n$  and has uniformly bounded complexity. But then, by Lemma 31.1, the sequence  $\{C_n\}$  has only finitely many different terms. Hence  $\beta$  is the translate of one of finitely many different polygons. ♠

Below we prove the following result.

**Lemma 31.4** *Let  $\beta$  be a low component of  $\widehat{\Gamma}(B_n)$ . There is some constant  $D'$  such that every  $D$ -low vertex of  $\beta$  can be connected to a low vertex of  $\beta$  in less than  $D'$  steps. Here  $D'$  depends on  $D$  and on  $A$ , but not on  $n$ .*

**Lemma 31.5** *Let  $\zeta \in U_A$  such that  $\|\zeta\| < N$ . Then there is some  $N'$  such that  $\psi^k(\zeta) \in \Xi$  for some  $|k| < N'$ .*

**Proof:** This is a fairly immediate consequence of our proof of the Return Lemma in §2 and the Pinwheel Lemma in §7. The Return Lemma takes care of the case when  $N$  is small, and the Pinwheel Lemma takes care of the case when  $N$  is large. ♠

Recall that  $J$  is the interval from Equation 2.

**Lemma 31.6** *Let  $\zeta \in \Xi$  be such that  $\|\zeta\| < N$ . Then there exists  $N'$  such that  $\Psi^k(\zeta) \in J$ .*

**Proof:** We choose a special interval relative to  $A_n$  whose closure contains  $\zeta$ . The term *special interval* refers to §2.2. Typically the choice is unique, but when  $\zeta$  lies in the boundary of a special interval there are two choices and we pick one arbitrarily. Let  $\beta_n$  be the component of  $\Gamma(A_n)$  that tracks this special interval. There is some uniform  $D$  such that the vertex of  $\beta_n$  corresponding to our special interval is  $N$ -low.

By the Continuity Principle,  $\text{diam}(\beta_n) \rightarrow \infty$ . By Corollary 31.3, we see that  $\beta_n$  is a low component for  $n$  sufficiently large. By Lemma 31.4, the vertex corresponding to  $\zeta$  can be connected to a low vertex within  $N'$  steps. But then there is a sequence  $\{k_n\}$  such that

$$\Psi_n^{k_n}(\zeta) \in [0, 2] \times \{-1, 1\}; \quad |k_n| < N'. \quad (437)$$

Here  $\Psi_n$  is the first return map defined relative to  $A_n$ . The important point here is that  $N'$  is independent of  $n$ . This lemma now follows from the Continuity Principle from §2. ♠

**Lemma 31.7** *If  $x \in \Xi$  is such that  $|x| < R$ , then there is some  $R'$  such that the portion of the  $\psi$ -orbit of  $x$  between  $x$  and  $\Psi(x)$  has cardinality at most  $R'$ .*

**Proof:** same proof as Lemma 31.5. ♠

Statement 1 of the Comet Theorem now follows from Equation 2, Lemma 31.5, Lemma 31.6, and Lemma 31.7.

Our work is almost done. The two remaining details are Lemma 31.2 and Lemma 31.4. We establish these results in the sections below.

## 31.2 Proof of Lemma 31.2

### 31.2.1 Traps

For  $j = 0, 1$ , let  $\Delta_j$  denote the region of agreement between  $\widehat{\Gamma}_j$  and  $\widehat{\Gamma}_2$ , as in Lemma 28.4. Call a parallelogram  $X_j$  a *trap* if  $X_j \subset \Delta_j$ , and no hovering component relative to  $A_j$  crosses  $\partial X_j$ . Say that a pair  $(X_1, X_2)$  is a *D-trap* if  $X_j$  is a trap relative to  $(A_j, A_2)$  and if every  $D$ -low vertex, relative to  $A_2$ , is translation equivalent to a vertex in one of the traps. As usual, the translation takes place in  $\mathbf{Z}V_2$ .

Below we will prove the following result.

**Lemma 31.8** *If  $A_2$  has high complexity, then there exists a  $D$ -trap.*

Lemma 31.2 follows immediately from Lemma 31.8. Let  $\beta_2$  be a  $D$ -hovering component of  $\widehat{\Gamma}_2$ . Let  $v$  be a  $D$ -low vertex of  $\beta$ . We can translate so that  $v$  lies in either  $X_0$  or  $X_1$ . Suppose that  $v \in X_0$ . Let  $\beta_0$  be the component of  $\widehat{\Gamma}_0$  that contains  $v$ . Since  $X_0$  is a trap,  $\beta_0 \subset X_0$ . But  $X_0$  is a region of agreement between  $\widehat{\Gamma}_0$  and  $\widehat{\Gamma}_2$ . Hence  $\beta_0 = \beta_2$ . The same argument works if  $v \in X_1$ .

Now we define the traps. First we make some general comments. The rational  $A_0$  is odd and the rational  $A_1$  is even. The parallelogram  $X_0$  is always bounded by the lines used in the Decomposition Theorem. The parallelogram  $X_1$  is the one we used in the proof of the Pivot Theorem. The reader can see the traps drawn, in all cases, using Billiard King.

Now we get down to specifics. There are 4 cases:

1.  $A_2$  is odd and  $A_1 < A_2$ .
2.  $A_2$  is odd and  $A_1 > A_2$ .
3.  $A_2$  is even and  $A_1 < A_2$ .
4.  $A_2$  is even and  $A_1 > A_2$ .

In our proof of the Pivot Theorem, we considered Cases 1 and 3. Here we will consider Cases 1 and 3 in detail, and just remark briefly on Cases 2 and 4. The reader will see that Case 2 is essentially identical to Case 1 and Case 4 is essentially identical to Case 2.

The reader can see the traps drawn in Billiard King, for any desired smallish parameter.

### 31.2.2 Case 1

We first reconcile some bits of notation. In this case we have

$$A_0 = (A_2)_-; \quad A_1 + A_0 = (A_2)_+. \quad (438)$$

Both  $A_0$  and  $A_2$  are odd rationals.

We define  $X_0 = R_1(A_2)$ , the parallelogram used in the decomposition Theorem for  $A_2$ . We define  $X_1 = R$ , the parallelogram defined at the end of §29.6.

In §29.9 we showed that  $R_1 \subset \Delta_1$  when  $A_2$  has high complexity. Lemma 21.6 shows that  $R_0 \subset \Delta_0$  when  $A_2$  has high complexity. However, since our notation has changed slightly, and since we are considering the opposite case from the one in Lemma 21.6 – namely,  $R_0$  here lies to the left of the origin – we will re-work the proof.

**Lemma 31.9**  $X_0 \subset \Delta_0$ .

**Proof:** We will apply the Diophantine Lemma. We work with the linear functionals  $G_2$  and  $H_2$  associated to the parameter  $A_2$ . Let  $u$  and  $w$  denote the top left and right vertices of  $X_0$  respectively. The interval in the Diophantine Lemma is

$$[-(q_2)_- - q_0 + 2, q_0 - 2]. \quad (439)$$

The lower bound comes from Case 2 of Lemma 18.5.

Hence, it suffices to show that to show that

$$G_2(u) \gg -(q_2)_- - q_0 \quad H_2(w) \ll q_0 \quad (440)$$

The ( $\gg$ ) symbol means an inequality in which the difference between the two sides tends to  $\infty$  with the complexity of  $A_2$ .

We have the estimates

$$u \approx -(V_2)_- + \lambda W_2; \quad w \approx \lambda W_2; \quad \lambda = \frac{q_2^*}{q_2} \leq \frac{q_0}{q_2}. \quad (441)$$

Here  $A_2^* = p_2^*/q_2^*$  is the superior predecessor of  $A_2$ . The approximation becomes arbitrarily good as the complexity of  $A_2$  tends to  $\infty$ . In particular, the approximation is good to within 1 unit once  $A_2$  has sufficiently high complexity.

We compute

$$G_2(u) \approx -(q_2)_- - \lambda \frac{q_2^2}{p_2 + q_2} \gg -(q_2)_- - \lambda(q_2) \geq -(q_2)_- - q_0.$$

This takes care of the vertex  $u$ . Now we compute

$$H_2(w) \approx \lambda \frac{q_2^2}{p_2 + q_2} \ll \lambda q_2 = q_0.$$

This takes care of the vertex  $w$ . ♠

Now we know that  $X_j \subset \Delta_j$  for  $j = 0, 1$ . Indeed, our proof shows that a large neighborhood of  $X_j$  is contained in  $\Delta_j$  once the complexity of  $A_2$  is large.

**Lemma 31.10**  $X_0$  is a trap.

**Proof:** By the Decomposition Theorem, the only component of  $\widehat{\Gamma}_2$  that crosses  $X_0$  is  $\Gamma_2$ , a low component. The crossings occur within 1 unit of the bottom vertices of  $X_0$ . Since  $\widehat{\Gamma}_0$  and  $\widehat{\Gamma}_2$  agree in a neighborhood of  $X_0$ , the same structure holds for  $\widehat{\Gamma}_0$ . The only places where a component of  $\widehat{\Gamma}_0$  crosses  $X_0$  are at low vertices. In particular, no hovering component of  $\widehat{\Gamma}_0$  crosses  $X_0$ . ♠

**Lemma 31.11**  $X_1$  is a trap.

**Proof:** We already saw in §29.7 that the only components of  $\widehat{\Gamma}_1$  that cross  $X_1$  are the ones on major components of  $\widehat{\Gamma}_1$ . But, such components are not hovering components. Hence  $X_1$  is a trap. ♠

Here is the last remaining step.

**Lemma 31.12** The pair  $(X_0, X_1)$  is a  $D$ -trap once  $A_2$  has high complexity.

**Proof:** The left bottom vertex of  $X_0$  is  $-(V_2)_-$  whereas the bottom right vertex of  $X_1$  is  $(V_2)_+$ . These two vertices differ by  $V_2$ . The bottom right vertex of  $X_0$  is  $(0, 0)$ , the same as the bottom left vertex of  $X_1$ . Figure 31.1 shows the picture.

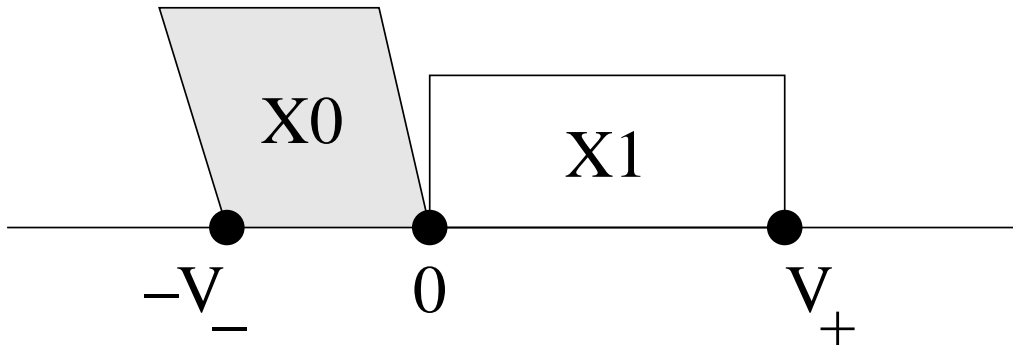


Figure 31.1: The trap

Suppose for the moment that the sides of  $X_0$  have the same slope as the sides of  $X_1$ . Then, once  $A_2$  has high complexity, the tops of both parallelograms are more than  $D$  units from the baseline. But then the union of translations

$$\bigcup_{k \in \mathbf{Z}} (X_0 + X_1 + kV_2) \quad (442)$$

contains all  $D$ -low vertices, as desired.

The slight complication is that the sides of  $X_0$  are parallel to  $W_2$  whereas the sides of  $X_1$  are parallel to  $W_1$ . These are the vectors from Equation 21, relative to  $A_2$  and  $A_1$ . As the complexity of  $A_2$  tends to  $\infty$ , the slopes converge, and no  $D$ -low lattice point lies between the two lines emanating from the same point. Thus, our union in Equation 442 still contains all  $D$ -low vertices once  $A_2$  has high complexity. ♠

### 31.2.3 Case 2

In this case we have  $A_1 > A_2$ . We take  $X_0 = R_1(A_2)$ , the smaller of the two parallelograms in the Decomposition Theorem. This time  $X_0$  lies to the right of the origin. We take  $X_1$  to be just like the parallelogram defined at the end of §29.6, except that  $-(V_2)_-$  replaces  $(V_2)_+$ . Here  $X_1$  lies to the left of the origin. The picture looks exactly like Figure 31.1, except that the roles of left and right are reversed, and the subscripts  $(+)$  and  $(-)$  are switched in the labels. Aside from switching the roles placed by left and right, and  $(+)$  and  $(-)$ , the proofs for Case 2 are exactly the same as the proofs for Case 1.

### 31.2.4 Case 3

We first reconcile some bits of notation. In this case we have

$$A_0 = (A_2)_+; \quad A_1 = (A_2)_-. \quad (443)$$

Here  $A_1$  and  $A_2$  are even and  $A_0$  is odd. We define  $X_1$  exactly as in Case 1, using the rectangle  $R$  described at the end of §29.6. The same argument as in Case 1 shows that  $X_1$  is a trap.

We define  $X_0$  to be the parallelogram bounded by the following lines.

1. The baseline relative to  $A_0$ .

2. The line parallel to  $V_0$  and containing  $W_0$ . This is the top of the room  $R(A_0)$  from the Room Lemma.
3. The line parallel to  $W_0$  and containing  $(0, 0)$ .
4. The line parallel to  $W_0$  and containing  $-(V_2)_-$ .

**Lemma 31.13**  $X_0 \subset \Delta_0$  once  $A_2$  has sufficiently high complexity.

**Proof:** We will apply Lemma 28.4. This time, we work with the linear functionals  $G_0$  and  $H_0$  associated to the parameter  $A_0$ . Let  $u$  and  $w$  denote the top left and right vertices of  $X_0$  respectively. The interval in the Diophantine Lemma is

$$[-q_2 + 2, q_0 - 2]. \quad (444)$$

Hence, it suffices to show that to show that

$$G_2(u) \gg -q_2 \quad H_2(w) \ll q_0 \quad (445)$$

We have

$$u = -(V_2)_- + W_0; \quad w = W_0. \quad (446)$$

We compute

$$G_0(u) \approx -(q_2)_- - \frac{q_0^2}{p_0 + q_0} \gg -(q_2)_- - q_0 = -(q_2)_- - (q_2)_+ = -q_2.$$

This takes care of the vertex  $u$ . Now we compute

$$H_2(w) = \frac{q_0^2}{p_0 + q_0} \ll q_0.$$

This takes care of the vertex  $w$ . ♠

**Lemma 31.14**  $X_0$  is a trap.

**Proof:** The same argument as in Lemma 29.6 shows that

$$-(V_2)_- = -(V_0)_- + kV_0. \quad (447)$$

for some  $k \in \mathbf{Z}$ . Geometrically, this says that

$$X_0 = Y_1 \cup \dots \cup Y_k \cup Z; \quad Y_j = R(A_0) - jV_0. \quad (448)$$

Here  $R(A_0)$  is the parallelogram from the Room Lemma. The parallelogram  $Z$  is  $\mathbf{Z}V_0$  translate of the parallelogram  $Z'$  bounded by the following lines.

1. The baseline relative to  $A_0$ .
2. The line parallel to  $V_0$  and containing  $W_0$ . This is the top of the room  $R(A_0)$  from the Room Lemma.
3. The line parallel to  $W_0$  and containing  $(0, 0)$ .
4. The line parallel to  $W_0$  and containing  $(V_2)_+$ .

But each  $Y_j$  separately is a trap by the Room Lemma. The parallelogram  $Z'$  is also a trap, by the same argument we gave in the proof of the Decomposition Lemma. This argument is repeated in the proof of Lemma 29.1. Hence, by symmetry  $Z$  is also a trap.

Hence,  $X_0$  is a finite union of traps, all meeting edge to edge. Hence,  $X_0$  is also a trap. ♠

It only remains to show that the pair  $(X_0, X_1)$  is a  $D$ -trap. The bottom vertices in this case have the same description as in Case 1, and the argument there works here word for word.

### 31.2.5 Case 4

We define  $X_1$  just as in Case 2. We define  $X_0$  as in Case 3, except that we replace the vector  $-(V_2)_-$  by the vector  $(V_2)_+$ . The rest of the proof is the same as in Case 3, modulo the same switching of “left” and “right”.

## 31.3 Proof of Lemma 31.4

### 31.3.1 Major Components

We keep the notation from the previous section.

**Lemma 31.15** *When  $A_2$  has sufficiently high complexity, the set*

$$(\Gamma_2 - P\Gamma_2) \cap X_1$$

*consists of 2 connected arcs, each joining an endpoint of  $\gamma_2$  to the top of  $X_1$ .*

**Proof:** In the even case, this is a restatement of Lemma 29.13.

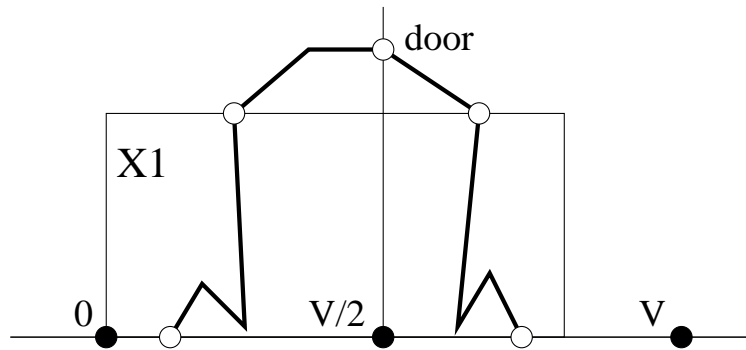


**Figure 31.2:** The arc  $\gamma_2$  in the odd case.

We consider the odd case. We describe the case when  $A_1 < A_2$ . The other case is entirely similar. The two endpoints of  $\gamma_2$  are  $E_2^+$  and  $E_2^- + V_2$ . Both these points belong to  $X_1$ . The line parallel to  $W_2$  through  $V_2/2$  divides  $X_1$  into two pieces. By the Hexagrid Theorem,  $\gamma_2$  crosses a door on this line. This door lies above the top of  $X_1$ . At the same time,  $\gamma_2$  can only cross the top of  $X_1$  twice. This follows from the Barrier Theorem, as applied to  $A_1$ , and from the fact that  $\hat{\Gamma}_1$  and  $\hat{\Gamma}_2$  agree in a neighborhood of  $X_1$ . This structure forces the following structure. Starting from the left endpoint of  $\gamma_2$ , some initial arc of  $\gamma_2$  rise up to the top of  $X_1$ . Following this, the next arc of  $\gamma_2$  crosses through a door and returns to the top of  $X_1$ . The final arc of  $\gamma_2$  connects the top of  $X_1$  to the right endpoint of  $\gamma_2$ . ♠

Now we derive some corollaries from our structure result. We say that a  $D$ -arc of  $\Gamma_2$  is a connected arc  $\alpha$  that joins a low vertex to a  $D$ -low vertex. Let  $|\alpha|$  denote the smallest integer  $N$  such that  $\alpha$  contains no vertices that are  $N$  vertical units above the baseline. So  $\alpha$  remains within  $N$  vertical units of the baseline. Given a  $D$ -low vertex  $v \in \alpha$ , let  $f(v; A_2) = \min |\alpha|$ , where the minimum is taken over all  $D$ -arcs having  $v$  as an endpoint. Let  $F(A_2) = \max f(v; A_2)$ , where the maximum is taken over all  $D$ -low vertices  $v$  of  $\Gamma_2$ . These functions depend implicitly on  $D$ , which is fixed throughout the discussion.

**Lemma 31.16** *If  $A_2$  has sufficiently high complexity, then*

$$F(A_2) \leq \max(F(A_0), F(A_1)).$$

**Proof:** Suppose first that  $A_2$  is odd. Choose a vertex  $v \in \Gamma_2$  such that  $F(A_2) = f(v)$ . By symmetry, we can choose  $v \in P\Gamma_2 \cup \gamma_2$ . Suppose that

$v \in P\Gamma_2$ . By the Copy Theorem,  $P\Gamma_2 \subset \Gamma_0$ . Hence  $v \in \Gamma_0$ . The argument in Lemma 29.2 shows that a vertex on  $P\Gamma_2$  is  $E$ -low relative to  $A_0$  if and only if it is  $E$ -low relative to  $A_2$ . Here  $E \in \{1, 2, 3, \dots\}$ . Call this the *low principle*. Let  $\alpha$  be a  $D$ -arc of  $\Gamma_0$  such that  $f(v; A_0) = |\alpha|$ . Since both endpoints of  $P\Gamma_2$  are low relative to both parameters, we can take  $\alpha \subset P\Gamma_2$ . Hence

$$F(A_0) \geq f(v; A_0) = |\alpha| \geq f(v; A_2) = F(A_2).$$

Note that  $|\alpha|$  is the same relative to both parameters, by the low principle.

Suppose that  $v \in \gamma_2$ . Then  $v$  is in one of the two arcs from Lemma 31.15. Let's say that  $v$  is on the left arc,  $\lambda$ . The left endpoint of  $\lambda$  is common to  $\Gamma_1$  and  $\Gamma_2$ , and  $\lambda \subset X_1$ , a region of agreement for the two arithmetic graphs. Hence  $\lambda \subset \Gamma_1$ . The low principle applies to any vertex in  $X_1$ . Let  $\alpha$  be a  $D$ -arc of  $\Gamma_1$  such that  $f(v; A_1) = |\alpha|$ . The left endpoint of  $\lambda$  is low, and the right endpoint lies on the top of  $X_1$ . When  $A_2$  has high complexity,  $\alpha \subset \lambda$ . The idea here is that the  $D$ -arc connecting  $v$  to the left endpoint of  $\lambda$  remains in  $X_1$  whereas any  $D$ -arc exiting  $\lambda$  must pass through the top of  $X_1$ . Since  $\alpha \subset \lambda$ , we get  $F(A_1) \geq F(A_2)$  by the same argument as in the previous case.

When  $A_2$  is even, the proof is the same except for two small changes. First, we need to invoke Lemma 29.13 (rather than just symmetry) to get  $v \in P\Gamma_2 \cup \gamma_2$ . Second, when  $v \in P\Gamma_2$ , we use Lemma 28.11 in place of the Copy Theorem. ♠

Now let  $\{B_n\}$  be the sequence in Lemma 31.4.

**Corollary 31.17**  *$F(B_n)$  is uniformly bounded, independent of  $n$ .*

**Proof:** Applying the previous result recursively, we see that there is some parameter  $C_n \in T(B_n)$ , of uniformly bounded complexity, such that

$$F(B_n) \leq F(C_n).$$

But the sequence  $\{C_n\}$  has only finitely many distinct members, by Lemma 31.1. ♠

**Corollary 31.18** *Let  $v_n$  be a  $D$ -low vertex on  $\Gamma(B_n)$ . Then  $v_n$  can be connected to a low vertex of  $\Gamma_n$  by an arc of length less than  $D'$  for some  $D'$  that is independent of  $n$ . Hence, Lemma 31.4 is true for points that lie on major components.*

**Proof:** By Corollary 31.17 we can find a  $D$ -arc  $\alpha_n$  connecting  $v_n$  to a low vertex of  $\Gamma(B_n)$  such that  $|\alpha_n| < N$  and  $N$  is independent of  $n$ . But the same argument as in the proof of Lemma 5.5 shows that the diameter of  $\alpha_n$  is uniformly bounded. The idea here is that  $\alpha_n$  cannot grow a long way in a thin neighborhood of the baseline. This takes care of  $D$ -low vertices on  $\Gamma(B_n)$ . Any other major component of  $\widehat{\Gamma}(B_n)$  is translation equivalent to  $\Gamma(B_n)$ . ♠

### 31.3.2 A Quick but Unjustified Finish

It remains to prove Lemma 31.4 for points that lie on minor components. First we will give a short proof that we cannot quite justify. Then we will patch up the argument. Experimentally, we observe the following strengthening of the Inheritance Lemma.

**Conjecture 31.19** *Let  $A_2$  be any rational, having the predecessors  $A_0 \leftarrow A_2$  and  $A_1 \leftarrow A_2$ . Then every minor low component of  $\widehat{\Gamma}_2$  is either the translate of a low component of  $\widehat{\Gamma}_0$  or the translate of a low component of  $\widehat{\Gamma}_1$ .*

Assuming this conjecture, we can quickly finish the proof of Lemma 31.4. Suppose that Lemma 31.4 is false. Then we can find a sequence of triples  $\{(v_n, \beta_n, B_n)\}$  with the following properties.

1.  $\beta_n$  is a minor component of  $\widehat{\Gamma}(B_n)$ ;
2.  $v_n$  is a vertex of  $\beta_n$  that lies within  $D$  units of the baseline;
3. The  $n$ -neighborhood of  $v_n$  in  $\beta_n$  contains no low vertices.

By Conjecture 31.19, the component  $\beta_n$  is the translate of  $\Gamma(B'_n)$  for some  $B'_n \in T(B_n)$ . Since the diameter of  $\beta_n$  tends to  $\infty$  with  $n$ , the complexity of  $B'_n$  tends to  $\infty$ . Hence, by Lemma 30.5,  $B'_n \rightarrow A$ . Thus, Thus, a counterexample to Lemma 31.4 involving minor components leads to a counterexample involving major components.

We can't quite prove Conjecture 31.19. Our approach to Lemma 31.4 is to prove a slightly weaker version of Conjecture 31.19, and then scramble to finish the proof.

### 31.3.3 The End of the Proof

Let  $A$  be an even rational. Previously, we had divided the polygon  $\Gamma(A)$  into two arcs, the pivot arc  $P\Gamma(A)$  and the upper arc. These two arcs join together at the pivot points.

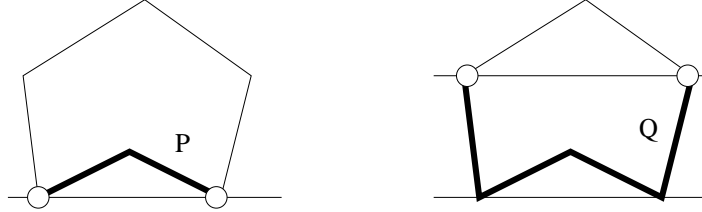


Figure 31.3:  $P\Gamma$  and  $Q\Gamma$ .

Now we consider a new decomposition of  $\Gamma$ . Referring to the Barrier Theorem, recall that  $\Gamma(A)$  passes through the barrier at 2 points. One arc of  $\Gamma$  lies below the barrier and one above. Let  $Q\Gamma$  denote the component that lies below. Then  $P\Gamma \subset Q\Gamma$ . We call  $Q\Gamma$  an *extended pivot arc*. We think of  $Q\Gamma$  as a kind of compromise between the whole component  $\Gamma$  and the pivot arc  $P\Gamma$ . If  $A$  has sufficiently high complexity, then  $Q\Gamma$  contains all the vertices within  $D$  of the baseline. This is a consequence of the Barrier Theorem.

So far we have only defined  $Q\beta$  when  $\beta = \Gamma(A)$  and  $A$  is an even rational. Our strengthening of the Inheritance Lemma extends this definition to all polygonal low components of  $\hat{\Gamma}(A)$ , when  $A$  is any rational parameter.

**Lemma 31.20** *Let  $A_2$  be any rational, having the predecessors  $A_0 \leftarrow A_2$  and  $A_1 \leftarrow A_2$ . If  $A_2$  has sufficiently high complexity, then every low component of  $\hat{\Gamma}_2$  has a well-defined extended pivot arc, and this pivot arc is the translate of an extended pivot arc of  $\hat{\Gamma}_j$  for one of  $j = 0, 1$ .*

**Proof:** We will use the existence of the traps  $X_0$  and  $X_1$ . Let  $\beta$  be a low component of  $\hat{\Gamma}_2$ . Let  $v$  be a low vertex of  $\beta$ . If  $v \in X_0$  then  $\beta$  is copied whole from  $\hat{\Gamma}_0$ . If  $\beta \in X_1$ , then  $\beta$  is copied whole from  $\hat{\Gamma}_1$  unless (in the language of §29.9)  $\beta = C_1$  or  $\beta = C_{k-1}$ . In these cases,  $QC_1$  and  $QC_{k-1}$ , both subsets of  $X_1$ , are copied whole by  $\hat{\Gamma}_2$ . Hence, the portion of  $\beta$  lying in  $X_2$  is copied from  $\hat{\Gamma}_1$ .

Let  $\tilde{\beta}$  denote the component of  $\hat{\Gamma}_2$  that contains  $\beta \cap X_1$ . We define  $Q\tilde{\beta} = Q\beta$ . Then  $Q\tilde{\beta}$  is copied from  $\hat{\Gamma}_1$  by construction. ♠

The following result is an *addendum* to the proof of Lemma 31.20. We would like to say that the components  $\tilde{C}_0$  and  $\tilde{C}_{k-1}$ , though perhaps imperfect copies of  $C_0$  and  $C_{k-1}$ , still retain a basic property of the original components.

**Lemma 31.21** *Let  $N$  be fixed. If  $A_2$  has sufficiently high complexity, then  $\tilde{C}_1 - Q\tilde{C}_1$  does not contain any vertices within  $N$  units of the baseline. The same goes for  $C_{k-1}$ .*

**Proof:** As in our proof of the Pivot Theorem, we consider the case when  $A_1 < A_2$ . The other case is entirely similar.

Let  $\gamma = \tilde{C}_1 - Q\tilde{C}_1$ . Here  $\gamma$  is an arc of  $\hat{\Gamma}_2$ . Let  $R$  be the parallelogram we used in the proof of the Pivot Theorem. We defined  $R$  at the end of §29.6. Recall that  $\hat{\Gamma}_1$  and  $\hat{\Gamma}_2$  agree in  $R$ . The component  $\tilde{C}_1$  has a low vertex in  $R$ . The arc  $\gamma$  has both its endpoints on the top edge of  $R$ .

Let  $S$  denote the infinite strip obtained by extending the left and right sides of  $R$ . We claim that  $\tilde{C}_1$  does not cross either side of  $S$ . To prove this claim, let  $S_L$  and  $S_R$  denote the left and right boundaries of  $S$ . Then  $\tilde{C}_1$  does not cross  $S_L$  by the Hexagrid Theorem applied to  $A_2$ . Likewise,  $\iota(\tilde{C}_1)$  does not cross  $S_L$  by the Hexagrid Theorem. Here  $\iota$  is the same symmetry as in Lemma 29.1. By construction,  $\iota$  swaps  $S_L$  and  $S_R$ . Hence,  $\tilde{C}_1$  does not cross  $S_R$ . This establishes our claim.

Now we know that  $\gamma$  does not cross the sides of  $S$ . Hence, if  $\gamma$  contains a vertex within  $N$  units of the baseline, this vertex must lie in  $R$ . But then  $\tilde{C}_1$  crosses the top edge of  $R$  at least 4 times. But these 4 crossing points are then copied from  $\hat{\Gamma}_1$ . This contradicts the Barrier Theorem, because the top edge of  $R$  is contained in the barrier line for  $\hat{\Gamma}_1$ . ♠

Let  $\{B_n\}$  be the sequence from Lemma 31.4.

**Corollary 31.22** *Let  $\{\beta_n\}$  be a sequence of components, with  $\beta_n$  a low component of  $\hat{\Gamma}(B_n)$ . Suppose that the diameter of  $\beta_n$  tends to  $\infty$ . Then the distance from any point on  $\beta_n - Q\beta_n$  to the baseline of  $\hat{\Gamma}(B_n)$  tends to  $\infty$  as well.*

**Proof:** This is a fairly immediate consequence of the previous result. Each  $\beta_n$  is a translate of a component of the form  $\tilde{C}$ ,  $C = \Gamma(B'_n)$ . Here  $B'_n$  is on the tree of predecessors of  $B_n$ . Since the diameter of  $\tilde{C}$  tends to  $\infty$  with  $n$ , we see that the complexity of  $B'_n$  tends to  $\infty$  with  $n$  by Lemma 31.1. Hence,

the distance from  $\tilde{C} - Q\tilde{C}$  to the relevant baseline tends to  $\infty$  with  $n$ . ♠

Now we redo the argument in §31.3.2 equipped with our weaker but sufficient results. From Lemma 31.20, we conclude that  $Q\beta_n$  is the translate of  $Q\Gamma(B'_n)$  for some other sequence  $B'_n \rightarrow A$ . This is just as in the proof of Lemma 31.22. Thus, a counterexample to Lemma 31.4 involving minor components leads to a counterexample involving major components. Since we have already taken care of the major components, our proof is done.

## 32 References

- [B] P. Boyland, *Dual Billiards, twist maps, and impact oscillators*, Nonlinearity **9** (1996) 1411-1438
- [De] N .E. J. De Bruijn, *Algebraic Theory of Penrose's Nonperiodic Tilings*, Nederl. Akad. Wentensch. Proc. **84** (1981) pp 39-66
- [Da] Davenport, *The Higher Arithmetic: An Introduction to the Theory of Numbers*, Hutchinson and Company, 1952
- [D], R. Douady, *These de 3-eme cycle*, Universite de Paris 7, 1982
- [DF] D. Dolyopyat and B. Fayad, *Unbounded orbits for semicircular outer billiards*, preprint (2008)
- [DT] F. Dogru and S. Tabachnikov, *Dual Billiards*, Math Intelligencer vol. 27 No. 4 (2005) 18–25
- [G] D. Genin, *Regular and Chaotic Dynamics of Outer Billiards*, Penn State Ph.D. thesis (2005)
- [GS] E. Gutkin and N. Simanyi, *Dual polygonal billiard and necklace dynamics*, Comm. Math. Phys. **143** (1991) 431–450
- [H] M. Hochman, *Genericity in Topological Dynamics*, Ergodic Theory and Dynamical Systems **28** (2008) pp 125-165
- [Ke] R. Kenyon, *Inflationary tilings with a similarity structure*, Comment. Math. Helv. **69** (1994) 169–198
- [Ko] Kolodziej, *The antibilliard outside a polygon*, Bull. Polish Acad Sci. Math. **37** (1989) 163–168
- [M1] J. Moser, *Is the Solar System Stable?*, Mathematical Intelligencer, 1978
- [M2] J. Moser, *Stable and Random Motions in Dynamical Systems, with Special Emphasis on Celestial Mechanics*, Annals of Math Studies **77**, Princeton

University Press (1973)

[MM] P. Mattila and D. Mauldin, *Measure and dimension functions: measurability and densities* Math. Proc. Cambridge Philos. Soc. *121* No. 1 (1997)

[N] B.H. Neumann, *Sharing Ham and Eggs*, summary of a Manchester Mathematics Colloquium, 25 Jan 1959 published in Iota, the Manchester University Mathematics students' journal

[S] R. E. Schwartz, *Unbounded Orbits for Outer Billiards*, Journal of Modern Dynamics **3** (2007)

[T1] S. Tabachnikov, *Geometry and Billiards*, A.M.S. Math. Advanced Study Semesters (2005)

[T2] S. Tabachnikov, *A proof of Culter's theorem on the existence of periodic orbits in polygonal outer billiards*, preprint (2007)

[VL] F. Vivaldi and J.H. Lowenstein, Arithmetical properties of a family of irrational piecewise rotations, *Nonlinearity*, (2006) 19:1069-1097

[VS] F. Vivaldi, A. Shaidenko, *Global stability of a class of discontinuous dual billiards*, Comm. Math. Phys. **110** (1987) 625-640